NATIONAL ACADEMY OF SCIENCES OF UKRAINE
DEPARTMENT OF GEOSCIENCES

INSTITUTE OF GEOLOGICAL SCIENCES OF THE NAS OF UKRAINE
M.P. SEMENENKO INSTITUTE OF GEOCHEMISTRY, MINERALOGY AND ORE FORMATION OF THE NAS OF UKRAINE
SUBBOTIN INSTITUTE OF GEOPHYSICS OF THE NAS OF UKRAINE
INSTITUTE OF GEOGRAPHY OF THE NAS OF UKRAINE
STATE INSTITUTION SCIENTIFIC CENTER FOR AEROSPACE RESEARCH OF THE EARTH OF THE INSTITUTE OF GEOLOGICAL SCIENCES OF THE NAS OF UKRAINE
UKRAINIAN MINERALOGICAL SOCIETY
INTERNATIONAL ASSOCIATION OF SEDIMENTOLOGISTS
INTERNATIONAL ASSOCIATION ON THE GENESIS OF ORE DEPOSITS

# IDEAS AND INNOVATIONS IN EARTH SCIENCES

## PROCEEDINGS OF THE 10$^{TH}$ INTERNATIONAL GEOSCIENCES CONFERENCE OF YOUNG RESEARCHERS

**Kyiv, 23-24 May, 2024**

**Kyiv 2024**

# SCIENTIFIC COMMITTEE

**Oleksandr Ponomarenko**, academician, NAS of Ukraine, Semenenko Institute of Geochemistry, Mineralogy and Ore Formation of the NAS of Ukraine, Kyiv, Ukraine;
**Stella Shekhunova**, academician, NAS of Ukraine, Institute of Geological Sciences of the NAS of Ukraine, Kyiv, Ukraine;
**Vitaliy Starostenko**, academician, NAS of Ukraine, Subbotin Institute of Geophysics of the NAS of Ukraine, Kyiv, Ukraine;
**Leonid Rudenko**, academician, NAS of Ukraine, Institute of Geography of the NAS of Ukraine, Kyiv, Ukraine;
**Oleksandr Kendzera**, corresponding member, NAS of Ukraine, Subbotin Institute of Geophysics of the NAS of Ukraine, Kyiv, Ukraine;
**Leonid Stepanyuk**, corresponding member, NAS of Ukraine, Semenenko Institute of Geochemistry, Mineralogy and Ore Formation of the NAS of Ukraine, Kyiv, Ukraine;
**Mykhailo Popov**, corresponding member, NAS of Ukraine, State Institution “Scientific Centre for Aerospace Research of the Earth” of the Institute of Geological Science of the NAS of Ukraine, Kyiv, Ukraine;
**Eugenia Maruniak**, corresponding member, NAS of Ukraine, Institute of Geography of the NAS of Ukraine, Kyiv, Ukraine;
**Oleksandra Olshtynska**, doctor of geological sciences, Institute of Geological Sciences of the NAS of Ukraine, Kyiv, Ukraine;
**Myron Kovalchuk**, doctor of geological sciences, Institute of Geological Sciences of the NAS of Ukraine, Kyiv, Ukraine;
**Olga Sedlerova**, PhD, State Institution “Scientific Centre for Aerospace Research of the Earth” of the Institute of Geological Science of the NAS of Ukraine, Kyiv, Ukraine;
**Stephen Lokier**, PhD, School of Built and Natural Environment, University of Derby, Derby, UK;
**Reimar Seltmann**, PhD, Research Leader and Head of CERCAMS, Natural History Museum, London, UK.

# ORGANISING COMMITTEE

**Anatolii Kushnir**, PhD, Institute of Geography of the NAS of Ukraine, Kyiv, Ukraine;
**Anna Khyzhniak**, PhD, State Institution “Scientific Centre for Aerospace Research of the Earth” of the Institute of Geological Science of the NAS of Ukraine, Kyiv, Ukraine;
**Bohdan Zanoz**, Institute of Geological Sciences of the NAS of Ukraine, Kyiv, Ukraine;
**Dmytro Hlavatskyi**, PhD, Subbotin Institute of Geophysics of the NAS of Ukraine, Kyiv, Ukraine;
**Eugen Lunov**, PhD, Semenenko Institute of Geochemistry, Mineralogy and Ore Formation of the NAS of Ukraine, Kyiv, Ukraine;
**Kateryna Vovk**, PhD, Semenenko Institute of Geochemistry, Mineralogy and Ore Formation of the NAS of Ukraine, Kyiv, Ukraine;
**Kateryna Yaroshovets-Baranova**, Institute of Geological Sciences of the NAS of Ukraine, Kyiv, Ukraine;
**Kyrylo Starodubets**, PhD, Institute of Geological Sciences of the NAS of Ukraine, Kyiv, Ukraine;
**Olena Ganzha**, PhD, Institute of Geological Sciences of the NAS of Ukraine, Kyiv, Ukraine;
**Sergii Mychak**, doctor of geological sciences, Subbotin Institute of Geophysics of the NAS of Ukraine, Kyiv, Ukraine;
**Vitaliy Dernov**, PhD, Institute of Geological Sciences of the NAS of Ukraine, Kyiv, Ukraine;
**Yevhenia Nezdolii**, Institute of Geological Sciences of the NAS of Ukraine, Kyiv, Ukraine;
**Yuliya Dudchenko**, Institute of Geological Sciences of the NAS of Ukraine, Kyiv, Ukraine.

**Ideas and Innovations in Earth Sciences:** Proceedings of the 10-th International Geosciences conference of young researchers, Kyiv, Ukraine. May 23-24, 2024, Kyiv. 2024. P. 130.
Conference proceeding contains materials presented at the 10-th International Geosciences conference of young researchers, which covering modern trends in geological science. The materials represents generalized results of researches of young researchers in the following fields: General and Regional geology; Marine geology; Mineral resources; Petroleum geology; Paleontology and Stratigraphy; Palynology and Paleoclimatology; Lithology and Sedimentology; Geochemistry, Mineralogy and Petrology; Geoinformatics; Hydrogeology and Engineering geology; Geomagnetism, Paleomagnetism and Electromagnetism; Physical geography, Geomorphology and Paleogeography; Geographical research and Sustainable development; Environmental geology. The materials of each report presented in English.
Proceedings of the conference recommend for a wide range of geologists.

Proceedings of the conference recommended for publication by the decision of conference organizing committee (protocol No. 2 dated April 16, 2024).

ISBN 978-617-7852-48-2

Materials published in author’s version.

# CONTENTS

**GEOGRAPHICAL RESEARCH AND SUSTAINABLE DEVELOPMENT**



**ENVIRONMENTAL GEOLOGY**

DOI: https://doi.org/10.30836/igs.iies.2024.45

**Kasianshuk Y., Alyokhin V.**

*Institute of Geological Sciences of the National Academy of Sciences of Ukraine, Kyiv, Ukraine.*
*E-mail: kasyanchukyroslav@gmail.com*

# THE SYSTEM OF DISCONTINUOUS DISLOCATIONS OF THE SOLOTVYNO DEPOSIT AND THE METHODOLOGY OF THEIR STUDY ON THE EXAMPLE OF ONE EXPOSURE

The study of discontinuous dislocations is one of the main tasks of geological mapping of all scales. Disruptive faults and zones of tectonic fracture control the location of many mineral deposits, determine their quality, mining and geological conditions of development. Studying them, it is important not only to identify and trace discontinuous dislocations in space, but also to establish their systems, kinematic types, conditions of formation, age and stages of their activation both in space and time [1]. Often on state geological maps, kinematic types of discontinuous dislocations, possible stages of activation and the conditions of the stress state of the subsoil at these stages have not been fully clarified.

The purpose of this work was a detailed study of discontinuous dislocations of different levels (from tectonic cracks to discontinuous faults) on one of the rock outcrops near the area of the Solotvyno salt deposit. The research area tectonically refers to the Solotvyno depression of the Transcarpathian depression and consists of tuffaceous and sandy-clay rocks of early Neogene age [2-4].

Main tasks of the research: study the lithological composition of rocks and their stratigraphic position on the outcrop, to determine the elements of rock formation; establish discontinuities and zones of tectonic fracturing in the rocks of the lower Neogene; carry out mass measurements of the elements of the occurrence of discontinuous dislocations (rupturing faults, tectonic cracks, shale disintegration); determine its kinematic type and elements of the occurrence of grooves and sliding strokes on sliding mirrors; reconstruct the paleostress fields of the rock massifs at observation point; determine whether this system of dislocations can be favorable for the migration of groundwater in the studied area.

Since rupture tectonics directly affects the mining, geological and hydrogeological conditions of the development of salt deposits and, in general, the ecological state of the environment, it was advisable to conduct detailed complex field studies of rupture dislocations in rock outcrops with the involvement of special tectonophysical methods [1-6]. The methodology of field research near the city Solotvyno, both on this outcrop and on others, included both traditional structural geological methods and methods of tectonophysical research. Mass measurements of the elements of rock formations and deformational mesostructures (tectonic cracks, veins, discontinuity faults, folds) were carried out, typification of cracks into detachments and chips was carried out, veins and crack filling material were studied. The composition of rocks was determined with the selection of samples (including those oriented in space) for petrographic studies under a microscope. Tectonophysical studies were carried out using the methods of structural and paragenetic analysis and the method of kinematic analysis [1, 3]. Types of tectonic cracks and faults (R, R', L – systems), T-structures, inversions of layers and shale formations of rocks under fractures and their spatial relationships were determined.

On the basis of field studies and results processing, a rose-diagrams of the extension of discontinuous dislocations of the research area were simulated (Fig. 1, 2).

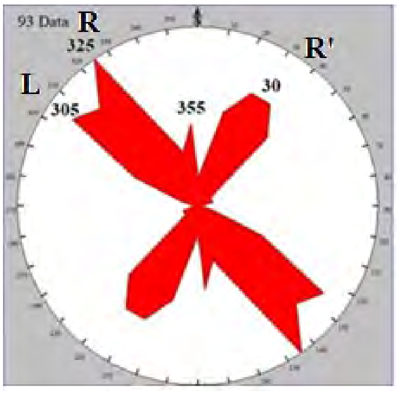


Fig. 1. System of tectonic cracks and faults


Fig. 2. Tectonic schistosity systems

The fault was established in the rock outcrops, which is presented by a zone of tectonic breccia and rock cataclase with a thickness of up to 40 cm, which is limited on both sides by L-cracks with sliding mirrors (Fig. 3). On these fractures, right-shear and right-slide-shear. The suture zone has a northwesterly extension along an azimuth of 300° with a dip to the northeast at an angle of 70°. L- systems tectonic cracks with furrows and slip strokes on planes are developed in the wings of the discontinuous fault. The angle of incidence of furrows changes from 25-30° to 40°.


Fig. 3. Fault seam zone (red lines show the L-systems tectonic cracks with slip lines (slickensides))

The stress state of the rock massifs was studied by tectonophysical methods. Based on the results of research, it was established that in the area is dominated shear type of stress field. Against the general background of the shear stress field, the established fault was formed in the mode of the reset field with the axis of tension across the strike of the fault.

In general, according to the research results, it was established that the "Solotvyno" site has a complex of geological and tectonic structures with the development of folded and discontinuous dislocations. Disruptive dislocations are represented by tectonic cracks and discontinuous faults, cleavage zone and flaking of rocks.

*This study was carried out under the funding of the state budget program CPCEL 6541230 in the framework of the R&D Project “Strategic mineral raw materials for the recovery of the economy of Ukraine: analysis of resources and reserves, development of search criteria for increasing their mineral resource base”.*

**References**

1. Gintov O.B. Field tectonophysics and its application in the study of deformations of the earth's crust. Kyiv: Phoenix, 2005. 572 p.

2. Shekhunova, S.B., Aleksieienkova, M.V., Stadnichenko, S.M., Siumar, N.P. 2015. The integrated geological model of Solotvyno structure as a tool to assess geoecological sustainability of Solotvyno rock-salt deposit. Collection of Scientific Works of the Institute of geological Sciences NAS of Ukraine, 8, 233-250. https://doi.org/10.30836/igs.2522-9753.2015.146791

3. Stoeckl L., Banks V., Shekhunova S., Yakovlev Y. 2020. The hydrogeological situation after salt-mine collapses at Solotvyno, Ukraine. Journal of Hydrology: Regional Studies. vol. 30, 100701. pp. 1-16. https://doi.org/10.1016/j.ejrh.2020.100701

4. Shekhunova S.B., Stadnichenko S.M., Aleksieienkova M.V., Kril T.V., Siumar N.P. 2021. Risk mapping of the slope mass movement processes for public awareness and community risk preparedness (on the example of Solotvyno). Materials of the Third EAGE Workshop on assessment of landslide hazards and

impact on communities, 20-23 September, 2021, Odessa, Ukraine. https://doi.org/10.3997/2214-4609.20215K1028
5. Murovska A., Amashukeli T., Alyokhin V. Stress fields and deformation regimes within the Ukrainian part of the Eastern Carpathians according to tectonophysical data. Geophysical journal. 2019. No. 2, T. 41. 84-97.
6. Alyokhin V.I., Boyarska A.D., Ishkov V.V. Peculiarities of dislocations and paleostress fields in tuffs of the Teresvina world of the Transcarpathian depression in the basin of the Tyachevets River. Scientific works of DonNTU. Series: "Mining and geological". 2022. 1(27)-2(28). P. 7-15.

DOI: https://doi.org/10.30836/igs.iies.2024.18

**Kravets M.**

*Institute of Geological Sciences of the National Academy of Sciences of Ukraine, Kyiv, Ukraine.*
*E-mail: marusya.kravets@ukr.net*

# GEOLOGICAL STRUCTURE AND FORMATION CONDITIONS OF THE VOYUTYCHI CLAY DEPOSIT (LVIV OBLAST): EXAMINATION OF GEOLOGICAL FORMATIONS AND THEIR PROPERTIES

Expanded clays are a type of mineral resources that is increasingly being used in the production of lightweight aggregate for the construction industry. The geological conditions of formation and properties of clays are critical in determining their potential for use as building materials. The aim of this paper is to explore the geological conditions of formation and properties of clay and their influence on the prospects of its use in the industry of building materials, particularly in the substitution of traditional aggregates. The findings of this study can provide insights for further research on the use of mineral resources in building materials and their potential to contribute to sustainable development in the construction ceramics industry.

The geological structure of the mineral deposit consists of formations of the Proterozoic eon theme, Paleozoic, Mesozoic and Cenozoic. Neogene, Miocene and Upper Pleistocene formations of the Carpathian regional layer of the Balytsia Formation N1bl are located on the field area directly under the Quaternary sediments [1]. The mineral resources of the deposit belong to the Desnianska Suite of the Upper Quaternary [1].

The deposit is located in the valley of the Strviazh River, stretches from west to east, and is confined to the first floodplain terrace. The height of the terrace is 6–8 meters [1].

Geomorphologically the study area belongs to the Sambirsko-Khyrivska (B.1.2.c) moraine-zandrova denudation-accumulative upland with sloping accumulative alluvial floodplain tiers [1].

The relief of the site is calm, gentle, and inclined in the eastern direction along the Strviazh River. The absolute depth of the field in the eastern part is 286.6 m; in the western part, it is 288.4 m (well 189) [1].

The geological section of the deposit is as follows:

1. On the eroded surface of Miocene clays, there is a pebble layer composed of well-crushed pebbles of Carpathian rocks (sandstones, siltstones, hornblende, quartz, etc.) with admixtures of different-grained sands and clays. The ratio of pebbles to sand in pebble layers varies widely. The exposed thickness of the pebble reaches 2 meters. According to literature data, the total thickness of pebbles is 8–10 meters [1].

2. Gray, quartz, fine-grained, and clayey sands lie on the roof of pebble layers. The sands are not widespread and occur in the form of individual lenses of various configurations and sizes. The thickness of the sands varies from a complete outcrop to 5×50 meters. The quality of sand is also not constant, as are the conditions of its occurrence. The particle size distribution of sands and the content of clay particles in them vary widely. Without clearly defined boundaries, clayey sands turn into sandy slugs [1].

3. Gray clays with a bluish or brownish shade, sandy, in many places with inclusions of sandstone fragments lie along the roof of sands, sometimes replacing them in extent. They contain plant remains and peat layers. And they are not widespread, occurring as lenses of various configurations and sizes. The largest lenses are found in the western and central parts of the southern region. The thickness of the clays varies mainly within 1–3 meters, reaching up to 7.3 meters in some wells (well 39) [1].

4. Dense, moderately and moderately plastic clays lie on top of bluish-gray clays or sands. The color of the rocks is uneven: spotted brown, yellowish brown, and yellowish gray. There are no regularities in the mineral's color changes [1].

The clays occurrence in the form of a layer with a thickness ranging from 0.0 to 6.5 m. Their bottom elevations range from 280.7 to 286.0 meters [1].

The roof of the minerals basically follows modern relief. Its elevations range from 282.8 to 288.2 m [1].

5. Yellowish-brown, dense, moderately plastic loams occur on the clay cover in the form of separate, small lenses. Contact between loams and underlying clays is gradual. The thickness of loams does not exceed 2.7 m [1].

6. There is a soil layer on top of loam and clay. The thickness of the soil layer in a large part of the study area is so insignificant that during plowing, mineral resources or loam are pulled to the surface. In the rest of the area, the thickness of the soil-plant layer does not exceed 40 cm [1].

To conduct research on the geological conditions of the formation and properties of expanded clay, it will be necessary to use a variety of materials and a strict methodology. Here are some steps and materials:

1. Literature Review: To provide a thorough review of the existing literature on expanded clay, including geologic form, properties, and applications. This will help identify research gaps and formulate research questions.

2. Fieldwork: Introduce fieldwork to collect expanded clay samples from various geological formations. The samples should be representative of different geological formations that contain expanded clays.

3. Laboratory analysis: Introduce laboratory analysis of samples to determine their physical and chemical properties. This may include tests such as grain size analysis, X-ray diffraction, scanning electron microscopy, and thermogravimetric analysis.

4. Data Analysis: Use statistical analysis to analyze data collected during laboratory tests. This will help to develop regularities and connections between the properties of expanded mineral resources and their geological formations.

During the exploration work, loams and clays of the Quaternary age were considered mineral resources. Tests were carried out in accordance with the requirements of the technical specifications for raw materials.

The clays within the reserve estimates occur in the form of a layer with a thickness of 0.00 m to 7.0 m and an average thickness of 3.3 m. Above, clay is replaced by loams, which do not differ in quality from mineral resources.

The particle size distribution of the clays determines the mineralogical composition; thermographic and X-ray diffraction studies and microscopic descriptions of siltstone fractions were performed at the laboratories. The microscopic examination of siltstone fractions (over 0.075 mm) revealed a high content of quartz (70–80%), iron oxides, magnetite, granite, and single grains of gluconate, which was determined by the Rutkovskiy method with the separation of clayey, dusty, and sandy fractions.

The particle size distribution of clays: the content of clays fractions ranges from 26.0 to 56.7%, dusty fractions from 31.3 to 63.9%, and sandy fractions from 6.0 to 12.0%.

The plasticity of clays varies widely, from 8.0 to 17.3.

Table 1. Mineralogical composition of the expanded clays from the Voyutytske deposit

| Fluctuations and the average composition | Composition of the components | | | | | | | | | | | | |
|---|---|---|---|---|---|---|---|---|---|---|---|---|---|
| | $SIO_2$ | $Al_2O_3$ | $Fe_2O_3$ | $TIO_2$ | MnO | CaO | MgO | $K_2O$ | $Na_2O$ | $SO_3$ | $H_2O$ | dust | from the original |
| From | 55,0 | 8,20 | 2,68 | 0,40 | | 0,84 | 0,65 | 1,50 | 0,60 | 0,06 | 1,17 | 2,50 | 0,23 |
| To | 81,0 | 15,54 | 6,94 | 0,85 | 0,21 | 3,37 | 2,26 | 2,32 | 1,23 | 0,30 | 3,32 | 8,43 | 1,78 |
| Average | 68,8 | 11,1 | 4,45 | 0,68 | 0,11 | 1,62 | 1,42 | 1,92 | 0,89 | 0,18 | 3,04 | 4,92 | |

Table 2. Physical and mechanical properties of the expanded clays from the Voyutytske deposit

| Sample ID | Density (kg/m³) | Porosity (%) | Compressive strength (MPa) | Water absorption |
|---|---|---|---|---|
| 1 | 640 | 49.3 | 3.1 | 23.6 |
| 2 | 645 | 48.9 | 3.6 | 21.5 |
| 3 | 650 | 48.6 | 4.2 | 20.1 |
| 4 | 636 | 49.5 | 2.8 | 25.1 |
| 5 | 655 | 48.3 | 3.8 | 19.8 |

As a result of the research, the following results were obtained:

1. It was established that expanded clays have high mechanical properties and chemical stability, which makes them promise for use in building materials.

2. It was found that the influence of expanded clays on the post-war state of building materials depends on their chemical and physical-mechanical composition, as well as on their interaction with other components of building materials.

The laboratory's conclusion on the quality of the raw materials was confirmed by semi-factory tests. The clays and loams in the area of the reserve's estimation are suitable for expanded clays gravel production.

Thus, this study investigated the geological conditions of formation and properties of expanded clays from the mineral deposit and their potential for use in the building materials industry. Mineralogical analysis showed that the predominant clays present in the samples were kaolinite and ilmenite. The physical and mechanical properties of the samples were also determined, including their density, porosity, compressive strength, and water absorption.

In conclusion, the geological conditions of formation and properties of clays are critical in determining their suitability for use in the construction industry. The unique properties of mineral resources, including their lightweight, high-strength, and insulation properties, make them a promising alternative to traditional aggregates. The substitution of traditional aggregates with clays can also reduce the use of non-renewable resources and decrease the carbon footprint of the construction industry. Further research and development of mineral resources and their applications in the building materials industry are necessary to fully explore their potential and contribute to sustainable development.

**References**

1. “Project for the development and reclamation of Site No. 1 of the Voyutytske deposit expanded clays”.

DOI: https://doi.org/10.30836/igs.iies.2024.1

**Santana-Martí L.A.[1], Rey-Villiers N.[1], Ortiz-Hernández M.C.[2], Sánchez A.[1]**

*(1) Instituto Politécnico Nacional, Centro interdisciplinario de Ciencias Marinas, Avenida IPN, S/N Colonia Playa Palo de Santa Rita, CP 23096, La Paz, Baja California Sur, México.*
*E-mail: isantanam2300@alumno.ipn.mx, nestorrvilliers@gmail.com, alsanchezg@ipn.mx*
*(2) El Colegio de la Frontera Sur, Unidad Chetumal, Chetumal, Quintana Roo, México.*
*E-mail: macortizh@gmail.com*

# EFFECTS OF THE MASSIVE INFLUX OF PELAGIC SARGASUM IN CARBONATED SEDIMENTS FROM MEXICAN CARIBBEAN

The beaches of the Mexican Caribbean are composed of carbonate sediments of biogenic origin. According to previous studies, the textural characteristics of these sediments correspond to medium-sized, moderately selected sands, mesokurtic kurtosis towards the north and more leptokurtic towards the south and asymmetry towards coarse sands. The sediments are mainly composed of pellets, foraminifera, mollusks and calcareous algae. Meanwhile, its mineralogy corresponds to aragonite (61.4%), calcite (37.1%) and 1.5% to terrigenous [1, 2].

Sargassum is a brown macroalgae of the genus *Sargassum* of the holopelagic type. This means that it spends its entire life floating in the sea. Since the summer of 2014, the beaches of the Mexican Caribbean have been affected by the massive influx of *pelagic sargassum* [3, 4, 5]. From a geoecological point of view, this massive influx can alter the sedimentological, mineralogical and geochemical characteristics of carbonate sediments. Sargassum leachates cause a reduction in pH, due to sulfidation conditions [4], making carbonate sediments to dissolve, especially in the finer fractions, which does not occur in medium- and coarse-grained sediments. Another important aspect to consider of sargassum is its function as a sediment exporter from the communities of calcareous that colonize this macroalgae. [6]. Species such as serpulid worms (polychaetes) and red algae (Rhodophyta) are common. However, bryozoans are the most abundant and can cover a third or more of the surface of this macroalgae, which suggests that sargassum provides an important pelagic source of magnesian calcite [7].

This research aims to analyze the influence of massive arrivals of pelagic *Sargassum* on the sands of the Mexican Caribbean, particularly in Puerto Morelos (Figure 1), and determine the impact of this macroalgae on sediments.

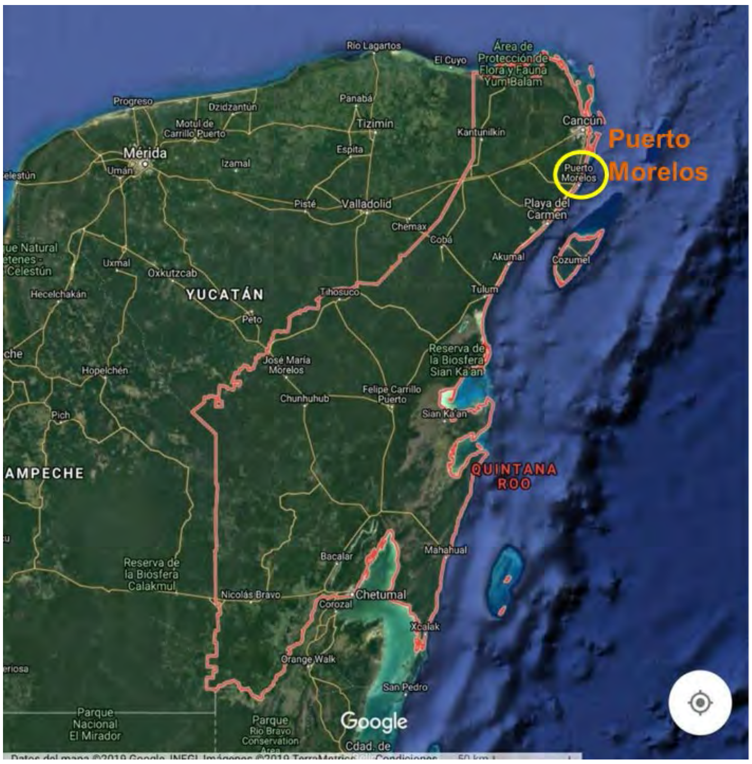


Fig. 1. Location of the study area. In the circle Puerto Morelos, Quintana Roo, México

There is a total of 30 sediment samples, collected between 2015 and 2022, in the months of February/March, April/May, June/July and October/November. Of them, 4 samples correspond to the year 2015, 6 to 2016, 2 to the year 2017 and 18 samples to 2022. On Puerto Morelos beach, surface sediment sampling was carried out biweekly for the period from April to October 2022.

Textural parameters were determined on a laser particle analyzer (LS 13 320). An X-ray diffraction (XRD) analysis was performed on the 18 samples corresponding to 2016 and 2022 in Puerto Morelos, to determine the mineralogy of the sediments and to know if any variation of the composition of the same has occurred over time, based on the fact that there is a prior knowledge of the mineralogical composition of the sites under study.

The results of the analysis of the textural parameters obtained to date seem to indicate that the effect of sargassum leachates has not affected the average grain size of the carbonate sediments of Puerto Morelos. Which have a granulometry with a medium grain size, with an average of 327 µm, with some small variations that have occurred over the years (1982 – 2022). However, in the period (2017 – 2022) there has been a trend towards a decrease in grain size, from 583 µm in 2017 to 381 µm in 2022, in Puerto Morelos. This decrease in average grain size coincides with the periods of highest influx of pelagic sargassum to these coasts. This suggests a decrease in grain size due to mechanical breakage due to the method of cleaning and transporting the sargassum on the beach and/or the action of the sargassum leachate on the calcareous sediment. The X-ray diffraction (XRD) analysis showed a tendency to modification in the mineralogical composition of the carbonate sediments of Puerto Morelos, taking into account previous studies and from calcareous epiphytic species exported by sargassum such as bryozoans, which are a pelagic source of magnesian calcite, being able to cover a third or more of the surface of this macroalgae and are incorporated into the existing sediment, adding up to a considerable percent of the total carbonate sediment. Such is the case of the year 2022 where there is an increase in the percentage of magnesian calcite compared to previous years to the detriment of the percentage of aragonite. The decrease in the average grain size and the mineralogical modification occurred in the period of highest mass influx of Sargassum. This indicates a real impact of the pelagic sargassum arrivals on the carbonate sediments of Puerto Morelos.

**References**

1. Carranza-Edwards A., Márquez-García A.Z., Tapia-Gonzalez C.I., Rosales-Hoz L. & Alatorre-Mendieta M.A., “Morphological and sedimentological changes on beaches in the southern Gulf of Mexico and the northwest Caribbean”, BULLETIN OF THE MEXICAN GEOLOGICAL SOCIETY, Vol. 67, No. 1, 2015, pp. 21-43.

2. González M.I., “Regional sedimentological study of beaches of Quintana Roo, Mexico; textural and compositional parameters of surface sands”, Master's Thesis, UNAM, Mexico City, Mexico, 2017.

3. Rodríguez-Martínez R.E., van Tussenbroek B. & Jordán-Dahlgren E. “Massive influx of pelagic sargassum to the Mexican Caribbean coast (2014-2015)”, In book: Harmful algal blooms in Mexico, Edition: 1, Chapter 5, Editorial: CICESE, Editors: García-Mendoza E., Quijano- Scheggia S.I., Olivos-Ortiz A., Núñez-Vázquez E.J., 2016.

4. Van Tussenbroek B., Hernández-Arana H.A., Rodríguez-Martínez R.E., Espinoza-Avalos J., Canizales - Flores H.M., González-Godoy C.E., Barba-Santos M.G., Vega-Zepeda A. & Collado-Vides L., “Severe impacts of brown tides caused by Sargassum spp. on near -shore Caribbean seagrass communities”, Marine Pollution Bulletin 122 (2017) 272-281.

5. Chávez V., Uribe-Martínez A., Cuevas E., Rodríguez-Martínez R.E., van Tussenbroek B., Francisco V., Estévez M., Celis L.B., Monroy-Velázquez L.V., Leal-Bautista R., Álvarez-Filip L., García-Sánchez M., Masia L. & Silva R., “Massive Influx of Pelagic *Sargassum* spp. on the Coasts of the Mexican Caribbean 2014–2020: Challenges and Opportunities”, Water, 2020, 12, 2908; DOI: https://doi.org/10.3390/w12102908.

6. Salter M.A., Rodríguez-Martínez R.E., Álvarez-Filip L., Jordán-Dahlgren E. & Perry C.T., “Pelagic Sargassum as an emerging vector of high-rate carbonate sediment import to tropical Atlantic coastlines”, Global and Planetary Change, Vol. 195, 2020, 103332.

7. Fabry V.J. & Deuser W.G., “Aragonite and magnesian calcite fluxes to the deep Sargasso Sea”, Deep-Sea Research. Vol.38, No. 6, 1991, pp. 713-728.

DOI: https://doi.org/10.30836/igs.iies.2024.42

**Merezhko M., Kuzmanenko H., Okholina T.**

*Institute of Geological Sciences of the National Academy of Sciences of Ukraine, Kyiv, Ukraine.*
*E-mail: geoinsgeo@gmail.com, geology7@ukr.net, svilya@ukr.net*

# CRITICAL MINERALS IN THE ALLUVIAL DEPOSITS OF THE TROSTYANYTSYA PLACER DEPOSIT OF ILMENITE

Mineral raw materials that have a specific application in industry (including high-tech and strategic industries) and for which there is no substitute at the current level of technological development, and whose supply is dominated by one or more producers, belong to the critical category. These minerals are economically important, and the stability of their supply is characterized by a high degree of risk [4].

The list of critical mineral raw materials differs not only for regions and countries of the world, but also changes over time for the same region due to the importance of mineral raw materials and the ways of their supply [1].

The State Geology and Subsoil Service of Ukraine analyzed minerals perspective of significance for national economic security and consumption trends in the world and selected 20 critical minerals, the confirmed reserves of which allow increasing their production in Ukraine [6]. These raw materials are divided into two groups: "Raw materials for import substitution" and "raw materials for innovative industries". The first group includes: natural gas and oil, uranium, coking coal, lead, zinc, gold, flux limestone, fluorite, potassium salts. The second group includes: titanium, zirconium, lithium, nickel, cobalt, beryllium, rare earths, tantalum, niobium, graphite.

According to the calculations of Ukrainian scientists, about 20% of reserves and resources of titanium minerals are concentrated within the Ukrainian placer subprovince, which includes 13 titanium-bearing regions [3].

The Volyn titanium-bearing region is one of the first places in terms of reserves. Ilmenite deposits are located not far from each other and represent a single group spatially connected with a series of main rocks of the Korosten intrusive complex. All deposits are essentially ilmenitic, with appreciable amounts of apatite (eluviall) and zircon (Irshynskyi placer) [5]. In some deposits, scandium and vanadium are present in ilmenite, and hafnium in zirconium. One of these deposits is Trostyanytsya, which was discovered during geological surveying in 1964-1970.

From a geological and structural point of view, the Trostyanytsya deposit is confined to the northern part of the Volodarsk-Volynskyi massif of the main rocks of the Korosten pluton [2], in the northwest it borders the Middle area of the Mezhyrichny placer ilmenite deposit, in the northeast it borders the Bukinsky deposit.

The main rocks of the Lower Proterozoic and the products of their physical and chemical weathering, as well as loose sedimentary formations of the Mesozoic-Cenozoic age, take part in the geological structure of the Trostyanytsya deposit.

The alluvial deposit fills a valley-like depression of a complex configuration, stretched in the northeast direction for a distance of up to 5 km, with a width of 2.5 km. The thickness of the productive deposits varies widely, on the sides of the subsidence it is 2-4 m, in the center it reaches 20 m. The bed of alluvial placer is the weathered kaolin crust, which is the source of the accumulation of ilmenite, which after the destruction of the crust is eroded into the placer.

Alluvial deposits make up 50% of the ore-bearing layer of the deposit and are represented by Middle Jurassic-Lower Cretaceous sands – 3%, secondary kaolins – 25%, Paleogene-Neogene sands – 4%, secondary kaolins – 5%, Lower Quaternary sands – 13%.

The main ore mineral of sedimentary deposits is ilmenite, the content of which ranges from 5-10 to 400 kg/$m^3$, sometimes up to 523 kg/$m^3$. High concentrations of ilmenite are characteristic of secondary kaolins. without the main ore component in the deposit, the following are present (kg/$m^3$): zircon – 0,44; rutile – 0,09; apatite – 0,2; magnetite – up to 0,03; in significant quantities - monazite, disten, titanomagnetite, as well as some components strategically important for the economy of our country.

Ilmenite from the alluvial deposits of the Trostyanytsya deposit in the form of isomorphic impurities contains elevated concentrations of vanadium and scandium ($V_2O_5$ – 0.265%, and $Sc_2O_5$ – 95.5 g/t). Vanadium can be extracted at existing titanium-magnesium enterprises during the metallurgical process.

Comprehensive development of this deposit will simultaneously solve several important issues for the sustainable development of the state, namely: it will continue the activity of Mezhyrichny GZK, it will bring a significant profit to the economy of the district, and it will partly provide critical raw materials for the necessary branches of industry. The deposit is promising, but requires detailed research using modern methods.

**References**

1. Baryatska N.V. The concept of critical mineral raw materials is a tool for stimulating the development of subsoil use in Ukraine. Mineral resources of Ukraine, 2020. No. 2. P. 13-18.
2 Bazaliyska L.M. Report on geological exploration works: Exploration of the Trostyanytsya ilmenite deposit. Book 1. Kyiv, 2008. "Geoinform of Ukraine".
3. Galetskyi L.S., Remezova O.O. International conference "Ti 2007 in the CIS". Geologist of Ukraine, 2007. No. 1. P. 3-5.
4. Shekhunova S.B. Critical and strategic mineral raw materials for the economic security and post-war development of Ukraine. Bulletin of the National Academy of Sciences of Ukraine, 2023. No. 25. P. 25-30.
5. Shvaiberov S.K. and others. Report on the results of prospecting and evaluation work on the Stavyshche, Trostyanytsya, and Ocheretyanka ilmenite placers, 1991. “Geoinform Ukraine”.
6. Strategic Minerals: Development Roadmap for Ukraine. [Electronic resource]. – Mode access: https://www.geo.gov.ua/wp-content/uploads/presentations/ukr/analiz-rozvytku-haluzey-krytychnykh-korysnykh-kopalyn.pdf

DOI: https://doi.org/10.30836/igs.iies.2024.43

**Quintana J., Gibson C.**

*Prismo Metals Inc, Suite 1100 - 1111 Melville St., Vancouver V6E 3V6, Canada.*
*E-mail: jquintana1208@gmail.com*

# GEOLOGY AND RESOURCE POTENCIAL OF THE PALOS VERDES PROJECT, MEXICO

The Palos Verdes Property location in Sinaloa State, northwestern Mexico in the Panuco Copala district, approximately 65 kilometers NE of Mazatlán, Sinaloa, in the Municipality of Concordia and comprises the Palos Verdes concession that covers 22.7707 hectares, as shown in Figure 1.

In the concession, veins with two main trends have been mapped: veins with a NW trend and others with a NE trend. The northeast system is the main trend of mineralized structures that occur as veins, stockwork and hydrothermal breccias that are structurally controlled by fractures and faults. Within this northeast system is the Palos Verdes vein with an orientation of N60ºE and a dip of 70 to 80º towards the southeast, hosted in andesitic volcanic rocks with a possible displacement through a shear zone with a NW-SE trend, it has a thickness variable from 0.2 to 5m and in parts up to 10 meters, composed of quartz and hydrothermal breccia with moderate to strong silicification, crustiform texture and various stages of mineralization. The economic minerals that the Palos Verdes vein presents are: silver galena, sphalerite, chalcopyrite, pyrite and gold.

The concession largely presents propylitic alteration with chlorite-epidote-pyrite on the volcanic rocks. In the fault and shear zones there is presence of argillic and intermediate argillic alteration with illite-smectite-kaolinite.

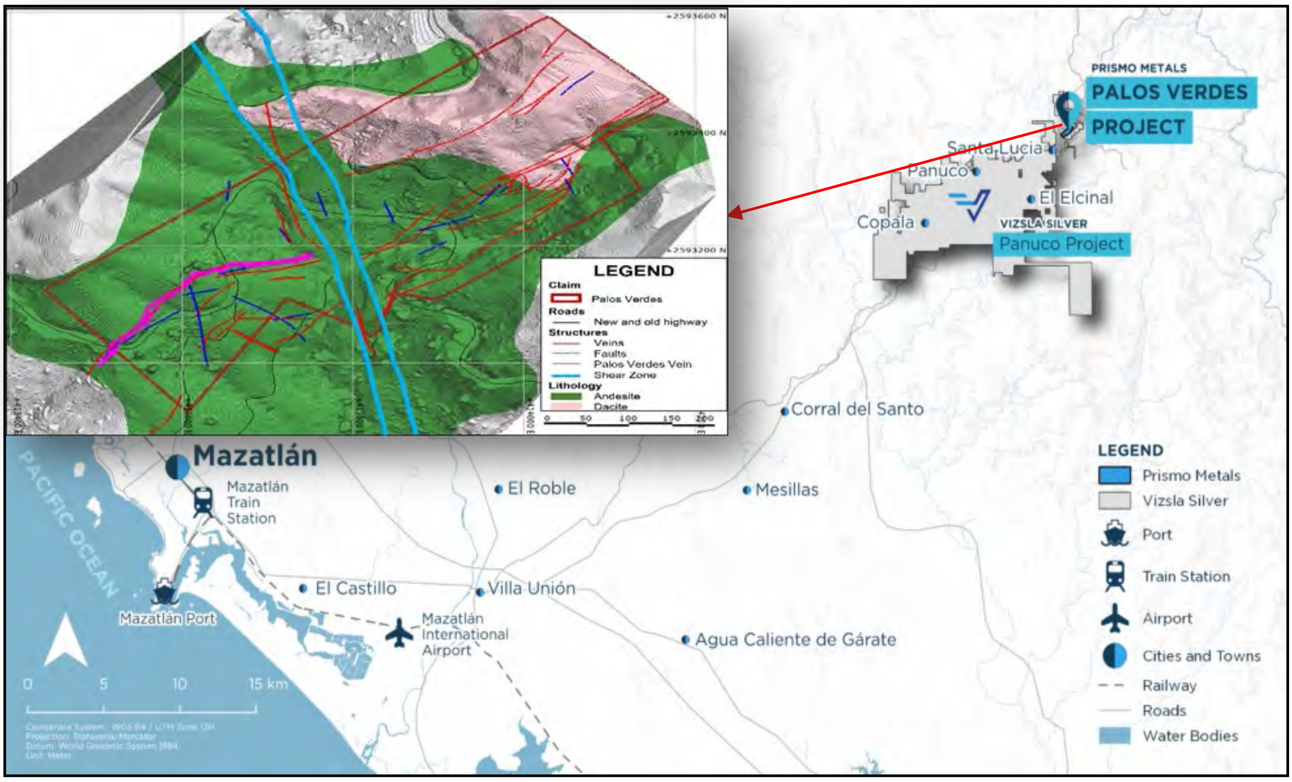


Fig. 1. The Palos Verdes Property is located in west central Sinaloa, about 50 km northeast of Mazatlán

33 drillings were carried out within the concession to delimit the Palos Verdes vein and other possible structures, which were analyzed with the fire assay and ICP14B methods, obtaining high values of Ag, Au, Zn and Pb, for which the equivalent silver value of each hole intercepted with the Palos Verdes vein. The results show good potential in the Panuco district as shown in Table 1.

Table 1. Silver equivalent grades of the holes intercepted with the Palos Verdes vein

| Hole | From (m) | To (m) | Width (m) | Ag eq (g/t) |
|---|---|---|---|---|
| PV-18-01 | 23.90 | 28.80 | 4.90 | 227.43 |
| PV-18-02 | 40.35 | 49.70 | 9.35 | 735.19 |
| PV-18-03 | 31.30 | 40.65 | 9.35 | 182.51 |
| PV-18-04 | 55.45 | 58.00 | 2.55 | 98.50 |
| PV-18-05 | 54.25 | 57.40 | 3.15 | 80.39 |
| PV-20-06 | 73.95 | 75.85 | 1.90 | 221.86 |
| PV-20-08 | 92.70 | 96.05 | 3.35 | 67.79 |
| PV-20-09 | 87.10 | 88.95 | 1.85 | 284.46 |
| PV-20-10 | 125.30 | 126.50 | 1.20 | 77.41 |
| PV-22-12 | 126.00 | 127.85 | 1.85 | 80.73 |
| PV-22-13 | 132.70 | 133.70 | 1.00 | 80.34 |
| PV-22-14 | 193.00 | 195.90 | 2.90 | 100.98 |
| PV-22-15 | 263.50 | 272.50 | 9.00 | 195.18 |
| PV-22-17 | 47.6 | 52.55 | 4.95 | 138.50 |
| PV-23-24 | 150.22 | 152.5 | 2.28 | 438.12 |
| PV-23-29 | 122.90 | 123.50 | 0.60 | 121.90 |
| PV-23-30 | 141.40 | 143.50 | 2.10 | 38.59 |
| PV-23-31 | 217.85 | 218.20 | 0.35 | 61.01 |
| PV-23-32 | 150.10 | 155.65 | 5.55 | 103.76 |
| PV-23-33 | 225.65 | 226.40 | 0.75 | 253.40 |

Silver equivalent values are calculated using the following metals prices: Au, US$1.750/oz, Ag, $21.24/oz, Pb, $0.97/lb and Zn, $1.34/lb.

The Palos Verdes vein was interpreted and represented in 3D as shown in Figure 2.

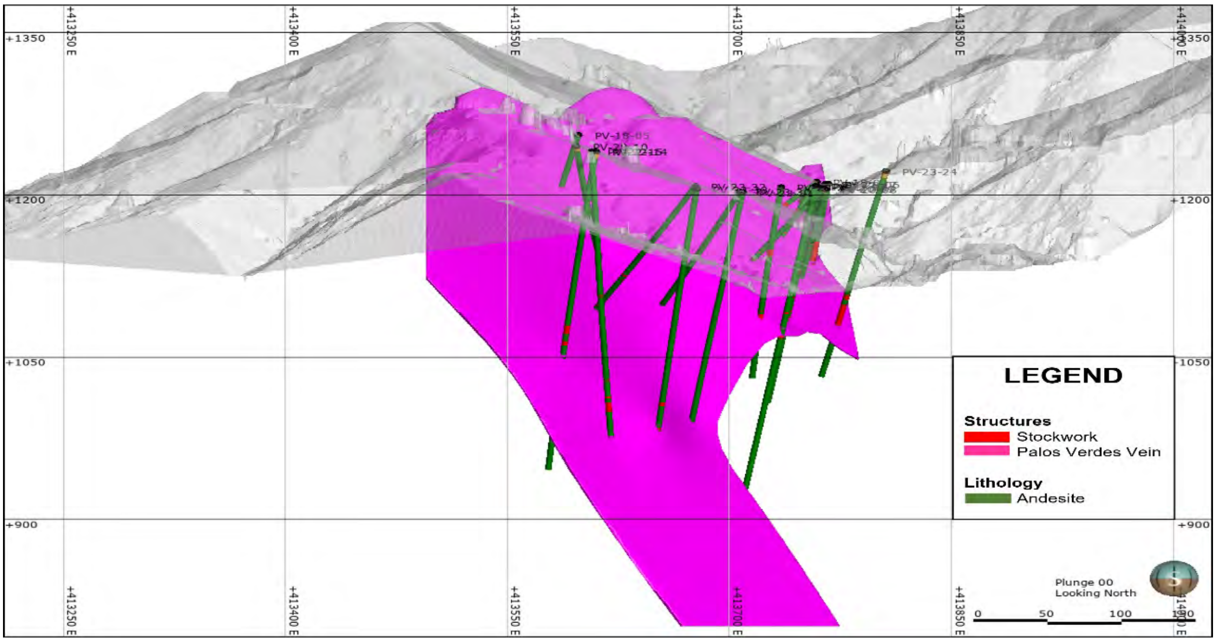


Fig. 2. North looking section, intersections of the drill hole with the Palos Verdes vein

## References


1. Prismo Metals Inc. [Electronic resource]. – Access mode: https://prismometals.com/project/the-palos-verdes-property.

DOI: https://doi.org/10.30836/igs.iies.2024.14

**Adizua O.F., Eke C.O.**

*Geophysics Research Group – GRG, Department of Physics, Faculty of Science, University of Port Harcourt, Port Harcourt, Rivers State, Nigeria. E-mail: okechukwu.adizua@uniport.edu.ng, ekeconfidence@gmail.com*

# APPLICATION OF SIGNAL ENVELOPE AND ITS DERIVATIVES TO ENHANCE RESERVOIR CHARACTERIZATION OF "X" FIELD IN THE NIGER DELTA BASIN

When analyzing traditional seismic data, seismic attributes could be a helpful tool for identifying hidden structures and features [1, 2, 3, 4, 9]. Our study focused on using the signal envelope and its derivatives to uncover and illuminate hidden features and structures in a post-stack depth migrated seismic volume in order to support the reservoir characterization objectives of the Niger Delta Basin's "X" field. The work's objective was to investigate how the envelope attributes and its derivatives can improve or illuminate seismic data as proposed by the works of [5, 6, 7, 8, 10], for the purpose of identifying bright spots, gas accumulations, sequence boundaries, significant lithologic changes, and porous media as this will foster and increase the field's overall goals for reservoir characterization. Well logs, 3D post-stack depth migrated seismic data, and time-depth relationship surveys obtained from the field were among the data requirements employed in the study's execution. The data was processed and visualized using the Schlumberger Petrel and Opendtech tools. The resistivity logs were utilized to identify the presence of hydrocarbons, while the gamma ray log helped to determine the lithology. The well logs were given a time function using the time-depth relationship function, allowing events found in the logs to be displayed on the seismic data. In order to create time-slices, the envelope attribute and its derivatives were created from the initial seismic volume and conditioned into time gates. Following the application of the signal envelope and its derivatives, the rock and fluid properties on the seismically enhanced volume were then interpreted. It was found that the envelope attribute was useful in identifying bright spots, gas accumulations, sequence boundaries, significant lithologic changes, and porosity. The first derivative of the envelope did not work as well as the envelope. While they performed rather well in spotting bright spots on inlines, they were unable to distinguish them along the time slices. They performed poorly when it came to identifying porous material, significant lithologic changes, and sequence boundaries. When it came to highlighting bright spots, gas accumulations, sequence boundaries, significant lithologic changes, and porous medium, the second derivative of the envelope performed just as poorly. This study has therefore successfully shown the effectiveness of the envelope attributes for the detection of bright spots, gas accumulations, sequence boundaries, major lithologic changes and has also shown its robustness in identifying porous media within the X field. The inherent limitations of the envelope derivatives have also been established. In conclusion, we have successfully demonstrated and shown that the envelope attribute works better than its derivatives (the first and second derivatives) when deployed for illuminating bright spots and associated structures and can be successfully utilized as an important tool at an early stage for a reservoir characterization project.

**References**

1. Brown, A. (2001). Understanding seismic attributes. GEOPHYSICS 66(1), 47-48. DOI: https://doi.org/10.1190/1.1444919.
2. Chopra, S. and Marfurt, K.J. (2005). Seismic attributes for prospect identification and reservoir characterization. SEG Geophysical Development Series No. 11, 464p.
3. Chopra, S. and Marfurt, K.J. (2008). Emerging and future trends in seismic attributes. The Leading Edge 27(3), 298-318. DOI: https://doi.org/10.1190/1.2896620.
4. Coren, F., Volpi, V. and Tinivella, U. (2001). Gas hydrate physical properties imaging by multi-attribute analysis – Blake Ridge BSR case study. Marine Geology 178(1), 197-210.
5. Koson, S., Chenrai, P. and Choowong, M. (2014). Seismic attributes and their applications in seismic geomorphology. Bulletin of Earth Science of Thailand, 6(1), 1-9.
6. Radovich, B.J. and Oliveros, R.B. (1998). 3D sequence interpretation of seismic instantaneous attributes from the Gorgon Field. The Leading Edge, v17, 1286-1293.
7. Sarhan, M.A. and Safa, M.G. (2017). Application of seismic attributes for detecting different geologic features within Kafr El Sheikh Formation, Temsah Concession, Nile Delta Basin. Scientific journal for Damietta Faculty of science. 7(1), 26-34.
8. Subrahmanyam, D. and Rao, P.H. (2008). Seismic attributes - a review. Hyderabad International Conference and Exposition on Petroleum Geology. 398-403.
9. Taner, M.T. (2001). Seismic attributes, CSEG Recorder 26, September 2001, p.48-56.

10. Tounkara, F., Ehsan, M., Nasar Iqbal M., Al-Ansari, N., Hajana, M.I., Shafi, A. and Elbeltagi, A. (2023). Analyzing the seismic attributes, structura and petrophysical analysis of the lower Goru Formation: A case study from Middle Indus Basin Pakistan. Front Earth Sci. 10: 1034874. DOI: https://doi.org/10.3389/feart.2022.1034874.

DOI: https://doi.org/10.30836/igs.iies.2024.2

**Giunti S., Bojanowski M.J.**

*Institute of Geological Sciences – Polish Academy of Sciences, Ul. Twarda 51/55, 00-818, Warsaw, Poland.*
*E-mail: s.giunti@twarda.pan.pl*

# HYDROCARBON-DERIVED THROMBOLITES FROM THE OUTER CARPATHIANS (POLAND)

Shallow marine thrombolites from a newly discovered Lower Cretaceous cold seep in the Outer Carpathians (Poland) were analysed in order to untangle the complex sedimentological and biogeochemical processes involved in their formation and their diagenetic modifications. The studied thrombolites are made of two components, (i) microcrystalline mesoclots and (ii) fine spar-filled framework cavities. These components are dominated by calcite and show a complex spatial relationship, resulting in a heterogeneous, clotted fabric. The mesoclots exhibit digitate structures, often concentrically-laminated, and are composed of fine spar-cemented micrite with $\delta^{13}C$ values from -34.8 to -19.4‰ PDB. Biomarkers characteristic of anaerobic methanogenic archaebacteria were detected within the mesoclots. The mesoclots host <5 mm-wide microtubes filled with isopachous calcite recording even lower $\delta^{13}C$ values of (from -39.0 to -20.5‰ PDB). The morphology of the mesoclots relative to their internal lamination and their geochemistry indicate that their growth was dependent on anaerobic oxidation of methane (AOM), while the microtubes acted as conduits for hydrocarbon-charged fluids. The framework cavities are internally lined with framboidal pyrite, and are cemented by fine spar with relatively high $\delta^{13}C$ of (-15.1 to -7.3‰ PDB) and low $\delta^{18}O$ values (-9.3 to -4.4‰ PDB). Carbonate precipitation within the framework cavities is interpreted to be related to bacterial sulphate reduction. U-shaped trace fossils attributed to the ichnogenus Balanoglossites cross-cut both mesoclots and framework cavities. The mechanisms involved in the formation and diagenesis of thrombolites at cold seeps are yet to be fully understood, and this work provides new insights on these complex biogeochemical and sedimentological processes.

*This work was supported by Polish National Science Centre grant no. 2020/37/B/ST10/01769.*

DOI: https://doi.org/10.30836/igs.iies.2024.39

**Hadiatskyi O.**

*Institute of Geological Sciences of the National Academy of Sciences of Ukraine, Kyiv, Ukraine.*
*E-mail: oleg.gadiatskyi@gmail.com*

# TOMOSTATICS SOLUTION IN THE REGION WITH COMPLEX SURFACE AND GEOLOGICAL ENVIRONMENTS

The statics problem is a vital sense of our work in seismic data processing. Why is this important? Because their function is a major to minimize artifacts in the definition of geological structures. The ability to accurately near-surface velocity modeling and statics solution is a necessity in seismic processing for future petroleum exploration.

Several examples, including models of generalized linear inversion (GLI) and tomography methods of statics corrections calculation, are discussed. Tomostatics solution was analyzed in this research (example of 3D seismic survey, North Africa), whose territory has difficult surface environments, topography (elevation varies from 190 m to 305 m) and geology as 65% sand-dunes and 35% gravel plain, also with varying velocity in the near-surface.

The geology of the near-surface consists of sand, clay, sandstone (weathered rocks), and limestone (bedding hard rock). Near-surface statics are always a significant concern, primarily since the existing surface conditions during acquisition influence the accuracy of the resulting time structure. In this case, the first arrivals produced from the vibroseis source were of reasonable quality and provided reliable first arrival pick times. First breaks were picked and then used for first-arrival traveltime tomography.

The statics calculation problem, whether short wavelength, long wavelength, or residual has always been one of the more time-consuming and problematic steps in seismic data processing. Although the sand dunes produced a severe statics issue, this was relatively easy to remove through simple refraction statics methods on the first arrivals of the field shot records, which solved the short (< 500 m) and medium (200 m - 3000 m) wavelength statics. The longer period statics (> 3000 m) were harder to quantify and quality control.

Refraction tomography methods and generalized linear inversion GLI (based on a 2-layer velocity model) are not always the control of the long-wave anomaly. This article will demonstrate the techniques of accurate control (Figure 1, c) of the long wavelength refraction statics with up-hole (UH) locations on the 3D survey. A detailed build of the near-surface velocity model is the basis of this.

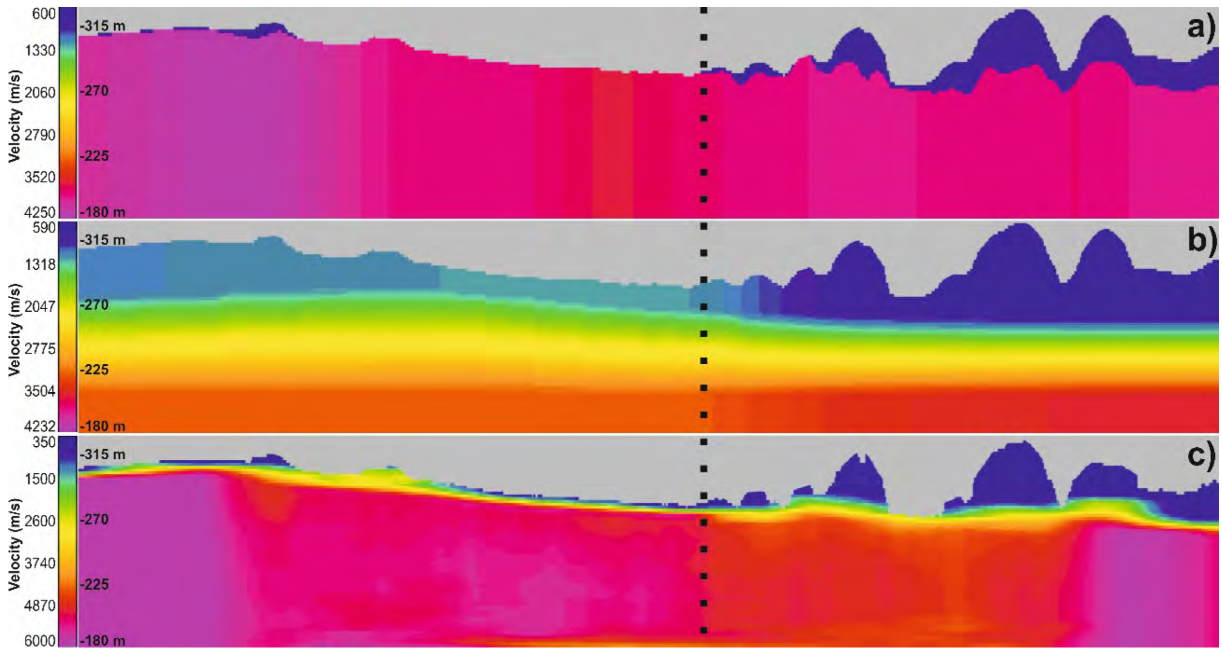


Fig. 1. Presents the results of velocity modeling using GLI a), tomography b) and tomography with accurate up-hole control c). Left - gravel plain, right - sand-dunes

This study was based on practical experiences and applies to well-established modeling techniques from up-hole and refraction statics [1]. The advantage of the tomography method with up-hole control is the construction of grids with fewer artifacts compared with classical tomography or GLI.

Synthetic modeling is fundamental for a plethora of tasks in seismic processing, most notably for comparing to observed seismic data and thus testing hypotheses [2]. It also proposed to check the practical experience of using synthetic modeling of near-surface velocity for statics corrections. In addition, it may be necessary to adapt this methodology to minimize the risks associated with exploration drilling without long-wave artifacts on the southern edge of the Dnieper-Donetsk depression. It is worth noting that this area is a perspective zone for hydrocarbon accumulation in non-anticlinal traps.

It can be concluded that a good technique for statics calculation requires accurate velocity models to be presented. Based on the 3D velocity-depth tomography model with up-hole control we have an excellent result for minimizing the near-surface confusion related to the long-wave. The best statics solution is the most important in the subsurface imaging and truth configuration of target horizons.

**References**

1. Cox, M.J.G. Static corrections for seismic reflection surveys. SEG, 1999. P. 546. DOI: https://doi.org/10.1190/1.9781560801818.

2. Krischer, L. On-demand custom broadband synthetic seismograms. Seismological Research Letters, Volume 88 (4), 2017. P. 1127-1140. DOI: https://doi.org/10.1785/0220160210.

*DOI: https://doi.org/10.30836/igs.iies.2024.12*

**Dernov V., Yefimenko V.**

*Institute of Geological Sciences of the NAS of Ukraine*, *Department of Stratigraphy and Palaeontology of the Palaeozoic Sediments, Kyiv, Ukraine. E-mail: vitalydernov@gmail.com*

# TAPHONOMIC AND PALAEOECOLOGICAL SIGNS OF DIASTEMS IN THE CARBONIFEROUS SUCCESSION OF THE DON-DNIPRO THROUGH, UKRAINE

No more than 10-25% of the Earth's history is documented in the sedimentary record, and most of this corresponds to diastems, a short interruption in deposition with little or no erosion before resumption of sedimentation [1, 3]. Stratigraphic gaps (or hiatuses, breaks) are an integral feature of any sedimentary sequence and their presence is guaranteed by the so-called Principle of the incompleteness of the stratigraphic record, i.e. the stratigraphic record in the form of rock sequences of the Earth's sedimentary cover is incomplete because a significant part of geological time in each particular section is not documented by rocks and corresponds to stratigraphic gaps [2]. Stratigraphic gaps occur in various ways: as a result of erosion in subaerial or aquatic environments, non-deposition of sediments due to hydrodynamic activity of the environment or lack of sedimentary material, and leaching of fine components [6]. Thus, formally, stratigraphic gaps can be divided into (1) syn-sedimentary and early diagenetic, (2) post-sedimentary [1, 8].

In addition to determining the correlation between the duration of sediment accumulation in the Earth's sedimentary cover and physical time, stratigraphic gaps analysis is necessary to restore the peculiarities of geotectonic processes in the geological past, to identify the mechanisms of anticline uplift formation, and to search for stratigraphic, lithological, and combined hydrocarbon traps [6, 7]. In recent decades, due to the gradual depletion of anticline hydrocarbon traps in the Dnipro-Donets Depression, more and more attention has been paid to the search for non-anticline traps, especially stratigraphic traps, the search criterion for which is often the presence of signs of stratigraphic gaps [5]. For example, ten stratigraphic gaps have been identified in the Tournaisian (Mississippian) sedimentary succession of the Hnidentsivska Uplift, to which the T1–T5 productive horizons are confined [7].

The presence of stratigraphic gaps in the Carboniferous succession of the Don-Dnipro Trough is recorded by radiometric, lithological and palaeontological (biostratigraphic, taphonomic and palaeoecological) methods. Among the taphonomic and palaeoecological signs of diastems in the Carboniferous succession of the Don-Dnipro Trough are: (1) characteristic trace fossils (e.g., bioerosions *Rogerella, Gnathichnus* and *Cyclopuncta* (Fig. 1A, D, E), burrows *Bergaueria* opened onto the erosional surface (Fig. 1J) or bioerosion traces on the hard- or rockground surfaces (e.g., see [8: Fig. 2B]); (2) microbially-induced sedimentary structures (Fig. 1I); (3) biotic communities that existed on compacted and hard substrates (e.g., skeletons of dead and living animals (Fig. 1F), rock- and hardgrounds, etc.); (4) paleosoil horizons and evidences of soil-forming processes (Fig. 1G); (5) biogenic buildups (bioherms, biostromes) and microbialites (stromatolites, thrombolites, oncolites) (Fig. 1B, H); (6) trunks and roots of arborescent lycopsids and sphenopsids preserved *in situ* (Fig. 1C), etc.

However, only biostratigraphic criteria allow us to determine the stratigraphic extent of a stratigraphic gap, i.e. to estimate the number of stratigraphic units that are missing in the sedimentary sequence as a result of erosion or non-deposition, and thus to determine the duration of the gap in absolute terms (i.e. in years). The above taphonomic and palaeoecological evidences allow us to detect the presence of diastems, but they are not sufficient to estimate the physical time that is not documented in the sedimentary sequence.

*The research was conducted within the framework of the programme “Strategic Mineral Resources for Economic Recovery of Ukraine: Analysis of Resources and Reserves, Development of Search Criteria for Increasing the Mineral Resource Base” (State Registration No. 0123U100855).*

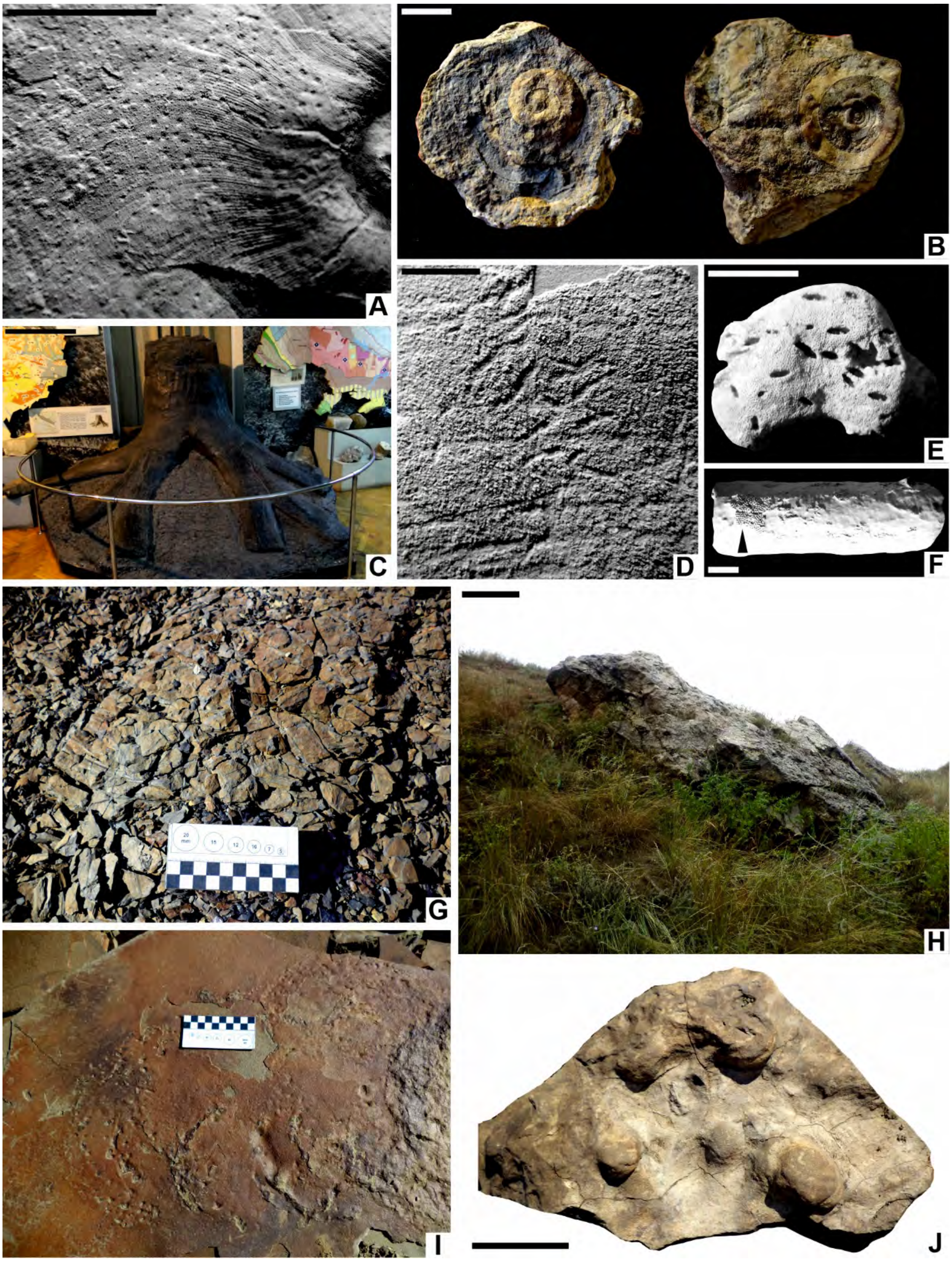


Fig. 1. Palaeoecological and taphonomic evidences for the presence of diastems in the Carboniferous of the Don-Dnipro Trough. A – bierosion trace fossils *Cyclopuncta* on the cephalopod conch (Visean, Dnipro-Donets Depression); B – oncolites with ammonoid conchs (Serpukhovian, Donets Basin); C – trunk of the arborescent lycopsid *Sigillaria* preserved *in situ* (Moscovian, Donets Basin); D – bierosion trace fossils *Gnathichnus* on the orthocerid nautiloid (Serpukhovian, Donets Basin); E – bierosion trace fossils *Rogerella* in an oncolite or limestone pebble (Moscovian, Donets Basin); F – crinoid stem with attached epibiontic bryozoan (Visean, Donets Basin); G – histosol below the $g_3$ coal bed of the Mospyne Formation (Bashkirian, Donets Basin); H – microbial limestone layer $L_7$, which lies on sandstone bed with an erosion contact (Moscovian, Donets Basin); I – microbially-induced sedimentary structure on the sandstone bedding plane (Bashkirian, Donets Basin); J – sandstone slab with sea anemone burrows *Bergaueria hemispherica* Crimes et al., 1977 (Bashkirian, Donets Basin). Scale bars = 5 mm (D), 10 mm (A, B, E, F), 0.1 m (G, I, J), 0.5 m (C, H).

**References**

1. Baraboshkin E.Yu., Weimarn A.B., Kopaevich L.F., Naydin D. P. Study of stratigraphic breaks during geological survey: Methodical recommendations. Moscow: Moscow University Press, 2002. 163 p.

2. Mesezhnikov M.S., Stepanov D.L. General stratigraphy. Principles and methods of stratigraphic studies. Leningrad: Nedra, 1979. 423 p.

3. Nalivkin D.V. 1974. Problem of stratigraphic gaps. In: Yanshin A.L. (Ed.), Etudes on stratigraphy. Moscow: Nauka, p. 10–21.

4. Ogar V.V. On the genesis of carbonate rocks of the Mokra Volnovakha Group (Lower Carboniferous of the southern Donets Basin). Collection of scientific works of the Institute of Geological Sciences of the NAS of Ukraine. 2008. Vol. 1. P. 132–139.

5. Popova T.L. Geological criteria for preserving the productivity of non-anticlinal traps in the Tournaisian–lower Visean terrigenous deposits of the Dnipro-Donets Depression. Collection of scientific works of the Institute of Geological Sciences of the NAS of Ukraine. 2009. Vol. 2. P. 47–51.

6. Staroverov V.N. Stratigraphic gaps in the Palaeozoic deposits of the SE part of the Russian Plate. Bulletin of the Voronezh University, Geology. 2013. No. 2. P. 40–45.

7. Vakarchuk G.I., Havrysh V.K. Stratigraphic breaks and unconformities in the Palaeozoic deposits of the Dnipro-Donets Depression. Geological Journal (Ukraine). 1991. No. 1. P. 119–130.

8. Zaitsev A.V., Baraboshkin E.Yu. Stratigraphic gaps in the Lower and Middle Ordovician deposits of the NW part of the Russian Plate. Bulletin of the Moscow University, Geology. 2006. No. 3. P. 17–24.

DOI: https://doi.org/10.30836/igs.iies.2024.3

**Domínguez-Samalea Y., Sánchez-González A.**

*Centro Interdisciplinario de Ciencias Marinas, Instituto Politécnico Nacional, La Paz, Mexico.*
*E-mail: ydominguezs2200@alumno.ipn.mx, alsanchezg@ipn.mx*

# OXYGENATION CHANGES IN THE MEXICAN PACIFIC BASED ON THE SEDIMENTARY RECORD OF BENTHIC FORAMINIFERA

Oxygen minimum zones (OMZ) are located below upwelling systems and are characterized by a dissolved oxygen (DO) concentration <0.5 ml $L^{-1}$ [1, 2]. Dissolved oxygen in seawater is crucial in many biogeochemical processes. The formation of the modern OMZ in the Eastern North Pacific (ENP) is primarily due to a combination of two factors: (1) the high rate of dissolved oxygen consumption by remineralization of exported organic matter and (2) limited ventilation due to a slow ocean circulation [2-5].

Over the past decades, the scientific community has put considerable effort into understanding the past dynamics of the OMZ. The importance of reconstructing OMZ reoxygenation and deoxygenation events and mechanistically explaining their climatic causes is essential in light of the ocean's current and potential future responses to modern global warming [6].

Benthic foraminifera (BF) are considered sensitive biological tracers of temporal and spatial variations in OMZ intensity [7-15], since DO and the flux of organic matter are usually the main limiting factors of the assemblages of foraminifera in these areas [17]. From the adaptation of benthic foraminiferal assemblages (BFA), the levels of qualitative dissolved oxygen concentrations have been proposed as oxic (>1.5ml $L^{-1}$), suboxic (0.5 to <1.5ml $L^{-1}$) and dysoxic (<0.5 ml $L^{-1}$) [10-18].

The study of the BFA in the Southwestern margin of Baja California Sur (SW-BCS) is extremely scarce, so it is necessary to carry out a paleoecological analysis of the community of BF. With the aim of analyzing the relative abundances of BF, estimating the concentration of DO in the OMZ and comparing the trends of OD estimation with denitrification tracers obtained by [22] of the (SW-BCS). The sediment core MAGD-MC02, collected at 680 m depth, is 1200 years old.

The study area is located in the transition zone of the ENP where the equatorial, subarctic, tropical subsurface [19] and intermediate water masses of the North Pacific converge [20]. The current system in this transitional zone is characterized by the California Current that flows towards the equatorial zone, the North Equatorial Current with a west-northwest direction and the California Countercurrent that flows towards the North Pole. The California Current transports cold, less saline, oxygenated and nutrient-rich water from the subarctic water mass, while the California Countercurrent, which transports properties of the equatorial subsurface mass, is characterized by being warm, more saline and poor in oxygen (Fig. 1).

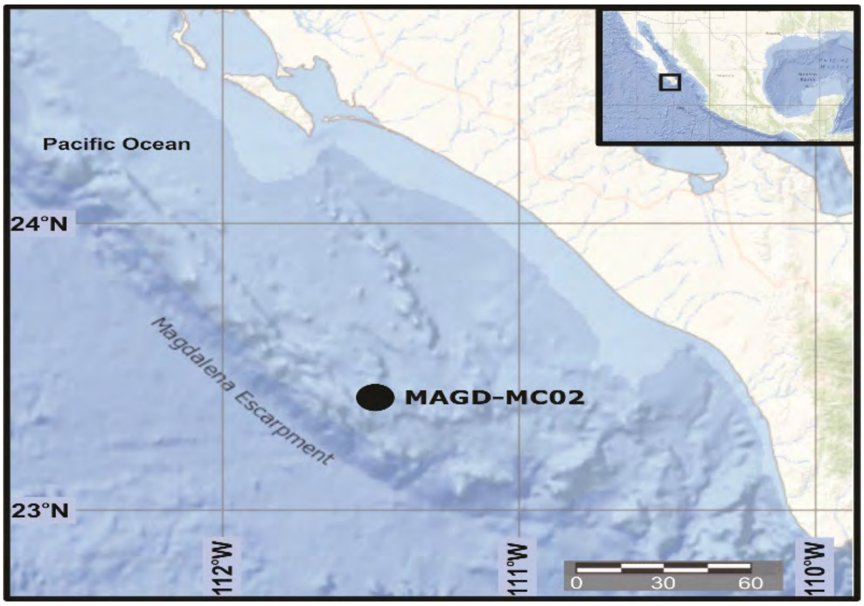


Fig. 1. Location of multicore MAGD-MC02 in SW-BCS, Mexico [21]

The correspondence analysis showed that the abundances of foraminifera are divided into two main groups (dysoxic [*B. subadvena*, *B. seminuda*, *B. exilis*] and suboxic [*B. argentea*, *U. peregrina, C. carinata, T. delicata*, *E. pseudobeyrichi*]). The concentration of DO was estimated by quantifying the percentages of dysoxic, suboxic and oxic foraminifera. In the last 1200 years CE, the OMZ has maintained dysoxic. The $\delta^{15}N$ values of the organic matter (denoted a trend opposite to what was observed for the estimation of dissolved oxygen inferred from the abundance of the group of dysoxic species. The $\delta^{15}N$ values of the organic matter suggested that the water column showed a trend towards a decrease in denitrification i.e. increased oxygenation [23] of the water column, which contrasted with the opposite trend of the estimation of dissolved oxygen during the MWP. The $\delta^{15}N$ of the sedimentary record reflects a lower use of nitrates. While, the $\delta^{15}N$ values of the organic matter had a tendency of increasing from the LIA to the recent, consistent with the dysoxic conditions inferred from the BF. This suggests that the OMZ has maintained dysoxic conditions over the past 1200 years.

**References**

1. Codispoti, L.A., Christensen, J.P. Nitrification, denitrification and nitrous oxide cycling in the eastern tropical South Pacific Ocean. Marine chemistry, 16(4), 1985, 277-300 p.
2. Gilly, W.F., Berman, J.M., Litvin, S.Y., Robison, B.H. Oceanographic and biological effects of shoaling of the oxygen minimum zone. Annual review of marine science. 5, 2013, 393-420 p.
3. Wyrtki, K. (1962). The oxygen minima in relation to ocean circulation, Deep Sea Res., 9, 11-23 p.
4. Paulmier, A., Ruiz-Pino, D. Oxygen minimum zones (OMZs) in the modern ocean, Prog. Oceanogr., 80, 2009, 113-128 p.
5. Praetorius, S.K., Mix, A.C., Walczak, M.H., Wilhowe, M.D., Addison, J.A., Prahl, F.G. North Pacific deglacial hypoxic events linked to abrupt ocean warming, Nature, 527, 2015, 362-366 p.
6. Choumiline, K., Pérez-Cruz, L., Gray, A.B., Bates, S.M., Lyons, T.W. Scenarios of deoxygenation of the eastern tropical north pacific during the past millennium as a window into the future of oxygen minimum zones. Frontiers in Earth Science, 7, 2019, 237 p.
7. Bernhard, J.M., Reimers, C.E. Benthic foraminifera population fluctuations related to anoxia: Santa Barbara Basin, Biogeochemistry, 15, 1991, 127-149 p.
8. Sen Gupta, B.K., Machain-Castillo, M.L. Benthic foraminifera in oxygen-poor habitats. Marine Micropaleontology, 20, 1993, 183 – 201 p.
9. Jorissen, F.J., Stigter, H.C.d., Widmark, J.G.V. A conceptual model explaining benthic foraminiferal microhabitats. Marine Micropaleontology, 26, 1995, 3-15 p.
10. Cannariato, K.G., Kennett, J.P. Climatically related millennial-scale fluctuations in strength of California margin oxygen-minimum zone during the past 60 k.y. Geology, 27, 1999, 975-978 p.
11. Cannariato, K.G., Kennett, J.P., Behl, R.J. Biotic response to late Quaternary rapid climate switches in Santa Barbara Basin: Ecological and evolutionary implications. Geology, 27(1), 1999, 63-66 p.
12. Jorissen, F.J., Fontanier, C., Thomas, E. Chapter seven paleoceanographical proxies based on deep-sea benthic foraminiferal assemblage characteristics. Developments in marine geology, 1, 2007, 263-325 p.
13. Ohkushi, K., Kennett, J.P., Zeleski, C.M., Moffitt, S.E., Hill, T.M., Robert, C., Beaufort, L., Behl, R.J. Quantified intermediate water oxygenation history of the NE Pacific: A new benthic foraminiferal record from Santa Barbara basin. Paleoceanography, 28(3), 2013, 453-467 p.
14. Tetard, M., Licari, L., Beaufort, L. Oxygen history off Baja California over the last 80 kyr: A new foraminiferal-based record. Paleoceanography, 32, 2017a, 246–264 p.
15. Tetard, M., Licari, L., Ovsepyan, E., Tachikawa, K., & Beaufort, L. Toward a global calibration for quantifying past oxygenation in oxygen minimum zones using benthic Foraminifera. Biogeosciences, 18(9), 2021a, 2827-2841 p.
16. Kaiho, K. Benthic foraminiferal dissolved-oxygen index and dissolved-oxygen levels in the modern ocean. Geology, 22, 1994, 719-722 p.
17. Moffitt, S.E., Hill, T.M., Ohkushi, K., Kennett, J.P., Behl, R.J. Vertical oxygen minimum zone oscillations since 20 ka in Santa Barbara Basin: A benthic foraminiferal community perspective. Paleoceanography, 29, 2014, 1–14 p,
18. Palmer, H.M., Hill, T.M., Roopnarine, P.D., Myhre, S.E., Reyes, K.R., Donnenfield, J.T. Southern California margin benthic foraminiferal assemblages record recent centennial-scale changes in oxygen minimum zone. Biogeosciences, 17, 2020, 2923-2937 p.
19. Durazo, R. Seasonality of the transitional region of the California Current System off Baja California. Journal of Geophysical Research-Oceans 120, 2015, 1173-1196 p.
20. Talley, L. Distribution and Formation of North Pacific lntermediate Water. Journal of Physical Oceanography, 23(3), 1993, 517-537 p.
21. Sánchez, A., Juárez-Fonseca M., González-Yajimovich O., Márquez-Portillo M. Decremento en las condiciones anóxicas en el Pacífico mexicano durante la Pequeña Edad de Hielo. En F. Paz y R. Torres (editores). Estado Actual del Conocimiento del Ciclo del Carbono y sus Interacciones en México: Síntesis a 2016. Serie Síntesis Nacionales. Programa Mexicano del Carbono en colaboración con la Universidad Autónoma del Estado de Hidalgo. Texcoco, Estado de México, México, 2016, 246-250 p.
22. Sánchez, A., Juárez, M., Ortiz-Hernández, M.C., Domínguez-Samalea, Y. (2022). Variability of the oxygen minimum zone associated with primary productivity and hydrographic conditions in the Eastern North

Pacific during the last 1200 years. Deep Sea Research Part I: Oceanographic Research Papers, 186, 103810.
23. Altabet, M.A., Pilskaln, C., Thunell, R., Pride, C., Sigman, D., Chavez, F., Francois, R. The nitrogen isotope biogeochemistry of sinking particles from the margin of the Eastern North Pacific. Deep Sea Research Part I: Oceanographic Research Papers, 46(4), 1999, 655-679 p.

DOI: https://doi.org/10.30836/igs.iies.2024.40

**Ivanov D.V.[1], Anistratenko O.Yu.[1, 2]**

(1) *Institute of Geological Sciences of the National Academy of Sciences of Ukraine, Kyiv, Ukraine.*
*E-mail: akiyo99@ukr.net*
(2) *I.I. Schmalhausen Institute of Zoology of the National Academy of Sciences of Ukraine, Kyiv, Ukraine.*
*E-mail: olga.anistrat@gmail.com*

# VOLODYMYR M. SEMENENKO`S COLLECTION OF NEOGENE MOLLUSCS

Natural collections are of crucial importance for modern scientific research, which significantly expands the field and methodology of information extraction. Moreover the locaties of fossil fauna and flora for various reasons become inaccessible for collecting new samples. Therefore, the importance of paleontological scientific collections as a source and repository of information only grows with the passage of time and will grow even more in the future. The inventory, arrangement and cataloging, first of all, of historical paleontological collections stored in the Institute of Geological Sciences of the National Academy of Sciences of Ukraine is one of the key problem [1].

The Department of Stratigraphy and Paleontology of Cenozoic Deposits stores collections of various groups of Paleogene and Neogene fauna and flora. Mostly these are working and monographic collections of current and former researchers of the department, collected in numerous expeditions within Ukraine and abroad. There are also collections donated by scientists from other institutions and countries.

The collection of Volodymyr Mykolayovych Semenenko (1934-2012), a Corresponding Member of the National Academy of Sciences of Ukraine, is mainly based on his own samplings from the outcrops and wells of the Sea of Azov region and other parts of the Eastern Paratethys Basin. These collections served as the material basis of his theoretical works on the stratigraphy of the Paratethys, realized in numerous scientific publications, including large generalizing monographs [2, 3, 4].

Organizing the collection of V.M. Semenenko is currently ongoing. More than 230 lots originated from over 45 wells have been pre-processed. Most of the lots represented by boxes of selected and identified bivalve and gastropod shells. Altogether we have pre-catalogued more than 60 species. Although V.M. Semenenko did not describe new taxa, his collection has a didactic value as a collection of shells identified to species rank (the so-called reference collection). In addition, part of the samples is primary ("stone") material from wells and outcrops, suitable for further lithological and paleontological study.

Integral parts of the collection of V.M. Semenenko also are his field note-books. They are currently pre-digitized and will be decrypted and correlated with material lots.

After the preliminary inventory, the arrangement and cataloging of the collection is planned. Based on the results of this work, a database will be developed in the Microsoft Access environment.

Microsoft Access is a database management system that has a large number of functions, including linked queries, sorting by various fields, and communication with external tables and databases. This will allow in the future to quickly find information for each element of the collection and the location of the well, accordingly to quickly find and sort the necessary information and communication for each position of the database.

Thus, the collection of Neogene molluscs of V.M. Semenenko will be ready for the work of taxonomists and stratigraphers.

*This work was carried out within the program #0122U001698 "The elaboration and testing of the stratigraphic model of Paleogene, Neogene and Quaternary sedimentary basins of Ukraine".*

**References**

1. Anistratenko O.Yu., Vernyhorova Yu.V. 2022. Universal coding system for paleontological collections as an effective basis for creating a unified electronic collections catalog at the Institute of Geological Sciences of the NAS of Ukraine. Geologičnij žurnal, 4 (381): 101-112. https://doi.org/10.30836/igs.1025-6814.2022.4.264991
2. Bondarchuk V.G. (Ed.) Stratigraphy of the UkrSSR. Volume 10. Neogene. Academy of Sciences of the UkrSSR. Institute of Geological Sciences. Kyiv: Naukova Dumka, 1975. 171 p. (In Ukrainian)
3. Muratov, M.V., Nevesskaya, L.A. (Eds) Stratigraphy of the USSR. Neogene System. Moskov: Nedra, 1986. 420 p. + 443 p. (In Russian)
4. Semenenko V.N. Stratigraphic correlation of the Upper Miocene and Pliocene of the Eastern Paratethys and Tethys. Kiev: Naukova Dumka, 1987. 230 p. (In Russian)

DOI: https://doi.org/10.30836/igs.iies.2024.15

**Prylypko S.[1], Alpert S.[2]**

*(1) Institute of Geological Sciences of the National Academy of Sciences of Ukraine, Kyiv, Ukraine. E-mail: sergijprilipko146@gmail.com*
*(2) Scientific Centre for Aerospace Research of the Earth of the Institute of Geological Science of the National Academy of Sciences of Ukraine, Kyiv, Ukraine. E-mail: sonyasonet87@gmail.com*

# GEOCHRONOLOGICAL RESEARCH OF ANTROPOGENIC SEDIMENTS

Geochronology is the science of determining the age of rocks and geological processes. Geochronology allows to establish quantitative and qualitative changes that occur in nature. Geochronology studies paleogeography, sediment provenance, depositional timing and basin development. The main aim of sampling for the analysis of deep horizons is the study of the sequence of processes and their regularities, that took place in the past and affect the present [3, 5].

There are many different geochronological methods of studying sediments. Geochronological data indicate relative age and chronostratigraphic data indicate the absolute age. Let's consider a brief description of various dating methods.

Paleomagnetism is the study of Earth's magnetic field, that fixed in sediments. Paleomagnetism allows to determine the direction of the paleomagnetic field during the formation of rocks. Paleomagnetism utilizes the reversals of Earth's magnetic field through time. Then time-scale is assigned by analyzing the magnetic changes recorded in sedimentary sequencees.

Radiocarbon dating can determine the age of organic materials which are no more than sixty thousands years old.

Paleontology is the relative dating method. It is based on the comparison of fossil assemblages of sediments and assigning them to an interval of time when these fossils are known to have existed. The fossil assemblage is compared with fossils of similar physical characteristics, and by knowing both age and the spatial extent of particular species, we can determine an interval of time.

Geological expertise of deposits includes description of deposits, determination of age, analysis of the sequence of their formation and composition. Samples for analysis has been taken from Quaternary sediments.

Determing the age requires a systematic approach to identifying fossil soils, loess and other types of deposits. It should be noted, that the whole range of different methods, such as stratigraphic, physical and mathematical are applied for solution of these tasks.

The thermoluminescence method (TL-method) is one of most efficient methods for determining the age of sediments [1]. The knowledge of the age of the studied objects helps to understand laws, sequences and development of processes and phenomena.

After determining the age, opportunities open up for comparison and correlation of various fairly remote areas, sections and phenomena. The main criteria for correlations are the age of the deposits, physical properties and their mineral composition. Covering deposits in the conditions of their natural position are influenced by environmental factors constantly [4].

The TL-method of determining the "absolute" and relative age of subaerial deposits is based on the properties of crystals to accumulate energy of decay of radioactive elements and to radiate it under the influence of heat. This energy is accumulated in crystalline lattices [2]. During heating process, the accumulated energy is emitted in the form of photons of light. We register this luminescence using our devices. Thermoluminescence dating of sediments depends on time of their burial.

The thermoluminescence effect is fixed in the form of curves of thermal influence. Dividing the amount of measured energy to the background radioactivity of the rock, we get the value, that characterizes the age of the sample.

Different optically transparent crystalline minerals-dielectrics are used as paleodosimeters. We are interested in such minerals, that can act as a paleodosimeter, that accumulate and save the age-related information for a long period of time. Quartz is the such a suitable mineral.

Our research allows to compare the geological structure of Quaternary sediments and to determine the age of sediments. It permits to conduct the structural analysis of sediments.

Analyzing the obtained results of TL-method, we can make a conclusion, that the geological processes recorded in the deposits of the sections are identical to those in other regions. It means, that these geological processes occurred under the influence of the same external factors of the Quaternary period.

Let's note, that the thermoluminescence effect is fixed in the form of curves of thermal light, determing the area bounded the curve or the intensity of the peak. Older sediments have larger age indices and younger sediments have lower age indices. We should use such minerals, that can act as a paleodosimeter, that accumulates and preserves the age-related information for a long period of time. Quartz is the such a suitable mineral. Quartz is one of the most common minerals of the earth's crust. Crystals of quartz have certain structural defects, that characterize a sufficient depth of the trap to ensure the saving of metastable state of the electrons for a long time [1].

The technique is best suited to the age determination of sediments which have been zeroed by influence of solar radiation during transposition.

Aeolian sediments are more likely to have undergone considerable solar exposure prior to deposition and therefore are more likely to have been effectively zeroed. Study must also be taken ensure that the sample is taken from an undisturbed area and has not been has not been exposed to any influence.

TL dating may be applied to aeolian, fluvial, coastal and, in some cases, marine sediments. The technique is also successfully applied to volcanic materials and heated firehearth samples and therefore may be directly applicable in certain archaeological contexts [4].

The main problem with determining the age of Pleistocene rocks by the TL-method consists in accurately calculation of some value (let's name it as age parameter (T)). The value of this age parameter is directly proportional to the time of formation of the investigated rocks. Therefore, for determining of the age of Pleistocene rocks by the TL-method, we can use this age parameter [1].

The age parameter is represented by the expression: $T = \frac{D}{P}$,

where *T* – time, *D* – dose, that was accumulated by the sample, *P*-annual dose.

Apha, beta and gamma radiation during whole burial period form structural defects with constant velocity $(V_{\alpha,\beta,\gamma})$ in quartz.

Let’s note, that velocity of formation of radiation defects is determined as:

$$V_{\alpha,\beta,\gamma} = \beta \cdot E, \tag{1}$$

where $\beta -$ the sensivity of the dose of the mineral, $E -$ the capacity of the expositional dose of gamma radiation.

The velocity of annihilation is proportional to the concentration of localized electrons in quartz at the selected moment of time:

$$V_A = k \cdot n, \tag{2}$$

where, *k* is the constant of the velocity of the of annihilation of localized electrons or a coefficient of proportionality.

Let’s note, that at saturation the velocity of formation of radiation defects will be equal to the velocity of their annihilation:

$$V_{\alpha,\beta,\gamma} = V_A. \tag{3}$$

From equations (1)-(3) we get the next equation (4):

$$\beta \cdot E = k \cdot n. \tag{4}$$

At the saturation concentration of localized electrons is denoted as *N*:

$$\beta \cdot E = k \cdot N. \tag{5}$$

From equation (5) we get the constant of the velocity of the of annihilation of localized electrons (coefficient of proportionality):

$$k = \frac{\beta \cdot E}{N}. \tag{6}$$

The velocity of change of the concentration of localized electrons is equal to the first derivative from concentration of localized electrons:

$$\frac{dn}{dt} = V_{\alpha,\beta,\gamma} - V_A = \beta \cdot E - \frac{\beta \cdot E}{N} \cdot n. \tag{7}$$

We have obtained the differential equation:

$$\frac{dn}{\beta \cdot E - \frac{\beta \cdot E}{N} \cdot n} = dT. \tag{8}$$

After the integration of this equation we have got the next formula:

$$T = \int \frac{dn}{\beta \cdot E - \frac{\beta \cdot E}{N} \cdot n} = \left| \begin{array}{l} \beta \cdot E - \frac{\beta \cdot E}{N} \cdot n = z \\ dn = \frac{N}{\beta \cdot E} dz \end{array} \right| = \int \frac{N}{\beta E} \cdot \frac{1}{z} dz = \frac{N}{\beta E} \ln \left| \beta E - \frac{\beta E}{N} \cdot n \right|. \tag{9}$$

Taking the upper limit of the integral – $n_0$ (accumulated concentration of localized electrons) and taking the lower limit of the integral – $n_{\min}$ (residual concentration of electrons after whitening), we get equation (10):

$$T = \frac{N}{\beta \cdot E} \left[ \ln \left( \beta \cdot E - \beta \cdot E \cdot \frac{n_{\min}}{N} \right) - \ln \left( \beta \cdot E - \beta \cdot E \cdot \frac{n_0}{N} \right) \right] = \frac{N}{\beta \cdot E} \ln \frac{1 - \frac{n_{\min}}{N}}{1 - \frac{n_0}{N}}. \tag{10}$$

So, we have found the equation (10) for the determination of the age of the rocks.

In this work we proposed the mathematical apparatus, that can be applied for calculating the age of anthropogenic sediments. This mathematical apparatus is based on the solution of the differential equation. A mathematical formula for the age parameter has been considered in this work. The velocity of annihilation, the velocity of the formation of radiation defects and the energy that was accumulated by the investigated sample over time were applied for derivation of this formula. It also was noted, that this mathematical apparatus helps to conduct correlation of various Quaternary sediments from various areas. It shows which rocks of a section are older and which are younger. It also determines the sequence of the rock accumulation.

**References**


1. Prylypko S.K., Alpert S.I. Mathematical model of the dynamics of accumulation light sum in subareal deposits. Conference Proceedings. Ideas and innovations in geosciences. Kyiv, 2019. P. 90-91.
2. Durcan J.A., King G.E., Duller G.A.T. DRAC: Dose Rate and Age Calculator for trapped charge dating. Quaternary Geochronology, 2015. Vol. 28. P. 54-61.
3. Gozhik P., Komar M., Łanczont M., Fedorowicz S., Bogucki A., Mroczek P., Prylypko S., Kusiak J. Paleoenvironmental history of the Middle Dnieper Area from the Dnieper to Weichselian Glaciation: A case study of the Maksymivka loess profile. Quaternary International, 2014. Vol. 334-335. P. 94-111.
4. Liritzis I., Vafiadou A., Zacharias N., Polymeris G.S., Bednarik R.G. Advances in surface luminescence dating: new data from selected monuments. Mediterranean Archaeology and Archaeometry, 2013. Vol. 13 (3). P. 105-115.
5. Komar M., Krokhmal O., Derevska K., Łanczont M., Mroczek P., Nawrocki J., Standzikowski K., Hołub B., Prylypko S. Środowisko i klimat w dolinie Dolnego Dniepru w czasie MIS 64-12 na podstawie danych paleontologicznych. Skurzyński, J., Jary, Z., Błaszkiewicz, M. (red.), XXVII Konferencja Naukowo-Szkoleniowa Stratygrafia Plejstocenu Polski „Późnoczwartorzędowe środowiska sedymentacyjne Pomorza Wschodniego". Stara Kiszewa, IGiRR UW. Wrocław, 2022. P. 129-131.

*DOI: https://doi.org/10.30836/igs.iies.2024.31*

**Nezdolii Ye.**

*Institute of Geological Sciences of the National Academy of Sciences of Ukraine, Kyiv, Ukraine.*
*E-mail: yevheniia.nezdolii@gmail.com*

# ON THE TAPHONOMIC STUDIES OF SMALL MAMMAL REMAINS FROM PELLETS OF BIRDS OF PREY: THE UKRAINIAN CONTEXT

Research in the field of taphonomy provide paleontology with biological and physical events, processes that operated after death and during removal from the environment [1]. Correct identification is critical to modeling how and why assemblages of animal remains (small mammals) accumulate on paleontological and archaeological sites. But just as important is the interpretation of identification, the explanation of the connection between the process and the agent [1, 13].

Identification of the agent is mandatory for successful taphonomic interpretation. Apart from natural or artificial death (due to an accident, human impact) predation (mammalian predators, birds of prey) is one of the causes for the accumulation of the remains of small mammals in pellets form on paleontological localities and archaeological sites [1, 2, 3, 14]. These finds contain perfectly preserved skeletal remains of the prey (a small mammal). Thus, we can make a detailed taphonomic and taxonomic analysis, which will provide information about the interaction between the predator and prey, as well as outline the environmental conditions during the formation of taphocenosis [1].

In nature, small mammals are associated with specific biotopes, so their remains are potentially an indicator of paleoenvironmental conditions [5, 15]. And here there are problems between questions of direct correlation. Predators have the ability to remove prey from the primary environment, they choose prey based on their specialization (size, behavior, etc.) and accumulate remains in nesting and/or roosting places [1, 14].

Methodological guidelines for taphonomic reconstructions based on small mammals remains contained in pellets of birds of prey was developed by Andrews in the 1990s [1]. His method is based on the degrees of modification bones of the skeleton, which have undergone mechanical and digestive effects of predators. The obtained results were used by the author as analogues for the assessment of fossil and archaeofaunal complexes in different parts of the world. Bones and teeth of rodents (Arvicolinae, Muridae) and insectivores (Soricidae, Talpidae and Erinaceidae) were extracted from the pellets birds of prey. Also studied coprolites of carnivorous mammals (Felidae, Canidae, Mustelidae and Mephitidae). To date, we have a large number of relevant researches based on Andrews' taphonomic methodology [13, 14].

In Ukraine, the pellet method was first proposed by I.H. Pidoplichko [7, 8]. But it was used in zoology in order to study and record the modern fauna of small mammals [4, 6]. In Ukraine, there are not enough studies related to Quaternary taphonomy, pellet taphocenoses based on the Andrews' methodology in the context of paleofaunistic interpretations [9-12].

First of all, it is necessary to adapt taphonomic methods to regional conditions, because the local fauna includes various taxa. For example, the simplest is the local seasonal collection of pellets of various species of birds of prey. Their analysis will make it possible to connect predators and seasonal fluctuations of their prey. And this will give an opportunity to better interpret ancient ecosystems in different seasons. An interesting question is the primary and secondary nature of the find. Because many prehistoric sites include species that are not modern. Such artificial assemblages can unite mammals from different environments or even from different geological periods [10]. There is another option, fossil species found nearby can live at the same time, but in different places. How they ended up together, united by a certain agent, predator or river. Recently, we tried to adapt Andrews' taphonomic model. It included only the level of mechanical breakage to the bones of the skull and lower jaw and bones of the postcranial skeleton of small mammals from pellets [11, 12]. In part, I succeeded in obtaining primary results for interpretation of taphonomic stages. In the future it will allow get a higher level of detail and better interpretation of pellet assemblages of small mammal remains removed from paleontological and archaeological sites of Ukraine.

**References**

1. Andrews P. Owls, caves and fossils. Predation, preservation, and accumulation of small mammal bones in caves, with the analysis of the Pleistocene cave faunas from Westbury-sub-Mendip, Somerset, UK. Chicago: University of Chicago Press. 1990. 231 p.
2. Andrews P., Evans E. Small mammal bone accumulations produced by mammalian carnivores. Palaeobiology. 1983. Vol. 9. No.3. P. 289-307.
3. Efremov I.A. Taphonomy: new branch of paleontology. PanAmerican Geologist. 1940. Vol. 74. P. 81-93.
4. Drebet M. Research on the small mammal fauna by analysis of pellets of birds of prey: algorithms of collection and analysis. Proceedings of the Theriological School. 2017. Vol. 10. P. 10-17. (In Ukrainian).

5. Gromov I.M., Polyakov, I.Y. Voles (Microtinae). Fauna of the USSR. Mammals. Moscow-Leningrad: Nauka. 1977. Vol. 8. No.3. P. 1-504. (In Russian).
6. Kuznetsov V., Kondratenko O. Microteriofauna of protected areas of Lugansk region for the results of the analysis of bird pellets. Proceedings of the Theriological School. Luhansk. 2006. Vol. 7. P. 75-76. (In Ukrainian).
7. Pidoplichko I.G. Analysis of pellets for 1925-1929. Issue 1. Issue of the commission of Pr. Land. VUAN. Kyiv. 1932. P. 5-6. (In Ukrainian).
8. Pidoplichko I.G. Results of the study of pellets for 1924-1935. Collection of works of the Zoological Museum of the Ukrainian Academy of Sciences. Kyiv.1932. Vol.19. P. 101-170.
9. Popova L., Kulakovska L. Microteriophauna of the Late Paleolithic site Corman (Chernivtsi Region, Ukraine): Paleoecological interpretation of pellet taphocenoses. Zoology in the modern world: challenges of the XXI century. Studies of vertebrates. 2021. P. 36. (In Ukrainian).
10. Popova L., Krochak M., Krochmal O., Nezdolii Y. Middle Pleistocene small mammal fauna of the cave locality Viniavy (L'viv region). Visnyk of the Taras Shevchenko National University of Kyiv. Geology. 2019. Iss. 2 (85). P. 16-22. (InUkrainian).
11. Nezdolii Ye. Small mammal remains from pellets of birds of prey: a contribution to taphonomy. Zoology in the modern world: challenges of the XXI century. Studies of vertebrates. 2021. P. 30. (In Ukrainian).
12. Nezdolii Ye., Yanevych O. Taphonomic analysis of small mammal bones accumulations from the location of the Buran-Kaya IV. Organic world of the Precambrian and Phanerozoic: theoretical and applied aspects of research: Materials of the International Scientific Conference and XLI Session of the Ukrainian Paleontological Society of the NAS of Ukraine (Kyiv, October 11-12, 2023). Kyiv. 2023. P. 82.
13. Fernandez-Jalvo Y., Andrews P. Atlas of taphonomic identifications. Dordrecht, Heidelberg, New York, London: Springer. 2016. 359 p.
14. Fernandez-Jalvo Y., Avery D.M. Pleistocene micromammals and their predators at Wonderwerk Cave, South Africa. The African Archaeological Review. 2015. Vol. 32. No. 4. P. 751-791.
15. Rekovets L.I. Quaternary small mammals of the southern part of East Europe. Kyiv: Naukova Dumka. 1994. 372 p. (In Russian).

DOI: https://doi.org/10.30836/igs.iies.2024.11

**Acevedo-Tirado T., Sánchez-González A.**

*Instituto Politécnico Nacional, Centro Interdisciplinario de Ciencias Marinas, La Paz, Baja California Sur, Mexico. CP 23096. E-mail: tacevedot2300@alumno.ipn.mx, alsanchezg@ipn.mx*

# PRODUCTIVITY DYNAMICS IN THE TRANSITIONAL ZONE OF THE MEXICAN PACIFIC: INSIGHTS FROM GEOCHEMICAL TRACERS

Currently, the ocean absorbs approximately 30% of the anthropogenic $CO_2$ released into the atmosphere each year [1]. The concentration of this greenhouse gas has varied throughout the history of the planet. This change in CO2 concentration is modulated by the atmosphere-ocean, atmosphere-biosphere exchange, and by geological and biological processes. These processes are related to the biological carbon and carbonate pump [2, 3].

This is how the biological pump and its effect, the burying of organic carbon and calcium carbonate on the ocean floor, relates variations in atmospheric $CO_2$ to carbon fluxes on the seabed [1]. The factors and mechanisms that increase or decrease the burial of carbonates and organic carbon in sediments therefore represent important outputs that control the flow of carbon from the active or surface carbon cycle to the long-term geological cycle [4].

Global warming may cause the land surface to warm relatively faster than the ocean, which could lead to a greater land-ocean pressure gradient and intensify winds along the coast in regions of eastern boundary currents and drive more intense and frequent coastal upwellings [5, 6, 7].

The Mexican Pacific Transitional Zone is a complex region in its oceanographic conditions, which leads to changes in primary and exported productivity. Geochemical tracers: organic carbon (CO), biogenic opal, and calcium carbonate are used to assess primary and exported productivity in sedimentary records.

Organic carbon is commonly used as an indicator of carbon export from the photic zone. Over the past two millennia, there has been a global increase in organic carbon, indicating an overall increase in exported productivity [11]. However, organic carbon is subject to diagenesis and sudden depositional events that lead to misinterpretations about exported productivity [1]. To exclude these interpretations an independent indicator of exported productivity is needed, calcium carbonate is a productivity indicator that represents the production of biogenic carbonate (mainly foraminifera and coccolithophores). Both tracers of exported productivity will be coherent if the preservation of organic carbon has not been altered by diagenetic processes and sudden depositional events [8]. Biogenic opal (mainly produced by diatoms and silicoflagellates) is another major contributor to exported productivity, especially during coastal upwelling events [9].

Global warming may cause marine and export productivity to increase, as winds along the coast drive more intense and frequent coastal upwelling. In this sense, the climatic and oceanographic reconstruction, based on the use of biogeochemical tracers (organic carbon, carbonate and biogenic opal) in the warming episodes of the recent past, i.e. the Holocene Climate Optimum or Medieval Warming Period may be key to understanding the future interactions of marine plankton functional groups in future climate change scenarios in eastern boundary current systems, like the California Current.

The objective of the present study is to quantify the content of organic carbon, biogenic opal and calcium carbonate to infer changes in primary and exported productivity during warming episodes in the transition zone of the Mexican Pacific. The southwestern margin of Baja California Sur is located in the transition zone of the Mexican Pacific, where the current system in this transitional zone is characterized by the California Current flowing into the equatorial zone, the North Equatorial Current flowing west-northwest, and the California Countercurrent flowing toward the North Pole. The California Current carries cold, less saline, oxygenated, nutrient-rich water from the subarctic body of water. Meanwhile, the California Countercurrent, which carries properties of the equatorial subsurface mass, is characterized by being warmer, more saline and poor in oxygen.

The sediment core GC-2 was recovered at a depth of 680 m on the southwestern margin of Baja California Sur, during the October 2009 oceanographic campaign, aboard the RV New Horizon (Figure 1). The sediment core with a length of 144 cm was sectioned at intervals of 1 cm, representing a total of 144 sediment samples. [12]. A subsample of each interval was freeze-dried, macerated in an agate mortar and weighed for analysis. The Organic carbon analysis was performed on a COSTECH 4010 elemental analyzer with an estimated analytical accuracy of 0.2% of BBOT and Urea certified standards. The quantification of biogenic opal will be estimated from 500 mg of sediments and with the technique described by [10]. The extracted silica will be quantified by UV-vis spectrophotometry at 812 nm. A sodium silicofluoride solution with an analytical accuracy of 0.5% will be used as standard.

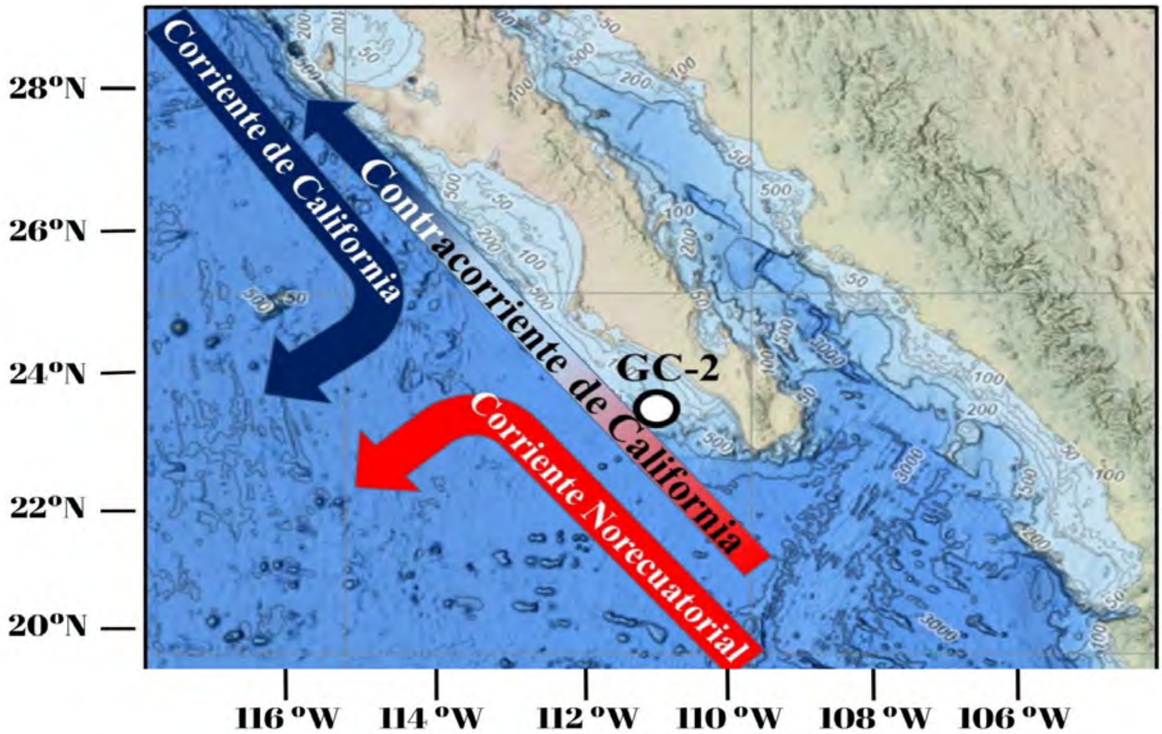


Fig. 1. Diagram of the California, Norequatorial, and California Countercurrent Currents in the Northeast Pacific Transitional Zone [13]. The dot indicates the location of the GC-2 gravity core collected

The organic carbon content ranged from 9% to 14%, with a minimum value of 9.54% and a maximum of 14.35%. Whereas, biogenic opal ranged from 0.2 to 19%, with a minimum value of 0.19% and a maximum of 19.33%. A spectral analysis was performed using the REDFIT procedure [14], which is included in the PAST 2.17b program. The organic carbon content showed periodicity of ~300, ~170 and ~100 years. Biogenic opal showed periodicity of ~310, ~270, and ~70 years. The values of organic carbon and biogenic opal showed a positive correlation with each other, showing an increase in warm periods such as the Roman Warm Period (1800 to 2200 years ago) and the Medieval Warming Period (700 to 1100 years ago). This suggests that primary and exported productivity responds to oceanographic conditions over various time scales.

**References**

1. Keil, R. (2017). Anthropogenic forcing of carbonate and organic carbon preservation in marine sediments. Annual Review of Marine Science, 9, 151-172.
2. Sanchez, A., & Carriquiry, J. (2007). Sedimentary organic carbon fluxes along the continental margin of the northeastern Mexican Pacific during the last 50000 years. Carbon in Aquatic Ecosystems of Mexico: Ensenada, Ministry of Environment and Natural Resources-National Institute of Ecology-Center for Scientific Research and Higher Education of Ensenada, 427-436.
3. Hajima, T., Yamamoto, A., Kawamiya, M., Su, X., Watanabe, M., Ohgaito, R., & Tatebe, H. (2020). Millennium time-scale experiments on climate-carbon cycle with doubled CO 2 concentration. Progress in Earth and Planetary Science, 7(1), 1-19.
4. Fennel, K., Alin, S., Barber, L., Evans, W., Bourgeois, T., Cooley, S., ... & Wang, Z.A. (2019). Carbon cycling in the North American coastal ocean: a synthesis. Biogeosciences, 16(6), 1281-1304.
5. Sydeman, W. J., Garcia-Reyes, M., Schoeman, D. S., Rykaczewski, R. R., Thompson, S. A., Black, B. A., & Bograd, S. J. (2014). Climate change and wind intensification in coastal upwelling ecosystems. Science, 345(6192), 77-80.
6. Xiu, P., Chai, F., Curchitser, E.N., & Castruccio, F.S. (2018). Future changes in coastal upwelling ecosystems with global warming: The case of the California Current System. Scientific reports, 8(1), 1-9.
7. Howard, E. M., Frenzel, H., Kessouri, F., Renault, L., Bianchi, D., McWilliams, J. C., & Deutsch, C. (2020). Attributing causes of future climate change in the California Current System with multimodel downscaling. Global Biogeochemical Cycles, 34(11), e2020GB006646.
8. Abella-Gutiérrez, J., & Herguera, J.C. (2016). Sensitivity of carbon paleoproductivity in the Southern California Current System on different time scales for the last 2 ka. Paleoceanography, 31(7), 953-970.
9. Pichevin, L.E., Ganeshram, R.S., Geibert, W., Thunell, R., & Hinton, R. (2014). Silica burial enhanced by iron limitation in oceanic upwelling margins. Nature Geoscience, 7(7), 541-546.

10. Mortlock, R.A., & Froelich, P.N. (1989). A simple method for the rapid determination of biogenic opal in pelagic marine sediments. Deep Sea Research Part A. Oceanographic Research Papers, 36(9), 1415-1426.
11. Wang, Y., Hendy, I.L., & Thunell, R. (2019). Local and remote forcing of denitrification in the northeast Pacific for the last 2,000 years. Paleoceanography and Paleoclimatology, 34(8), 1517-1533.
12. Sánchez, A., Juárez, M., Ortiz-Hernández, M.C., Domínguez-Samalea, Y. (2022). Variability of the oxygen minimum zone associated with primary productivity and hydrographic conditions in the Eastern North Pacific during the last 1200 years. Deep Sea Research Part I: Oceanographic Research Papers, Volume 186, ISSN 0967-0637.
13. Durazo, R. (2015). Seasonality of the transitional region of the California Current System off Baja California. Journal of Geophysical Research: Oceans, 120(2), 1173-1196.
14. Schulz, Michael & Mudelsee, Manfred. (2002). REDFIT: Estimating red-noise spectra directly from unevenly spaced paleoclimatic time series. Computers & Geosciences. 28. 421-426. 10.1016/S0098-3004(01)00044-9.

*DOI: https://doi.org/10.30836/igs.iies.2024.4*

**Arenas F.[1], Fujita H.[2], Sanchez A.[1], Medina-Contreras D.[1]**

*(1) Instituto Politécnico Nacional, Centro Interdisciplinario de Ciencias Marinas, La Paz, B.C.S., México.*
*E-mail: farenasg2000@alumno.ipn.mx, alsanchezg@ipn.mx, dmedinac1900@alumno.ipn.mx*
*(2) Instituto Nacional de Antropología e Historia, Centro Baja California Sur, La Paz, B.C.S., México.*
*E-mail: harumifuj@gmail.com*

# SURFACE SEA TEMPERATURE RECONSTRUCTION OF LA PAZ BAY, GULF OF CALIFORNIA: NEW EVIDENCE FROM PINCTADA MAZATLANICA $\delta^{18}O$

Through the use of stable oxygen isotopes in bivalve shells, Holocene oceanic characteristics can be reconstructed from past surface sea temperatures (SSTs), allowing the study of climatic patterns and phenomena that affect marine and human communities. The goal of this study was to calculate Holocene summer SSTs for La Paz Bay through the novel analysis of $\delta^{18}O$ in *Pinctada mazatlanica* shells from a $^{14}C$ dated Holocene open camp site of Baja California Sur, México. Presently summer season aragonite $\delta^{18}O$ of *P. mazatlanica* is -1.8 ± 0.2‰, varying between -1.3‰ and -1.9‰ during the last 8.4 ky; For the years 8396 BP, 7708 BP and 7070 BP $\delta^{18}O$ was enriched 0.2‰ to 0.1‰, suggesting slightly colder SSTs vs. the present, while in 7805 BP, $\delta^{18}O$ values were depleted -0.1‰, suggesting slightly warmer SST; in 6945 BP and 2087 BP, $\delta^{18}O$ was enriched 0.4‰ to 0.5‰, suggesting significantly colder SSTs vs. the present. The resulting Holocene SST tendencies align with and support a number of local and regional paleotemperature studies, establishing it as a novel paleotemperature proxy for La Paz Bay.

**References**

1. Arenas F., Fujita H. and Sánchez A. (2021) Paleoenvironmental reconstruction in La Paz Bay, Gulf of California: Evidence from δ 18 O in Chione californiensis. The Holocene: 095968362110665. DOI: http://doi.org/10.1177/09596836211066594.
2. Fujita H., Hernández A., Bulhusen K., et al. (2018) Trans-Holocene Occupations at Cañada de la Enfermería Sureste #3 (Site A119), Baja California Sur, México. SCA Proceedings 32: 59–77.
3. Barron J.A., Metcalfe S.E. and Addison J.A. (2012) Response of the North American monsoon to regional changes in ocean surface temperature. Paleoceanography 27(3). DOI: http://doi.org/10.1029/2011PA002235.

DOI: https://doi.org/10.30836/igs.iies.2024.44

**Biletskyi O.**

*Institute of Geological Sciences of the National Academy of Sciences of Ukraine, Kyiv, Ukraine.*
*E-mail: biletskyi.ol@gmail.com*

# RESEARCH AND CURRENT STATE OF UPPER VENDIAN (EDIACARAN) OUTCROPS IN THE HORYN FACIES ZONE

The Ediacaran Period lasted from approximately 635 to 541 million years ago and was characterized by global geological and ecological processes that had a significant impact on the evolution of life. During the Cryogenian and Ediacaran, several key processes occurred, including the warming after the global glaciation, continental drift, which involved the breakup of the supercontinent Rodinia and the formation of Gondwana, as well as the impact of an asteroid, the evidence of which is the Acraman impact structure.

The Ediacaran Period is notable for the emergence of the Ediacaran biota, which consisted of several groups of metazoans with a rather complex morphology. These were soft-bodied organisms, mostly not similar to modern biotic groups, which complicates their genetic classification and understanding their role in the evolutionary history of life.

In Ukraine, Ediacaran deposits are widespread in the Volyn-Podillia Plate and partly in the Pereddobruzkyi Through, which situated in the southwest part of the East European Platform [1-8]. The upper Vendian (Ediacaran) in Volyn and Podillia is represented by the Mohyliv-Podil's'kyy and Kanyliv group, which represent the Novodniester and Ushytsa horizons of the regional stratigraphic scheme [1].

In contrast to the Vendian of Podillia, which is characterized by a unique completeness of a sedimentary sequence, detailed stratigraphic subdivision, and a sufficiently high level of lithological study [1-8], the deposits of the Upper Ediacaran of the Horyn facies zone (FZ) lie monoclinally and most of the rocks are overlaid by a thick sedimentary cover, which significantly complicates their study.

They are exposed only in the valley of the Horyn River and its tributary, the Vilia River (from the town of Ostroh to the village of Khotyn, Rivne Region). The Vendian deposits were previously investigated primarily using core material from deep geological mapping boreholes of 1980-1984 (sheet M-35-XV; Rivne). The cores of these boreholes have been lost, and the methods and tools for examining Ediacaran rocks have recently undergone significant changes. The monograph "Vendian of Ukraine" by Velikanov et al. [4] describes six outcrops of Vendian deposits in Volyn (NW Ukraine).

The lowest stratigraphic interval includes outcrops in the village of Rozvage to the north of the town of Ostroh. A small outcrop of deposits similar in stratigraphic position can be observed at the mouth of Tatarskyi Yar in the town of Ostroh (in the yard of the house on 146a, Dzerzhynskogo Street). One of the largest outcrop is an abandoned quarry in the village of Slobidtsi, the right bank of the Vilia River. The only outcrop of the Kalyus Beds in Volyn is located in the area of the village of Khotyn, north of the city of Rivne [4].

Of the six outcrops in the Horyn FZ described in the monograph “Vendian of Ukraine”, the author found that only the man-made outcrop (abandoned quarry) in the village of Kamianka on the right bank of the Vilia River (Fig. 1, a) is accessible. Other outcrops are flooded (quarries) or sodden (gullies).

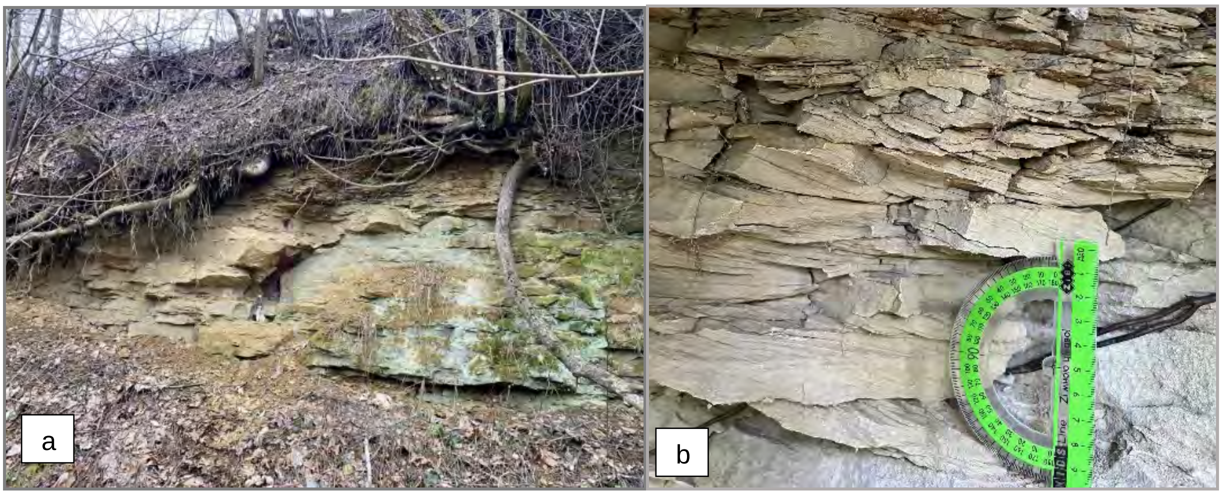


Fig. 1. Ediacaran rocks exposed in the village of Kamianka:
a) Outcrop panorama; b) Textural features of siltstones

The section in the quarry in the village of Kamianka comprises sandstones and siltstones. The lower part of the section consists of a 1.1 m-thick layer of a massive, gray-red, fine-grained, feldspar-quartz and micaceous sandstone. The upper part of the section is consists of thin- and wavy-layered, micaceous, weathered siltstones. In some places, mica forms thin lenses and layers over 0.4 m thick (Fig. 1, b).

V.A. Aseeva [4] identified an assemblage of microscopic phytofossils in the sandstone bed, which is typical of the lower part of the Kanyliv Group. Although these deposits are similar to the rocks of the Mohyliv Formation of Podillia in terms of lithological parameters and depositional conditions (Fig. 2) [5]. Therefore, they require further research.

Fig. 2. The Lomoziv Beds of Podillia (photo by A.I. Martyshyn)

The Kanyliv Group was initially described as the Kanylov strata of the Lower Cambrian by O.V. Krasheninnikova [6] in the basin of the Horyn River. It was subsequently divided into two lithostratigraphic units: the lower sandstone bed and the upper thin-bedded sandstone-mudstone-siltstone bed [7]. These strata were initially established based on the well log charts and compared by stratigraphic position and volume with the Zharniv, Krushaniv and Studenytsi formations of the Podillian ledge of the Ukrainian Shield. However, the lithological composition, structure, and organic remains were not characterized due to the lack of core material.

V.Ya. Velikanov [8] was the first to successfully correlate the Kanyliv Group in Volyn with its analogues in Podillia and eastern Poland. This correlation led to the creation of the lithostratigraphy of the Kanyliv Group and monitoring of the evolution of the sedimentary basin.

Therefore, it can be concluded that the study of the depositional conditions of the upper Vendian (Ediacaran) sediments of Volyn is in its initial stage and requires further research. This includes a detailed examination of the geochemical, mineralogical, and lithological features, which are crucial for reconstructing the ecology of the Ediacaran paleobasin. These tools enable the monitoring of paleoenvironmental changes and the development of new models of climate change, as the mineral composition of rocks is controlled by various factors, such as geotectonic setting, source of clastic material, degree of weathering, and depositional conditions (e.g. grain size and hydraulic sorting of minerals with different densities and grain shapes), as well as diagenesis and hydrothermal events.

*This study was carried out under the funding of the state budget program CPCEL 6541030 in the framework of the R&D Project "Sedimentation conditions and lithogenesis of the Upper Ediacaran (Vendian) sediments of the East European Platform southwestern part".*

**References**

1. Stratigraphy of the Upper Proterozoic, Paleozoic and Mesozoic of Ukraine, Chief editor P.F. Gozhik – K.: IGN NAS of Ukraine. Logos, 2013. 113 p.

2. Shekhunova S.B., Stadnichenko S.M., Paliy V.M., Permyakov V.V., Gudzenko V.V. Lithogenesis of the Ediacaran (Vendian) "Kalius beds" according to the lithological and geochemical studies of the Podillia sequence. Collection of scientific works of the IGS NAS of Ukraine, 2018, Issue 11, p.129-146. DOI: http://doi.org/10.30836/igs.2522-9753.2018.153094.

3. Paliy V., Shekhunova S., Stadnichenko S. Cyclicity of Ediacaran (Vendian) Deposites of Volyno-Podillia (Ukraine). Abstracts of the 20th International Sedimentological Congress, 13-17 August 2018, Quebec, Canada. 184-4tt8-193.
4. Vend of Ukraine. Velikanov V.A., Asyeeva E.A., Fedonkin M.A. 1983. 70-72 p.
5. Martyshyn A.I. Association of benthic macrobiota of the Late Ediacaran of Podillia in the deposits of the grave-Podilsky series in the quarry near the Dniester hydroelectric power station. Collection of scientific works of the Institute of Geological Sciences of the National Academy of Sciences of Ukraine. 2022. Vol. 15, issue 1. p. 44–64. DOI: https://doi.org/10.30836/igs.2522-9753.268218
6. Krasheninnikova O.V. Ancient Formations of the Western Slope of the Ukrainian Crystalline Shield. – Kyiv: Nauk. dumka, 1956. – 193 p.
7. Sokolov B.S. Precambrian and Cambrian Boundary Problems, Geology and geophysics. – 1974. – No. 2. – p. 3-29.
8. Velikanov V.A. On the correlation of Upper Vendian deposits of Ukraine and Eastern Poland, Izv. Academy of Sciences of the USSR. Ser. geol. – 1988. – No. 2. – p. 16-22.

DOI: https://doi.org/10.30836/igs.iies.2024.16

**Dröllner M.[1], Danišík M.[2], Barham M.[1], Kirkland C.L.[1]**

*(1) Timescales of Mineral Systems Group, School of Earth and Planetary Sciences, Curtin University, GPO Box U1987, Perth, WA 6845, Australia. E-mail: maximilian.drollner@curtin.edu.au*
*(2) Western Australia ThermoChronology Hub (WATCH) Facility, John de Laeter Centre, Curtin University, GPO Box U1987, Perth, WA 6845, Australia.*

# CAPTURING THE THERMAL FINGERPRINT OF SOURCE AREAS WITH DETRITAL RUTILE U-PB-HE DOUBLE-DATING: REFINING SOURCE-TO-SINK RELATIONSHIPS IN THE MURRAY BASIN, SOUTHEASTERN AUSTRALIA

Detrital rutile is receiving increasing attention as a valuable complement to detrital zircon due to its ability to record geological processes to which zircon is often unresponsive. As a primary metamorphic mineral, U-Pb dating of rutile provides insights into middle- to shallow-crustal processes, while rutile geochemistry has been applied to better understand protolith composition and growth temperatures. To better capture the thermal history of metamorphic source terranes, we present an integrated approach combining U-Pb geochronology and (U-Th)/He thermochronology ("double-dating") applied to detrital rutile from late Neogene heavy mineral sand deposits in the Murray Basin, southeastern Australia. In addition, we performed $^{4}He$ diffusion experiments on rutile of the same samples to understand the closure temperatures of the analyzed samples. Combined with trace element geochemistry, using Cr-Nb systematics and the Zr-in-rutile thermometer, U-Pb-He double-dating allows for the reconstruction of a thermal fingerprint for individual rutile grains, offering less ambiguous provenance information. In the Murray Basin, the application of double-dating and geochemistry aids in identifying the ultimate source terrane, and thereby resolves complex, multi-cycle sediment pathways from an exotic and distal ultimate source through near-surface intermediate storage units. This finding posits the recycling history as a key mechanism in upgrading the rutile grade in one of the world's most significant Ti resources. Incorporating (U-Th)/He systematics into the detrital rutile analytical toolkit enhances the mineral's versatility and highlights its potential in generating a more comprehensive understanding of sedimentary systems.

*DOI: https://doi.org/10.30836/igs.iies.2024.17*

**Kompanets H.[1], Ganzha O.[1], Kushnir A.[2]**

*(1) Institute of Geological Sciences of the National Academy of Sciences of Ukraine, Kyiv, Ukraine.*
*E-mail: oag2909@gmail.com*
*(2) Institute of Geography of the National Academy of Sciences of Ukraine, Kyiv, Ukraine.*
*E-mail: kushnirpaleogeo@gmail.com*

# TITANIUM DEPOSITS CHARACTERISTICS OF THE VOLYN REGION

Volyn titanium region is located in the northern part of the Ukrainian shield, located within the development of basic and partially acidic rocks of the Korostensky pluton. The sedimentary cover of this territory is represented by deposits of different ages from the Cretaceous to the Quaternary period, in which placers of titanium-bearing rocks have been explored. The composition of the Korostensky pluton is dominated by rapakivi granites, anorthosite, gabbro-anorthosite, and gabbro-norite of the Volodarsk-Volynsky, Chopovytsky, Krovotynsky, and Ushomirsky massifs.

Researching of the paleogeographic characteristics of the formation of placers and placer deposits for this territory were carrid out of Veklich M.F., Komlyev O.O., Remezova O.O., Okholina T.V., Ganzha O.A. etc. [1, 3, 5]. In this article, the authors analyzed and summarized the results of research on the Volyn titanium region.

Magmatogenic deposits of titanium are concentrated within the Volodarsk-Volynsky massif of basic rocks (one of the largest is the Stremyhorod deposit). They have apatite mineralization and are complex apatite-ilminite.

The thickness of weathering crusts within this massif varies from 0.1 to 40.0 m, on average it is 9.0-10.0 m. In the weathering crust profile, a zone of disintegration and initial leaching, partial kaolinization, and complete kaolinization can be distinguished. The amount of ilmenite in the product zones of the weathering crust varies from 30 to 130 kg/m3 and is lower than in the parent rocks. A trend of relative accumulation of titanium minerals from bottom to top along the section of the weathering crust as other components are removed is noted.

Exogenous titanium deposits of the Volyn titanium region are also concentrated within the Volodarsk-Volynsky Massif. These are ancient alluvial and deluvial placers of the Mesozoic and Cenozoic, Quaternary alluvial placers of buried and modern river valleys. The largest Mesozoic (Lower Cretaceous, Irshansk suite) deposits of this type are Lemnenske, Mezhyrichne deposits, Ushytskyi, Ushomyrskyi, Selyshchanskyi, Ivanivskyi placers; Cenozoic - Livoberezhne, Zlobytske [2], Valky-Gatskivke, Pravoberezhne, Poromivske [4] deposits, Quaternary – Irshinske, Vernyo-Irshynske, Katerynivske, Trostyanetske, Stavyshchanskyi and Ocheretyanskyi placers (Fig. 1). Almost all deposits have a paragenetic connection, where the weathered crust and the loose part are ore-bearing.

Lower Cretaceous placers are composed of multi-grained kaolinic sands with a significant amount of gravel material, secondary kaolins and carbonaceous clays. Ore minerals are represented by ilmenite, leucoxenized ilmenite, leucoxene. Their amount in these placers varies significantly: from 20-30 to 300-1100 $kg/m^3$. These placers are confined to buried valleys and depressions in the topography of the crystalline basement. The length of placers of this age varies from 0.5 to 9.0 km, the width - from several tens of meters to 4.0 km, the thickness reaches 10 - 15 m.

Cenozoic placers also fill the buried valleys produced in the relief of bedrock and their weathering crusts. They are 0.2 to 5.0 km long and 0.05 to 2.0 km wide. The thickness of the product deposits is 0.2–15 m. Ore minerals are the same with Lower Cretaceous placers; their amount is from 50 to 400 $kg/m^3$.

Quaternary placers are divided into Early Pleistocene, Late Pleistocene and Holocene (modern). Early Pleistocene placers consist of a layer of sands, sandy loams, and loams with patches of secondary kaolins that underlie fluvioglacial sands (Verkhno-Irshinske, Katerynivske, and others). Late Pleistocene placers are confined to the terrace of the Irsha River (Irshynske deposit, in which the amount of ilmenite is 10 - 100 $kg/m^3$).

In general, placer deposits located of the Volodarsk-Volynsky massif are characterized by: placers are limited to relatively wide, vaguely defined valleys with smooth sides; productive deposits consist of sedimentary formations of different genesis and age; the thickness of the ore-bearing deposit and the amount of ilminite does not change significantly both along the length and across the length of the placer; minerals accompanying ilmenite in placers are no industrial importance.

The formation of exogenous deposits of the Volyn titanium region was influenced by many factors. These are primarily tectonic and paleographic conditions. Thus, in the early Cretaceous, in connection with upward epeirogenic movements, a continental regime was established in this territory. The valleys and depressions of river systems were formed in the large depressional structures of the foundation. In the riverbeds were accumulation of ilmenite-bearing coarse-grained sands of the Irshansk suite. From the second part of the Late Cretaceous to the present time, continental conditions dominated the area. Ilmenite was also accumulated in river valley of Middle Quaternary, Late Quaternary, and modern deposits. And the main thing is the presence of titanium-bearing weathering crusts that were formed on the main rocks of the Volodarsk-Volynsky massif, which do not form deposits of the residual type. These weathering crusts were the source of wear and accumulation of ilmenite in sedimentary deposits of different ages with which placers of this mineral are associated.

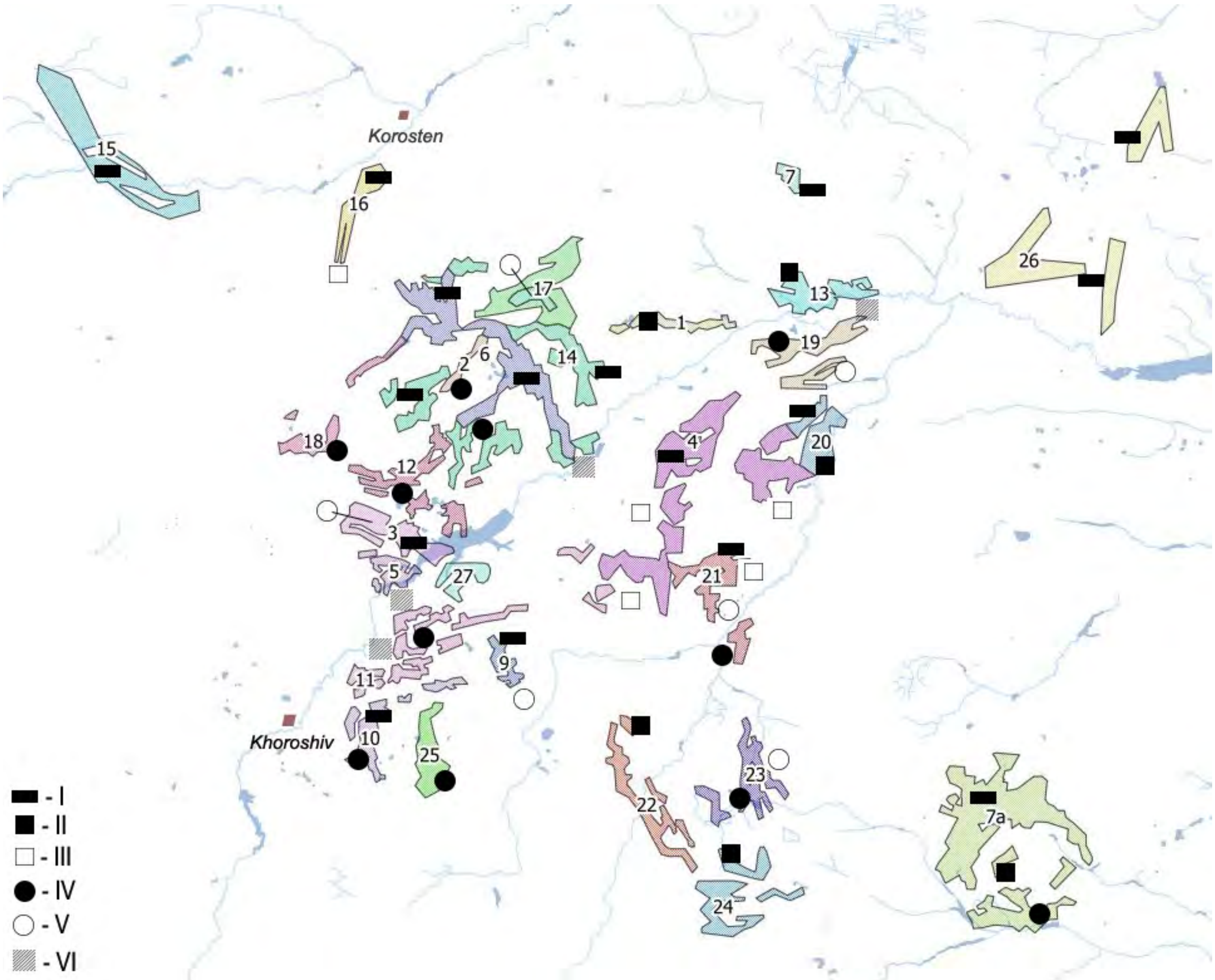


Fig. 1. Overview map of the geological time and paleogeographic conditions of the formation of deposits and placers of the Volyn Placer Region

I – Middle and Late Mesozoic continental deposits and placers in the weathering crust of crystalline rocks; II – Paleogene-Neogene continental deposits and placers; III – marine placers of the Upper Cretaceous; IV – Early and Middle Quaternary alluvial placers (partially undissected); V – Middle Quaternary water-glacial placers; VI – Late Pleistocene and Holocene (modern) placers.

1. Shershnivske; 2. Lemnenske; 3. Verkhnyo-Irshynske (including Katerynivske); 4. Irshynske; 5. Livoberezhne; 6. Northern part of the Lemnenske deposit; 7a. Torchynske; 9. Krasnorichenske; 10. Poromivske; 11. Pravoberezhne; 12. Valky-Gatskivske; 13. Zlobytske; 14. Lemnenske (residual); 15. Ushytskyi placer; 16. Ushomyrskyi placer; 17. Ivanivskyi placer; 18. Stavyshchanskyi placer; 19. Selyshchanskyi placer; 20. Bukinska ilmenite area (Mezhyrichne deposit); 21. Trostyanetska ilmenite area; 22. Ocheretyanskyi placer; 23. Vydybirskyi placer; 24. Fedorivskyi placer; 25. Poromivske deposit; 26. Shevchenkivska area; 27. Kropyvenske deposit.

### References

1. Ganzha, O.A., Kuzmanenko, H.O., Okholina, T.V., Remezova, O.O., Current state of mineral base of titanium deposits of Ukraine, Vol. 99, No. 4, 2022, pp. 60-66. https://doi.org/10.17721/1728-2713.99.08 (in Ukrainian).

2. Ganzha, O., Okholina, T., Kroshko, Yu., Kuzmanenko, H. & Kovalchuk, M. ‘Structural and Lithological Models of Ilmenite Placer Deposits in Ukraine’, Anuário do Instituto de Geociências, 46:55949. 2023, https://doi.org/10.11137/1982-3908_2023_46_55949.
3. Komlyev O.O. Historical and dynamic basin geomorphosystems of geomorphological formations of the Ukrainian Shield: Dissertation of Doctor of Geographical Sciences: 11.00.04. 2011. 523 pp. Kyiv. (in Ukrainian).
4. Kuzmanenko, G.O., Okholina, T.V., Ganzha, O.A., Yaremenko, O.V. Ore yield of the Poromivskoe ilmenite deposit. Mineral Resources of Ukraine, No. 3, 2023, pp. 3-7. https://doi.org/10.31996/mru.2023.3.3-7 (in Ukrainian).
5. Veklich M.F., Dyachenko M.G., Tsymbal S.N. Titanium content of sedimentary deposits on the territory of the USSR (Ukrainian Crystalline Shield). Alluvial titanium deposits of the USSR. M.: Nedra. 1976. 107- 112 pp. (in Russian).

*DOI: https://doi.org/10.30836/igs.iies.2024.30*

**Streltsova I.**

*Institute of Geological Sciences of the National Academy of Sciences of Ukraine, Kyiv, Ukraine.*
*E-mail: ivanna.tit@gmail.com*

# SEISMIC FACIES ANALYSIS OF PERMIAN SEDIMENTS OF PIVDENNO-KHRESTYSCHE AREA (DNIPRO-DONETS BASIN, UKRAINE)

The Pivdenno-Khrestysche area located in the central axial part of the Dnipro-Donets basin (DDB, Ukraine). The DDB is a Late Palaeozoic intracratonic rift basin, with sedimentary thicknesses up to 19 km, displaying the effects of salt tectonics of Upper Devonian salt formation during its entire history, from Late Devonian rifting to the Tertiary. Hundreds of concordant and discordant salt structures formed during this time [3, 4, 6, 7]. There are three evaporite formations in the Dnipro-Donets depression: Upper Frasnian (lower saline stratum), Lower Famennian (upper saline stratum) and Lower Permian Formation. The postrift-platform Lower Permian Formation occupies the larger part of the depression. The depth of the formation base ranges from 50 to 4060 m and its thickness varies from 40 m in the NW to 1737 m in the SE part of the depression. The formation is underlain by the Kartamysh red-coloured terrigenous formation [3, 4]. The study area characterizes by high distribution of Lower Permian sediments that interact with Krestyschensky salt dome. Lower Permian formation is subdivided into two subformations: the rock-salt-bearing Mykytivka-Slovyansk and Kramatorsk K-Mg-salt-bearing ones. The rock-salt subformation, which is up to 1200 m thick, is represented by alternating layers of rock salt (up to 75 m thick), limestones, mudstones, marls, anhydrites and halopelites. The K-Mg-saltsubformation, up to 960 m thick, is composed of rock-salt with anhydrites, salt-siltstones, sandstones and halopelites, as well as K-Mg- and Mg-salt seams. Up to six large-scale cycles are distinguished in this subformation, with halite-siliciclastic rocks and/or anhydrites in the base and with thick rock-salt or salt-siliciclastic bed at the top. The lowest cycles are covered by the aforementioned K-Mg salt and bisschofite seams [3]. The Khrestysche salt structure is a mushroom-shaped dome consisting of Upper Devonian salt formation that penetrates into the Lower Permian formation. Mushroom-shaped diapirs have an overhanging bulb fringed by one or more skirts (peripheral pendant lobes), which can curl inward to form vortices capable of entraining cover rocks to various degrees [5]. The complex history of Lower Permian facies sedimentation and salt dome development lead us to made seismic facies analysis. The goal of this study is presenting new data on structure and tectonic settings of Lower Permian depositional environment and found areas with economic interests using seismic data.

Data and Methodology

The makeup of a seismic image reflects the interaction between the substrate geology and the seismic waves traveling through the rocks, modulated by the physical properties of the rocks. The amplitude, frequency, continuity, terminations, and distribution of reflectors define various seismic facies units, which were subsequently grouped into seismic facies associations defining progradational, retrogradational or aggradational geometries. They are controlled by the rate of accommodation and the sediment supply. In spite of the technological progress, seismic data still provide only indirect information lithology in the subsurface, so calibration with borehole data is essential for fine tuning the seismic facies-lithofacies relationship, for velocity measurements, or for time-depth conversions [1].

This study used 100 km$^2$ 3-D seismic data set. All seismic data are displayed in milliseconds two-way travel time. Wireline-log and stratigraphic data from six boreholes in the basin constrain the composition and age of the salt and its overburden, and checkshot data tie this borehole information to our seismic data.

Results

Six seismic facies units have been differentiated in the Pivdenno-Khrestysche area of the Dnipro Donets Basin (Figure 1). Although the seismic characteristics depend on the seismic acquisition and processing methodology of various seismic data, a general pattern can be established [2]. All of them have special seismic amplitude and frequency characteristics described below (Figure 1). Some of the seismic facies contained rock salt that have special seismic reflection because diapiric salt is typically acoustically transparent. This acoustic characteristic of salt helps us rightly distinguish salt dome.

First three facies units subparallel fairly continuous, subparallel continuous to semicontinuous, parallel continuous (units 1,2 and 3) are characteristic for stable Permian «shallow water» basin with laminated anhydrite-carbonate (formed after bacterial gypsum-carbonate) [3, 4]. This three facies units distributed through all Pivdenno-Khrestysche area. We also can observe flaked Lower Permian salt in the third seismic facies unit. The fourth facies unit represented salt dome and show Devonian salt breakthrough Lower Permian sediments. Oblique (5) facies unit occurs near salt dome steam and it was formed by salt diaper developing. Sub-parallel hummocky facies unit (6) occur near steam, under main bulb, in “pocket” caused by complex geometry of salt dome (Figure 2, red circle). The location of the pocket we can see on the horizontal reflection seismic slice. It situated between two salt walls. Also we can see part of mushroom-shaped salt dome in the left part of seismic section on the Figure 2. The part of seismic section beneath salt dome belongs to Lower Permian strata. The Triassic strata overlaps Khrestysche salt dome.

| Seismic facies unit | Seismic examples | Amplitude and frequency characteristics | Spatial distribution, typical occurence |
|---|---|---|---|
| 1. (Sub-) parallel fairly continuous | 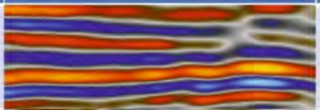 | High amplitude, meduim to high frequency | Occurs beneath salt dome |
| 2. Subparallel continuous to semicontinuous |  | Medium to high amplitude, Low to high frequency | Occurs beneath salt dome |
| 3. Parallel continuous |  | High amplitude, high frequency | Occurs beneath salt dome |
| 4. Chaotic discontinuous |  | Low to medium amplitude | Occurs inside salt dome (central part) |
| 5. Oblique | 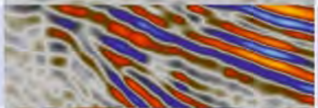 | Variable amplitude, Low to high frequency | Occurs near steam |
| 6. Sub-parallel hummocky |  | High amplitude, meduim to high frequency | Occurs near steam |

Fig. 1. Characteristic seismic facies units used in the seismic sequence stratigraphic interpretation

The most perspective for hydrocarbon prediction are facies units 5 and 6. Oblique (5) facies unit showed positive structure that can contain gas sealed by salt. Sub-parallel hummocky facies unit (6) also trapped by salt and have interesting inner structure that can point to good reservoirs.

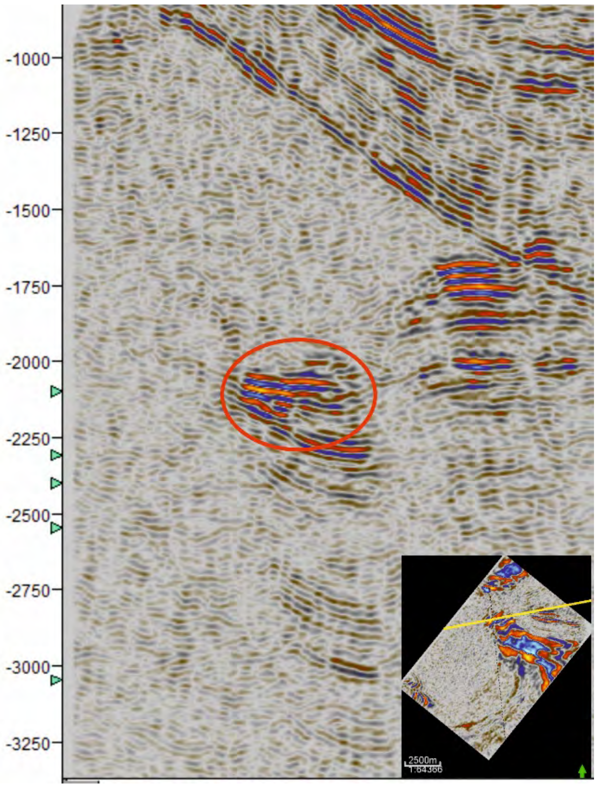


Fig. 2. Reflection seismic section across Krestysche salt dome

The seismic facies analysis helps us to understand depositional environment through Lower Permian time and also to distinguish two possible hydrocarbon traps. Diapiric salt acoustic transparent gave opportunity to outline a complex morphology of the Khrestysche salt dome. This method has to be using with other geological and geophysical methods to make the right conclusion and decision.

*This study was carried out under the funding of the state budget program CPCEL 6541230 in the framework of the R&D Project “Strategic mineral raw materials for the recovery of the economy of Ukraine: analysis of resources and reserves, development of search criteria for increasing their mineral resource base”.*

**References**

1. Catuneanu O. Principles of Sequence Stratigraphy. Cambridge: Elsevier, 2006. 55 p.
2. Balázs, A., Matenco, L., Magyar, I., Horváth F., Cloetingh S. The link between tectonics and sedimentation in back-arc basins: New genetic constraints from the analysis of the Pannonian Basin. Tectonics, 2016. V.35, P. 1526-1559.
3. Shekhunova S.B. Saliferous Formations: Patterns of Lithogenesis and Problems of Usage. Kyiv: Naukova Dumka. 2020. 335 p.
4.Shekhunova S., Stadnichenko S., Siumar N., Aleksieienkova M. The Lower Permian evaporite formation of the Dnipro-Donets Depression (Ukraine): Sedimentary and geochemical peculiarities // Abstract Book of 31* IAS Meeting of Sedimentology, 22-25 June. Kraków: 2015. 480 P.
5. Jackson, M.P.A., Talbot, C.J., Anatomy of mushroom-shaped diapirs. Journal of Structural Geology, 1989, V. 11, P. 211-230.
6. Stovba S.M., Stephenson R.A. Style and timing of salt tectonics in the Dniepr-Donets Basin (Ukraine): implications for triggering and driving mechanisms of salt movement in sedimentary basins. Marine and Petroleum Geology, 2002. V. 19, № 10, P. 1169-1189.
7. Shekhunova S.B. Peculiarities of salt bearing formations postsedimentary changes. Collection of Scientific Works of the Institute of Geological Sciences of the NAS of Ukraine, 2010. V. 3. P. 116-137.

DOI: https://doi.org/10.30836/igs.iies.2024.27

**Antonenko T., Kalinichenko O.**

*M.P. Semenenko Institute of Geochemistry, Mineralogy and Ore Formation of the National Academy of Sciences of Ukraine, Kyiv, Ukraine. E-mail: tetyana_savchenko@ukr.net, okalinichenko@nas.gov.ua*

# THERMAL TRANSFORMATION OF SYNTHETIC LEPIDOCROCITE BY DATA OF TERMEMAGNETOMETRY AND FEROMAGNETIC RESONANCE

The mechanisms of transformation of lepidocrocite (γ-FeOOH) heating under air remain unclear, regardless of numerical studies of thermal transformations of this mineral [1, 2, 3, 4]. Lepidocrocite is lower spread in nature, then goethite (α-FeOOH). The orthorhombic structure of lepidocrocite is formed by the hexagonal layers of $O^{2-}$/$OH^-$ anions, stacked in the [150] direction, $H^+$ ions are located along the line between of two $O^{2-}_{II}$ ions (O – H ··· O), and $Fe^{3+}$ ions occupy octahedral sites [2, 3]. Heating of lepidocrocite under air results, like goethite, in structure dehydroxylation – destruction of OH groups and remove of formed $H_2O$ molecules from the structure [1, 2, 4]. Dehydroxylation of γ-FeOOH, unlike α-FeOOH, occurs in some stages [3]. Initially weakly bound molecular water desorbs, then dehydroxylation results in forming of maghemite (2(γ-FeOOH) → γ-$Fe_2O_3$ + $H_2O$), which transforms to hematite (γ-$Fe_2O_3$ → α-$Fe_2O_3$) [2, 3]. Maghemite (γ-$Fe_2O_3$) forms at lower temperatures, $T$ ≈ 200 – 300 °C, and transform to hematite, α-$Fe_2O_3$ (hexagonal structure), at the temperatures from 350 to 600 °C [1, 2, 4]. The [150] direction of the orthorhombic unit cell corresponds to the [111] direction of a distorted cubic cell, that facilitates lepidocrocite dehydroxylation to the spinel phase – maghemite (Mgh) [2]. The dehydroxylation of lepidocrocite results in forming of aggregations of nanocrystalls (≈ 10 nm) of the cubic maghemite with the disordered distribution of iron vacancies ($V_{Fe}$) [2]. Heating of the cubic maghemite can result to enlarge of crystallites and forming of the tetragonal maghemite (Mgh2) with the ordered $V_{Fe}$ distribution and the relation of $c/a$ ≈ 3 for the lattice parameters [2]. These changes lead to significant changes in the properties, in particularly, to decrease in the Curie temperature from $T_C$ ≈ 650 to 580 °C (≈$T_C$ of magnetite). Lepidocrocite can transform to hematite (Hem) when dehydroxylation occurs very slowly [2].

The aim of the present work was to synthesize of lepidocrocite from the aqueous solution of iron (II) sulfate and to identify of iron oxides formed during the thermal conversion of lepidocrocite using by structural and magnetic methods. Lepidocrocite (Lps) was synthesized by low-temperature precipitation from the aqueous solution and divided into some samples. Some of the obtained samples were heated isothermally at temperatures $T$ = 250 – 550 °C and $T$ = 100 – 800 °C with the 100 °C step exposing for 20 and 60 min at each temperature, respectively. The samples were studied using methods of X-ray phase analysis (XRD), thermomagnetometry (TMA) and ferromagnetic resonance (FMR). Diffractogramms were obtained by the standard methodic using DRON 3M. TMA was performed using the device for measuring the Curie temperature [5] at a heating velocity of 60°/min up to 350 °C, espousing during 5 and 10 min at this temperature and cooling with the same velocity. The saturation magnetization ($M_s(T)$) and the first derivate, $dM_s/dT$ (differential thermomagnetic curve (DTMC)) in the magnetic field of 350 mT in dependence on the temperature were recorded. FMR spectra were recorded on LEXIS-580 spectrometer (Bruker, X-band).

A batch of lepidocrocite was synthesized in the following way, analogously by [3]. There were prepared of 300 ml water solution of iron (II) sulfate, dissolving 16.68 g of $FeSO^4$•$7H_2O$ in water, and 1 M NaOH, dissolving 7 g of NaOH in 250 ml of water. 1M NaOH was added to the iron (II) sulfate solution until pH = 6.7 - 6.9 was approached (the pH value needed for lepidocrocite precipitation), until the dark green color of the solution was obtained. The suspension was aerated with continuous magnetic stirring. The pH and temperature of the suspension were recorded. A small amount of 1M NaOH was added to adjust pH = 6.7 – 6.9, until the suspension color changed to yellow-orange. After the reaction was completed, the precipitate was removed from the suspension and washed with water (50 ml) by centrifuging and dried in a thermostat until an unchanged weight was approached.

XRD showed the following main reflexes of the precipitate: 0.618; 0.328; 0.246 and 0.193 nm. Such values practically correspond to the standard reflexes of lepidocrocite [3]. Heating of Lps for 20 minutes at $T$ = 250 and 350 °C resulted in forming of the X-ray amorphous phase, which transformed into the crystalline hematite at $T$ = 450 and 550 °C, respectively.

TMA showed the following. When the sample was heating the magnetization $M_s$ increased at 200 °C, to the extremum at 280 °C and, after a break, to 350 °C. The exposure for 5 min as this temperature was resulted in the slightly decrease of $M_s$. The cooling curve demonstrated the ferromagnetic (FM) phase with the Curie temperature of$T_C$ = 335 °C and the $M_s$ increase in ≈ 2 times. The magnetization has increased in ≈ 3.5 times, relative to Lps, after the heating/cooling cycle. When the sample was heating TMA with the exposure for 10 min at $T$ = 350 °C showed (Figure 1, a) the extremes of $M_s$ increase: insignificant – at ≈ 220 °C and two main – at 290 and 350 °C, with approximately the same contribution to magnetization. The value of $M_s$ increased by more than an order of magnitude during sample heating, did not change practically during 10 min and continued to increase when the sample was cooling. The value of $M_s$ was been in ≈ 20 times larger, then Lps (the original sample), after cooling. The cooling curve showed appearance of FM phases with $T_C$ = 310 °C (main) and additional phases with ≈ 260 and 200 °C (Figure 1, a).

FM phases were absent up to 350 °C when the heating/cooling velocity was 20°/min without stopping up to 650 °C. The magnetization $M_s$ at this temperature (350 °C) dropped almost to zero. This shows that the heating velocity was low, so the FM phases were forming during the dehydroxylation of lepidocrocite and transformed quickly to hematite.

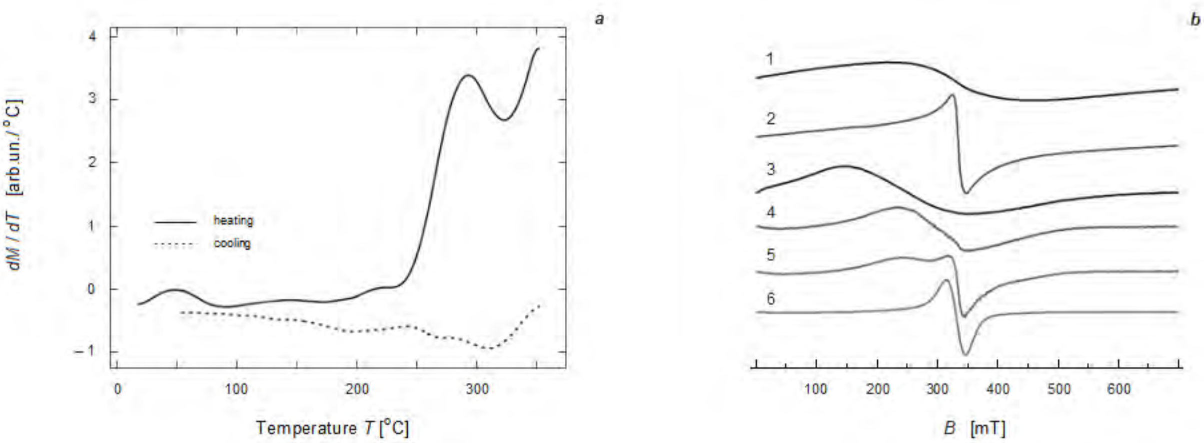


Fig. 1. The study of lepidocrocite Lps: (a) DTMA, (b) FMR spectra (the first derivative of the signal) of the synthesized Lps (1) and after isothermal heat at $T$ (°C) = 200 (2), 500 (3), 600 (4), 700 (5) and 800 (6)

FMR allows establish FM phases [6, 7]. In particularly, the parameters $B_1$, $B_{res}$ and $\Delta B$ of the cubic and tetragonal maghemite ($\gamma$-$Fe_2O_3$) are 270, 300, 80 and 220, 290, 210 mT, respectively [6]. Thus, these maghemites differ significantly by the parameters $B_1$ and $\Delta B$ of FMR signals.

The FMR spectrum (Figure 1, b, Table 1) of the synthesized Lps is presented by the broad band on the resonance magnetic field of $B_{res}$ ≈ 300 mT with the width of $\Delta B$ = 237 mT (curve 1). To clarify the structures of FM phases formed during thermolysis of lepidocrocite, the samples were heated isothermally to 800 °C (with the exposure of 60 min at each temperature).

Table 1. Parameters $B_{res}$, $B_1$, $B_2$ and $\Delta B$ and intensity ($I$) of the FMR spectra of the synthesized lepidocrocite and one after isothermal heat at the listed temperatures

| Parameter | Temperature, °C | | | | | | | | |
|---|---|---|---|---|---|---|---|---|---|
| | **20** | **100** | **200** | **300** | **400** | **500** | **600** | **700** | **800** |
| $B_{res}$ [mT] | 300 | 305 | 305 | 270 | 260 | 255 | 280 | 300 | 305 |
| $B_1$ [mT] | 166 | 155 | 295 | 260 | 220 | 270 | 250 | 290 | 294 |
| $B_2$ [mT] | 413 | 410 | 320 | 390 | 430 | 350 | 360 | 315 | 326 |
| $\Delta B$ [mT] | 237 | 245 | 25 | 106 | 137 | 207 | 117 | 25 | 32 |
| $I$ [rel. un.] | 0.00 | 0.02 | 0.04 | 1.00 | 0.90 | 0.52 | 0.02 | 0.01 | 0.02 |

Note. Parameters of the first derivative of the FMR signal: $B_{res}$ – the resonance magnetic field, $B_1$ and $B_2$ – extremums, $\Delta B = B_2 - B_1$ – the line width

The FMR signal was narrowed substantially with the intensity increase for the sample heated to 200 °C, in addition, the very narrow band was appeared at ≈ $B_{res}$, nearly an order of magnitude smaller in width (curve 2). Heating of Lps up for 300 °C leaded to (Table 1) the intensity increase, the shift to lower magnetic field and the significant broadening of the FMR signal. After heating at 400 and 500 °C (curve 3), the intensity of the signal gradually decreases with the band broadening. Heating of Lps at 600 °C (curve 4) resulted in the shift of the band to the higher magnetic field and division of the signal into two components – wide component ($\Delta B$ ≈ 150, $B_{res}$ ≈ 260 mT) and narrow one ($\Delta B$ ≈ 26, $B_{res}$ ≈ 300 mT). After heating of Lps at 700 °C (curve 5) and 800 °C (curve 6), the narrow component intensity increased gradually, but the wide component intensity droped at 700 °C. This component was absent after heating of Lps at 800 °C.

The narrow component for Lps heated up to 200 °C and the narrower component for the sample heated at $T$ ≥ 600 °C are due to hematite, based on the spectrum parameters [7]. FMR spectrum of Lps heated at $T$ ≤ 200 °C shows the mixture of amorphous phase and hematite, at $T$ = 500 °C – maghemite [6], the component of Hem, moreover, does not appear due to its low intensity. The FMR signals of Lps heated at $T$ = 600 and 700 °C are due to Mgh and Hem.

The comparison of the obtained TMA and FMR data shows that quickly heating of lepidocrocite to 200 °C does not lead to significant changes in its magnetic structure, but hematite forms during slow heating. When Lps was heated slowly to 300 °C, the FM phase formed at $T \approx 280$ °C. The FMR spectrum of this sample after cooling showed appearance of mixture of maghemites differed in structures, most likely, as a result of enlarged of some crystallites. TMA up to 350 °C with the exposure for 5 min showed the formation of the FM phase with the Curie temperature of $T_C = 310$ °C. The cooling curve clearly demonstrated it for the exposure for 10 min (Figure 1, a). This Curie point is significantly lower than that of cubic maghemite ($T_C$ = 650 °C) and tetragonal maghemite ($T_C \approx 580$ °C $\approx T_C$ of magnetite) [2]. This can indicate to Na impurities and the presence of $V_{Fe}$ in tetrahedral sites, which results in significantly reduces of the $T_C$ of maghemite [2].

FMR spectrum of the sample heated at 300 °C (Table) is caused by the cubic maghemite (Mgh1) with the tetragonal one (Mgh2) impurity based on the signal parameters. Content of Mgh2 increases significantly when the temperature of isothermal heating elevates to 400 and 500 °C. The ratios of the contents of different types of maghemites in samples heated in this temperature range are following: Mgh1> Mgh2, Mgh1≥ Mgh2 and Mgh1< Mgh2, respectively. The broadening of the FMR signal and its shifts to lower magnetic field (Figure, b, Table) indicates increase of Mgh2 content. Thus, elevate in the temperature of isothermal heating leads to enlarge of Mgh1 crystals and formation of the Mgh2 structure. Most of the Mgh2 phase is transformed to hematite during Lps heating at $T = 600$ °C. The rest part of this phase remains after heating at 700 °C. Therefore, the inversion temperature to hematite of the phase Mgh1 formed during the dehydroxylation of synthesized Lps and, possibly, containing the Na impurities, is $T_{inv} \approx 800$ °C. This value lies within the range of the inversion temperatures of maghemites of different genesis and origin [2].

Heating of lepidocrocite at 500 °C in the presence of starch (4%) leaded to quick dehydroxylation and partial reduction of the structure to magnetite. Lps heating for 5 min at these condition resulted in formation of the solid solution of Mgh in magnetite (Mag) with the Curie point of $T_C = 570$ °C and phase contents of Mag > Mgh by FMR data. The exposure for 20 min at this temperature resulted in formation of the FM phase with $T_C = 632$ °C, close to tetragonal maghemite (Mgh2) by FMR data.

The present study showed the effectiveness of using of the complex of magnetic methods, thermomagnetometry and FMR, for the identification of ferromagnetic (FM) phases formed during the thermal transformation of synthetic lepidocrocite. It was established that Lps heating up to 280 and 350 °C resulted in formation of two FM phases, the cubic (Mgh1) and tetragonal (Mgh2) maghemites, respectively. The Mgh1 phase is thermally unstable and transforms into hematite. The thermal stability of the Mgh2 phase, which structure close to tetragonal maghemite, possibly, with Na impurities and tetragonal iron vacancies, and the Curie point of $T_C = 310$ °C, is substantially higher: the inversion temperature to hematite is ≈ 800 °C. The comparison of TMA and FMR data shows that the lepidocrocite heating at 500 °C in the presence of starch (4%) leads to the rapid (for 5 min) partial reduction of the structure to magnetite, and the exposure for 20 min at $T = 570$ °C results in formation of the FM phase closed to tetragonal Mgh2. The obtained results can be used to identify maghemite in iron quartzites during their preparation before enrichment.

**References**

1. Cudennec Y., Lecerf A. Topotactic transformations of goethite and lepidocrocite into hematite and maghemite. Solid State Sciences, 2005. V. 7, № 5. P. 520-529.
2. Boer C.B. Rock-magnetic studies of hematite, maghemite and combustion – metamorphic rocks. Proefschrift: Utrecht University. Utrecht, The Netherlands. 1999. 245 p.
3. Guyodo Y., Bonville P., Till J.L., Ona-Nguema G., Lagroix F., Menguy N. Constraining the origins of the magnetism of lepidocrocite (γ-FeOOH): a Mossbauer and magnetization study. Frontiers in Earth Science, 2016. Vol. 4, № 3, article 28. P. 1-9.
4. Gendler T.S., Shcherbakov V.P., Dekkers M.J., Gapeev A.K., Gribov S.K., McClelland E. The lepidocrocite–maghemite–haematite reaction chain – I. Acquisition of chemical remanent magnetization by maghemite, its magnetic properties and thermal stability. Geophysical Journal International, 2005. V. 160, № 3. P.815-832.
5. Yanishpolsky V.V. et al. Device for measuring of the Curie temperature and identifying of magnetic minerals in ores and magnetic materials. 2014. Patent UA 94514 U. (In Ukrainian)
6. Coduri M., Masala P., del Bianco L. et al.. Local structure and magnetism of $Fe_2O_3$ maghemite nanocrystals: the role of crystal dimension. Nanomaterials, 2020. V. 10, Iss.5, 867. P. 1-28.
7. Snisar V.P., Kalinichenko A.M., Bagmut M.M., Ponomar V.P., Kalinichenko O.A., Ovsienko V.V. Thermal oxidation of natural magnetite by data of X-Ray diffraction, magnetometry and ferromagnetic resonance. Proceed. of the 7st International Scientific and Practical Conference "Global and Regional Aspects of Sustainable Development", 6-8 July, 2022, Copenhagen, Denmark. Scientific Collection Interconf., No 115, 2022. C.257-261. (In Ukrainian)

*DOI: https://doi.org/10.30836/igs.iies.2024.28*

**Lunov Ye.S.[1], Lunova I.M.[1], Chernysh D.S.[1], Nissen J.[2]**

*(1) Institute of Geochemistry, Mineralogy and Ore Formation of the National Academy of Sciences of Ukraine, Kyiv, Ukraine. E-mail: lunoeugen145@gmail.com*
*(2) Zentraleinrichtung Elektronenmikroskopie (ZELMI), Technische Universität Berlin, Germany*

# EVOLUTION OF FELDSPARS DURING ALBITIZATION (ON THE EXAMPLE OF THE PERGA DEPOSIT, NW UKRAINE)

Perga beryllium deposit is located in the NW of the Ukrainian Shield (Zhytomyr region). It is situated within the Proterozoic Perga complex, which is connected with the intersection of several deep faults [1]. Geologically it is the part of the Sushchano-Perga zone (SPz). The SPz is composed of various rocks of different ages. Among them, the most widespread are quartzites, disthenic quartzites, greisens, syenites, alkaline syenites, alkaline metasomatites, granites, granite-porphyries, and subalkaline granites [3].

The main ore mineralization of the SPz, including unique beryllium (genthelvite type) deposit, is associated with Perga granites. The ore field is characterized by extensive development of alkaline metasomatites, represented by quartz-feldspar, albite-K-feldspar and biotite-K-feldspar rocks [3]. Since alkaline feldspars are the main forming minerals of ore-bearing rocks and ores, our goal is to investigate the evolution of their composition and structure in the processes of polymetasomatism and the characteristic crystal chemical features of feldspars at different stages of ore formation.

The feldspars from a representative series of 17 samples of metasomatites, mostly from shaft No. 2, were investigated by means of EMPA, XRD, µ-XRF and optical microscopy. Quantitative EMPA were obtained on carbon-coated uncovered thin sections with a field emission electron microprobe JEOL JXA-8530F at ZELMI (TU Berlin). Parameters of the crystal structures of the feldspars were determined using Rigaku SmartLab high-resolution XRD system at TU Berlin. Optical microscopic study of the thin sections was carried out at IGMOF (Kyiv).

Most of the ore-bearing rocks contain two feldspars. K-feldspar, during the process of metasomatism, is replaced by albite with the formation of perthites and further progressive albitization [3]. This transformation with appearance of substitution perthites and their gradual growth into albitites with rare inclusions of resorbed orthoclase grains was studied in details and documented using EMPA and µ-XRF visualization. Both stages of albitization can be observed in Figure 1: the early phase with massive formation of perthites (Fig. 1, a) and the nearly complete replacement of K-feldspar by albite in the late stage (Fig. 1, b).

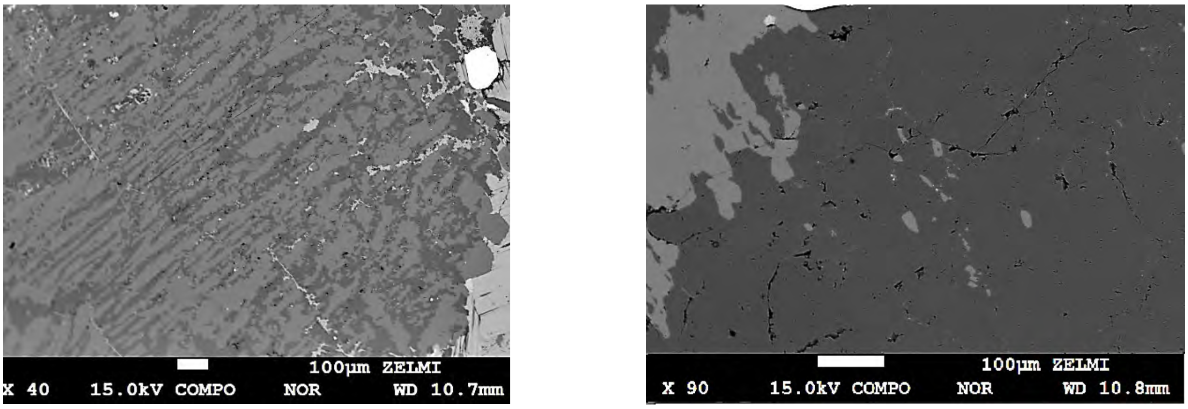


a b

Fig.1. Early (a) and late (b) stages of albitization of K-feldspar in Perga alkali metasomatites

The content of $K_2O$ and CaO in albite varies from 0.02 to 3.8 % and from 0.001 to 0.006 %, respectively. The content of $Na_2O$ in orthoclase ranges from 0.02 to 1.3 %.

According to K. Mehnert [2] the exsolution of primary K-Na-feldspars can occur at solvus temperatures (660-715°C), while crosshatched twinning of microcline formed as a result of rearrangement of earlier monoclinic orthoclase, at temperature not lower than 500°C.

In feldspar-quartz metasomatites formed during albitization, the ZnO content in albite increases sharply from 0.003 to 0.77 % near contacts or in inclusions within dissolved genthelvite crystals. This indicates the replacement of genthelvite by albite, as in the case of simultaneous crystallization of these minerals, all Zn would have been absorbed by genthelvite (Fig. 2).

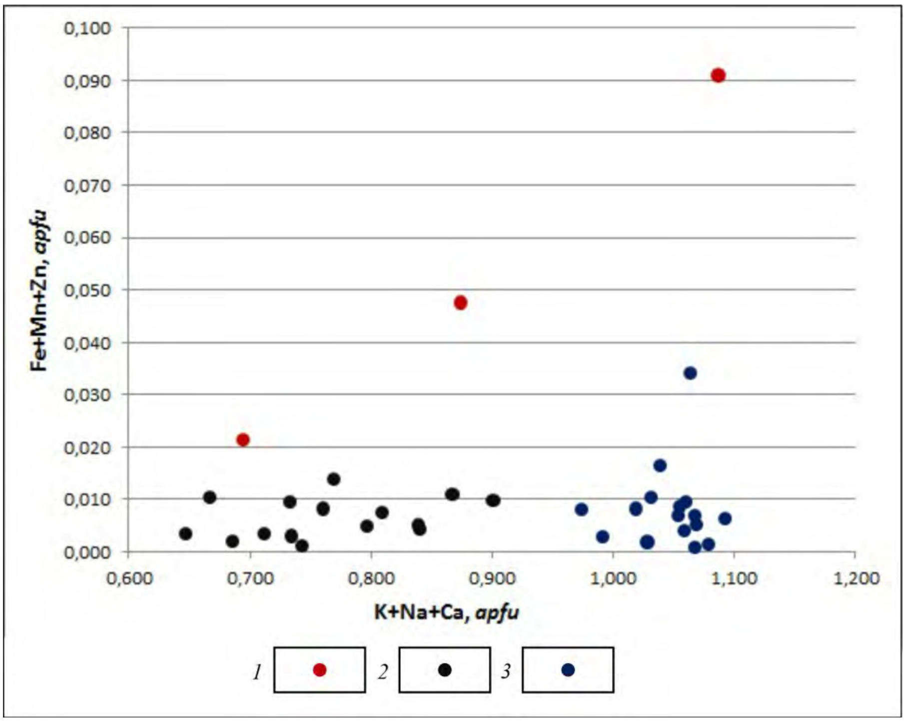


Fig. 2. Crystal chemical features of albite from metasomatites in early and late stages of albitization: relations between K+Na+Ca and Fe+Mn+Zn.
*1* – inclusions and near contacts with genthelvite; *2* – two-feldspar metasomatites (early); *3* – quartz-feldspar metasomatites (late).

The content of FeO in albite varies from 0,003 to 0,96 %, whereas in orthoclase − from 0.005 to 0.44 %. Bright blue amazonite with an elevated Pb content (0.03-0.08 % PbO) is characteristic of the late low-temperature stage of silicification.

Contrary to the previous works [3], our data revealed very insignificant amount of Rb in feldspars. Instead, increased concentrations of Rb were found in micas.

*Acknowledgement. The authors are very grateful to Cordelia Lange for technical assistance in XRD studies and Dr. Vladimir Khomenko for assistance and consultations.*

**References**

1. Bezpalko N.A. Petrolohiya ta aktsesorni mineraly hranitiv ta metasomatytiv Pivnichnoyi Volyni, Nauk. dumka, Kyiv. 1970. 160 p. (in Ukrainian).
2. Mehnert K.R. Migmatites and the Origin of Granitic rocks. Mir, Moscow. 1971. 328 p. (in Russian).
3. Metalidi S.V., Nechaev S.V. Sushchano-Perzhanskaia zona (heolohiia, mineralohiia, rudonosnost), Nauk. dumka, Kyiv. 1983. 136 p. (in Russian).

DOI: https://doi.org/10.30836/igs.iies.2024.20

**Makwela D.[1,2], Imai A.[1]**

*(1) Department of Earth Resources Engineering, Kyushu University, Fukuoka, 819-0395, Japan.*
*Email: makwela.denson.683@s.kyushu-u.ac.jp, imai@mine.kyushu-u.ac.jp*
*(2) Geological Survey Department, P.O Box 27, Zomba, Malawi.*

# PARAGENETIC STAGES OF RARE EARTH ELEMENTS MINERALIZATION AT THE TUNDULU CARBONATITE OF THE CHILWA ALKALINE PROVINCE, MALAWI

There is increased demand for rare earth elements (REEs) due to their use in green technology and supply imbalance [1, 2]. Carbonatites have become target for exploration as they are generally enriched in REEs compared to other igneous rocks [3]. However, carbonatites are fully endowed with their REEs budget during the initial short lived magma intrusion and its enrichment to economic level is commonly associated with hydrothermal or metamorphic events which result in REEs remobilization [4]. We studied Tundulu Carbonatite to characterize its petrogenesis to assess its REEs mineralization potential. We integrated field observation, X-ray diffractometry, optical microscopy and scanning electron microscopy combined with energy dispersive spectroscopy to decipher the textural and mineralogy of Tundulu Carbonatite and establish a paragenetic sequence.

The Tundulu Carbonatite belongs to the Chilwa Alkaline Province of Jurassic to early Cretaceous age. The Tundulu Carbonatite is spatially related to the nepheline syenite. Based on field and petrographic observations, the carbonatite is emplaced as a ring structure with at least two igneous centers [5]. The first center is associated with the initial intrusion that emplaced the medium to coarse grained sovite, and fine to coarse grained carbonatite agglomerate. The second center is associated with the emplacement of fine to medium grained apatite-rich carbonatite, and fine to medium grained siderite carbonatite (Figure 1). From detailed petrographic observation of the samples collected, all carbonatites have variable proportion of carbonates (calcite, siderite, ankerite, strontianite, dolomite and synchysite), silicates (feldspar and biotite), oxides (hematite, pyrolusite and quartz), sulfate and sulfide (barite, pyrite and celestine), phosphate (fluorapatite, apatite) and pyrochlore. Magmatic and hydrothermal processes were responsible for considerable changes in rock texture and mineralogy. Hydrothermal activities were more effective in the second center due to probable multiple brecciation that open more space for low temperature fluid percolation [6].

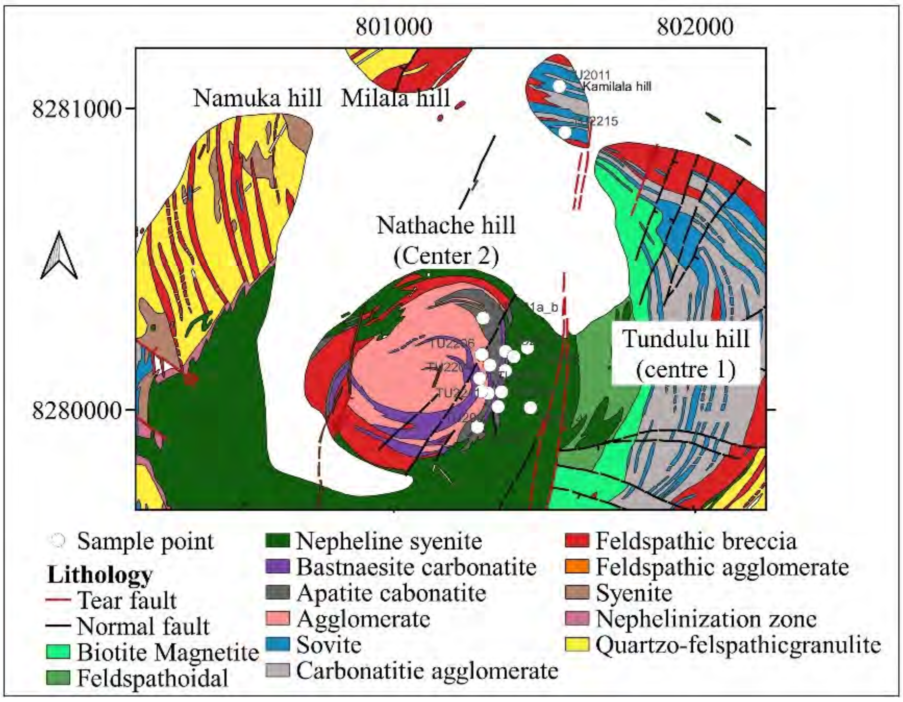


Fig. 1. Geological map of Tundulu Carbonatite showing the main two igneous centers and sample locations (Modified after [5])

Distribution of the ore minerals and micro-texture indicates variation in mineralization stages. The mineralization can be classified as primary and secondary during magmatic and hydrothermal processes, respectively. The primary REEs mineralization of the Tundulu Carbonatite characterized by calcite with comb texture and subhedral elongated apatite, synchysite occurred with syntaxial crystal intergrowth in hexagonal pseudomorphs associated with strontianite and barite [7] (Fig 2a-b). The secondary REEs mineralization is characterized by euhedral fluorapatite with dissolution texture and recrystallization that occurred as clear rim, associated with brecciated ankerite; synchysite occurs in interstitial between spaces of quartz and apatite, or overprinted hydrothermal quartz and recrystallized calcite [6] (Figure. 2c-d). The secondary minerals formed because of dissolution of carbonates and apatite as well as redistribution of REEs due to low temperature fluids that reacted with the solidified carbonate. The REEs mineralization paragenetic stages is shown in Fig. *3*.

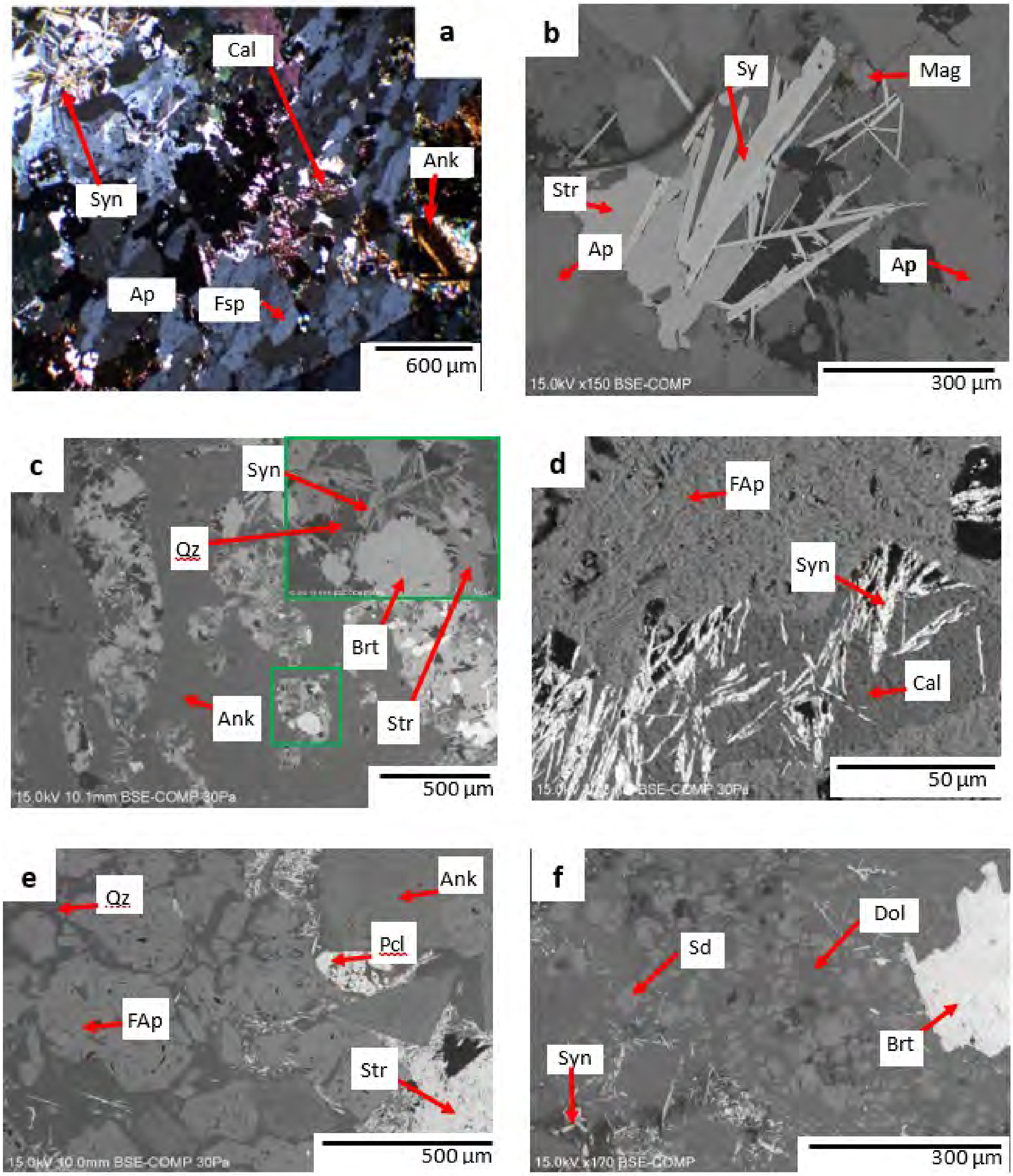


Fig. 2. Photomicrograph and back scattered electron images of samples from the Tundulu Carbonatite. (a -b) magmatic synchysite with syntax texture, subhedral elongated apatite and calcite with comb texture in soviet carbonatite (c) magmatic synchysite with syntax texture in association with strontianite and barite in

hexagonal pseudomorph in apatite-rich carbonatite, (d) re-crystallized calcite with inclusion of synchysite with fibrous texture in apatite-rich carbonatite, (e) Synchysite with fibrous texture inclusion in hydrothermal quartz in association with strontianite and apatite with dissolution texture in apatite-rich carbonatite, (f) Synchysite that overgrew dolomite that replaces siderite in siderite-rich carbonatite. Abbreviations: AFp, fluorapatite. Cal- calcite, Syn- synchysite, Qz- quartz, Pcl- pyrochlore, Str- strontianite, Brt- barite, Fsp- feldspar.

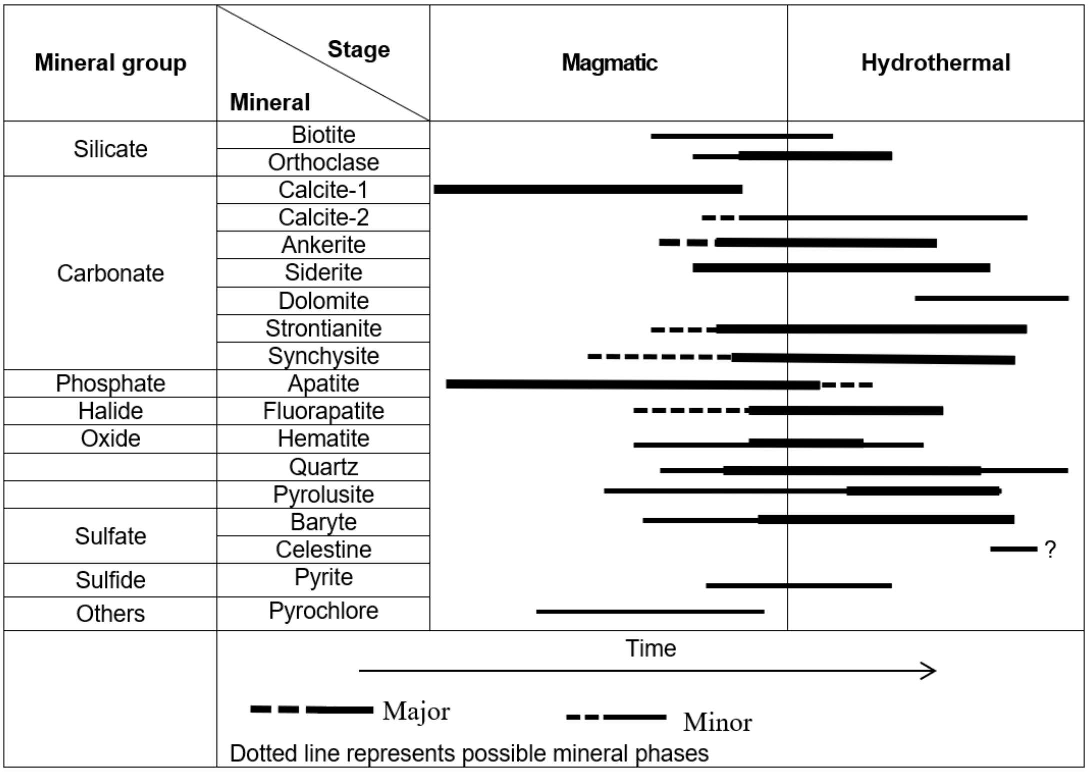


Fig. 3. REEs mineralization paragenetic sequence

*This works was supported by the Japan International Cooperation Agency (JICA). Special mention to member of the Economic Geology laboratory of Kyushu University for their support.*

**Reference**

1. Dushyantha, N., Batapola, N., Ilankoon, I. M.S.K., Rohitha, S., Premasiri, R., Abeysinghe, B., Ratnayake, N., Dissanayake, K. The story of rare earth elements (REEs): Occurrences, global distribution, genesis, geology, mineralogy and global production, Ore Geology Reviews, Vol. 122, 2020. 103521 p.
2. Wang, P., Yang, Y.Y., Heidrich, O., Chen, L.Y., Chen, L., Fishman, T., Chen, Wei, Q. Regional rare-earth element supply and demand balanced with circular economy strategies, Nature Geoscience, Vol. 17, 2024. pp. 94-102.
3. Woolley, A.R., Kempe, D.R.C. Carbonatites: Nomenclature, average chemical compositions, and element distribution. In Bell, K. Ed, Carbonatite: Genesis and Evolution, 1st ed., London, UnwinHyman, 1989, pp. 1–13.
4. Anenburg, M., Broom-Fendley, S., Chen, W. Formation of rare earth deposits in carbonatites, Elements, Vol. 17, №. 5, 2021, pp. 327-332.
5. Garson, M.S. The Tundulu Carbonatite ring-complex in Southern Nyasaland, Memoir 2, Government Printer, Zomba, 1962. 235p.
6. Broom-Fendley, S., Styles, M.T., Appleton, J.D., Gunn, G., Wall, F. Evidence for dissolution-reprecipitation of apatite and preferential LREE mobility in carbonatite-derived late-stage hydrothermal processes, American. Mineralarogist., Vol. 101, №. 3, 2016. pp. 596-611,
7. Dalsin, M.L., Groat, L.A., Creighton, S., Evans, R.J. The mineralogy and geochemistry of the Wicheeda Carbonatite Complex, British Columbia, Canada, Ore Geology. Reviews., Vol. 64, 2015. pp. 523-542.

DOI: https://doi.org/10.30836/igs.iies.2024.7

**Alpert S.**

*Scientific Centre for Aerospace Research of the Earth of the Institute of Geological Science of the National Academy of Sciences of Ukraine, Kyiv, Ukraine. E-mail: sonyasonet87@gmail.com*

# APPLICATION OF THE MODERN METHODS OF PROCESSING REMOTE SENSING DATA FOR SOLVING ECOLOGICAL PROBLEMS

Nowadays solution of different ecological problems, such as assessment of forests, water quality modeling, mapping of petroleum pollutions includes of an application of Remote Sensing (Figure 1). High resolution remote sensing hyperspectral images provide an important information about structure and details of objects. The procedure of hyperspectral image classification is a most important and difficult problem.

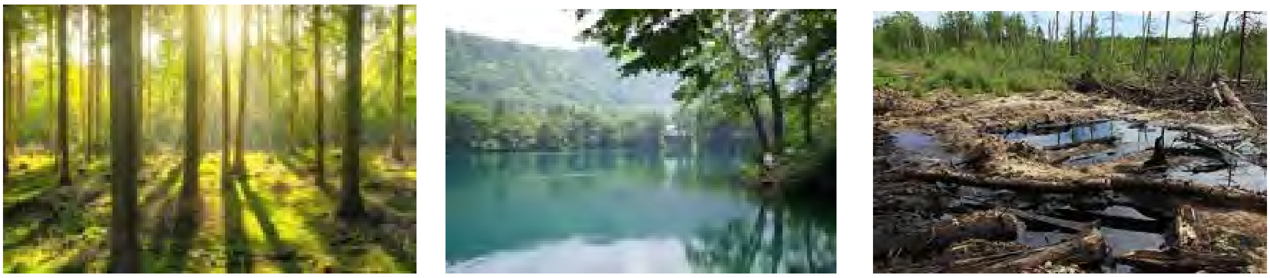

Fig. 1. Ecological tasks, that apply hyperspectral satellite images: assessment of forests, water quality modeling and petroleum pollutions

The main aim of this work is to consider the new hyperspectral image classification method, applying Normalized difference vegetation index (NDVI), Dempster-Shafer theory and Yager's combination rule. Consider the proposed classification algorithm using the following example. Suppose we have a territory on which the following classes are present: green vegetation, man-made objects, open soil, sand, roads, petroleum pollutions, water.

Our task is to determine the area with petroleum pollutions. Then we should identify and map these petroleum pollutions for conducting environmental monitoring of this studied area. The proposed method consists of two steps.

At the first step we apply NDVI and at the second step we apply main concepts of Dempster-Shafer theory and Yager's combination rule for mapping petroleum pollutions. Application of NDVI is the first step of classification procedure. At this step we can create mask based on NDVI and reduce the number of classes. This procedure reduces the volume of data and facilitates further calculations.

The NDVI is a dimensionless index, that describes the difference between visible and near-infrared reflectance of vegetation cover. Vegetation index can be used to estimate the density of green vegetation. NDVI will increase in proportion to vegetation growth [1-3].

The NDVI is calculated from these individual measurements as follows:

$$NDVI = \frac{NIR - RED}{NIR + RED}, \tag{1}$$

where $NIR -$ spectral reflectance measurement acquired in the near-infrared region,

$RED -$ spectral reflectance measurement acquired in the red (visible) region.

The NDVI takes on values between -1 and 1.

Let's note, that different values of NDVI correspond to different classes of objects, such as: soil, water, roads, sand, green vegetation, petroleum pollutions.

If $NDVI = 1,$ we have an area with dense, healthy vegetation.

If $NDVI = 0,$ we have an area with nothing growing in it.

If $NDVI < 0,$ we have a lack of dry land.

Let's note, that NDVI takes on values between 0,2 and 0,8 for green vegetation, NDVI takes on values between -0,3 and 0,2 for man-made objects, open soil, sand, roads. If $NDVI < -0,3,$ we have water objects.

NDVI takes on values between -0,25 and 0,15 for *petroleum pollutions.*

Then we form a mask based on the calculated values of the NDVI for the original image. This procedure excludes from further analysis all areas on the image for which the values of the NDVI index are outside the range [-0.25; 0.15]. Applying this procedure we exclude areas of forest, grass, bushes and water bodies. Then remaining objects can be divided into a smaller number of classes: *petroleum pollutions,* buildings and roads, water.

At the second step we describe main concepts of Dempster-Shafer theory (generalization of probability theory) and Yager's combination rule for classification hyperspectral image.

In Dempster-Shafer theory, with every hypothesis $A$ $\left(A \in 2^{\Omega}\right)$ there is associated basic mass (basic probability assignment) $m\left(A\right)$ [3-5]. The $m\left(A\right)$ mass value represents the degree of belief allocated to the hypothesis *A*. This mass *m* belongs to the interval [0, 1].

Let's note, that mass *m* also satisfies the such conditions:

$$\sum_{A \subseteq 2^{\Omega}} m\left(A\right) = 1; \quad (2)$$

$$m\left(\varnothing\right) = 0 .$$

Suppose the first source appointed to the hypothesis *A* a mass value $m_1$, and the second source independently appointed to the same hypothesis *A* a mass value $m_2$.

Yager's combination rule can can deal with highly conflicted information sources and process conflicting information [5-7]. Yager's combination rule assigns the masses of intersections of conflicting sets, which create an empty set in the intersection, to the base set. Non-null mass of the empty set is generally distributed among the elements of the frame of discernment.

Yager's combination rule is defined as:

$$m(A) = \sum_{B_1 \cap B_2 \cap \ldots \cap B_n = A} \prod_{1 \le i \le n} m_i(B_i), \ A \ne \varnothing, \ \theta, \quad (3)$$

where $\theta$ – set of hypotheses about membership of pixel (frame of discernment), $2^{\theta}$ – total number of subsets of the $\theta$, $m(\varnothing) = 0$,

$$m(\theta) = \sum_{B_1 \cap B_2 \cap \ldots \cap B_n = \theta} \prod_{1 \le i \le n} m_i(B_i) + K, \quad (4)$$

$$K = \sum_{B_1 \cap B_2 \cap \ldots \cap B_n = \varnothing} \prod_{1 \le i \le n} m_i(B_i). \quad (5)$$

The *K* is called the conflict coefficient. This coefficient reflects the degree of conflict among the sources. The range of values of the K lies within the interval [0, 1]. The more contradictions we have, the closer is the *K* value to 1. Zero value of conflict coefficient indicates the absence of contradictory assessments of the sources.

Consider an numerical example, where we determine the class of the pixel (object) $\pi_n$, applying basic probability assignments and Yager's combination rule. Suppose, that frame of discernment is $\theta = \left\{P, B, W\right\}$, where hypothesis $P$ means, that sample belongs to class "Petroleum pollution", hypothesis $B$ means, that sample belongs to class "Buildings and roads", hypothesis $W$ means, that sample belongs to class "Water".

Suppose, we have two spectral bands. The sensors provide two bodies of evidence $m_1$ and $m_2$, respectively:

$$m_1\left(\left\{P\right\}\right) = 0,6; \ m_1\left(\left\{W\right\}\right) = 0,2; \ m_1\left(\left\{P, B\right\}\right) = 0,2.$$

$$m_2\left(\left\{W\right\}\right) = 0,1; \ m_2\left(\left\{P, B\right\}\right) = 0,5; \ m_1\left(\left\{P, W\right\}\right) = 0,4.$$

The combination *m* can be obtained, applying Table 1.

Table 1. Yager's combination rule

| Basic probability assignment $m_1$ and $m_2$ | $m_1(\{P\})$ 0,6 | $m_1(\{W\})$ 0,2 | $m_1(\{P,B\})$ 0,2 |
|---|---|---|---|
| $m_2(\{W\})$ 0, 1 | $\varnothing$ 0,06 | $\{W\}$ 0,02 | $\varnothing$ 0,02 |
| $m_2(\{P,B\})$ 0,5 | $\{P\}$ 0,3 | $\varnothing$ 0,1 | $\{P,B\}$ 0,1 |
| $m_2(\{P,W\})$ 0,4 | $\{P\}$ 0,24 | $\{W\}$ 0,08 | $\{P\}$ 0,08 |

Then we define basic probability assignments and determine maximum value of basic probability assignments:

$m(\{P\}) = 0,6 \cdot 0,5 + 0,6 \cdot 0,4 + 0,2 \cdot 0,4 = 0,62$ – basic probability assignment, that sample belongs to class "Petroleum pollutions";

$m(\{W\}) = 0,2 \cdot 0,1 + 0,2 \cdot 0,4 = 0,1$ – basic probability assignment, that that sample belongs to class "Water";

$m(\{P,B\}) = 0,2 \cdot 0,5 = 0,1$ – basic probability assignment, that sample belongs to the class "Petroleum pollution" or "Buildings and roads".

$$m(\{\varnothing\}) = 0,6 \cdot 0,1 + 0,2 \cdot 0,5 + 0,2 \cdot 0,1 = 0,18.$$

Applying Yager's combination rule, we can make conclusion, that sample belongs to class "Petroleum pollutions".

A new classification method, based on NDVI and Yager's combination rule was proposed in this work. It was shown, that this method consists of two steps. Application of NDVI is the first step of classification. It also was noted, that different values of NDVI correspond to different classes of objects. Analyzing different values of the NDVI, we can select special classes, that we need. After application of Vegetation Index Yager's combination rule can be used for further classification. Main advantages of this combination rule were described in this work.

It was noted, that Yager's combination rule can process incomplete and conflicting data. Yager's combination rule has the advantage of simple calculations too. It was considered an numerical example, where NDVI and Yager's combination rule were applied for detection and mapping of petroleum pollutions. Application of this new proposed classification method can be applied in ecological monitoring, assessment of forests, mapping of petroleum pollutions and other practical tasks [7-8].

**References**

1. Crippen R.E. Calculating the Vegetation Index Faster. Remote Sensing of Environment, 1990. Vol 34. P. 71-73.
2. Abidi M.A., Gonzalez R.C. Data Fusion in Robotics and Machine Intelligence. New York: Academic, 1992. P. 562-569.
3. Alpert S. A new approach to applying the discount rule in hyperspectral satellite image classification. Management of Development of Complex Systems, 2020. Vol. 43. P. 76-82.
4. Popov M., Alpert S., Podorvan V., Topolnytskyi M., Mieshkov S. Method of Hyperspectral Satellite Image Classification under Contaminated Training Samples Based on Dempster-Shafer's Paradigm. Central European Researchers Journal, 2015. Vol.1, № 1. P. 86-97.
5. Shafer G. A Mathematical Theory of Evidence. Princeton. NJ: Princeton University Press, 1976. P. 875-883.
6. Yager R. On the Dempster-Shafer Framework and New Combination Rules. Information Sciences, 1987. Vol. 41. P. 93-137.
7. Alpert S.I. A new band selection method for multispectral data based on criterion function of information capability. Management of Development of Complex Systems, 2023. Vol. 53. P. 23-29,
8. Alpert S.I. Data combination method in Remote Sensing tasks in case of conflicting information sources. Ukrainian Journal of Remote Sensing, 2021. № 8(3). P. 44-48.

DOI: https://doi.org/10.30836/igs.iies.2024.37

**Arradj S.E., Chabou M.C.**

*Emerging Materials Research Unit (EMRU), Department of Earth and Universe Sciences, Farhat Abbas University, Algeria. E-mail: sifeddine.arradj@univ-setif.dz*

# LITHOLOGICAL DISCRIMINATION OF PHANEROZOIC MAGMATIC FORMATIONS IN THE DJANET TERRANE USING LANDSAT 9 AND SENTINEL 2 MSI SATELLITE IMAGE PROCESSING

The Saharan Platform in Algeria stands as a focal point for the investigation of magmatic events spanning the Phanerozoic era. While certain occurrences have received extensive scrutiny, such as the Triassic-Liassic magmatism linked to the opening of the Central Atlantic Ocean in southwestern Algeria, or the Cenozoic magmatism in the Hoggar region, others remain shrouded in limited understanding. Notably, the Paleozoic intrusive magmatic activities occurring in sedimentary basins situated east and south of the Targui Shield, along the western boundary of the Murzuq Basin, represent a prime example of such enigmatic phenomena [1].

To address these knowledge gaps, advanced remote sensing techniques were judiciously employed, leveraging multispectral satellite imagery obtained from various sensors, including the Landsat-9 Operational Land Imager (OLI) and the Sentinel-2 MultiSpectral Instrument (S2-MSI). The imagery underwent meticulous processing, including a spectral sampling of different geological formations based on fieldwork (Figure 1) and resampling to a spatial resolution of 10 meters and subsequent creation of an image stack.

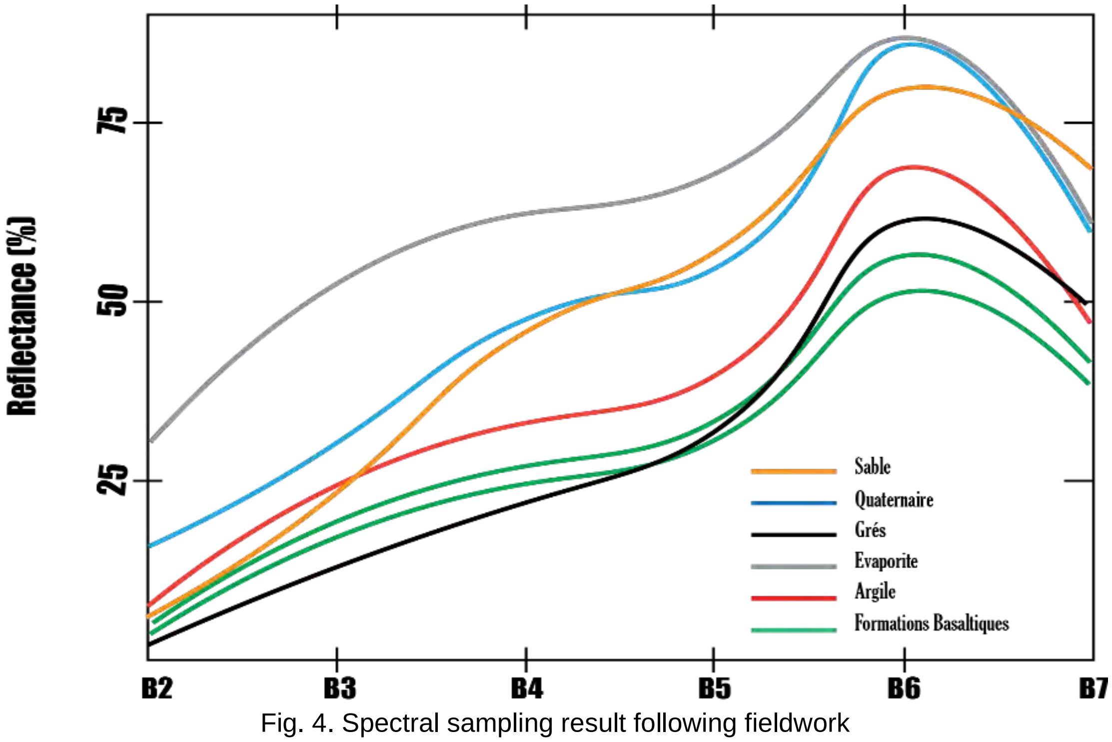


Fig. 4. Spectral sampling result following fieldwork

The Optimum Index Factor (OIF) served as a cornerstone in discriminating between magmatic rocks and sedimentary formations. By judiciously selecting specific bands from Landsat-9 and Sentinel-2 imagery – namely, Sentinel-2 band 4 (SB4), Landsat-9 band 6 (LB6), and Landsat-9 band 7 (LB7) – an optimal false-color combination was derived (Figure 2), facilitating enhanced visualization and discrimination of geological formations [2].

We utilized the Band Ratio algorithm integrated into the ENVI 5.3 software to map the magmatic formations. The combination (R: LB7/SB3, G: LB6/SB3, B: SB4/SB3) proved to be the most suitable. To ensure a clear interpretation of the results, we employed two algorithms integrated into the MNF software (Minimum Noise Factor) and IC software (Independent Component) [3].

In Figure 3, the extent of the Arrikine sill, notably to the north, is compared to Figure 2 where it appears in a dark violet hue. It is also worth noting a certain continuity of the sill to the southwest of the study area, as seen in Figure 4 and Figure 5. Fieldwork did not reveal this continuity; instead, it showed intense hydrothermal alteration in the periphery of the Silurian sedimentary formations around the sill, similarly in the southwest area.

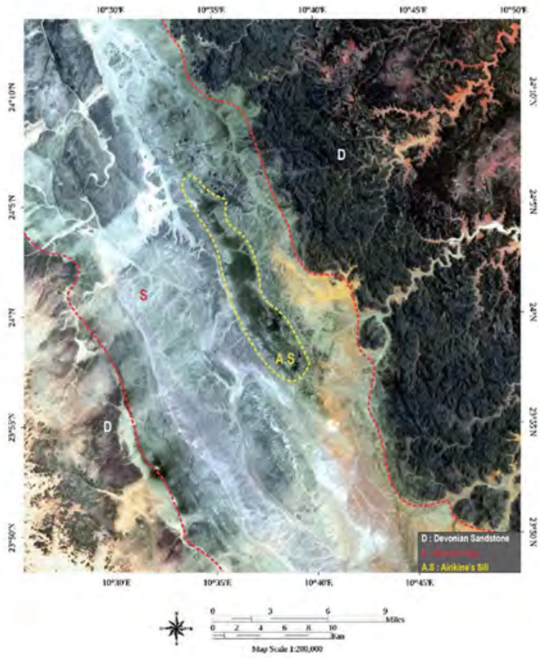


Fig. 2. Natural colors R: SB4, G: SB3, B: SB2

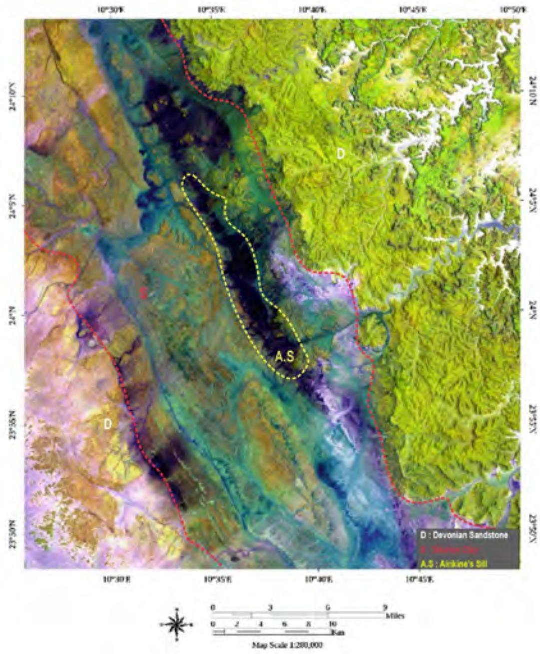


Fig. 5. Optimum index factor RGB (R: LB7 (Landsat 9), G: LB6 (Landsat 9), B: SB4 (Sentinel 2)

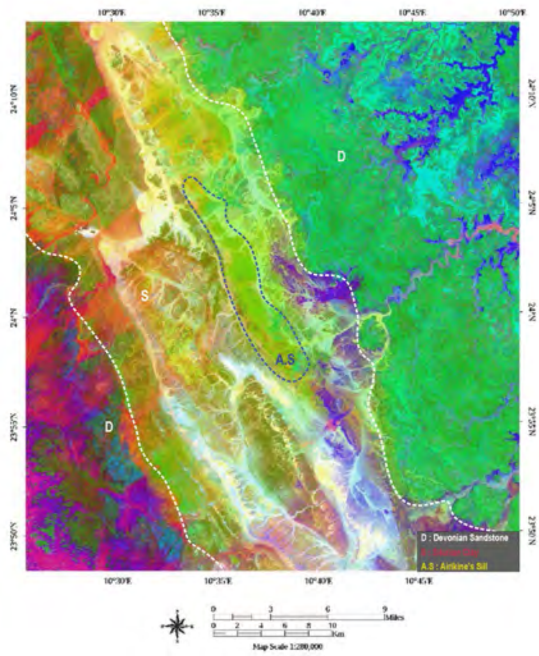


Fig. 4. Independent Component Analysis (ICA)

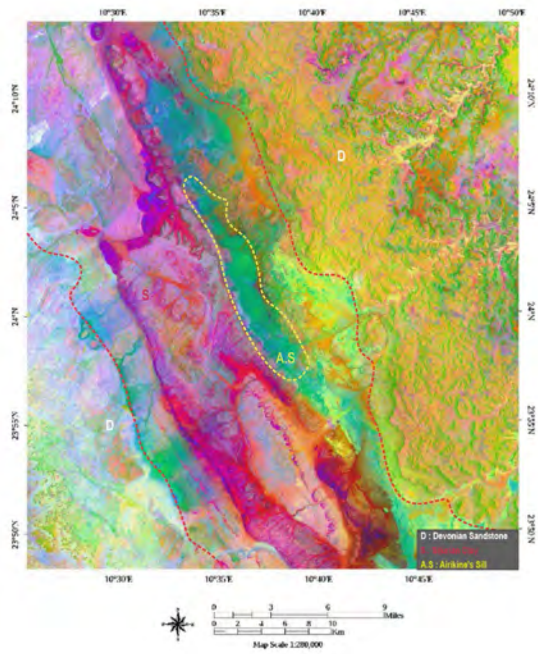


Fig. 5. Band Ratio (R: LB7/SB3 G: LB6/SB3 B: SB4/SB3)

The discovery of basaltic magmatism, exemplified by the Arrikine sill within the Silurian sedimentary formations along the western border of the Murzuk Basin in southeastern Algeria, has heralded a new era of insights into the Phanerozoic magmatic evolution of the Eastern Hoggar region. Recent advancements in multispectral satellite imagery, particularly those stemming from Landsat-9 and the Sentinel-2 MultiSpectral Instrument (S2-MSI), have significantly facilitated the mapping of this geological feature with unprecedented detail and precision.

## References

1. M.E.M. Derder, S. Maouche, J.P. Légeois, B. Henry, M. Ammena, A. Ouabadi, H. Bellon, O. Burguier, B. Bayou, R. Bestandji, O. Nouar, H. Bouabdallah, M. Ayach et M. Beddiaf. Descovery of a Devonian mafic

magmatism on the western border of the Murzuk basin (Sahara metacraton): paleomagnetic datind and geodynamical imlications; Journal of African Earth Sciences; 2016.
2. Bhattacharjee Debdip; Optimum Index Factor (OIF) for Landsat data: a case study on Barasat Town, west Bengal, India. International Journal of Remote Sensing & Geoscience, 2013.
3. Silvia Marchesi, Lorenzo Bruzzone; ICA and kernel ICA for change detection in multispectral remote sensing images. IEEE International Geoscience and Remote Sensing Symposium; 2009.

DOI: https://doi.org/10.30836/igs.iies.2024.23

**Frolov G.[1], Azimov O.[2]**

*(1) Institute of Geological Sciences of the National Academy of Sciences of Ukraine, Kyiv, Ukraine. E-mail: saintmer4ant@gmail.com*
*(2) State Institution «Scientific Centre for Aerospace Research of the Earth of the Institute of Geological Sciences of the National Academy of Sciences of Ukraine», Kyiv, Ukraine. E-mail: azimov@casre.kiev.ua*

# APPLICATION OF DIGITAL METHODS OF PROCESSING SATELLITE ALTIMETER DATA FOR RESEARCHING THE DYNAMICS OF SEA SURFACE CHANGE

The method of satellite altimetry as a relatively new approach of high-precision satellite imaging provides various fields of Earth sciences with the most complete information about the state of the ocean and its changes over time, which is used, in particular, in scientific research in geology, geodesy, oceanography and climatology [1, 11-15].

Satellite altimetry is one of the active methods of remote sensing of the surface from a spacecraft. It is basically a technique for measuring height. Satellite radar altimetry measures the time taken by a radar pulse to travel from the satellite antenna to the surface and back to the satellite receiver. Moreover, this measurement yields a wealth of other information that can be used for a wide range of applications [5, 12-14].

According to [3], sea surface heights, measured by satellite altimeters, can be converted to gravity anomalies. Gravity anomaly differences and characteristics between basins reflect variations in crustal thickness, basement properties, depth, stratigraphic framework, and overlying cover strata structures. Therefore, usage of altimetry data provides us with an opportunity to develop a much higher resolution gravity map for all offshore areas of the world. Such a detailed map might allow us to explore and map hydrocarbon locations for profitable oil and gas extraction.

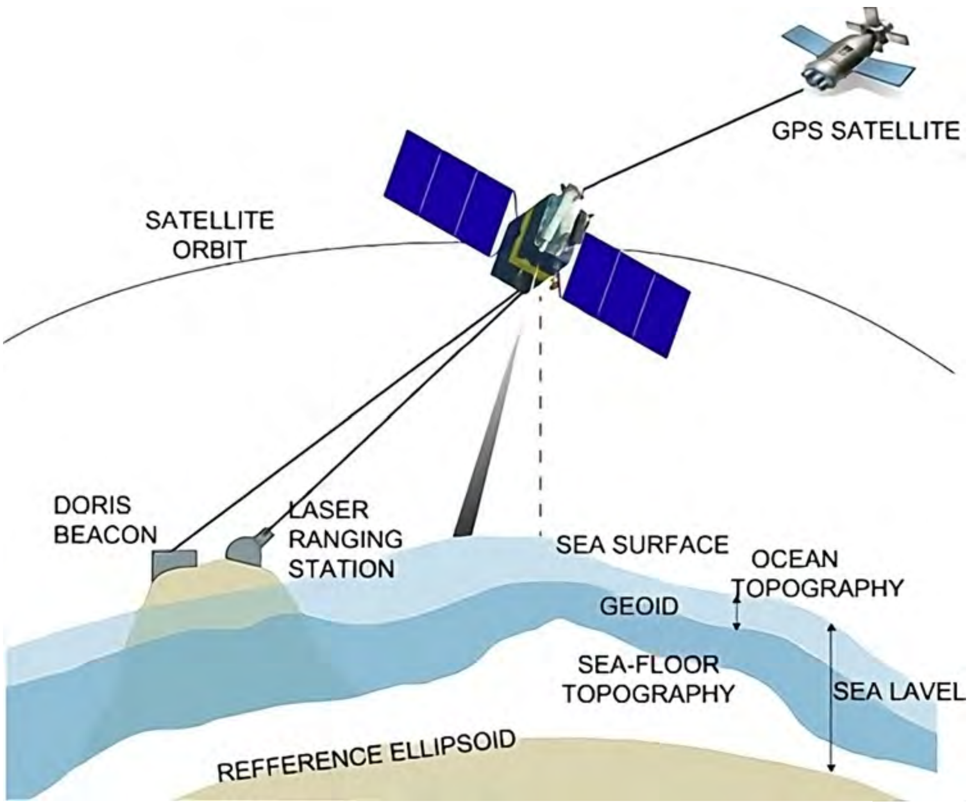


Figure 1. The essential principles of a satellite altimeter measuring system (according to [9])

A satellite altimetry system includes a radar to measure the height of a satellite above the earth's surface and a tracking system to determine the height of a satellite in a geocentric coordinate system. The system measures the sea level rise relative to the center of mass of the Earth. Thus sea surface form can be obtained.

The distance from the satellite to the underlying surface is calculated by the return time of the probing radio pulse, which makes it possible to determine the height of the sea surface.

There is a large number of altimetric satellites in outer space. All of them have sufficient accuracy to investigate the marine geoid and the influence of underwater relief elements on it.

The following key reference surfaces are used for the analysis of altimetric observations:

1. Geoid - model of global mean sea level that is used to measure precise surface elevations.

2. Mean sea surface (MSS) - the long-term average of the sea surface height (at least over one year). It is determined by averaging sea surface heights over a certain period of time, minus tidal forces.

MSS is generally derived by direct interpolation of the averaged sea surface height (SSH) observations or the along track SSH gradients using various sophisticated interpolation techniques [4]. The accuracy of the MSS determination has improved significantly over time due to the increase in the number of observations, improvements made in satellite orbit determination, etc. Throughout the history of the development of altimetry, an increase in the averaging period can be observed, which leads to a decrease in the influence of interannual fluctuations of the sea surface level on the results of observations.

Early altimetry products had a 7-year MSS calculation period, while modern altimetry datasets have a 20-year MSS calculation period [1].

Satellite altimetry provides us with data about sea surface heights (SSH). Sea level anomalies (SLA) represent the height of the water surface above the MSS at some point in time in the specified region. They are analyzed to study the dynamics of changes in sea surface level [2, 12-14].

$$SLAN = SSH - MSSN$$

Operational oceanography systems are heavily dependent on near-real-time sea surface height data from multiple satellite missions. In recent years, significant progress has been made in the development of high-quality altimetry products and many improvements have been made, primarily related to data processing algorithms and the timeliness of their acquisition.

Certain errors cannot be removed by calibration. These are classed as either random or bias errors. Let us dwell on a number of the main causes of errors in measurements, which to one degree or another affect the accuracy of the initial data, as well as methods for reducing their influence on research results:

1. Global ocean tidal atlases are used in order to provide altimetry missions with tidal de-aliasing correction at the best possible accuracy. The satellite data for the global tide model are based on data from four altimetry satellites. These satellites observe the distance between the satellite and the sea surface averaged over a region of 5 km along pre-selected ground tracks, and have done so for years at regular intervals [6].

2. Atmospheric delays are caused by the water vapor present in the atmosphere. To some extent, this effect is corrected using the measurements of the radiometer instrument on board the altimetry satellites. It's called a wet tropospheric correction (WTC). However, a large uncertainty is associated with these measurements. For further reduction of its impact on altimetry data, highly stable water vapor climate data records can be used. These can be obtained from independent microwave radiometer (MWR) measurements on board meteorological satellites [7].

3. Orbit errors in processing of satellite altimeter data are caused largely by inaccuracy of the gravity model which is required for the computation of the trajectory of the spacecraft. To reduce impact of such errors minimization of the crossover differences of profiles measured by the altimeter radar is required.

4. Instrument noise is mixed with oceanic SSH signals in altimetry measurements. According to [8], using nearly simultaneous observations from two altimeters, the white noise level of altimeter instrument noise was best estimated from the SSH spectral values at wavelengths of 25–35 km. The white noise spectrum can simply be subtracted from the SSH wavenumber spectrum to minimize the effects of instrument noise in the spectral estimates.

Nowadays, SSH are provided along-track for all available satellite altimetry missions. All measurements are already corrected by the most actual geophysical corrections. Moreover, as the data of all missions have been carefully harmonized and cross-calibrated in advance, it should be possible to merge and combine SSH of any mission in order to improve the spatial and temporal resolution.

Satellite altimetry has become an indispensable instrument in the observing climatological changes of the World Ocean's surface heights and the largest ice shields of Greenland and Antarctica. Altimetry observations of sea level are the only source of information that allows us to remotely display the subsurface state of the ocean. The use of results of such observation proves useful when it is necessary to quantitatively assess the consequences of climate change or when conducting geological, geophysical surveys, etc.

Tides, atmospheric delays, orbit determination and instrumental noise are the most notable sources of negative impact on the accuracy of altimetry data. Each of them require a special approach to be dealt with (i.e. to reduce its influence on research results).

Numerous studies have proved the connection between low-amplitude local anomalies of gravity and magnetic field with oil and gas deposits in both platform and geosynclinal areas [10]. Altimetry data can be converted to gravity anomalies, which allow us to better localize and track trap structures within potential hydrocarbon basins.

Recently, within the framework of scientific research, methods have been developed to reduce the influence of the main sources of errors on the accuracy of source data in general, and research results in particular. Combining different methods for processing altimetry data can allow us not only to better directly measure sea surface heights, but also to improve the accuracy of gravity model maps, etc.

*This study was carried out under the funding of the state budget program CPCEL 6541230 in the framework of the R&D Project "Strategic mineral raw materials for the recovery of the economy of Ukraine: analysis of resources and reserves, development of search criteria for increasing their mineral resource base".*

**References**

1. Stammer D., Cazenave A. Satellite Altimetry Over Oceans and Land Surfaces. CRC Press, 2018 – P. 50.
2. Copernicus marine environment monitoring service [URL] – http://marine.copernicus.eu.
3. Fletcher K. et. al. SWOT altimetry and the next generation of offshore gravity, 2023 [URL] – https://getech.com/blog/petroleum/swot-altimetry-and-the-next-generation-of-offshore-gravity/
4. Ole B. Anderse, Per Knudsen. DNSC08 mean sea surface and mean dynamic topography models, Journal of geophysical research, 2009 – P. 11002.
5. Rosmorduc V., Benveniste J., Bronner E., et. al. Radar Altimetry Tutorial. – European Space Agency, 2016 - P. 3.
6. MIKE 21 Toolbox. Global Tide Model – Tidal prediction, 2017 – P. 5.
7. Barnoud A. et. al. Reducing the uncertainty in the satellite altimetry estimates of global mean sea level trends using highly stable Water vapor climate data records. Journal of Geophysical Research. Oceans, 2023, 128 (3) - P. 1.
8. Yongsheng Xu, Lee-Lueng Fu. The effects of altimeter instrument noise on the estimation of the wavenumber spectrum of sea surface height - American meteorological society, 2012 – P. 2233.
9. Laboratory for Satellite Altimetry [URL] – https://www.star.nesdis.noaa.gov/socd/lsa/SeaLevelRise/LSA_SLR_background.php
10. Gadirov V. et. al. Use of Gravity and Magnetic Methods in Oil and Gas Exploration: Case Studies from Azerbaijan - International Journal of Earth Sciences Knowledge and Applications, 2022 – P. 143.
11. T. Bašić. Introductory Chapter: Satellite Altimetry – Overview, Satellite Altimetry - Theory, Applications and Recent Advances. IntechOpen, 2023 – P. 1-3. DOI: https://doi.org/10.5772/intechopen.112394.
12. Neill S. et. al. Fundamentals of Ocean Renewable Energy, 2018 – pp. 1-4.
14. Mertikas, S. et. a. Environmental applications of remote sensing. Pollution Assessment for Sustainable Practices in Applied Sciences and Engineering, 2021 – P. 139. DOI: https://doi.org/10.1016/b978-0-12-809582-9.00003-7
14. M. Grgić, T. Bašić, Radar Satellite Altimetry in Geodesy - Theory, Applications and Recent Developments, Geodetic Sciences – Theory, Applications and Recent Developments. IntechOpen, 2021 – pp. 1-7. DOI: https://doi.org/10.5772/intechopen.97349.
15. Jiang, L. et. al. CryoSat-2 Altimetry Applications over Rivers and Lakes. Water, 2017 (9) – P. 211.

DOI: https://doi.org/10.30836/igs.iies.2024.41

**Ivanyshyn V.[1], Kasiyanchuk D.[2]**

*(1) Department of Geodesy and Land Management, Ivano-Frankivsk National Technical University of Oil and Gas, 15 Karpatska Street, 76019 Ivano-Frankivsk, Ukraine. E-mail: vlad2016ivanyshyn@gmail.com*
*(2) Department of Geodesy and Land Management, Ivano-Frankivsk National Technical University of Oil and Gas, 15 Karpatska Street, 76019 Ivano-Frankivsk, Ukraine. E-mail: dima_kasiyanchuk@ukr.net*

# ANALYSIS OF THE NDVI INDEX ON THE EXAMPLE OF THE PEREHINSK TERRITORIAL COMMUNITY

Remote sensing, the process of collecting data from a distance, has revolutionized our ability to monitor and understand the Earth's surface. Among the plethora of indices and metrics used in remote sensing, the Normalized Difference Vegetation Index (NDVI) stands out as a powerful tool for assessing vegetation health and dynamics. Developed in the 1970s, NDVI has since become a cornerstone in environmental monitoring, agricultural management, and land cover analysis [1].

At its core, NDVI quantifies the density and health of vegetation by leveraging the reflectance properties of two key wavelengths: near-infrared (NIR) and red light. The formula for NDVI is straightforward (1):

$$NDVI= (NIR+Red)/(NIR-Red), \quad (1)$$

where NIR is the reflectance in the near-infrared spectrum and Red is the reflectance in the red spectrum. The resulting values range from -1 to 1, with higher values indicating denser and healthier vegetation. Negative values typically represent water bodies or clouds, while values close to zero suggest barren land or urban areas with little to no vegetation.

The strength of NDVI lies in its sensitivity to chlorophyll content and canopy structure. Healthy vegetation absorbs most of the visible red light for photosynthesis, while reflecting a significant portion of NIR light. Consequently, the NDVI values for healthy vegetation are relatively high due to the large NIR reflectance and low red reflectance. Conversely, stressed or sparse vegetation exhibits lower NDVI values, as seen in areas affected by drought, disease, or human activity.

One of the key advantages of NDVI is its applicability across various spatial and temporal scales. It can be computed from multispectral satellite imagery, aerial photography, or ground-based sensors, offering insights into vegetation dynamics at local, regional, and global levels. Additionally, NDVI facilitates the monitoring of seasonal changes, phenological shifts, and long-term trends in vegetation cover, providing invaluable information for land management, biodiversity conservation, and climate change research.

In agricultural contexts, NDVI is widely used to optimize crop production, monitor crop health, and assess the effectiveness of irrigation and fertilizer applications. By mapping NDVI spatial patterns within fields, farmers can identify areas of concern, implement targeted interventions, and maximize yields while minimizing inputs. Similarly, conservationists leverage NDVI to evaluate habitat quality, track deforestation, and prioritize areas for restoration efforts.

One of the main tasks of ensuring a high-quality information approach to the development of ATCs based on the content of the administrative reform is the development of regional GIS [2], which is the main objective of this study. The territory of the Perehinsk community lies within the Limnytsia River basin, which is one of the cleanest rivers not only in Ukraine but also in Europe. It is well known that the formation of the river's water balance often depends on the condition and quality of the vegetation cover. An equally important factor in shaping the structure of the territory's forest plantations is its altitude gradation from the Carpathian Mountains to the pre-Carpathian trough, which characterises the region as a zone of coniferous forests in the highlands and mixed forests in the Limnytsia River valley. The region's main industry is timber processing, so the study of the vegetation index is important not only for modelling and analysing economic benefits and risks, but also for studying the impact of global climate change and unauthorised logging on the ecosystem as a whole.

Google Earth Engine is a powerful tool for analysing geospatial data. It provides access to a large number of satellite images and other geospatial data, and has integrated tools for processing, analysing and visualising them.

Downloading a large number of satellite images and organising them for research takes time and a large amount of storage space. When using Google Earth Engine, there is no need to download satellite imagery, which is an advantage.

The Sentinel-2 satellite images with cloud cover not exceeding 10% were used in the script (Fig.1).

The data show a significant difference in biomass production between 2018 and 2023 (Table 1). The NDVI index in 2018 is higher due to more favourable conditions for vegetation development. Humidity at that time was quite high, precipitation was frequent and floods were not uncommon. The situation in 2023, as can be seen from the data obtained, was radically different - it was a dry period accompanied by extreme heat, precipitation was not as frequent as in 2018. The ability of tree leaves to photosynthesize decreases when their temperature becomes too high. Due to the abnormal heat, some of the leaves may have crossed a critical temperature threshold after which their ability to photosynthesize is impaired.

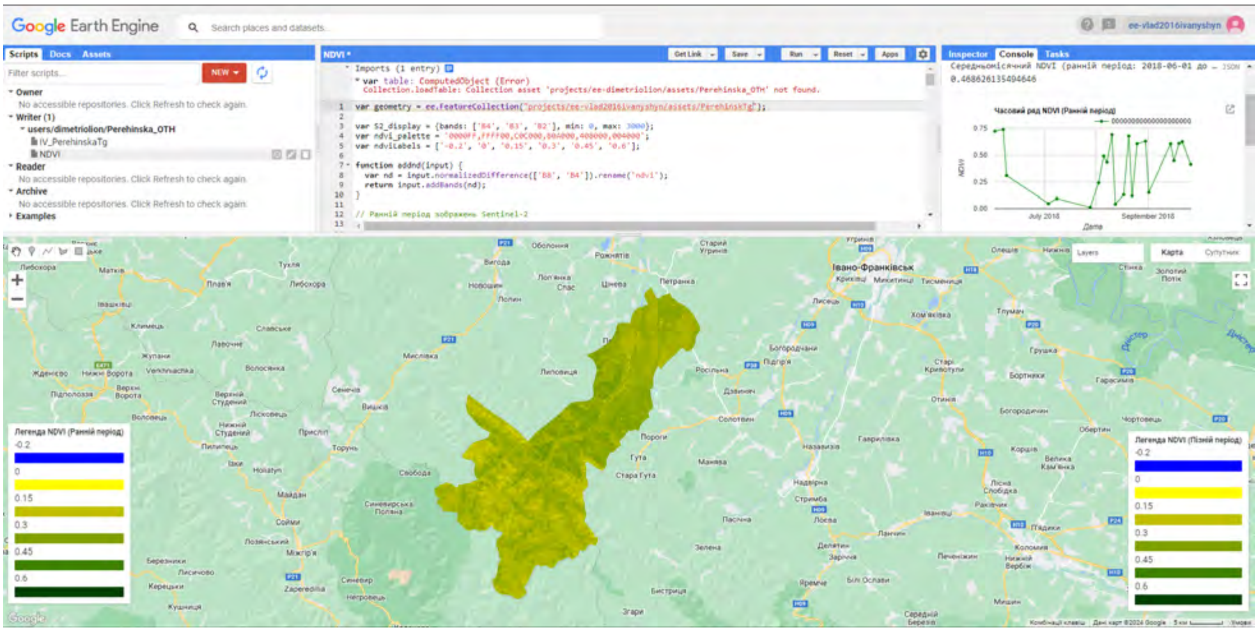


Fig. 1. NDVI index of Perehinsk territorial community

Analysing the results, it is difficult to assess which areas were most affected by this or that factor. Therefore, an additional difference model was built. The average difference value for the study area is -0.229. This is a fairly large figure. And as can be seen from the model, it is the mountainous areas that have undergone the greatest changes, which directly indicates significant deforestation in the study area.

Table 1. Average values of the NDVI index

| **Month** | **2018** | **2023** |
|---|---|---|
| June | 0,591 | 0,337 |
| July | 0,051 | 0,387 |
| August | 0,407 | 0,284 |
| September | 0,477 | 0,314 |
| Average | 0,464 | 0,330 |

Conclusion. The Perehinsk territorial community is a typical example that characterises the mountainous and foothill vegetation structure, which is important for sustainable development of the territory. 2 The vegetation index of a territory is dependent not only on forestry activities, but, as can be seen from the results of the study, is also dependent on the factor of global temperature changes in the water balance of the territory. The satellite image interpretation data allowed us to summarise the dynamics of the vegetation index change for two similar periods, in particular, for 2018 it is 0.464, for 2023 - 0.330. The interpretation of the results of this study can serve only as one of the initial stages for studying the index, taking into account all possible factors that may occur.

**References**


1. Rouse, J.W., Haas, R.H., Schell, J.A. and Deering, D.W. (1973) Monitoring Vegetation Systems in the Great Plains with ERTS (Earth Resources Technology Satellite). Proceedings of 3rd Earth Resources Technology Satellite Symposium, Greenbelt, 10-14 December, SP-351, 309-317.

2. Geoinformation system for forestry management [Electronic resource]. – Mode access: https://magneticonemt.com/geoinformatsijna-systema-dlya-lisovogo-gospodarstva/

DOI: https://doi.org/10.30836/igs.iies.2024.13

**Krakovskyi S.**

*Taras Shevchenko National University of Kyiv, Kyiv, Ukraine. E-mail: krakovsp@gmail.com*

# A COMPARATIVE ANALYSIS OF ELECTRONIC ATLAS AND GEOPORTAL: THE CASE OF SWITZERLAND

According to the most common definition, atlases are *"intentional combinations of maps or data sets, structured in such a way that specific objectives are reached."* [1] The definition highlights the following properties of atlases: structuring of information, compliance with a specific objective (intentionality), and the presence of specific elements (maps or data sets). The first two properties are too general and can characterize any structured combination of elements based on a certain idea (e.g., presentation slides). Therefore, the definition primarily emphasizes the presence of a set of maps or data sets. The data sets are added to make the definition more versatile and to include electronic atlases (EAs). However, an intentional combination of structured data sets can be an ordinary data catalog without any graphical representation (replacing "data" with "layers" would slightly reduce ambiguity). In addition, most contemporary mapping applications also consist of a set of maps. Hence, this definition is acceptable only for paper atlases.

For EAs, the above definition is modified by Kraak and Ormeling [1] as follows: *"intentional combinations of specially processed spatial data sets, together with the software to produce maps from them."* A new function of atlases was introduced: map creation (producing), which implicitly means the generation of maps from the given list of data sets by user choice (flexible concept of map information provision according to [2]). Without eliminating the shortcomings of the main definition, this modification raises a number of new questions: 1) What list of operations does "map creation" include? 2) What category of authors/users can create maps? 3) What kind of "software" is meant? 4) What category do e-book atlases and EAs with a restrictive concept fall into [2]? While this definition may be correct from a technical viewpoint (especially for EAs of the 1990s), it characterizes EA as a final product from the perspective of use quite poorly. Such important properties of atlases as "an atlas is more than the sum of individual maps", coherence of maps, enabling map comparisons (thematic, temporal, spatial), narrative structure are not included in both definitions.

Initially, geoportals or clearinghouses were associated with mechanisms for searching and administering geospatial data based on the provided metadata. With the cartographic revolution of Web 2.0, geoportal web applications have increasingly begun to incorporate maps as a search tool and/or a means of presenting search results. Nowadays, the map interface has become the main interface for a significant number of geoportals, especially national ones. Moreover, for some countries, the geoportal has replaced the national EA (e.g., Finland, Italy, Poland), being considered a website for map-based access to spatial data of the country. Nevertheless, the main functions of the geoportal remain [3]: monitoring the availability of datasets in scope; discovering suitable datasets based on their descriptions (metadata); accessing the selected datasets through their view or download services.

In addition to geoportals and web GIS, with the rise of cartography web 2.0, EAs faced such competitors as cartographic information systems, interactive maps, and story maps. Google Maps and similar mapping services hardly should be considered competitors since it is no longer appropriate for EAs to function as navigators. However, the aim of this study is not to find theoretical solutions but to analyze the differences in implementation between EAs and geoportals in practice.

To avoid discrepancies between the theory and its interpretation in practice, the theory should characterize EA as a whole and its main components. The whole implies defining the key properties of EA, the functions of EA (why to use it) or the "work it does," the typical scenario of its use (how to use EA), and the target users. The main components of EAs as end products include: 1) information architecture and navigation; 2) cartographic representation or visualization (EA may contain various forms of data visualization or spatial visualization); 3) functionality (primarily interactive functions (IF)); and 4) interface (layout, flexibility, aesthetics). Only understanding these two aspects of EA allows us to answer the question, "What is EA?"—that is, to reveal the concept of EA as a specific cartographic concept and product. The integration of thematic content is envisaged by the concept of a concrete EA.

To demonstrate this approach, Swiss cartographic products were used, which are world-renowned for their high-quality combination of cartographic traditions and modern technologies. The Atlas of Switzerland (AoS) 3 [4] and the Statistical Atlas of Switzerland (SAS) [5] were chosen as the main EAs. The latest version of the AoS is the AoS-online (2016) [4], but the author lost access to this EA after 2020. The main differences of the AoS-online are a complete transition to 3D (positioned as the main advantage of EA in competition with other mapping applications), a new interface, simplified functionality, and the possibility of updating. It is also worth mentioning the Swiss World Atlas interactive (SWAi) [6], which was notable for its navigation capabilities. The key strengths and drawbacks of these two EAs were taken into account. Describing the basic idea of the AoS, Sieber and Huber [7] used the metaphor of the atlas as a "story book" that should make users feel comfortable and fulfill their curiosity and demands. Simultaneously, the AoS is positioned as a system for geographic analysis and cartographic visualization in a multimedia environment, as well as *"a distinctive compilation of cartographically well designed maps emphasizing the characteristics of the thematic information depicted, and ready to be explored by tailored atlas tools."* [8]

The SAS was developed by the Federal Statistical Office using the Statatlas platform [5]. The Political Atlas of Switzerland, the Historical Atlas of the Federal Census, and the Statistical Atlas of Cities were also produced on the basis of this platform. The implementation of these EAs is identical, differing only in their thematic content. The Statistical Atlas of Cities is notable for its cartographic representation, which facilitates the comparison of the nine largest Swiss cities, each represented by a separate map. The SAS meets the rigid requirements for statistical atlases established in the dissertation [9] and is defined as follows: "*atlas, which in the form of an integral collection of mostly analytical maps and other information carriers (diagrams, tables, texts) graphically portrays current societal, and esp. socio-economic facts. In its true sense, it represents, by using primary sources and applying certain statistical methods, all spatial data gained by official statistics through special surveys or censuses for a broad societal insight*." [9]

Another Swiss federal institution, the Federal Office of Topography (swisstopo), has created the Maps of Switzerland (MoS) application [10], which is considered the "map viewer" of the Swiss geoportal. The main functions of the application are searching, viewing, organizing, and downloading geospatial data, along with printing maps. Although this application enables metadata browsing and supports address (geographic) and thematic search, its functionality related to accessing and searching metadata is inferior to other geoportals. Considerable attention is paid to the cartographic representation of a large number of themes and to "creating your own maps." What is the difference between MoS and EAs, especially the SAS and the AoS 3?

All three cartographic products are single-page applications. In AoS 3, switching between several visualization modes takes place in the same interface without losing the context/status of each view. The MoS interface is ahead of both EAs in terms of the amount of screen space allocated to the map. However, the interface elements (mainly sidebars) of the MoS, the SAS, and the AoS-online can be collapsed/expanded, while the layout of the AoS 3 is static. Infoboxes can be dragged and dropped in all applications. A full layout redesign is not supported by any application. The MoS and the SAS interface styles are coherent with each other (a feature of all federal applications). Also, only these two applications are accessible on mobile devices.

The information is organized by topic in all three applications. An important difference is in the approach to the provision of cartographic information. The SAS applies a restricted concept [2], which provides only ready-made maps without the ability to combine them. The AoS 3 approach can be called restrictive flexible [2], since each selected map can be supplemented with a second one from the list of system recommendations. In the MoS, users can select, combine, and reorder any layers—it's a flexible concept [2]. In addition, it is possible to change the theme classification in the Table of Contents (TOC), which is not supported by the mentioned EAs. A tree menu (TOC) is used for presenting themes in all three applications, although only the AoS 3 has graphical display elements (icons, colors) in the TOC. Also, only the AoS 3 shows all the subsections and elements of each section in a clear way (this overview advantage will be lost in the AoS-online). The AoS 3 and the MoS support a visual preview of themes, which is very rare among mapping applications in general. All three applications have geographic and thematic search (the most detailed in the AoS 3 due to an index (gazetteer)), but there are no advanced search options. Filtering elements is possible only in the AoS 3 index. The TOC sorting IFs that were implemented in SWAi are not offered. However, in AoS-online, users can sort maps by popularity or novelty. Similarly, the SWAi context-dependent navigation [6] has not been implemented in AoS versions.

The description of layers in the SAS and the MoS is limited to formal information, a metadata description, or a short summary. In contrast, the AoS 3 texts are longer, didactic in nature, and sometimes accompanied by multimedia. Still, texts and multimedia in all applications are linked to maps. Multimedia elements in the MoS only make up the content of individual layers without playing a supporting role for other themes. The MoS does not provide access to the attribute tables of thematic layers at all, unlike the SAS. There is no attribute table as such in the AoS 3, but users can view the selected values of the thematic indicator for territorial units in the "comparison" panel. The editors' publications of the above-mentioned atlases [7-9] note that it is desirable to supplement the topics of EAs with multimedia for better storytelling. Multimedia is partially implemented only in the AoS 3. However, none of the applications tell the story. Only the AoS 3 offers to add maps that would help users create meaningful storylines (connections). Both EAs do not provide alternative theme classifications (for the SAS, this is due to the standardization of themes in statistics). Neither the MoS nor the AoS 3 offer attribute tables, focusing instead on cartographic representation. The presence of tables in the SAS is explained by the statistics requirements.

The SAS basemap displays administrative boundaries, hydrography, and terrain. Only layers of the basemap can be switched. In the AoS 3, users can activate all the main layers of reference maps, including labels. The list of basemaps is extremely limited (the same applies to the AoS-online). Instead, the MoS provides a huge number of basemaps in the form of layers and layers of individual topographic elements. However, there is no intentional distinction between thematic and base layers of the map.

The symbolization of the SAS maps is mostly limited to choropleths, proportional symbols, and combinations of both. The AoS 3 and the MoS are characterized by the use of various types of maps. However, the AoS 3 has multivariate maps, although there are relatively few synthetic maps. In the MoS, the legend is a static image. The user can only modify the layer's transparency. In the SAS, the legend allows users to highlight individual classes of an indicator. Instead, the AoS 3 realizes a significant part of the "smart legend" [7] potential. Charts as standalone forms of visualization are not implemented in any application (in the AoS-online, charts are built when comparing map objects). In contrast to the Swiss atlases, the MoS 3D visualization focuses on displaying local objects (buildings, vegetation). However, the MoS 3D visualization also successfully represents thematic layers, and map navigation is smoother and faster. On the other hand, the AoS 3 has several 3D modes (panorama, block diagram, prism map).

The comparison capabilities play a key role in the functionality section. Animation is the only IF for comparing maps in the SAS. In the MoS, the animation is supplemented by a vertical slider for a map view. Instead, the AoS 3 provides the ability to open maps in different visualization windows, supports animation, and displays statistics for selected map objects. The map/data export IFs in the MoS and the AoS 3 are approximately at the same level (however, the MoS enables users to print any pages with information). The SAS is superior to the previous ones since a user can download layer output data in various formats (directly from the EA). In terms of extensibility, the MoS with "drawing" IFs (adding markers, lines, polygons, labels as single objects to the map) outperforms the mentioned applications.

Therefore, the essential differences between the MoS and the AoS (the SAS has many limitations due to its type [9]) are the opposition of layers and "ready-made maps" (although the basemaps are autonomous elements in both applications), the differences in the nature of map/data descriptions, the possibilities of manipulating symbolization in EAs, and a greater variety of means for comparing maps and objects in EAs. However, it is more about qualitative differences (how detailed and perfectly certain aspects are implemented). The MoS formally meets the definition of an atlas [1]. In both applications, maps or layers are classified not randomly but according to a certain idea and are divided into sections/subsections. Certainly, one could argue that the layers and their sequence are more carefully selected in the AoS, and they try to show certain cause-and-effect relationships. Instead, the MoS aims to simply provide as many layers cataloged in a certain way as possible. But neither application tells a story, even within sections.

The "map viewer" of the Bayern geoportal [11] is an application completely identical to the MoS (it seems to be a product of the same framework), but it is called the "Bayern Atlas." Although the "atlas nature" of the MoS remains debatable, it is no longer possible to ignore the fact that one interactive map can represent a large number of themes. If we focus on storytelling in EAs, which often implies a linear structure and combination with multimedia, we will have to look for differences between EAs and geonarratives (in particular, story maps). Turning EAs purely into "comparison machines" leads to competition with dashboards and geovisualization applications with multiple coordinated views. Betting on only one property of EA is unlikely to change the situation. Preserving the high status and uniqueness of EAs requires a new concept that would integrate the set of old and new properties of EAs into a single whole, clearly answering the question of the expediency of EAs and their functions. Nevertheless, existing concepts of EA need to be clarified and systematized. To achieve all of this, cartographers need to move the "cartographic horizon" beyond maps, looking at EAs as holistic systems from the user's perspective.

**References**


1. Kraak, M.J., & Ormeling, F. (2020). Cartography: visualization of geospatial data. CRC Press.
2. Resch, C., & Jordan, P. (2001, August 6-10). Characteristics in data management within a scientific multinational internet atlas [Paper presentation]. The 20th International Cartographic Conference, Beijing, China.
3. European Commission (n.d.). INSPIRE Geoportal. Retrieved March 22, 2024 [Electronic resource]. – Mode access: https://inspire-geoportal.ec.europa.eu/index.html.
4. Atlas of Switzerland (n.d.). Portfolio. Retrieved March 22, 2024 [Electronic resource]. – Mode access: https://www.atlasderschweiz.ch/portfolio.
5. Bundesamt fur Statistik (n.d.). Plattform Statatlas. Retrieved March 22, 2024 [Electronic resource]. – Mode access: https://www.atlas.bfs.admin.ch/de/index.html.
6. Cron, J., Marty, P., Bär, H.R., & Hurni, L. (2009, November 15-21). Navigation in school atlases: Functionality, design and implementation in the "Swiss world atlas interactive" [Paper presentation]. The 24th International Cartographic Conference, Santiago, Chile.
7. Sieber, R., & Huber, S. (2007). Atlas of Switzerland 2-A highly interactive thematic national atlas. In W. Cartwright, M. P. Peterson, G. Gartner (Eds.), Multimedia cartography (pp. 161-182). Berlin, Heidelberg: Springer Berlin Heidelberg.

8. Sieber, R., Hollenstein, L., Odden, B., & Hurni, L. (2011, July 3-8). From classic atlas design to collaborative platforms–The SwissAtlasPlatform Project [Paper presentation]. The 25th International Cartographic Conference, Paris, France.
9. Schulz, T. (2014). Der Statistische Atlas Untersuchungen zu klassifikatorischen, inhaltlichen, gestalterischen, technischen und kommunikativen Aspekten (Doctoral dissertation, Dresden University of Technology).
10. The federal geoportal (n.d.). Mapviewer. Retrieved March 22, 2024, from https://www.geo.admin.ch
11. Geoportal Bayern (n.d.). Bayern Atlas. Retrieved March 22, 2024 [Electronic resource]. – Mode access: https://geoportal.bayern.de/bayernatlas.

*DOI: https://doi.org/10.30836/igs.iies.2024.34*

**Marhes S.**

*State Institution "Scientific Centre for Aerospace Research of the Earth of the Institute of Geological Sciences of the National Academy of Sciences of Ukraine", Olesia Honchara Str., 55-b, Kyiv, 01054, Ukraine. E-mail: sergemarhes@gmail.com*

# SATELLITE GEOECOLOGICAL ANALYSIS OF THE PEAT-SWAMP SYSTEM OF THE SUPII RIVER

Supii is a young river of the Dnieper left bank with poorly developed terrace complexes. Its length reaches 144 km, and the basin equals 2165 km². It starts with swamp near the village of Svydovets in the Nizhyn district of the Chernihiv region (Figure 1). The mouth of Supii is concentrated in the conditions of the Dnieper-Donetsk depression and spurs of the Ukrainian crystalline shield [1].

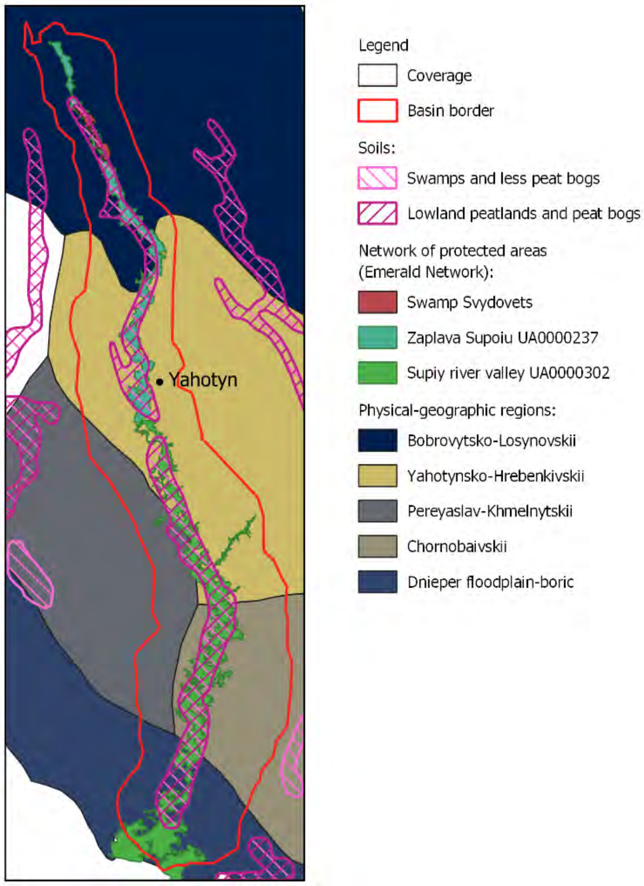


Fig. 1. Map-scheme of the Supii peat-swamp system

Characteristically, the narrowest sections of the valley are limited to the peripheral part of the positive morphostructure of the central type. There are two terrace levels in the valley: the floodplain and the 1-st (Desnian) supraflood terrace. The floodplain is two-sided, it is a bottom swamp, with a width of 500 m to 3-3.5 km, a height above the water cut from 0.5 to 1.0 m. It is mainly composed of peat, but closer to the slopes there are peaty sands and loams [2].

Limited distribution, weak water enrichment of the aquifer and low quality of underground water, high vulnerability and lack of protection from diffuse pollution by products of agricultural activity make it unsuitable not only for centralized water supply, but also for water supply of individual farms [1].

Intensive agricultural activity contributed to the further degradation of peatlands and the formation of large areas of flammable surfaces. General warming of the climate and long dry periods have become the leading factor in the occurrence of peat fires.

However, the territory has its own unique ecosystem. The river is fully and completely the approved territory of the Emerald Network of Ukraine as "Zaplava Supoiu" and "Supiy river valley" presented in Figure 1. The network aims to preserve species and ecosystems that have been recognized as rare at the level of the whole of Europe, according to the provisions of the Berne Convention on the Protection of Wild Flora and Fauna and Natural Habitats in Europe [3].

Restoring the balance of natural and anthropogenic processes for the conditions of sustainable development of the territories of the Supii river basin is of primary importance. Research in this area helps to solve a number of sustainable development goals. That is why it is advisable to correctly assess their value [4].

To prepare progress of physical characteristics of peatlands based on remote sensing data, soil analysis was carried out. There are Normalized Difference Water Index (NDWI), Soil-Adjusted Vegetation Index (SAVI).

To reflect qualitative indicators of water content in plant leaves calculated NDWI by Gao (1996). To reflect the amount of water in water bodies chosen NDWI by McFeeters (1996). For the influence of soil brightness in areas where vegetative cover is low was used SAVI [5]. Results are presented in Figure 2.

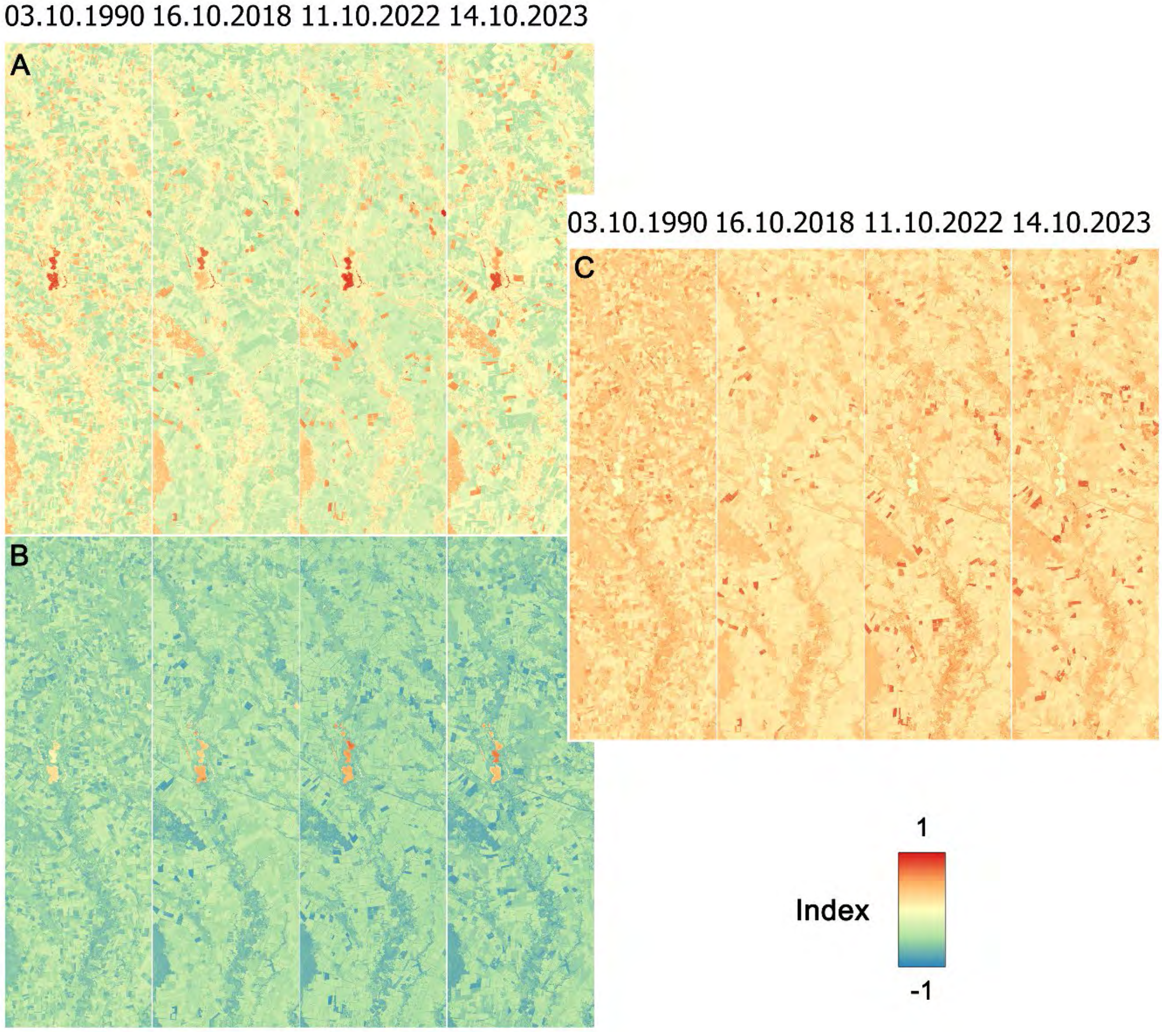


Fig. 2. Indexes of A) NDWI (Gao, 1996), B) NDWI (McFeeters, 1996) and C) SAVI

The degradation of land is quite noticeable in the images of recent years. To obtain a better result, such as an assessment of the risks of burning peatlands, it is planned to conduct an analysis of the temperature distribution of the land surface (LST).

**References**

1. Management plan of Dnieper river basin. Part 1(2025-2030), 2021. P.422.
2. Derii M.M. Report on the geological survey of the subsurface. Geological structure and minerals of the confluence of the Trubizh and Supii rivers. Book 1. Kyiv, 2007.
3. Berne Convention on the Conservation of European Wildlife and Natural Habitats (Bern, 1979). Kyiv, 1998. P. 76.
4. Rudenko L.H., Marunyak Y.O., Holubtsov O.H. Landscape planning in Ukraine. Kyiv, 2014. P. 144
5. Landsat Soil Adjusted Vegetation Index of Landsat missions [Electronic resource]. – Mode access: https://www.usgs.gov/landsat-missions/landsat-soil-adjusted-vegetation-index.

DOI: https://doi.org/10.30836/igs.iies.2024.36

**Saidi A.[1], Djabri M.[1], Arradj S.E.[2]**

(1) *Research Laboratory of Sedimentary Environment, Mineral and Water Resources of Eastern Algeria, Department of Earth and Universe Sciences, Echahid Cheikh Larbi Tebessi-Tebessa University, Algeria. E-mail: amani.saidi@univ-tebessa.dz, mohamed.djabri@univ-tebessa.dz*
*(2) Emerging Materials Research Unit (EMRU), Department of Earth and Universe Sciences, Farhat Abbas University, Algeria. E-mail: sifeddine.arradj@univ-setif.dz*

# EXPLORING LIQUEFACTION POTENTIAL THROUGH NUMERICAL MODELING

Liquefaction is a critical concern in seismic-prone regions, where the transformation of soil from a solid to a liquefied state can lead to catastrophic damage to infrastructure and loss of life. In this study, we investigate the liquefaction potential of a site located in a seismic region of Algeria, which has previously experienced two earthquakes of magnitude 6.5 (the 1856 Djidjili earthquake, 21 and 22 August 1856). The analysis is based on standard penetration test (SPT) data, and the numerical modeling is carried out using the Plaxis 2D [1, 2, 3].

We employed the UBCSand constitutive model within the Plaxis 2D software, which incorporates the effects of soil plasticity and liquefaction. The model parameters are obtained from correlations with Standard Penetration Test (SPT) data collected at the site [3, 4, 5].

The study area is located in Northeast Algeria, in the Skikda Province, with coordinates (36°49'20.40"N, 5°55'9.16"E). The terrain comprises a sequence of loosely consolidated Pleistocene sand deposits, exhibiting a reddish coloration, with varying degrees of relative density, ranging from 28% to 55%. The piezometric level is observed at a depth of 6 m (Fig.1).

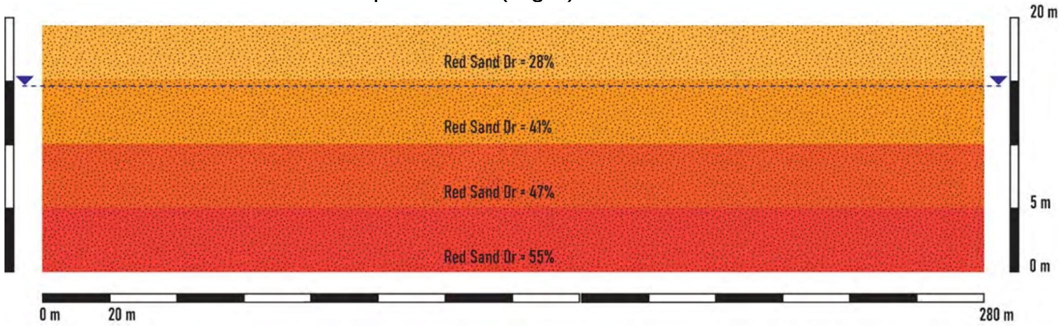


Fig. 1. Depth profile of relative soil densities within the study area

In the static analysis stages, the default model boundary conditions were used. Displacements were fixed in both directions at the base boundary (Ux=0 and Uy=0), while displacements were allowed in the y direction but not in the x direction at the vertical boundaries (Ux=0 and Uy≠0).

For the dynamic analyses, tied boundary conditions were applied on the vertical boundaries and the "none" option was used in the horizontal direction. Tied boundary conditions allow points located at the same elevation to move with the same displacements, reflecting the behavior of the laminar box more realistically. A prescribed displacement of 0.05 m in the S direction was applied to the model base to provide the earthquake input motion.

Since seismic signal data for the 1856 Djidjili earthquake is not available in the literature, we chose to use ground motion data from the 1952 Kern County earthquake. This earthquake occurred on July 21 in the southern San Joaquin Valley and had a moment magnitude of 7.3. The seismic signal data was obtained from the PEER Ground Motion Database.To ensure accuracy and reliability in our seismic simulations, we calibrated and corrected the data using the SeismoSignal 2024 software tool (Fig. 2) [6, 7, 8].

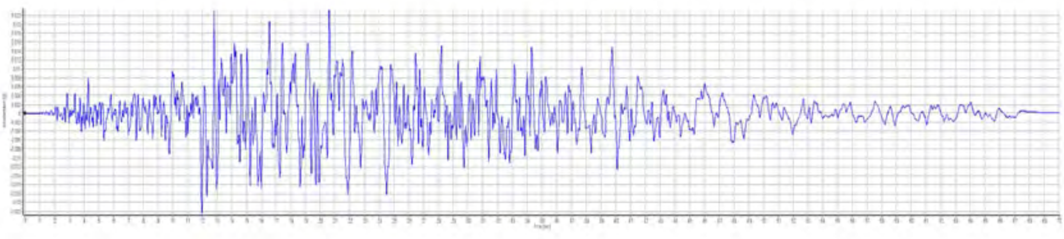

Fig. 2. Input signal

Excess pore water pressure (EPWP) is a critical parameter in assessing liquefaction potential. In this study, EPWP was calculated at three depths: 12 m (P2), 6 m (P5), and 3 m (P8). The results were compared to the effective stress at each depth to determine the liquefaction potential (Fig.3).

The results show that the EPWP at P8 and P5 exceeds the effective stress at those depths, indicating that liquefaction is likely to occur at these locations. At P2, the EPWP is lower than the effective stress, suggesting that liquefaction is less likely at this depth.

These findings are consistent with the observed liquefaction during the 1856 Djidjili earthquake. Liquefaction was reported to have occurred in areas with sandy soils and shallow groundwater, which are conditions that favor the development of high EPWP.

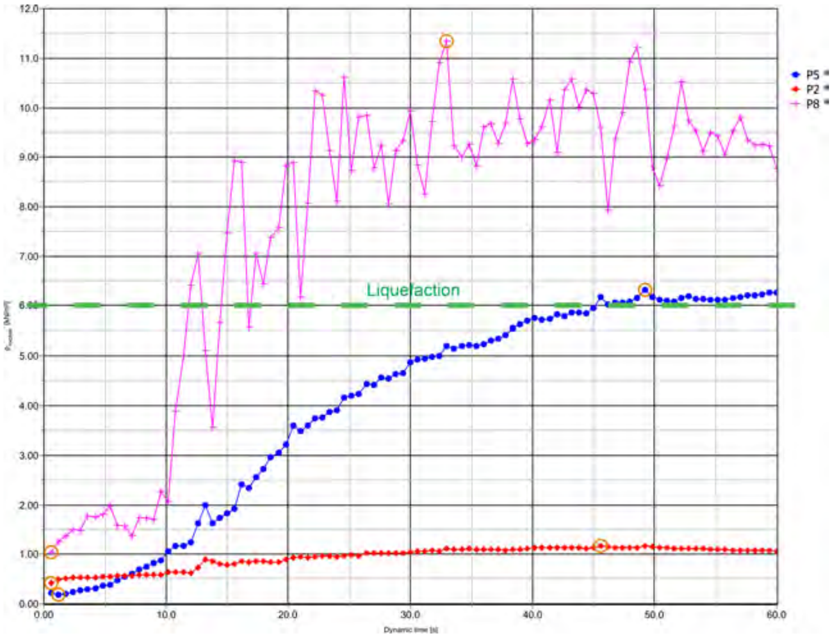

Fig. 3. Results

**References**

1. Boulanger, R.W., & Idriss, I.M. (2014). Soil liquefaction during earthquakes. Earthquake Engineering Research Institute (EERI).
2. Vucetic, M., & Dobry, R. (1991). Effect of soil plasticity on cyclic liquefaction. Journal of Geotechnical Engineering, 117(1), 89-107.
3. Iwasaki, T., & Tatsuoka, F. (1985). Soil liquefaction analysis by the finite element method. Journal of Geotechnical Engineering, 111(7), 772-791.
4. Zhang, J., & Liu, Y. (2019). Numerical simulation of soil liquefaction using Plaxis. Geomechanics and Engineering, 16(2), 197-210.
5. Idriss, I.M., & Boulanger, R.W. (2015). Soil liquefaction during earthquakes (2nd ed.). CRC Press.
6. Harbi, S.; Meghraoui, M.; Maouche, M. (2011), "The Djidjelli (Algeria) earthquakes of 21 and 22 August 1856 (I0 VIII, IX) and related tsunami effects Revisited", Journal of Seismology, 15 (1): 105-129.
7. Ambraseyes, N.N. (1982), "The seismicity of North Africa: the earthquake of 1856 at Jijeli, Algeria", Bollettino di Geofisica Teorica ed Applicata, 24 (93): 31-37.
8. Soloviev, S.L., Solovieva, O.N., Go, C.N., Kim, K.S., and Shchetnikov, N.A. Tsunamis in the Mediterranean Sea 2000 B.C.-2000 A.D: Advances in Natural and Technological Hazards Research (Kluwer Publications 2007). Vol. 13, 237 pp.

*DOI: https://doi.org/10.30836/igs.iies.2024.10*

**Tymchyshyn M.**

*State Institution "Scientific Centre for Aerospace Research of the Earth of the Institute of Geological Sciences of the National Academy of Sciences of Ukraine", Olesia Honchara Str., 55-b, 01054, Kyiv, Ukraine. E-mail: tymchyshyn.m.a@gmail.com*

# ASSESSMENT OF DEFORESTATION IN THE IVANO-FRANKIVSK OBLAST BASED ON REMOTE SENSING DATA

Deforestation is one of the urgent problems in the world. Deforestation is caused by natural and anthropogenic factors, therefore the need to monitor this problem is urgent. An operational and low-cost monitoring method for detecting deforestation is the use of remote sensing data. Thanks to satellite information, it is possible to solve several tasks related to the diagnostic assessment of this process and the development of recommendations for solving this problem [1-2].

In Ukraine, the problem of deforestation is large-scale, due to deforestation. Since our country is forest-deficient, the problem of deforestation is urgent and must be solved. The problem of deforestation has been studied by many scientists [3-11].

Ivano-Frankivsk Oblast was selected as the study area to assess the state of the forest cover, it is in this region that part of the Ukrainian Carpathians is located.

The online platform for working with space images Google Earth Engine (GEE) and the "Hansen dataset" database, which uses data from Landsat satellites since 2000, were used for calculations [12-14].

To assess the state of deforestation in the Ivano-Frankivsk oblast based on the remote sensing data, a program code was written in the JavaScript programming language, which is shown in (Figure 1).

```
Imports (1 entry)
  var geometry: Table users/businka0053/Ivano-Frank
var gfc2022 = ee.Image("UMD/hansen/global_forest_change_2022_v1_10");
var treeCoverCha_Vis = {
  min: 0,
  max: 100,
  palette: ['black', 'green'],
  bands: ['treecover2000']
}
Map.addLayer(gfc2022.clip(geometry), treeCoverCha_Vis, 'Hansen2000');
var lossImage = gfc2022.select(['loss']);
//Mapping tree cover loss from 2000
// Add the loss layer in red.
Map.addLayer(lossImage.clip(geometry).updateMask(lossImage),
             {palette: ['FF0000']}, 'Loss');
// Get the loss image.
// This dataset is updated yearly, so we get the latest version.
var lossImage = gfc2022.select(['loss']);
var lossAreaImage = lossImage.multiply(ee.Image.pixelArea());
var lossYear = gfc2022.select(['lossyear']);
var lossByYear = lossAreaImage.addBands(lossYear).reduceRegion({
  reducer: ee.Reducer.sum().group({
    groupField: 1
    }),
  geometry: geometry,
  scale: 30,
  maxPixels: 1e9
});
print(lossByYear);
```

Fig. 1. JavaScript program code for assessing the state of deforestation in the Ivano-Frankivsk oblast in the period from 2001 to 2022

For the period from 2001 to 2022, the results of deforestation of the studied territory were obtained, which are shown in (Figure 2).

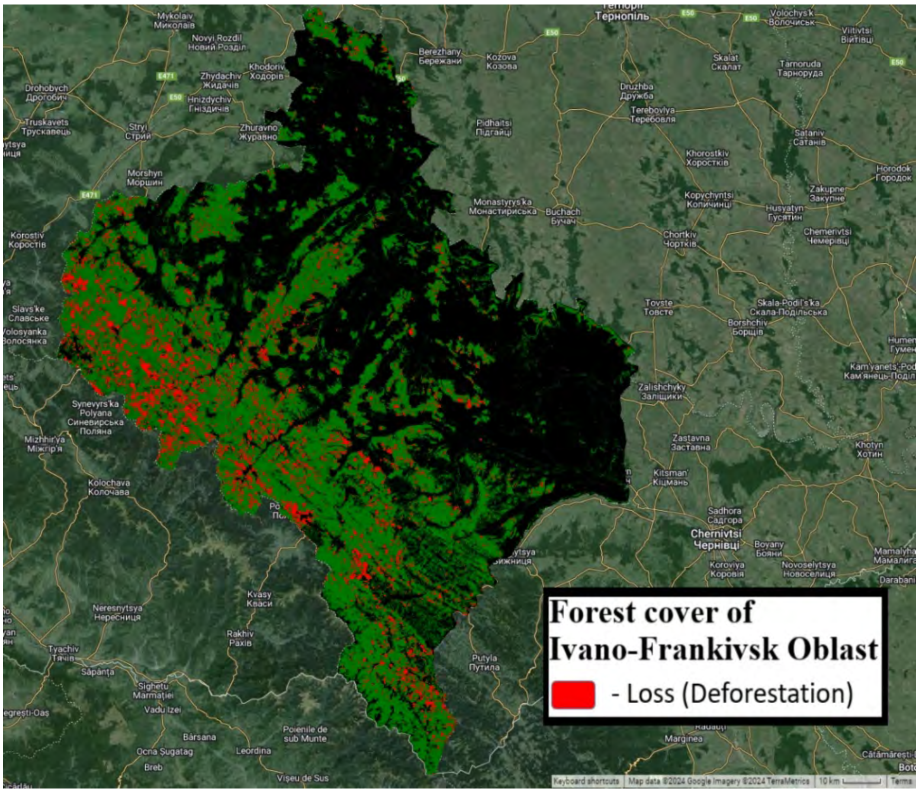


Fig. 2. Deforestation map of Ivano-Frankivsk Oblast for the period from 2001 to 2022

The forest cover change map of the Ivano-Frankivsk oblast shows the area of deforestation in red. Analysis of Fig. 1 shows that in the western and southern parts of Ivano-Frankivsk oblast, there are more areas with intensive deforestation over the past 22 years compared to the center and east of Ivano-Frankivsk oblast. One of the features, why the level of deforestation in the western and southern parts of the Ivano-Frankivsk oblast is higher than in other parts of the oblast, is that the territory of the Carpathians is located in the western and southern parts of the oblast, which have a large area of forests and forest ecosystems on their territory.

The Google Earth Engine online application provided data in CSV format and plotted the loss of forest cover in the Ivano-Frankivsk oblast for each year from 2001 to 2022.

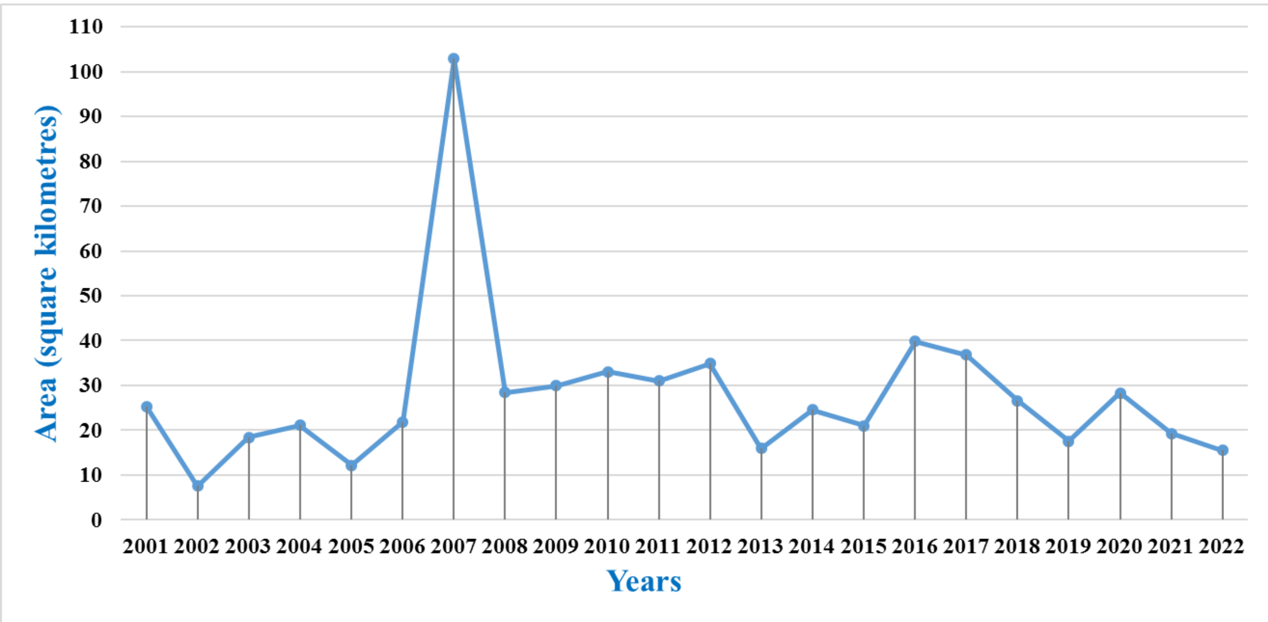


Fig. 3. Areas of deforestation in the Ivano-Frankivsk oblast for the period 2001-2022

The results of the graph (Figure 3) showed that for the period from 2001 to 2022, the greatest loss of forest cover in the Ivano-Frankivsk oblast was in 2007 and it amounted to 102.91 square kilometers. The smallest losses were in 2002 and they amounted to 7,523 square kilometers. According to the dynamics of deforestation, it can be noted that starting from the peak year of 2007, the level of loss decreased, but it was greater than in the period between 2001 and 2006. In the period from 2008 to 2012, the loss of forest cover gradually began to increase. Between 2013 and 2015, the rate of deforestation decreased. In 2016, the level increased but then began to decrease. In 2020, the level increased and between 2021 and 2022 gradually began to decrease, and in 2022 the area of deforestation was 15.54 square kilometers.

So, the total area of forest cover loss in the Ivano-Frankivsk oblast for the period from 2001 to 2022 was approximately 612.25 square kilometers.

The problem of deforestation is not only for the Ivano-Frankivsk oblast but also for the entire territory of Ukraine, that is, it is a nationwide problem and it is necessary to develop an action plan, carry out the necessary reforms, and implement norms and amendments to laws, improve our legislation and ratify the norms of the European Union in our legislation to solve the problem of the destruction of forest cover in our state.

Further research will be aimed at determining the deforestation of the forest massifs of the Carpathian Mountains and Ukrainian Polissia.

**References**

1. Tymchyshyn, M.A. Remote assessment of the Holosiivskyi forest ecosystem. Kyiv. National Aviation University. 2022. 53 p. [Electronic resource]. - Mode access: https://er.nau.edu.ua/handle/NAU/55478.

2. Tymchyshyn, M.A., Dudar, T.V. Remote assessment of the forest ecosystem (TATARIV Region, IVANO-FRANKIVSK Oblast case study). Materials of the XVIII All-Ukrainian scientific online conference of higher education graduates and young scientists with international participation "Modern problems of ecology" on October 6, 2022. Zhytomyr, "Zhytomyr Polytechnic", Ukraine. 2022. P. 59. [Electronic resource]. - Mode access: https://conf.ztu.edu.ua/suchasni-problemy-ekologiyi-6-zhovtnya-2022-r/.

3. Oral, H.V. Deforestation. In: Romaniuk, S., Thapa, M., Marton, P. (eds) The Palgrave Encyclopedia of Global Security Studies. Palgrave Macmillan, Cham. 2020. [Electronic resource]. - Mode access: https://doi.org/10.1007/978-3-319-74336-3_390-1.

4. Bodo, T., Gimah, B.G., & Seomoni, K.J. Deforestation and Habitat Loss: Human Causes, Consequences and Possible Solutions. Journal of Geographical Research. 2021.V. 4 № 2. P. 22–30. [Electronic resource]. - Mode access: https://doi.org/10.30564/jgr.v4i2.3059.

5. Von Hellermann, P. Deforestation. The International Encyclopedia of Anthropology. 2018. P. 1–5. [Electronic resource]. - Mode access: https://doi.org/10.1002/9781118924396.wbiea2006.

6. Ali, A., Riaz, S., and Iqbal, S. Deforestation And Its Impacts On Climate Change An Overview Of Pakistan. Papers on Global Change IGBP. 2014. V 21 № 1. P. 51–60. [Electronic resource]. - Mode access: http://dx.doi.org/10.1515/igbp-2015-0003.

7. De Andrade, R.B.; Mota, G.L.A.; da Costa, G.A.O.P. Deforestation Detection in the Amazon Using DeepLabv3+ Semantic Segmentation Model Variants. Remote Sens. 2022. V. 14. 4694. [Electronic resource]. - Mode access: https://doi.org/10.3390/rs14194694.

8. Wang, J.; He, Z.; Wang, C.; Feng, M.; Pang, Y.; Yu, T.; Li, X. Investigation of Long-Term Forest Dynamics in Protected Areas of Northeast China Using Landsat Data. Remote Sens. 2022. V. 14. 2988. [Electronic resource]. - Mode access: https://doi.org/10.3390/rs14132988.

9. Braun, A.C. Deforestation by Afforestation: Land Use Change in the Coastal Range of Chile. Remote Sens. 2022. V. 14. 1686. [Electronic resource]. - Mode access: https://doi.org/10.3390/rs14071686.

10. Matosak, B.M.; Fonseca, L.M.G.; Taquary, E.C.; Maretto, R.V.; Bendini, H.d.N.; Adami, M. Mapping Deforestation in Cerrado Based on Hybrid Deep Learning Architecture and Medium Spatial Resolution Satellite Time Series. Remote Sens. 2022. V. 14. 209. [Electronic resource]. - Mode access: https://doi.org/10.3390/rs14010209.

11. Torres, D.L.; Turnes, J.N.; Soto Vega, P.J.; Feitosa, R.Q.; Silva, D.E.; Marcato Junior, J.; Almeida, C. Deforestation Detection with Fully Convolutional Networks in the Amazon Forest from Landsat-8 and Sentinel-2 Images. Remote Sens. 2021. V. 13. 5084. [Electronic resource]. - Mode access: https://doi.org/10.3390/rs13245084.

12. Hansen, M. C., P. V. Potapov, R. Moore, M. Hancher, S. A. Turubanova, A. Tyukavina, D. Thau, S. V. Stehman, S. J. Goetz, T. R. Loveland, A. Kommareddy, A. Egorov, L. Chini, C. O. Justice, and J. R. G. Townshend. High-Resolution Global Maps of 21st-Century Forest Cover Change. Science 342. 850-53. 2013. [Electronic resource]. - Mode access: https://doi.org/10.1126/science.1244693.

13. Forest Changes Detection Using Hansen Dataset via Google Earth Engine API: A Case Study of Dhaka, Bangladesh. [Electronic resource]. - Mode access: https://medium.com/@sohelrana.aiubPro/forest-changes-detection-using-hansen-dataset-via-google-earth-engine-api-a-case-study-of-dhaka-46a5a5730f11.

14. Google Earth Engine [Electronic resource]. - Mode access: https://earthengine.google.com/.

DOI: https://doi.org/10.30836/igs.iies.2024.8

**Weldemikael B.T.[1], Woldetinsae G.[2], Neshir G.[1]**

*(1) Addis Ababa Science and Technology University, Department of Software Engineering, Ethiopia.*
*(2) Addis Ababa Science and Technology University Department of Mining Engineering, Ethiopia.*
*E-mail: girma.woldetinsae@aastu.edu.et*

# GENERATING LAND GRAVITY ANOMALIES FROM SATELLITE GRAVITY OBSERVATIONS USING DEEP LEARNING IMAGE TRANSLATION

Gravity anomalies are significant for various geophysical and geodetic applications, including mineral and oil exploration, determination of orbits, and the study of geodynamic processes within the Earth among others [1, 2]. The accuracy of gravity anomalies can be increased by improving the accuracy of gravimetric and geodetic measurements and by enhancing the methodology of anomaly detection [3]. Gravity data is collected through ground surveys, and are time-consuming, labor-intensive, and often limited by accessibility issues and instrumentation. Land-based gravity surveys are often expensive and difficult to obtain in remote areas [4]. With the advent of satellite technology, it became possible to collect gravity data on a global scale. However, satellite gravity data often lacks the resolution and accuracy due to the distance from the Earth's surface [5-7]. To overcome this limitation, deep-learning-based image translation techniques can be used to enhance the satellite-based data [8] with some limitations.

Image transaltion is the process of mapping characteristics from one domain to another and is used in remote sensing imagery analysis, movement of soil and rock materials [9]. It involves translating the characteristics of one domain (in this case, satellite gravity data to another domain (ground gravity data). The goal is to leverage the global coverage of satellite data and enhance it with the resolution and accuracy of ground data. The Pix2Pix Generative Adversarial Networks (GAN) model, a type of Generative Adversarial Network known for its image-to- image translation capabilities, presents a novel approach to this challenge. Despite its proven success in various fields, the potential of Pix2Pix GAN for geophysical images, such as gravity anomaly datasets, has not been fully explored. It is used to effectively map gravity anomalies from satellite to ground and adapt the Pix2Pix GAN model for large scale data transformation. The impact of varying patch sizes on model performance is investigated using key metrics to ensure improved accuracy in gravity anomaly mapping. The model used 1376 satellite and 1376 ground Bouguer gravity anomaly images from northern and northeast part of Ethiopia. 2200 images were used for training and 552 for testing. The findings indicate that larger patch sizes, particularly 142x142 pixels, significantly enhanced model accuracy by capturing global features and contextual information. Additionally, models incorporating L2 loss with LcGAN demonstrate superior performance across quantitative metrics compared to those with L1 loss. The study contributes to the improvement of geophysical exploration by providing a method that generates more accurate gravity maps (Fig. 1), thereby enhancing the precision of geological models and related applications.

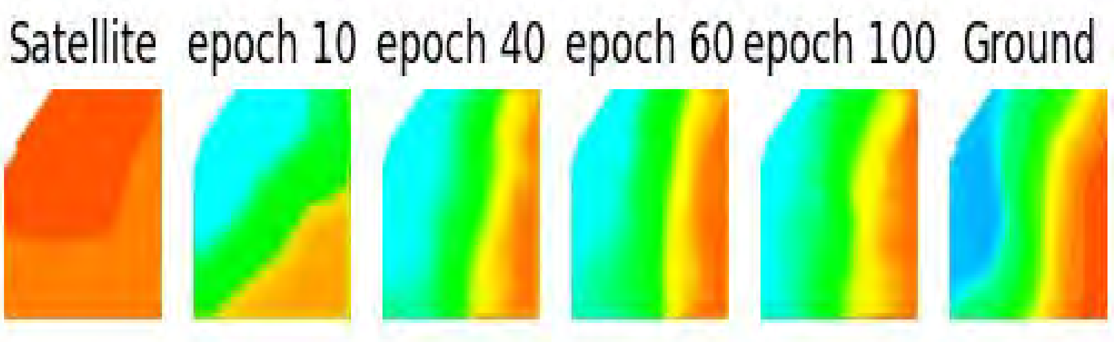


Fig. 1. Training steps for L2 + cGAN with epoch from epoch 5 to epoch 60

## References

1. L. Luis´ Luis´alvarez-Gaumé and M. A. Vázquez-Mozo, "Anomalies and the Green-Schwarz Mechanism," Nov. 2022. DOI: https://doi.org/10.48550/ARXIV.2211.06467.
2. V. Puškorius, E. Paršeliūnas, P. Petroškevičius, and R. Obuchovski, "An analysis of choosing gravity anomalies for solving problems in geodesy, geophysics and environmental engineering," Environ. Eng., 2020. DOI: https://doi.org/10.3846/ENVIRO.2020.684.
3. S. Hikami, A. I. Larkin, and Y. Nagaoka, "Spin-Orbit Interaction and Magneto resistance in the Two Dimensional Random System," Prog. Theor. *Phys.*, vol. 63, no. 2, pp. 707-710, Feb. 1980. DOI:

https://doi.org/10.1143/PTP.63.707.
4. O. Alaofin, Y. Zhang, J. Sharma, and X. Li, "Cross-Modality Super-Resolution of Satellite Gravity Data for Geophysical Exploration," Int. Geosci. Remote Sens. Symp., vol. 2022-July, pp. 7539-7542, Jul. 2022. DOI: https://doi.org/10.1109/IGARSS46834.2022.9883035.
5. R. Beránek and J. Mrlina, "Modelling 3D subsurface structures using gravity and enhanced gravity gradient method," EGU23, Feb. 2023. DOI: https://doi.org/10.5194/EGUSPHERE- EGU23-6032.
6. P.P. KHATRI, R. HONDA, and H. MORIKAWA, "Separation of Gravity Anomaly Data Considering Statistical Independence of Source Signals," J. Japan Soc. Civ. Eng. Ser. A1 76 (Structural Eng and Earthq. Eng., vol. 69, no. 4, p. I_549-I_558, 2013. DOI: https://doi.org/10.2208/jscejseee.69. i_549.
7. I. Ahmadi, A. Ghorbani, and A.H. Ansari, "3D Gravity Cross-Correlation imaging for large scale data analysis: Application to the Crustal structure of Iran," J. Earth Sp. Phys., vol. 46, no. 4, pp. 131-145, Sep. 2020. DOI: https://doi.org/10.22059/JESPHYS.2020.298815.1007197.
8. Y. Zhang, "Deep Learning Based Super Resolution of Gravity Data for Geophysical Exploration," no. November, 2021.
9. W.W. Choi, S.K. Hong, K.H. Kim, S.J. Park, and M.K. Kim, "A Study on the Cross-domain domain Terminology Mapping Based on Geospatial Information," Jihyeong gong'gan jeongbo, vol. 30, no. 4, pp. 35-46, Dec. 2022. DOI: https://doi.org/10.7319/KOGSIS.2022.30.4.035.

DOI: https://doi.org/10.30836/igs.iies.2024.46

**Havryliuk R., Nikitash O., Nikitash Iu., Negoda Iu.**

*Institute of Geological Sciences of the National Academy of Sciences of Ukraine, Kyiv, Ukraine.*
*E-mail: gavrilyuk.ruslan@gmail.com, olgagrig88@ukr.net, yn88@ukr.net, ynegoda2008@gmail.com*

# HYDROGEOLOGICAL ASPECTS OF THE SHALLOWING OF LAKE SYNE IN KYIV

Syne Lake is located in the northwestern part of Kyiv, on the western outskirts of the Vynohradar residential area. The ancient origin of the lake is evidenced by old maps, in particular the map of 1746, which shows the lake without a name [6]. The lake is shown and captioned on later maps of the XIX and XX centuries, and the reservoir is partially visible on an aerial photograph taken in September 1943.

The lake is located on the watershed plateau of the Dnipro and Irpin rivers within the upper part of the Gorenka River basin, the right tributary of the Irpin River, and is considered the largest watershed lake in Kyiv (Fig. 1).

The lake consists of two parts: the northern and southern reaches, although according to Vyshnevskyi (2021), in the past the lake consisted of one reach, the southern one. In the second half of the 1970s, during the active development of the adjacent Vynohradar residential area, the lake was artificially enlarged. The lake acquired its current configuration in the 1980s. The lake area reached 4.4 hectares, with an average depth of 0.85 m, a maximum depth of 1.85 m, and a volume of 37.6 thousand meters [3]. The absolute water level at the end of the last century was 152.5 m.


Fig. 1. Lake Syne (satellite image [4])

The watershed nature of Lake Syne's location has largely determined its vulnerability to external influences caused by natural and man-made changes in its water balance, which has led to the current problem of shallowing.

The lake has been shallowing since at least the early 2010s. According to the Pleso utility company, which manages Kyiv's water bodies, including Lake Syne, the problem became acute in the spring of 2019, when the lake began to rapidly shrink. By the fall of the same year, the water level had dropped by 1.5 meters, and the water had moved away from the cutoff by 10 meters, which led to the transformation of the lake into two separate shallow water bodies. An analysis of Google Earth satellite images shows that over the past 10 years, the lake has been losing its water surface, which eventually resulted in a complete loss of water in the lake in the summer of 2023. As of March 2024, a water mirror was observed in the lake, but in a limited area, critically small on the northern paddle.

Maintaining the water balance of the lake was partially ensured by the flow of technological water discharges from the Vinohradar-1 water supply station, where, according to the regulations, twice a year, drinking water tanks with a total volume of 14 thousand m were cleaned. After the introduction of the latest water treatment technologies (without the use of liquid chlorine), technological discharges stopped, which also negatively affected the lake's level regime [3]. According to local residents, the last filling of the lake with water from the Vynohradar-1 water supply station took place at the beginning of the full-scale Russian invasion in 2022, based on the need to create a reserve water supply.

Experience has shown that artificially filling the lake with water does not solve the problem of its shallowing, which is caused by a change in the water balance, namely a decrease in water inflow (underground and surface) and water losses due to increased evaporation.

The development of the adjacent territory and the regulation of surface runoff have significantly limited the surface water inflow to the lake, and also negatively affected the infiltration of groundwater.

The current morphology of the territory's relief surface shows the presence of depressions to which Lake Syne is confined, as well as Blue Lake, located to the east (Fig. 2). The analysis of the catchment area of Lake Syne (Fig. 3), conducted using the Surfer software based on the digital surface of Kyiv, shows that in the absence of development, it could have been 635 hectares, which is quite close to the estimates obtained by other researchers based on the analysis of topographic maps from the first half of the last century [3]. This was the surface watershed of the lake before the regulation of surface runoff in the second half of the 1970s, which has intensified in the last 10 years with the resumption of development of the adjacent territory. As a result of the development, which was accompanied by the regulation and diversion of surface runoff, the current area of the lake's surface catchment is probably about 20 hectares, actually limited to the hollow in which the lake was formed.

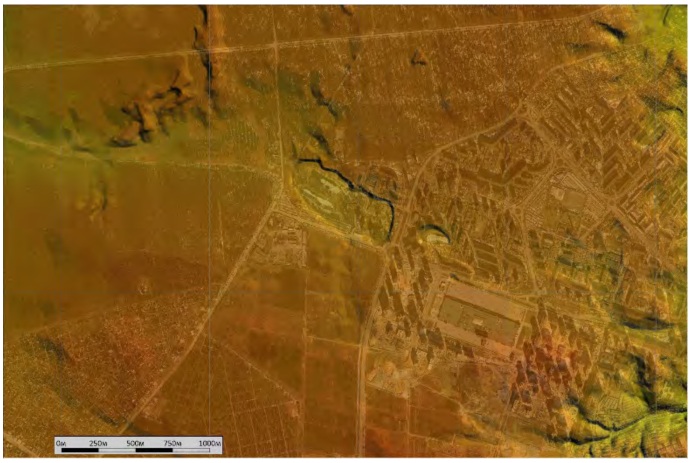

Fig. 2. Relief in the area of Lake Syne (based on a digital elevation map of Kyiv at a scale of 1:10,000) [5]

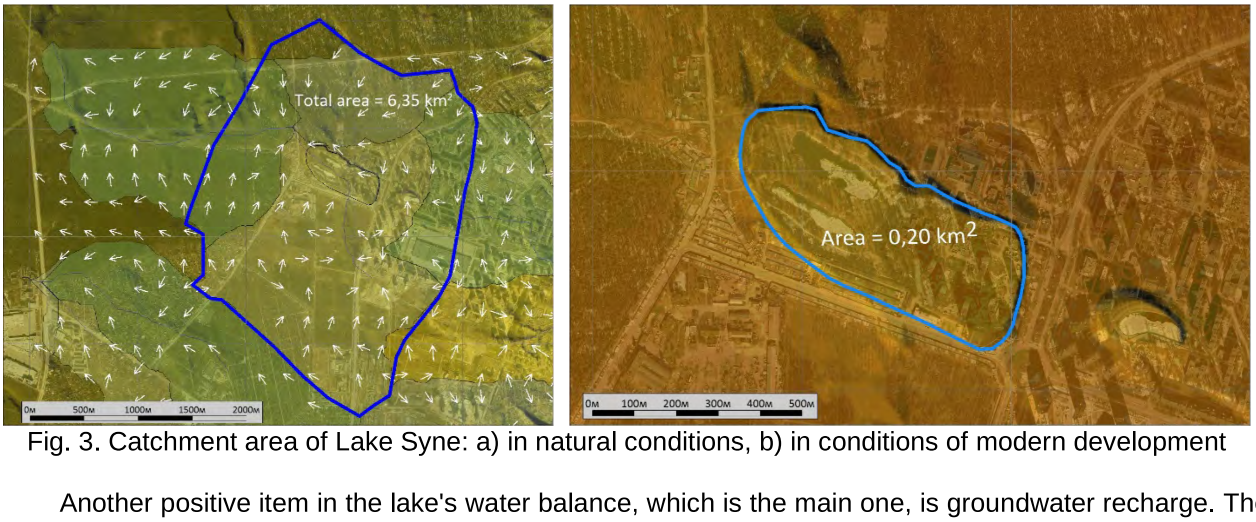


Fig. 3. Catchment area of Lake Syne: a) in natural conditions, b) in conditions of modern development

Another positive item in the lake's water balance, which is the main one, is groundwater recharge. The lake is believed to be of glacial origin [3]. Its formation is determined by the presence of a depression formed in Quaternary fluvio-glacial and glacial sediments. The first aquifer from the surface was formed in this rock layer, which lies on Miocene-Pliocene water-resistant clays and provides underground water supply to the lake.

According to the surveys [2], the lake is a drainage for the groundwater aquifer, and the surface water level in it reflects the level of the groundwater aquifer. The absolute surface elevation of the lake bed is about +150 m. As of summer 2020, the water surface elevation of the lake was +150.5 m, and groundwater elevations in wells drilled in the lake area were close to this value. This means that the lake's water supply and water level are primarily determined by the groundwater aquifer and its level.

The catchment area of the groundwater feeding the lake is complex and disturbed. Its boundary in the upper part of the groundwater flow from the Dnipro-Irpin watershed probably coincides to some extent with the contour of the surface water catchment area under natural conditions. To the west of the lake, the groundwater catchment area may be significantly smaller than the natural surface runoff catchment area and is determined by the ratio of water levels in the reservoir to groundwater. In order to establish the exact catchment area within which Lake Syne is groundwater fed, it is recommended to conduct additional hydrogeological surveys to build a hydrogeological map of the area.

The main factors affecting groundwater are climate change and anthropogenic factors related to the development of the territory. The downward trend in groundwater levels observed in the lake area is typical for Ukraine in recent decades. The decrease in water content in the Polissia region, which includes the study area, is mainly caused by climate change [1]. In the case of Lake Syne, the situation is further aggravated by the development of a large part of the territory where the underground runoff that feeds the lake is formed. As noted above, this significantly reduces groundwater infiltration, in particular due to the evaporation of precipitation from asphalt and other hard surfaces, as well as their collection and disposal. Thus, on the one hand, the development of the territory becomes an obstacle to surface runoff to the lake, and on the other hand, it reduces groundwater recharge, which leads to a decrease in its level. Development can also change the nature of the filtration flow, in particular, lead to a redistribution of flow directions due to the impact of foundations that become an obstacle in its path, and as a result of water reduction works during the construction and operation of buildings. Thus, a part of the groundwater flow may be directed towards the Dnipro River valley and not enter the lake's underground recharge zone.

With limited surface runoff to the lake, groundwater is becoming the dominant source of its recharge. At the same time, the development of the territory, as well as climate change, negatively affect groundwater recharge, resulting in a decrease in its level, which has led to the shallowing of Lake Syne.

*This work was supported by the National Academy of Sciences of Ukraine, project no 0123U100855 "Strategic mineral raw materials for the recovery of the economy of Ukraine: analysis of resources and reserves, development of search criteria for increasing their mineral resource base".*

## References

1. Boychenko S, Havryliuk R, Gusev O, Savchenko S, Yatskiv A. Changes in the environmental sphere of Polissya. Changes in the environmental sphere of Polissya: aspects of the influence of anthropogenic and climatic factors // Modern environmental problems of Ukrainian Polissya and adjacent territories (to the 30th anniversary of the Chernobyl accident): materials of the international scientific and practical conference. Nizhyn, 2016. - P. 170-173 (in Ukrainian).
2. Cleaning and improvement of Lake Syne in Podil district of Kyiv. Technical report on survey (research) work (comprehensive assessment of the state of the reservoir). Vodbud-Ukraine LLC. Kyiv, 2020 (in Ukrainian).
3. Kozytskyi O.M., Shevchuk S.A., Shevchenko I.A., Logunova N.V. Causes of lowering the levels of Lake Syne and measures to improve its ecological condition. Land Reclamation and Water Management, 2020. Issue 2. pp. 101-111 (in Ukrainian).
4. Microsoft Bing [Electronic resource]. – Mode access: https://www.bing.com/maps
5. Preparation of a digital cartographic database of the city of Kyiv on a scale of 1: 10,000. Research Institute of Geodesy and Cartography of State Geodesy Service. Kyiv, 2002 (in Ukrainian).
6. Vyshnevskyi V.I. Water bodies of Kyiv. Kyiv: Nika-Center, 2021.280 p. (in Ukrainian).

DOI: https://doi.org/10.30836/igs.iies.2024.29

**Honcharenko S.**

*Institute of Geological Sciences of the National Academy of Sciences of Ukraine, Kyiv, Ukraine.*
*E-mail: goncharenko.s@icloud.com*

# CHANGES IN GEOLOGICAL ENVIRONMENT IN THE DISPUTED LANDS WITHIN THE ALMAZNO-MAREVSKY GEOLOGICAL-INDUSTRIAL AREA

Extraction of coal in the mines "Pervomaisk", "Rodina", "Golubovskaya", "Gornaya", "Raduha" "Carbonit" within the boundaries of the Almazno-Marevsky geological-industrial area located within the urbanized territories, such as Pervomaisk, Zolote, Hirske and Kalinove led to changes in the geological environment, disruption of natural dynamics and the emergence of dangerous man-made and engineering-geological processes with corresponding environmental consequences (Figure 1).

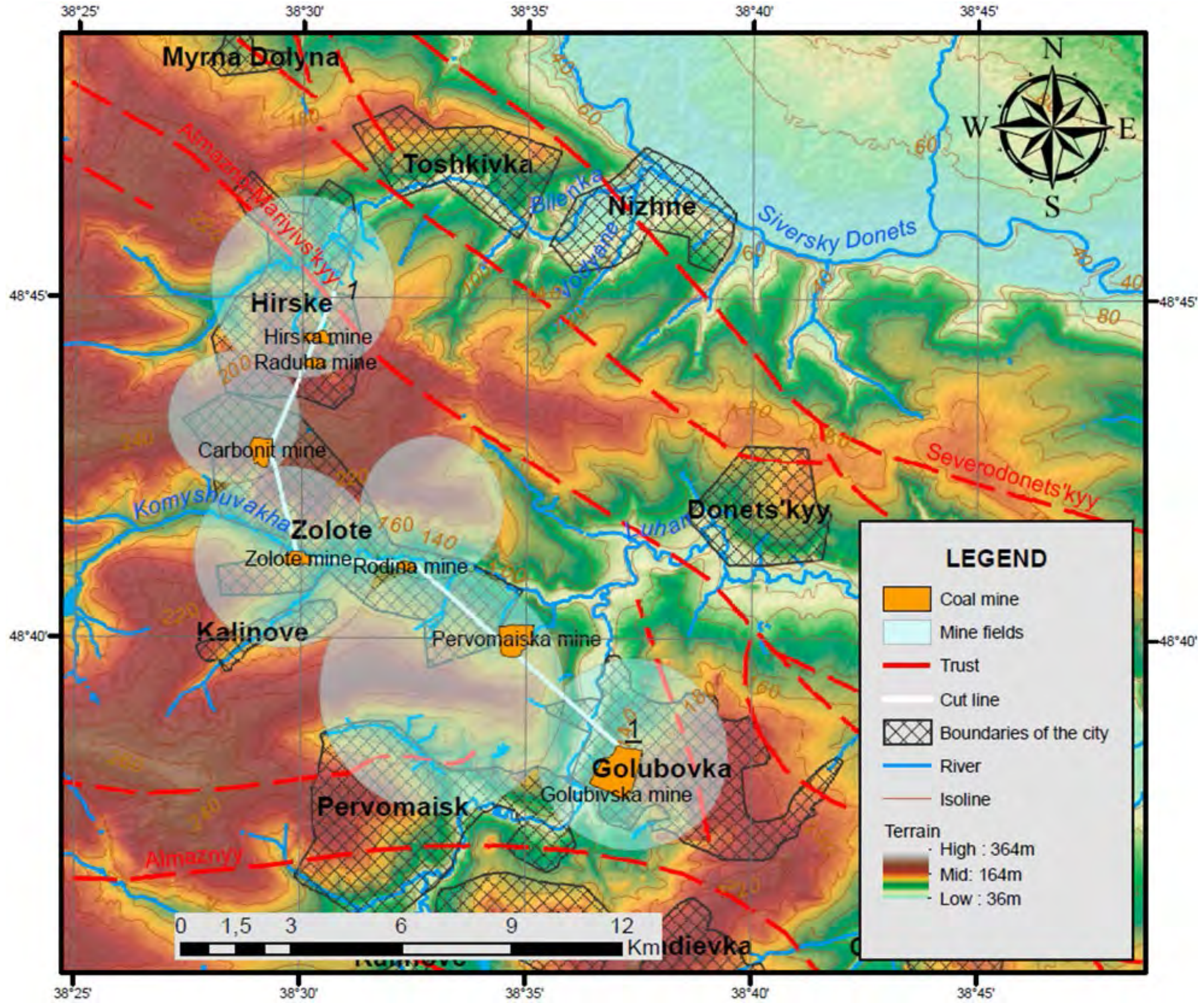

Fig. 1. Plan of the study territory of the Almazno-Marievsky geological-industrial area

The studied territory belongs to the Dnipro-Donetsk seismotectonic province [1] and has a shaking intensity 6 level on the Richter scale. In terms of geostructure, the territory is located in the zone of shallow folds of the Almazno-Mariivska synclinoria of the Donetsk fold structure, next to the Almazno-Mariivskii, Almaznii and Severodonetskii thrusts.

According to geomorphological zoning, territory belongs to the structural-denudational, strongly undulating elevated plain (some places with ridge-hollow relief), which occupies almost the entire territory, and is densely dissected by valleys and gorges of the Lugan' and Komyshuvakha rivers. The elevation difference in the relief ranges from +80 m to +250 m.

Taking into account that the lower boundaries of the geological research environment is determined by the depth of technogenic development territory [2], it was established that its thickness in the studied territory is 480 - 970 m with absolute marks from -330 to -720 m (Figure 2.), where coal deposits are spread, which are interlayered with argillites and siltstones, alternating with clayey and silty shales, sandstones and limestones, which contain thin layers of coal and are covered with quaternary deposits from the surface, mainly in places of river valleys.

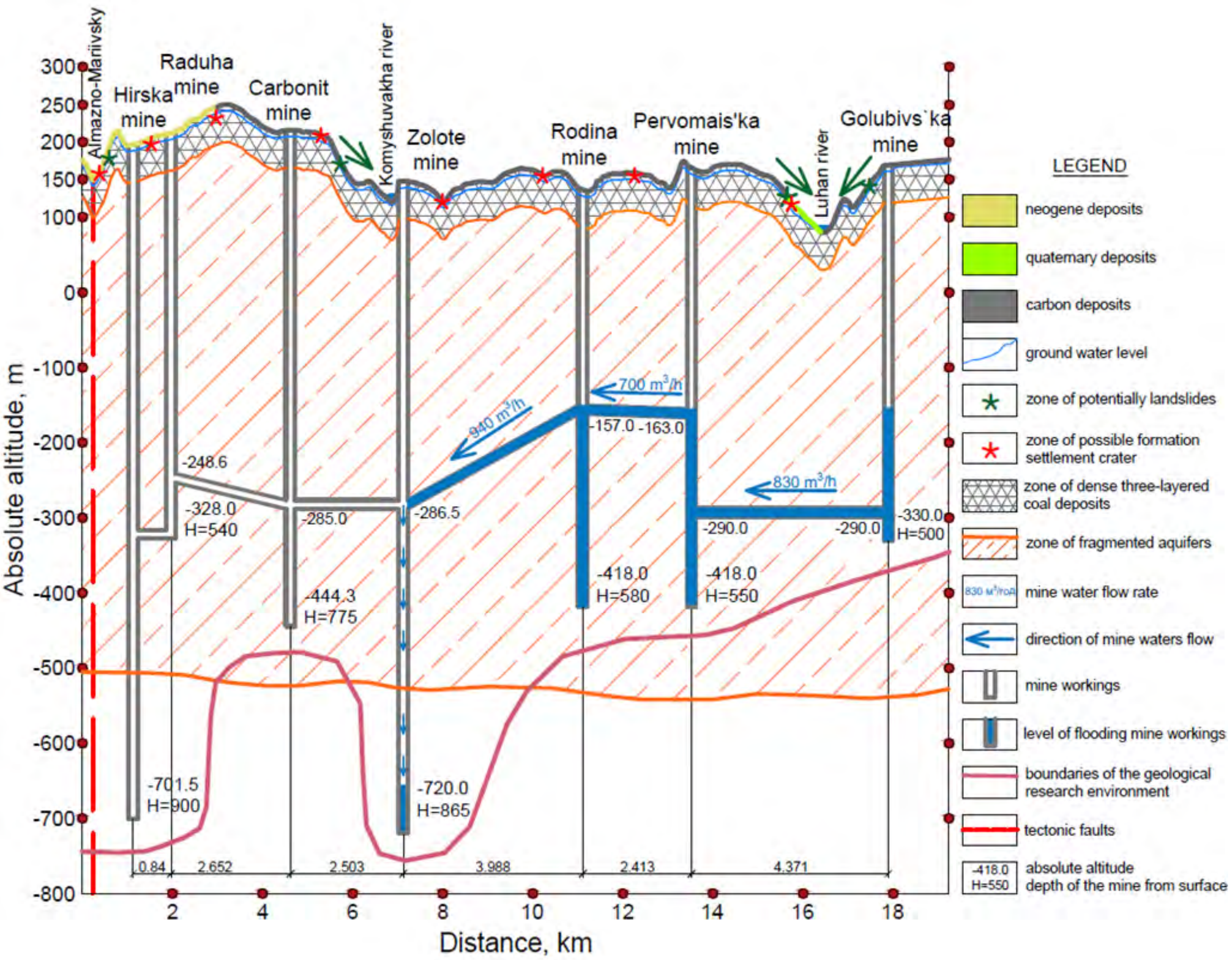


Fig. 2. Cut line 1-1 Figure 1. Geological environment of the Almazno-Marievsky geological-industrial area

Today, shutting down coal industrial enterprises as a result of military operations led to the uncontrolled flooding mines "Pervomaiska", "Rodina", "Golubivska", the flooding level of which is at the absolute mark of -163 m, which are dangerous due to the fact that they are in the zone fragmented aquifers and have a hydraulic connection with the "Zolote", "Girska", "Raduga", "Carbonite" mines, which are at risk of the next flooding. Mine water, passing through the mine at a speed of up to 940 $m^3/h$, is subject to various types of pollution and is characterized by increased mineralization, in particular, the presence of sulfates and chlorides, as well as a high level iron and other heavy metals [3-4].

The hydrogeological conditions of the study territory are caused by the fact that throughout the entire area of distribution of the aquifer in quaternary deposits, along the Lugan and Komyshuvakha rivers, recharge is carried out due to the infiltration of atmospheric precipitation, flood waters and the influx of water from bedrock and has a hydraulic connection with the underground lower deposits [5].

Therefore, threat of mine waters through spillage into the zone of fragmented aquifers, and further expansion in groundwater between the populated areas of Pervomaisk, Zolote, Girske, Golubivka and Kalinov poses serious threats of an environmental and man-made nature. Metals from polluted groundwater can enter the human body through agricultural products and well drinking water [6-7].

If mine waters rise to the surface zone of dense three-layered coal deposits, flooding of territories, subsidence of the surface, and activation of landslides will occur (Figure 2.) [8-9]. Shift of rocks in ravines and gullies of river valleys can lead to the opening of previously existing sources of groundwater, which leads to increased suffusion and activity of shear masses throughout the shear massif and on its slopes [10].

The influence of fractures and the decrease in strength due to the flooding of mine workings are the main factors of the intensity of the occurrence of cracks in coal seams, which leads to the release of methane and the development of deformations of the earth's surface and an increase in rock pressure in the massif, at the same time, with the development of engineering and geological processes, rock pressure becomes more dangerous, since the process of deformations along the mine decreases, but the stresses in individual areas increase [11]. Earthquakes can cause the growth of microcracks underground along mine workings [12].

The ratio of weak and solid rocks has a significant impact on the nature of deformations of the earth's surface [13]. The depth of the working space and methods of controlling rock pressure are key factors that in the future will determine the height of the spread of landslide zones, depth and width of the development of subsidence troughs and rock deformations. Due to the abrupt cessation of the activities of coal enterprises, there is no possibility of controlling roof subsidence and managing rock pressure.

Analysis of the above-mentioned changes in the geological environment provide the basis for a more detailed study of the impact uncontrolled flooding of coal mines. Integrated and differentiated risk assessment will make it possible to quantify the risk under worst-case scenarios and identify objects with the most likely degree of damage and specify the list of objects within the settlements of Pervomaisk, Zolote, Girske, Golubivka and Kalinov that may be damaged as a result of one of the engineering-geological hazardous processes [14].

Determining the boundaries of the geological environment within the Almazno-Marievsky geological-industrial area provides an understanding of the connection between mines that are flooded due to the abrupt cessation of the activities of coal enterprises, which will entail the development of processes such as deformation of the surface and underground space, the release of methane, the occurrence of local earthquakes, and the ingress of contaminated mine waters into underground and ground water, as well as into the Lugan and Komyshuvakha rivers.

**References**

1. Kushnyr A.N. Tectonic earthquakes of the Donbas anomaly of electrical conductivity, their possible connections. Geodynamics. – 2011. – № 2 (11). P. 150-152.

2. Demchyshyn M.G. Technogenic impacts on the geological environment of Ukraine. – K.: IGS NAS of Ukraine, 2004.

3. Shiv K., Kumar N. Ground Water Contamination in Coal Mining Areas: A Critical Review. International Journal of Engineering and Applied Sciences, vol. 3, № 2, Feb. 2016.

4. Carreras H.A., Wannaz E.D., Pignata M.L. Assessment of human health risk related to metals by the use of biomonitors in the province of Cordoba, Argentina. Environ. Pollut, 2009, pp.157-117.

5. Explanatory Note to the Hydrogeological Map of the USSR at a Scale of 1:200000, Donbas Series, Letter M-37-XXXIII, Kyiv 1975.

6. Haroon G., Khoiyangbam R., Ahmad S., Zuber S. Trace Metal Levels in the Muscle Tissues of Ctenopharyngodon Idella (Grass Carp) and Ophiocephalus (Snake Headed Fish) of Antiya Tal of Jhansi City (U.P.). International Journal of Applied Environmental Sciences. V (4), 505–512, 2010.

7. Tarasenko I. Chemical composition of groundwater in abandoned coal mines: Evidence of hydrogeochemical evolution. Applied Geochemistry, 2022.

8. Gojković Z., Kilibarda M., Brajović L., Marjanović M., Milutinović A., Ganić A. Ground Surface Subsidence Monitoring Using Sentinel-1 in the “Kostolac" Open Pit Coal Mine. Remote Sensing. 2023; 15(10):2519.

9.Shang H., Zhan H-Z., Ni W-K., Liu Y., Gan Z-H., Liu S-H. Surface Environmental Evolution Monitoring in Coal Mining Subsidence Area Based on Multi-Source. Remote Sensing Data. Front. Earth Sci. 2022; 10:790737.

10. Demchyshyn M., Anatskyi O. The path of aquifer development on the slopes of the Dnieper and Lybid valleys. ISSN 0367–4290. Geol. Journ. 2009. № 3.

11. Medyantsev A. Displacement of rocks and the earth's surface under the influence of mine workings. Novocherkassk: Novocherkassk Polytechnic Publishing House. Inst., 1976. – 83 p.

12. Külekçi G. Damages caused by earthquakes to mines and underground spaces and minimizing these damages. International Journal of Advanced Natural Sciences and Engineering Researches (IJANSER), 7(10), 199-206.

13. Avershin S. Displacement of Rocks in Underground Excavations. Ugletekhizdat Publ., 1947. – 245 p.

14. Shekhunova S.B., Kril T.V. Geological and economic risk assessment for territories of hazardous geological and technogenic processes (exemplified by Solotvyno township). Naukovyi Visnyk Natsionalnoho Hirnychoho Universytetu. 2022, (2): 079-085.

DOI: https://doi.org/10.30836/igs.iies.2024.38

**Nikitash O., Havryliuk R., Shpak O., Negoda Iu., Lohvinenko O., Nikitash Iu.**

*Institute of Geological Sciences of the National Academy of Sciences of Ukraine, Kyiv, Ukraine.*
*E-mail: olgagrig88@ukr.net, gavrilyuk.ruslan@gmail.com, shpak_lena@yahoo.com, ynegoda2008@gmail.com, lohvynenko.olha@gmail.com, yn88@ukr.net*

# MONITORING OF GROUNDWATER WATER QUALITY IN ECO-INDUSTRIAL PARK BILA TSERKVA

Over the course of the last decade, the whole world including Ukraine has been experiencing a growing problem associated with the deterioration of the environment due to the impact of anthropogenic activity and urbanization. Industrial enterprises generate large amounts of waste, which may be detrimental to overall health. Numerous environmental problems that arose from industrial development prompted the creation of eco-industrial parks (EIP). Groundwater monitoring in EIP becomes a key factor in ensuring sustainable development and preserving environment.

At present, Ukraine is a part of the global program of eco-industrial parks (GPEIP) implemented by the United Nations Industrial Development Organization (UNIDO). The goal of GPEIP is to demonstrate the benefits EIP, which are to increase resource productivity and improve the economic, environmental and social performance of enterprises, as well as to promote inclusive and sustainable development [5]. In 2020, Bila Tserkva Cargo Aviation Complex (BCAC) became a member of GPEIP in Ukraine [6].

This research carried out in the frame of the project “Hydrogeological substantiation of the control system of the impact of eco-industrial parks on the environment” included examination of subsurface contamination with petroleum products and monitoring of groundwater quality in EIP Bila Tserkva.

Subsurface contamination with petroleum products was found at the studied area in the early 1990s. The source of contamination was the former Bila Tserkva Aircraft Repair Plant (BARP), next to which the State Arboretum Olexandria and the Ros River locate (Fig. 1).

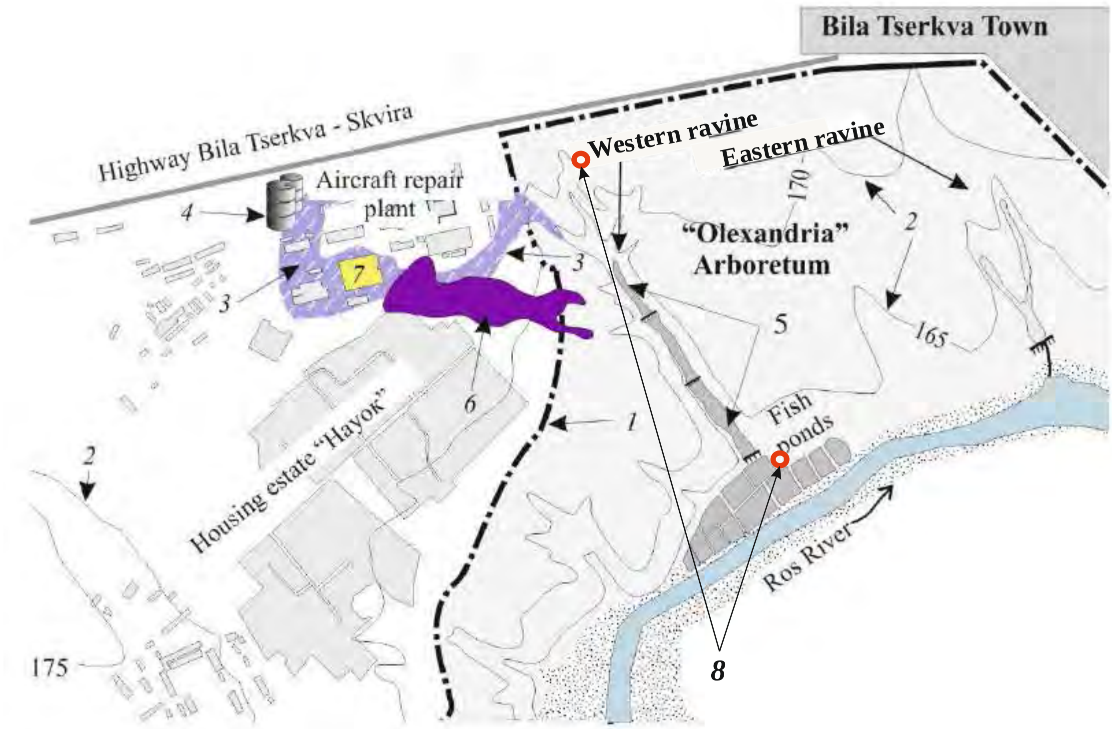


Fig. 1. The overview scheme of the research area: 1 – boundary of Olexandria arboretum; 2 – groundwater lines; 3 – subsurface contamination with petroleum products (by Pravoberezhna Geological Expedition, 1990); 4 – a fuel and lubricant warehouse; 5 – a cascade of artificial ponds (Poterchata, Rusalka and Vodyanik); 6 – a mobile petroleum products layer (by IGS, 2007); 7 – an aircraft repair workshop; 8 – wells recommended to the state groundwater monitoring system of Ukraine (by IGS, 2021)

In 1990, the appearance of petroleum products in surface water of ponds of the Western ravine in Olexandria arboretum was found. Petroleum product concentrations varied from 0.12 to 4.94 mg/l in the

Poterchata pond, from 0.07 to 4.40 mg/l in the Rusalka pond, and from 0.04 to 3.68 mg/l in the Vodyanik pond, which is tens and hundreds of times higher than maximum limited concentrations (0,01 mg/l) [8].

In 2000-2001 and 2006-2007, the research carried out by Institute of Geological Sciences revealed that the main contamination sources were the facilities of BARP such as fuel and lubricant warehouses, an aircraft repair plant, engine repair and testing shops, and a petrol station. Three lenses of mobile petroleum products with a thickness up to 2.5 m located on the water table of the submarine water-glacial aquifer were found and deliniated. [2]. Groundwater contamination with dissolved petroleum products covered all three ravines of the arboretum (Western, Central and Eastern) and the ravine “Forester's House”. The maximum contents of petroleum products in groundwater (30 mg/l) and bottom sediments (5600 mg/kg) were found at the place of groundwater discharge in the upper Poterchata ravine [7]. As the waters of all ponds are discharged into the Ros River, the ecological situation in the arboretum also significantly affected on the state of the Ros river basin, which is the main source of drinking water for the residents of Bila Tserkva and other towns downstream. Long-term contamination negatively affected on the state of the woody and herbaceous vegetation in the arboretum, and the high toxicity of soluble hydrocarbons killed fish in the Western cascade of ponds [3].

In 2019, within the agreement on scientific cooperation between Institute of Geological Sciences and Olexandria State Arboretum we carried out the ecological and geological survey, which showed that petroleum contamination of the cascade of ponds in the Western ravine continued. The signs of dissolve petroleum product flow discharge into the mouth of the lateral trough crossing the western slope of the ravine (the Poterchata pond) were revealed (Fig. 2). This gives reason to believe that contaminant migration from the groundwater recharge area, where contamination sources locate, to the place of groundwater drainage in the Western ravine through moraine sediments occurs in high conductivity layers formed by fluvioglacial sand [1]. In order to confirm this assumption and solve the problem of groundwater and surface water protection, observation posts must be set up in places where petroleum products are expected to enter the ponds.

Fig. 2. Petroleum contamination of surface water of the Poterchata pond and petroleum product flow discharge on the surface (2019)

Since 2021 study of the contaminated area has been continued. Field works included sampling of soil, surface water and groundwater within the cascade of ponds in the Western ravine to identify the places of primary petroleum product entry, inspection of existing observation wells, drilling and installation of additional ones, and periodic measurements of water and petroleum product levels in observation wells (Fig. 3).


Fig. 3. Drilling of observation wells and measuring of water and petroleum product levels (2021)

Several observation wells drilled more than 30 years ago into the aquifer in the fractured zone of crystalline Precambrian rocks were deconserved. Since this aquifer lies first below the surface, it has undergone the main contamination. Testing of the wells revealed groundwater contamination with petroleum products [4]. Two of these wells have been recommended to be included in the State Groundwater Monitoring Network of Ukraine. According to the latest monitoring data in 2023, a mobile petroleum product layer (0.07-0.19 m) was found in all observation wells located on the western slope of the Poterchata pond (Table 1). Dissolved hydrocarbon concentrations in waters of the Poterchata pond vary from 0.36 to 1.33 mg/l (Table 2).

Table 1. The results of measurements of petroleum product and groundwater levels

| No of well | Petroleum product level (m) | Groundwater level (m) | Petroleum product layer (m) | Petroleum product level (m) | Groundwater level (m) | Petroleum product layer (m) |
|---|---|---|---|---|---|---|
| | August 9, 2022 | | | May 26, 2023 | | |
| 1 | 10,02 | 10,23* | 0,21 | 9,93 | 10,11 | 0,18 |
| 2 | 10,05 | 10,38 | 0,33 | 9,98 | 10,10 | 0,12 |
| 3 | closed | | | 9,76 | 9,84 | 0,08 |
| 4 | 10,19 | 10,40* | 0,21 | 10,06 | 10,07 | 0,01 |
| 5 | 10,08 | 10,28* | 0,2 | 10,01 | 10,19 | 0,18 |
| 6 | 9,85 | 10,19* | 0,34 | 9,77 | 9,96 | 0,19 |
| 7 | 10,12 | 10,27 | 0,15 | 9,97 | 10,08 | 0,11 |
| 8 | 10,23 | 11,00* | 0,77 | 10,13 | 10,20 | 0,07 |

*– bottomhole

Table 2. The results of determination of petroleum product concentrations in water

| No p/p | Place of sampling | Petroleum product concentrations (mg/l) | Additional information |
|---|---|---|---|
| May 26, 2023 | | | |
| 1 | Well 3m | 1.68 | Water is clear |
| 2 | Well 5m | 2.90 | Sediment is observed |
| 3 | Poterchata pond, 2nd ravine (3 m from the bank) | 1.31 | Water is clear |
| 4 | Vodyanik stream | 0.44 | Water is clear |
| 5 | Rusalka pond | 0.03 | Water is clear |
| 6 | Poterchata pond (draining through the dam) | 0.36 | Water is clear |
| 7 | Poterchata pond, 1st ravine near the bank | 0.61 | Sediment is observed |
| 8 | Poterchata pond, 1st ravine (3 m from the bank) | 1.33 | Water is clear |
| 9 | Pore solution | 30.66 | Water is clear |

Thus, the results of this research indicate a negative impact of EIP Bila Tserkva on the environment. It is necessary to create a well network for monitoring groundwater quality, increase both environmental and economic efficiency of remediation measures, and promote the solution of current environmental problems related to soil and water contamination with petroleum products. Improvement of the ecological state of the contaminated area of Olexandria arboretum will contribute to the preservation of historical park compositions and valuable plant communities as well as the development of tourism.

**References**

1. Bricks, A.L., Gavryliuk, R.B., Negoda, Y.O. (2020). Hazard of petrochemical pollution of ponds of the “Olexandria” arboretum (Bila Tserkva). Journal of Geology, Geography and Geoecology. No 29(2), 243-251.
2. Bricks, A.L., Negoda, Y.A. (2008). Formation of a zone of petrochemical pollution near the “Olexandria” arboretum (Bila Tserkva). Geological Journal, No 4. 106-112.
3. Galkin, S.I. (2011) Dendrological parks of the National Academy of Sciences of Ukraine: problems of preservation of historical plantations related to the strengthening of anthropogenic impact on their territories (on the example of the dendrological park “Olexandria” of the National Academy of Sciences of Ukraine). Journal: Introduction of plants, No 2, 118-123.
4. Havryliuk R.B., Shpak O.M., Negoda Y.O., Lohvinenko O.I., Nikitash O.G. Study of environment contamination with petroleum products in the region of Bila Tserkva eco-industrial park // Proceedings of 16th International Conference Monitoring of Geological Processes and Ecological Condition of the Environment, Nov 2022, Volume 2022. DOI: https://doi.org/10.3997/2214-4609.2022580153.

5. [Electronic resource]. - Mode access: http://bcavia.com/article/kp-bilocerkivskij-vantazhnij-aviacijnij-kompleks-dolucha%D1%94tsja-do-mizhnarodnogo-pro%D1%94ktu-oon-zi-stvorennja-eko-industrialnogo-parku.html.
6. Implementation handbook for eco-industrial parks. (2017). United Nations Industrial Development Organization.
7. Negoda, Y.O., Golub, G.I., Shpak, O.M. (2014). Assessment of subsurface contamination with petroleum products and heavy metals within the state dendrological park “Olexandria” (Bila Tserkva). National Natural Parks - Past, Present, Future: Proceedings of the International Scientific and Practical Conference dedicated to the 30th anniversary of the Shatsk National Park (Svityaz, April 23-25, 2014). Kyiv, 168-172.
8. Pleskach, L.Y. (2004). Contamination of water reservoirs of the dendrological park “Olexandria” and its impact on the state of vegetation. Journal: Introduction of plants, 80-89.

*DOI: https://doi.org/10.30836/igs.iies.2024.22*

**Pokshevnytska T., Khrutba O.**

*National Transport University, Kyiv, Ukraine. E-mail: officenttn@gmail.com*

# DISTRIBUTION PATTERNS AND HYDROGEOLOGICAL ASPECTS OF ANTHROPOGENIC WATER POLLUTION

Ukraine possesses a considerable amount of water resources, such as rivers, lakes, and ponds. However, these water bodies face various forms of pollution due to intensive industrial and agricultural activities in the country. Anthropogenic pollution problems include discharges of industrial wastewater, agricultural waste, oil spills, and other sources of pollution.

The war's impact on hydrological bodies in Ukraine could be significant and negative. During armed conflict, water sources can become polluted, groundwater levels can decrease, waterways and aquifers can be destroyed, and the ecological balance of rivers and lakes can be disrupted.

Additionally, water infrastructure, including water intakes, water pressure structures, sewage systems, and other hydro-ecological systems, may be impacted. This damage can result in drinking water shortages and sanitation issues (Figure 1).

Furthermore, warfare can result in the contamination of waterways and rivers due to the discharge of oil, explosives, or other dangerous materials. This can have adverse effects on aquatic ecosystems and the well-being of individuals who reside in the vicinity and rely on these water sources for their daily requirements [1].


Fig. 1. The main ways of pollution of the hydrosphere

State water monitoring data has revealed significant water pollution problems in various regions of Ukraine, particularly in the central part of the country and some regions in the east and west [2].

The map of monitoring and environmental assessment of water resources of Ukraine shows the level of water pollution in Ukraine (Figure 2). Green dots indicate areas where pollution does not exceed the norm and are scattered across the map. Yellow dots show places where the level of pollution exceeds the norm by up to 2 times. Orange dots indicate places with pollution levels 3 to 4 times higher than the norm. Red dots, which are more common, indicate locations with pollution levels 5 times or more above the norm. The highest levels of pollution are shown by red dots, which are concentrated in central Ukraine and some regions in the east and west of the country. Blue dots indicate missing data.

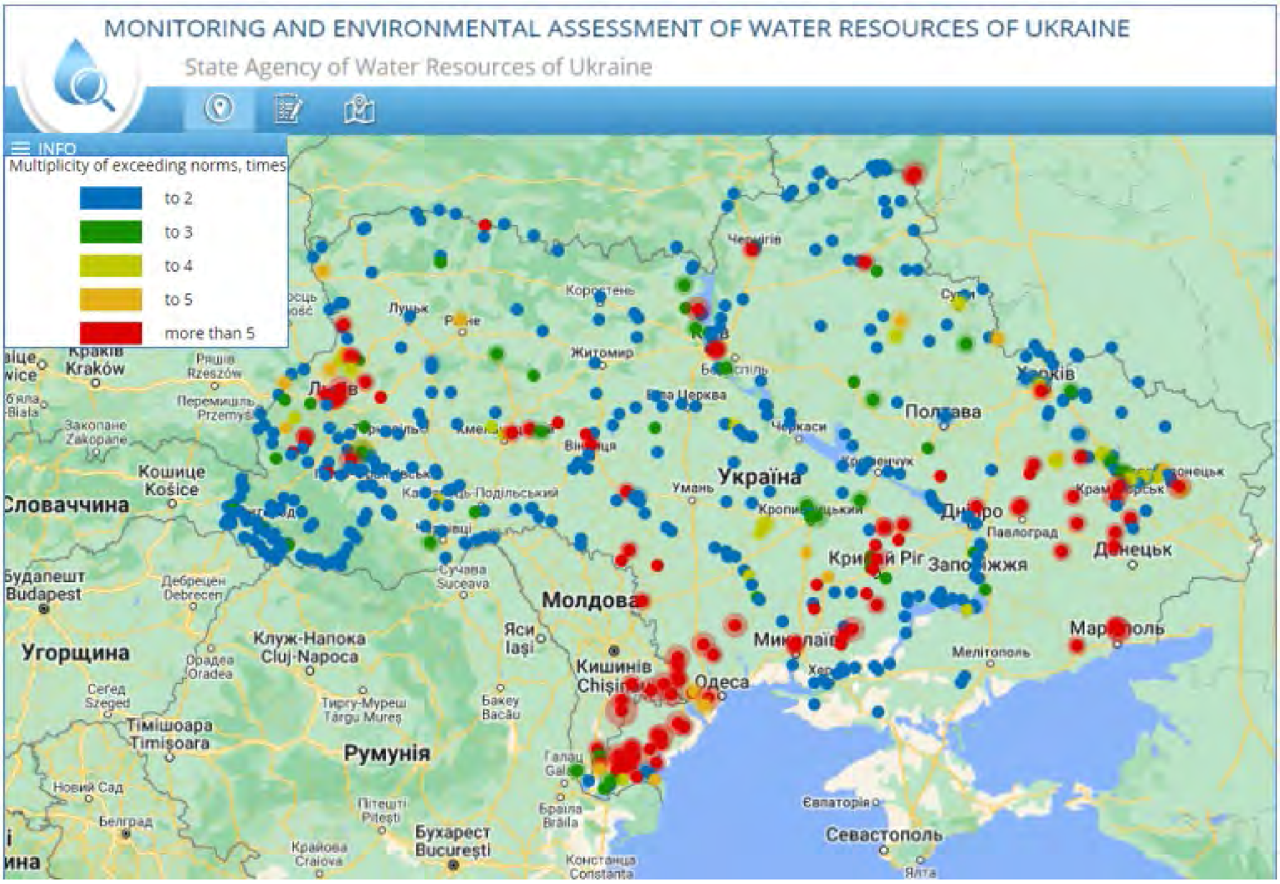

Fig. 2. Monitoring and environmental assessment of water resources of Ukraine

To evaluate the effect of human-made pollution on hydrogeological processes and water resources, a thorough analysis is necessary. The collected data will be linked with existing data on hydrogeological processes and water resources to assess the impact of anthropogenic pollution. Simulation models will be used to predict the possible effects of anthropogenic impacts on hydrogeological processes and water resources. Determination of the potential risk of anthropogenic pollution to water bodies by using existing metrics and standards. Strategies and measures will be developed and implemented to minimize anthropogenic impacts and preserve hydrogeological processes and water body resources (Figure 3).

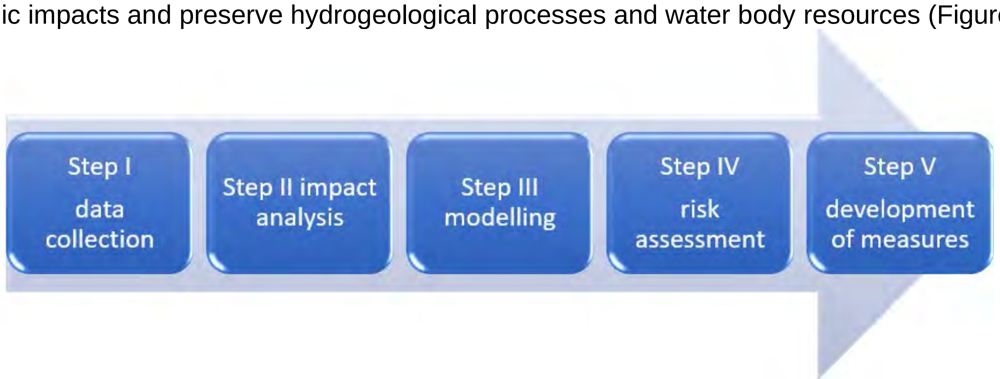

Fig. 3. The evaluation steps

The distribution of pollution varies in different water systems depending on several patterns [3]. Pollution of water systems can be concentrated in certain geographical areas due to the concentration of industrial zones, urban centers or agricultural areas. Water systems used for industrial purposes, such as power generation or industrial beneficiation, may be subject to more intense pollution than water systems used for natural or recreational use. Population size can affect the level of anthropogenic pollution in a water system. Larger population centers tend to have higher levels of waste entering water systems. Technological development also plays a role in controlling and reducing pollution. The distribution of anthropogenic pollution can be influenced by the extent to which technologies are developed. Regions with a strong technological base may have more advanced water treatment and pollution control systems.

Additionally, the characteristics of the natural water environment, such as river systems, lakes or coastal areas, can contribute to the accumulation or distribution of pollutants. For instance, the sluggish flow of water in rivers may promote the buildup of pollution, whereas a tidal system may facilitate the dispersion of pollution (Figure 4).

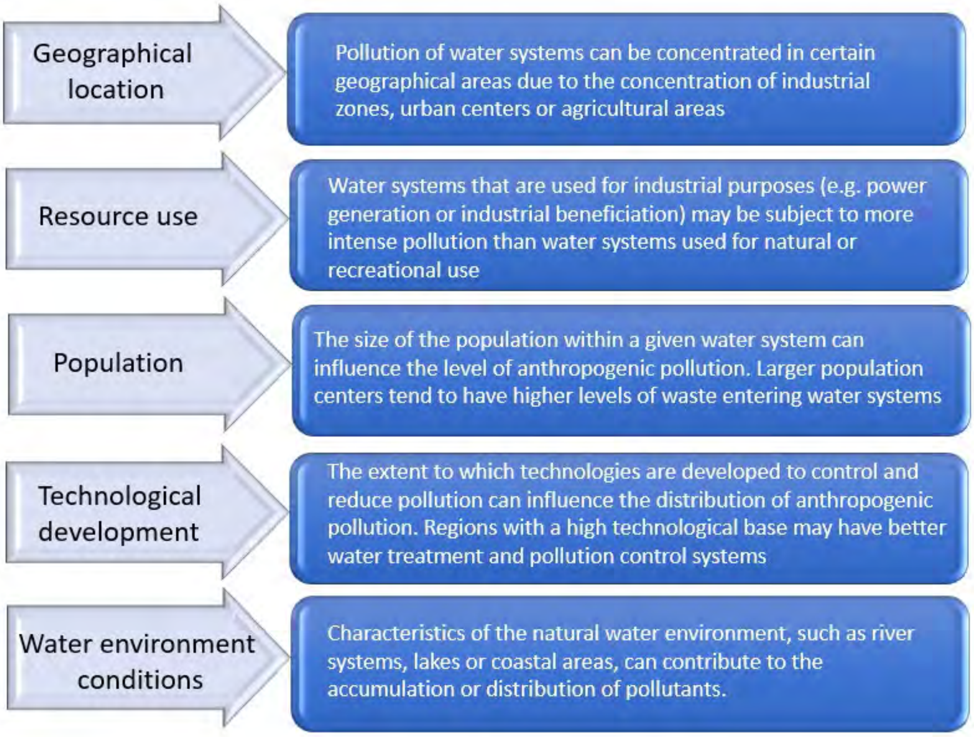


Fig. 4. The distribution of the water pollution

To minimise emissions and discharges of pollutants into water bodies, it is recommended to use environmentally friendly production and processing methods. Consider implementing new technologies that are less harmful to the environment.

Efficient use of resources can significantly reduce water pollution. To reduce emissions and discharges of pollutants into water sources, it is advisable to reduce the use of water, energy and raw materials.

The implementation of wastewater treatment systems in both industrial and residential areas can significantly reduce the discharge of harmful substances into water bodies. The use of modern filtration systems and biological treatment methods can be highly effective.

Additionally, conducting educational campaigns and raising environmental awareness in society can positively impact people's behavior towards water use and pollution. Promoting rational consumption and raising awareness of the importance of water conservation are essential aspects.

Regular monitoring of water quality and compliance with environmental standards will help to quickly identify pollution problems and develop effective measures to reduce them. It is necessary for government agencies, citizens' associations, and enterprises to work together to ensure effective control.

Ukraine's water resources are at anthropogenic pollution due to both human-made pollution and the effects of armed conflict. The contamination of water bodies poses a significant threat to ecosystems, biodiversity, and the health of those who depend on these water sources. It is essential for the government, industries, and communities to collaborate to tackle these challenges and implement sustainable practices to safeguard and conserve Ukraine's precious water resources for future generations.

**References**


1. *Protection of water resources of Ukraine: from crisis to recovery – WAREG - European Water Regulators*. (2023, October 30). WAREG - European Water Regulators. https://www.wareg.org/articles/protection-of-water-resources-of-ukraine-from-crisis-to-recovery/.

2. Map *"Exceeding the maximum limit of water quality indicators at monitoring stations"*. (n.d.). http://monitoring.davr.gov.ua/EcoWaterMon/GDKMap/Index.

3. Snitinsky V., Khirivsky P., Zelenko O., Ivankiv M., & Gnativ I. (2022). Injection of anthropogenic factors on the rivers of the western region of the Ukrainian Carpathians. Bulletin of Lviv *National Ecological University "Agronomy", 26*, 22–26. https://doi.org/10.31734/agronomy2022.26.022.

*DOI: https://doi.org/10.30836/igs.iies.2024.35*

**İlayda Sapmaz[1], Sena Uyar[2], Mutlu İçhedef[1]**

*(1) Ege University Institute of Nuclear Sciences, 35100, Bornova, Izmir, Türkiye.*
*E-mail: ilaydaeda19@gmail.com, mutlu.ichedef@ege.edu.tr*
*(2) Ege University Faculty of Education, Department of Mathematics and Science Education, 35100, Bornova, Izmir, Türkiye. E-mail: sena.uyarr@hotmail.com*

# DETERMINATION OF RADIOACTIVITY AND HYDROGEOLOGICAL PROPERTIES OF AGORA HISTORICAL SITE AND HALKAPINAR UNDERGROUND WATER RESOURCES

Izmir is the third most populous city in Turkey, after Istanbul and Ankara, with a population of 4,479,525 people as of 2024. While most of this population, approaching five million, is concentrated in the city center around the Gulf of Izmir, the remaining part of the population is scattered in the districts on the periphery. It has been observed that migration to Izmir city center and its surroundings has accelerated in recent years. With the increasing population, urbanization is also gaining momentum, and as a result, population density (population per unit area; person/km$^2$) is also increasing. According to the last assessment, the population density in the city center was calculated as 366 people/km$^2$ [1]. Izmir is not considered a city rich in water resources sufficient for its dense population. While there are underground water sources in Izmir, the city can face drought risks due to its climate conditions and geographical structure. Especially during the summer months, the city may experience water scarcity. Therefore, it is important to use water efficiently and to conserve water resources.

One of the most significant sources of water for the city is supplied by Halkapınar Springs. Halkapınar springs, located within the Izmir city area and providing water to the city from the lake in the region for 122 years since 1897, are an important water source for Izmir. The total number of wells was 25 by opening 3 wells (research wells) in 1972, 10 wells in 1973, 6 wells in 1975-1976, and 6 wells in 2009. A total of 19 wells are currently active. The water produced from deep wells is collected in the tank in Halkapınar, purified in the Halkapınar Arsenic Treatment Plant, and transmitted to the city through 2 pump stations with 9 motor pumps [2]. Another water source emerges within the ancient city of Agora. The Agora Archaeological Site, located in Kemeraltı, Konak District of Izmir, is the city center of the ancient city of Symrna, founded between Kemeraltı and Kadifekale, with administrative, social, cultural, and religious functions during the Hellenistic and Roman periods. A significant part of the ruins in the Agora date back to the 2nd century AD.


Fig. 1. The map of study area

This study aims to determine the radioactivity, physical, and chemical properties of Agora and Halkapınar water resources. We began working in September 2023, and approximately 100 water samples have been analyzed in the ongoing study. The radioactivity content (radon and radium), temperature, and silica content of the waters from Halkapınar and Agora are being studied. Radon activity concentrations of waters were determined by RAD7H2O (Durridge, USA). Water samples were taken from each water source with special 250 ml bottles, and measurements were made in the laboratory. Radium concentrations were determined indirectly by measurements using the radioactive balance between radon and radium. For this purpose, water samples in which radon was measured were kept for 1 month and measured again. Temperature and pH were determined on-site using a hand-held pH meter. Silica measurements were performed using the colorimetry method. The obtained results are presented in Table 1.

Table 1. Mean values of groundwaters

| **Name** | **Radon ($Bq\ l^{-1}$)** | **Radium ($Bq\ l^{-1}$)** | **Temperature (°C)** | **pH** | **Silica ($mg\ l^{-1}$)** |
|---|---|---|---|---|---|
| AGK1 | 8.4 | 5.0 | 19.5 | 7.3 | 32.4 |
| AGK2 | 5.8 | 3.8 | 19.5 | 7.2 | 35.6 |
| AGK3 | 12.0 | 7.5 | 19.5 | 7.4 | 33.7 |
| K4 | 2.9 | - | - | 7.1 | 13.6 |
| K5 | 3.8 | - | - | 7.2 | 13.9 |
| K9 | 2.9 | - | - | 7.1 | 14.2 |
| K11 | 3.1 | - | - | 7.1 | 14.4 |
| K12 | 3.6 | - | - | 7.1 | 13.5 |
| K14 | 3.7 | - | - | 7.1 | 13.4 |

The studied areas are important because they are strongly connected to the Izmir Fault Zone. Therefore, the water radon levels at the Agora Historical Site show very large variations during the study period. The ongoing study will focus on collecting more data on these sites. Specifically, we will add measurements of $^{2}H$ and $^{3}H$ to obtain information on the sources of these waters and the connections between them.

**References**

1. Türkiye İstatistik Kurumu (TÜİK), "İstatistik Veri Portalı" https://data.tuik.gov.tr/Kategori/GetKategori?p=nufus-ve-demografi-109&dil=1 Son Erişim Tarihi:05.04.2021.
2. IZSU, "https://www.izsu.gov.tr/tr/TesisDetay/1/4/2#:~:text=Halkap%C4%B1nar%20derinkuyular%C4%B1ndan%20%C3%BCretilen%20su%2C%20%C5%9Fehrin,Toros%20b%C3%B6lgeleri%20direkt%20olarak%20beslenmektedir. Access Date: 15:03.2024.

DOI: https://doi.org/10.30836/igs.iies.2024.32

**Streltsov A.**

*Institute of Geological Sciences of the National Academy of Sciences of Ukraine, Kyiv, Ukraine.*
*E-mail: streltsov.kiev.ua@gmail.com*

# ANALYSIS OF ENGINEERING AND GEOLOGICAL CONDITIONS AND THE ASSURANCE OF SLOPE STABILITY ON ONE OF THE DNIEPER SLOPE SECTION WITHIN THE PECHERSKY DISTRICT OF KYIV

The high investment attractiveness of real estate in the central part of Kyiv and the limited land fund for new construction cause great interest in the development of plots with complex engineering and geological conditions. Administratively, the studied territory is located between Ivan Mazepa Street, 1 and Parkova Road in the Pechersk District of Kyiv.

The studied territory is located at the intersection of the mixed forest zone and the forest-steppe zone of the Dnipro highland region. Orographically, the territory belongs to the Dnipro Highlands (Kyiv Plateau), dissected by systems of ravines and gullies. In terms of geomorphology, the research site is located in the edge of the Kyiv Loess Plateau and the slope edge to the Dnipro Valley [1]. The relief of the studied territory was formed as a result of the territory planning with bulk soils. In the north-eastern part, the site is bordered by a steep slope to the Dnipro River.

The geological structure of the area up to 30.0 m consists of this sediments [2]:

- (t H) – modern bulk soils, which are composed of sandy and dusty, dark gray, black, brownish-gray, hard and plastic loams, in places with an admixture of organic substances, with inclusions of construction debris up to 25% (broken bricks, rubble stones, wood, glass, scrap metal and others), with layers and lenses of hard-soft plastic loam 15%, capacity up to 10.4 m;
- (d, dz, b H) – a Holocene complex of deluvial, deluvial-slide and swampy soils, which is composed of sandy loams, dusty, from solid to fluid consistency, light rigid-plastic loams, in places with an admixture of organic substances and lenses of heavily peated soils. The capacity of the complex in some places is up to 11.8 m;
- (edv PIII-H) – eluvial-deluvial-eolian Late Neopleistocene-Holocene soils, which are represented by sandy loams, dusty, loess-like, subsidence, hard and plastic, loams light and heavy dusty, tightly plastic. The thickness of the layer is up to 12.1 m.
- (f,l-g PII) – a complex of Middle Neopleistocene rocks of fluvio-, limnoglacial, and glacial genesis, represented by dusty, dense sands, sandy loams, light and heavy loams, of various consistencies. The thickness of the layer reaches 9.0 m;
- (l PI-II) – a complex of Lower Neopleistocene rocks of limnic genesis represented by hard and semi-hard clays, light and heavy loams, with a total thickness of up to 9.7 m;
- ($N_2$čb) – deposits of the Pliocene Neogene system (red-brown clays), represented by light and heavy dusty, semi-hard and hard clays, up to 7.5 m thick;
- ($N_{1\text{-}2}$sg) – deposits of the Neogene system of the Lower Pliocene-Upper Miocene (variegated clays), which are composed of light and heavy, semi-hard and hard clays, up to 8.1 m thick;
- ($N_1$np) – deposits of the Neogene system of the Poltava series, which are represented by sandy, hard sandstones with weakly cemented sandstone lenses, with an open thickness of up to 6.3 m.

The hydrogeological conditions of the research area are characterized by the presence of one pressure-free mixed aquifer: the groundwater horizon in Holocene sediments and an aquifer complex in glacial and lacustrine sediments of the Neopleistocene [2,3].

Groundwater levels in the wells were established at depths of 7.7 m - 14.5 m. Within the upper flat part of the site, the absolute marks of the aquifer mirror vary from 179.59 m near the street. Mazepy up to 175.05 m on the edge of the slope. Along the slope, the levels change in the range of 175.00 m - 162.35 m. In some wells, an abnormally high level of underground water is noted - 175.00 m. This is connected with the formation of head water due to losses from water-bearing communications that pass along the edge of the slope.

A calculation of the slope stability in the natural and forecast states was performed according to profiles II-II', III-III' and IV-IV' (Fig. 1) to assess the slope state (stable, landslide-prone, landslide) from a geological point of view at the time of the investigations [2].

The work was performed in RocScience Slides 6 software. The Slides 6 program analyzes the sliding surfaces stability using methods of vertical compartments limit equilibrium. It makes it possible to analyze individual slip surfaces or to apply search methods to determine the critical slip surface for a given slope.

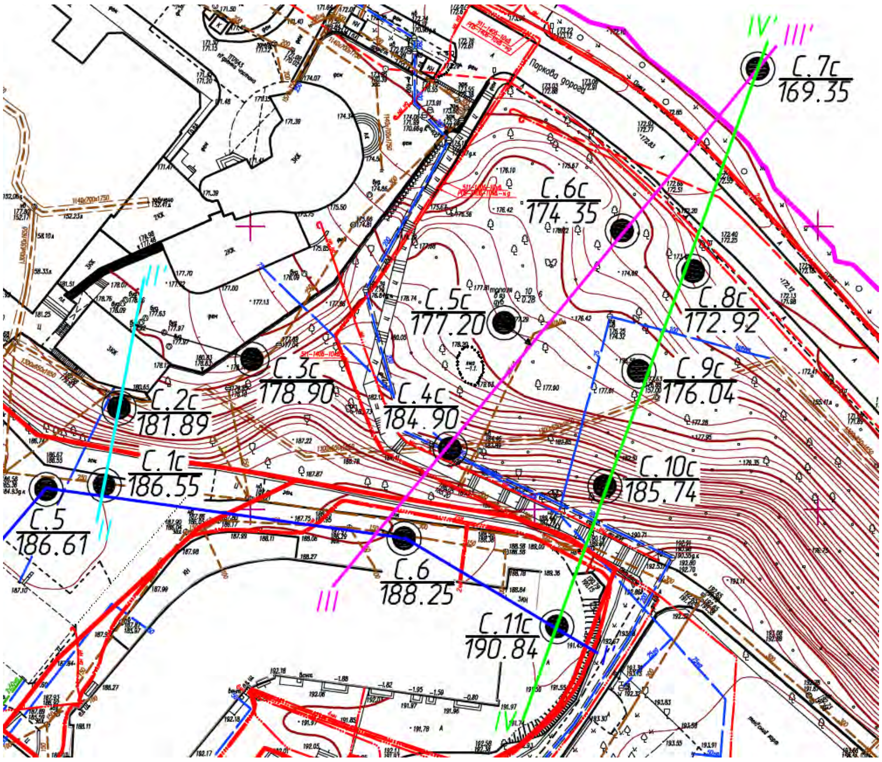


Fig. 1. Layout of calculation profiles

Calculations were carried out on a round-cylindrical sliding surface. The properties calculated characteristics of the selected engineering and geological elements are accepted at a confidence probability = 0.95. Walls and foundations of existing buildings are applied to profiles III-III' and IV-IV', taking into account the loads from them.

The forecast state was modeled taking into account a possible rise in the groundwater level by 1.5 m and wetting of the upper soil layers due to precipitation. According to table B.5 of DBN B.1.1-46:2017 [4], the normative factor of the stability margin under these conditions is 1.25.

Calculation results:

1. The slope along the II-II' profile is organized by several tiers of retaining walls, which were erected during the residential complex construction on the street. Hrushevskyi 11, therefore, together with the structure of the building, they perceive the main shear pressure from the slope. In its natural state, the probable sliding plane passes in the upper part of the slope on bulk soils, Kst (stability margin coefficient) is 1.41, which is greater than the normative value and indicates its stable condition. In the forecast state, Kst = 1.19. This value is below the norm, but the slope remains stable.

2. According to the III-III' profile in its natural state, the sliding plane originates behind the wall of the Komendatura building and passes through Lower Neopleistocene deposits of limnic genesis, which are lithologically represented by clays and loams. Kst = 1.47. The slope is in a stable state and is fully provided with a normative coefficient.

In the forecast state, the sliding curve shifts to the slope steepest part and then spreads to weak, heterogeneous deluvial-slide and bulk soils. Kst = 1.14, which is below the norm, and indicates that the slope is approaching the state of ultimate equilibrium.

3. According to the IV-IV' profile, in its natural state, the sliding surface passes over bulk soils and has Kst = 1.040. The obtained coefficient of the stability reserve is much smaller than the normative one, and indicates that this section of the slope is in a state of limit equilibrium.

When surveying this part of the slope, the presence of erosion processes is noted, which manifests itself in the form of planar and linear erosion, deep gullies, and the inclined growth of trees - "drunk forest", indicates the already existing landslide processes.

In the forecast state, the coefficient of stability reserve Kst =0.932. Under such conditions, there is a loss of stability and activation of shear processes within the slope.

The nature of the development of the most likely slip lines within the studied slope section indicates that under these conditions, the development of landslide processes will occur on bulk, deluvial-slide and limnic soils.

The specific topography of the site in the lower part of the III-III' profile indicates that in the past there was flooding of the soil mass of deluvial-slide soils.

Based on the results of slope stability calculations coefficients based on the calculated profiles obtained during searches, the following conclusions can be drawn:

1. The slope within the construction site is prone to landslides, and a separate part of it along the IV-IV' profile is landslide-prone;

2. The slope has a complex geomorphological structure, there are man-made sources of water saturation of the soil, which determines the differential moistening of the slope soil and different activity of surface erosion processes;

3. In the event of a part of the slope sliding on loose soils, it is possible to form a puncture of new sliding surfaces behind the wall of the existing building closest to the slope.

Based on the results of the work, technical decisions were substantiated in the design and construction of the anti-slide structure, which is a retaining wall on injection-molded piles with a monolithic reinforced concrete grid.

**References:**

1. Barshevskiy N.E., Kuprash R.P., Shvydkyi Y.N. Geomorphology and relief-forming deposits of the Kyiv city region. Kyiv: “Naukova dumka”. 1989. P. 181-185.

2. Technical report on engineering-geological surveying “Multifunctional administrative and public complex with apartments and parking, with reconstruction and restoration, with the adaptation of the architectural monument "Mykolaivski Vorota" with adjacent buildings (1846-1850) along the street Ivan Mazepa, 1 in the Pechersk district of Kyiv”. Kyiv: LLC “OSNOVA”. 2020. 78 p.

3. Technical report on engineering-geological surveying “Multifunctional administrative and public complex with apartments and parking, with reconstruction and restoration, with adaptation of the architectural monument "Mykolaivski Vorota" from adjacent buildings (1846-1850) along the street. Ivan Mazepa, 1 st. Pechersk district of Kyiv". Kyiv: State Enterprise of the Ministry of Defense of Ukraine "Central Project Institute". 2012. 150 p.

4. DBN B.1.1-46:2017. Ingineering protection of the territories, buildings and structures from landslides and rockfalls main principles. Kyiv. Minregionbud. 2017.

DOI: https://doi.org/10.30836/igs.iies.2024.33

**Cherkes S., Poliachenko I., Hlavatskyi D., Melnyk G., Bakhmutov V.**

*Subbotin Institute of Geophysics of the National Academy of Sciences of Ukraine, Akademika Palladina Ave. 32, 03142 Kyiv, Ukraine. E-mail: semyoncherkes@gmail.com, poliachenkoib@gmail.com, hlavatskyi@gmail.com, melnykgv@gmail.com, bakhmutovvg@gmail.com*

# PALAEOGEOGRAPHY OF UKRAINE FROM THE PRECAMBRIAN TO THE QUATERNARY: RECENT ACHIEVEMENTS OF THE KYIV PALAEOMAGNETIC SCHOOL

**Introduction.** Among modern fundamental problems of geology – the problem of geodynamic evolution of the Earth (continental drift, supercontinental cycles, mantle convection and processes in the Earth's core), the problem of geomagnetic field evolution (its genesis, configuration, and generation modes), and contradictions in the correlation and dating of continental and marine sediments, which complicates the solution of palaeoclimatology problems (determination of spatial and amplitude features of climate change, climate rhythmicity, development of forecast global and regional climate models, etc.) – can be highlighted.

One of the main tools for solving the abovementioned problems is the palaeomagnetic method, which is used to reconstruct palaeogeographical conditions and behavior of the geomagnetic field during ancient geological epochs. Palaeomagnetic data allow to interpret the movement of individual blocks of the Earth's crust at a quantitative level, to assess the geometry of the geomagnetic field and modes of its generation, and to correlate distant geological cross-sections. Furthermore, magnetic minerals in rocks reflect not only the peculiarities of the geomagnetic field at the place and time of their origin, but are also extremely sensitive indicators of environmental conditions (and changes), which makes it possible to successfully use the rock magnetic method in palaeoclimatology and ecology. The advantage of the palaeomagnetic (and rock magnetic) method is the relative ease of specimen preparation and its expressiveness (compared to classical methods), which determines its high productivity and efficiency, especially when combined with other geological, geochemical and geographical methods.

**Activities of the Kyiv Palaeomagnetic School (KPS).** The territory of Ukraine is geologically diverse and generally well studied. There is a full range of specific geological structures and formations that store information about the key stages of the Earth's evolution from ancient times to the present. Based on the palaeomagnetic method, the use of a modern integrated approach to the study of geological formations in Ukraine allows to obtain unique fundamental and applied valuable knowledge. Taking into account the development of rock magnetic techniques, the availability of new equipment (see Table 1 in [1]) and publication activity, the activities of the KPS in the study of various rocks of Ukraine can be divided into several stages, which marked the key works.

The first (1962–1994) stage began in 1962 and ended with the publication of the generalised Pleistocene magnetostratigraphic scale of Ukraine in 1994 [2]. At this time, the KPS was formed on the basis of the Subbotin Institute of Geophysics of the National Academy of Sciences of Ukraine. The school was founded by such distinguished scientists as Z.A. Kurtykhovska, N.P. Mykhailova, A.M. Glevaska, V.N. Tsykora, S.V. Kravchenko, A.Y. Karzanova, O.N. Tretiak, O.M. Rusakov, G.F. Zagniy, V.N. Kovalenko-Zavoisky, M.I. Orlova, and others. This stage was characterised by the development of the basic principles of palaeomagnetic stratigraphy, the beginning of the study of the "fine structure" of the geomagnetic field, the construction of the first regional magnetostratigraphic scales of the Cenozoic and the rise of the problem of palaeomagnetic stratification of loess-soil strata [1]. In addition, a significant work was performed on the study of Precambrian rocks, and palaeomagnetic characteristics of various rocks of the territory of Ukraine were obtained, among which palaeomagnetically informative varieties were identified [3].

At the second stage (1995–2012), extensive studies of the subaerial sediments of the reference cross-sections were carried out, and the boundaries of the Matuyama/Brunes and Gauss/Matuyama were defined. Particular attention was paid on the stratigraphic correlation of Ukrainian subaerial sediments with loess-soil records from other regions and with the MIS marine scale [1]. During this phase, palaeomagnetic and magnetostratigraphic studies of the Ediacaran rocks of the Volyn Large Igneous Province and terrigenous sediments of Podillia were carried out, the results of which were rather ambiguous [3, 4]. The main researchers of the KPS at this stage were O.N. Tretiak, A.M. Glevaska, S.V. Kravchenko, L.I. Vigilianska, V.G. Bakhmutov and G.V. Slyvinska.

The third stage (2013 to the present) is characterised by the use of new magnetometric equipment by Ukrainian scientists and the intensification of palaeomagnetic and rock magnetic research. The research is aimed at solving the problem of correlation of key sections in the glacial and non-glacial zones and reliable determination of palaeomagnetic inversions [1]. A significant part of the research was carried out to clarify the model of development of the East European Platform in the Middle Palaeozoic [5] and Palaeoproterozoic

[4]. The study of the Ediacaran rocks of Volyn-Podillia was continued to determine the features of the geomagnetic field anomalous behaviour in the Ediacaran [3, 4]. This phase also covered studies of the relationship between the geomagnetic field and climate [6]. The active members of the KPS at the third stage of its development are V.G. Bakhmutov (the head of the School), I.B. Poliachenko, D.V. Hlavatskyi, G.V. Melnyk, S.I. Cherkes and V.V. Shpyra.

**Studied objects.** The research within the third stage of KPS development covers several geological intervals – from the Palaeo- and Neoproterozoic, Lower Devonian, Silurian, Jurassic/Cretaceous boundary to the Quaternary. The research focused on the full range of rocks (sedimentary, plutonic, volcanic) sampled from different parts of Ukraine (Fig. 1), mainly within the structures of the Ukrainian Shield and its slopes, the Volyn-Podillia plate, as well as the Black Sea Lowland and Crimean Mountains.

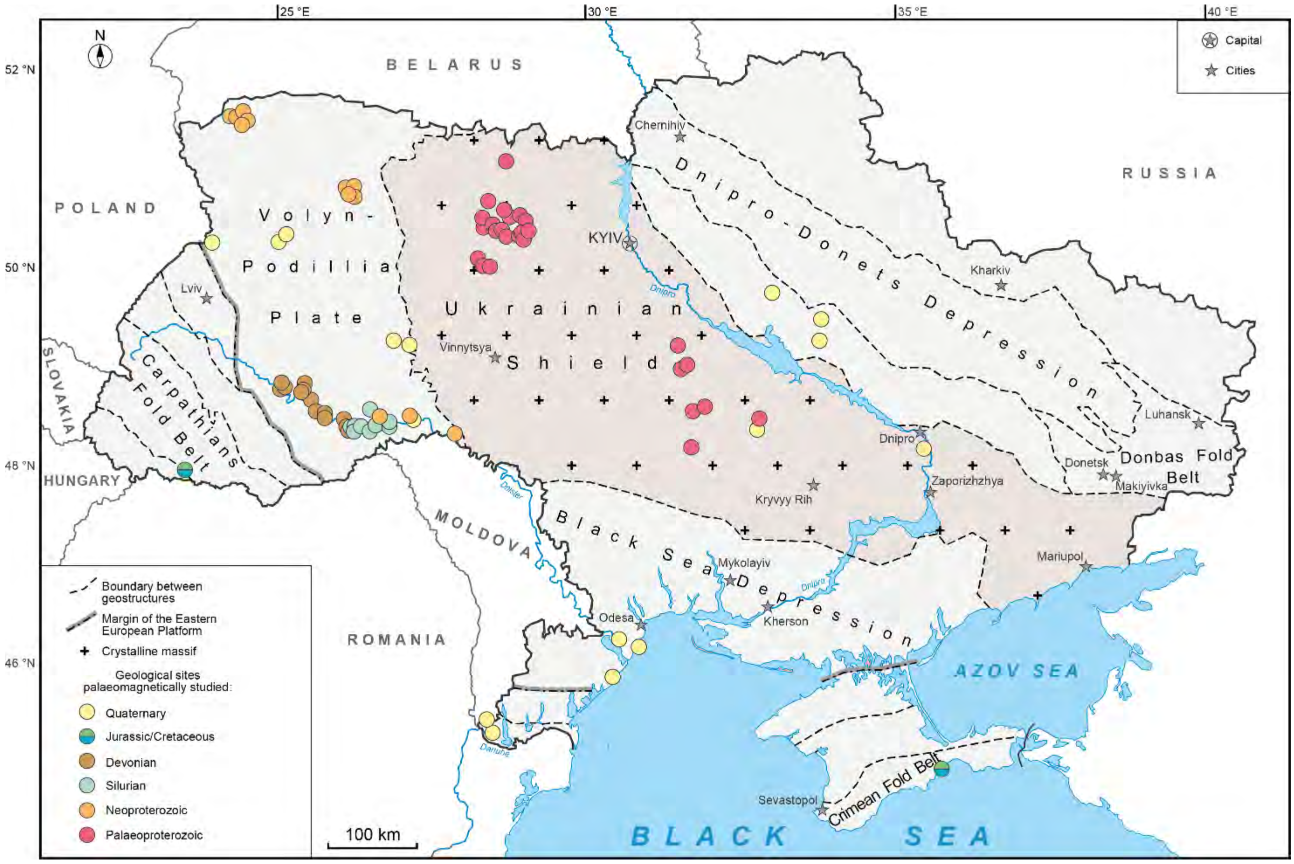

Fig. 1. Location of the studied sections/sites on the schematic map of the main geostructures of Ukraine

**Results and conclusion.** The results of the study of the most ancient rocks sampled within the Buky and Novoukrainka massifs are presented in [3, 7]. Based on the temperature demagnetisation data, a high-temperature characteristic component of magnetisation was identified for the gabbro-monzonites of the Novoukrainka massif (2035 ± 10 Ma) and the monzonites of the Buky massif (1987 ± 14 Ma). The calculated corresponding palaeomagnetic determinations of the massifs are in good agreement with the data obtained for the Proterozoic dikes of the northwestern Volyn megablock with an age of ~2 Ga. According to the new palaeomagnetic data, the Volyn and Ingul domains did not experience significant movements relative to each other after ~2 Gya and since then may have developed within a single structure of the Ukrainian Shield. At the same time, the Ukrainian shield occupied palaeolatitudes of about 20–25°.

Based on the results of studies of rocks with an age of about 1.76–1.75 Ga from the Korosten and Korsun-Novomyrhorod plutons [8], a characteristic component of magnetisation was identified for anorthosites, gabbro-anorthosites, gabbro, and monzonites. The characteristic component is bipolar, and rock magnetic and microscopic data indicate its primary nature. The new results are in good agreement with data obtained earlier for other rocks of similar age within the Volyn and Inhul domains of the Ukrainian Shield, indicating that these domains have been developing as a single tectonic unit since at least 1.76 Gya. According to palaeomagnetic data for Fennoscandia and Volga-Sarmatia, ~1.76 Ga. Fennoscandia occupied a sub-equatorial position within palaeolatitudes of 5–20°, and Volgo-Sarmatia was located near the equator and rotated counterclockwise relative to Fennoscandia by ~40° compared to its present position within the East European Platform. Thus, the final formation of the East European Platform occurred no earlier than 1.76 Gya.

The results of studies of volcanogenic rocks of the Volyn series of the Volyn Large Igneous Province (580–560 Ma) [4] and red tuffites of the Grushka suite (Volyn series) of Podillia support the hypothesis of anomalous behaviour of the geomagnetic field in the Ediacaran. The anomaly is reflected in an increased frequency of reversals and a different from dipole configuration of the Earth's magnetic field. This indicates significant transformations of the geodynamo mechanism in Ediacaran and reflects one of the key moments in its evolution. It is concluded that there is no clear palaeotectonic interpretation of palaeomagnetic determinations for the Ediacaran.

According to the results of palaeomagnetic studies of Silurian and Lower Devonian sedimentary sequences of Podillia [5], a characteristic component of magnetisation was identified. According to the data obtained, in the Ludlow epoch, the East European Platform was located in the near-equatorial latitudes of the Southern Hemisphere and moved north to the equatorial latitudes of the Southern Hemisphere in the Pridoli epoch. Then the drift pattern changes – the platform moves southward, and in the Lochkovian and Pragian times its position stabilises in the equatorial latitudes of the Southern Hemisphere. The latitudinal drift velocity was ~3–5 cm/year.

Based on the new data and the most reliable palaeomagnetic determinations from palaeomagnetic databases, we calculated kinematic parameters of the East European Platform and its segments in the Proterozoic and Palaeozoic intervals.

In addition, our new results on comprehensive rock magnetic and terrestrial-climatic reconstruction of the conditions of Quaternary sedimentary environment in different parts of Ukraine allows for their perfect stratification and correlation, which is the basis for reliable regional and global palaeoclimatic reconstructions. The proposed stratigraphic correlations indicate the outstanding completeness of continental subaerial deposits in Ukraine, which is a unique region for determining Quaternary palaeoclimatic changes in Europe. The new scheme of climatostratigraphic correlation of the reference loess-palaeosol sequences of the glacial and periglacial parts of Ukraine is proposed as a basis for further forecasting of climatic changes of a higher (thousand-year) rank.

Consequently, the results of the palaeomagnetic studies of the geological formation of Ukraine in different age ranges were synthesized for the first time. In view of newly obtained data, it is possible to trace the change in the palaeogeographical situation from the Precambrian to the Quaternary period.

**References**

1. Bakhmutov V., Hlavatskyi D., Poliachenko I. Magnetostratigraphy of the Pleistocene loess-palaeosol sequences in Ukraine and Moldova: a historical overview and recent developments. Geological Quarterly, 2023. V. 67, № 4. 35.

2. Tretyak A.N., Vigilyanskaya L.I. Magnetostratigraphic scale of Pleistocene of Ukraine. Geophysical journal, 1994. V.16, №2. P. 3-14. (in Russian)

3. Bakhmutov V.G., Poliachenko I.B., Cherkes S.I. Problems of Precambrian paleomagnetism on the territory of Ukraine. Geophysical journal, 2018. V. 40, № 5. P. 245-268. (in Russian)

4. Bakhmutov V.G., Poliachenko I.B., Cherkes S.I., Shcherbakova V.V., Hlavatskyi D.V. Palaeomagnetism of the Vendian traps of Volyn, southwestern margin of the East European platform. P. 1: palaeomagnetic directions and poles. Geophysical journal, 2022. V. 43, № 6. P. 70-119. (in Russian)

5. Bakhmutov V.G., Poliachenko I.B. New paleomagnetic data on the Silurian and Devonian sedimentary rocks from Podolia, SW Ukraine, and kinematics of the East European platform in the Middle Paleozoic. Geodynamics & Tectonophysics, 2014. V 5, № 4. P. 1045-1058. (in Russian)

6. Kilifarska N.A., Bakhmutov V.G., Melnyk G.V. The hidden link between Earth's magnetic field and climate. Elsevier, 2020. 218 p. ISBN: 978-0-12-819346-4.

7. Cherkes S., Bakhmutov V., Poliachenko I., Mytrokhyn O., Shpyra V., Yakukhno V. Palaeomagnetism of the Palaeoproterozoic rocks of the ~2 Ga Novoukrainka and Buky massifs of the Ukrainian Shield. XVII International Scientific Conference "Monitoring of Geological Processes and Ecological Condition of the Environment", 7–10 November 2023, Kyiv, Ukraine. Kyiv, 2023. Mon23-199.

8. Bakhmutov V.G, Mytrokhyn O.V., Poliachenko I.B., Cherkes S.I. New palaeomagnetic data for Palaeoproterozoic AMCG complexes of the Ukrainian Shield. Geophysical Journal, 2023. V. 45, № 4. P. 3-19.

DOI: https://doi.org/10.30836/igs.iies.2024.25

**Bonchkovskyi O.[1], Hlavatskyi D.[2]**

*(1) Taras Shevchenko National University of Kyiv, Faculty of Geography, Volodymyrska St. 60, 02000 Kyiv, Ukraine. E-mail: oleksandr.bonchkovskyi@knu.ua*
*(2) Institute of Geophysics, National Academy of Sciences of Ukraine, Akademika Palladina Av. 32, 03142 Kyiv, Ukraine. E-mail: hlavatskyi@gmail.com*

# PALAEOPEDOLOGY AND ROCK MAGNETISM OF THE UPPER PLEISTOCENE LOESS-PALAEOSOL SEQUENCE AT SMYKIV (NW UKRAINE)

The Upper Pleistocene sequence at Smykiv is one of the best developed loess-palaeosol sections of north-western Ukraine. The section is situated in the central part of the Volyn Upland (50°28.18' N, 25°08.22' E), on the slope of the deep road cut near Smykiv village (Rivne region). The section is on the right slope of the Dezha River (middle stream), a small left tributary (only 10 km long) of the Styr River.

The loess-palaeosol sequence comprises 13 stratigraphic units: 6 palaeosols and 7 non-soil beds. The section was studied by palaeopedological, micromorphological, grain-size and rock magnetic methods. The palaeosols were classified according to the World Reference Base for soil resources [1], and micromorphological features of palaeosols were described according to the terminology of [3, 4]. Grain size has been measured according to the pipetting technique [2].

The lowermost unit in the section, Dnipro, is represented by thick (over 5 m) laminated loamy sands with several levels affected by cryoturbation that enabled to interpret these sediments as periglacial alluvium.

The Kaydaky unit (MIS 5e) is represented by a soil with distinct textural differences: AEb@ and EBtb@ horizons are loamy sands, whereas Btgb@ horizon is a silt loam. Albeluvic glossae here penetrates the argic horizon, which, along with an abrupt textural difference, meet criteria of Retisol [1]. Micromorphology of the soil is characterized by numerous clay coatings with humus impurities in the Btgb@ horizon, platy microstructure with bleached micromass in the EBtb@ horizon and by an expressed microzonality in the AEb@ horizon.

The Pryluky unit (MIS 5c-a) includes three relatively thin soils separated by cryogenic levels (namely solifluction and soil veins). The lower soil ($pl_{1b}$) is the darkest in the section and is leached from carbonates, therefore the soil is classified as Haplic Phaeozem. This soil is characterized by a weak granular microstructure, and thin Fe-Mn hypocoatings, and has no signs of b-fabric. The middle soil ($pl_{3b1}$) is a thin humified soil, not affected by solifluction, which consists only of the Ab horizon. Thus, the soil is classified as Brunic Solimovic Regosol. This soil has a platy microstructure with pronounced brown humus punctuations. Here, the roundness of the sand grains increases, indicating intense sedimentation. The upper soil ($pl_{3b2}$) comprises the Akb@ and Bwkb@ horizons. The soil is disturbed by cryogenic features (solifluction, soil veins and reticulate post-cryogenic texture). The soil is characterized by many carbonate pedofeatures, particularly calcite hypocoatings and needle-fiber calcite. Thus, the soil is classified as Calcaric Solimovic Regosol.

The Uday unit (MIS 4) comprises loess and solifluction beds, both calcareous and silty. Carbonates are both secondary and primary with an explicit predominance of calcified root cells and soft nodules. The micromass is micritic and microstructure is rather platy with occasional granular peds.

The Vytachiv unit (MIS 3) is represented by Gleyic Cambisol with Agb and Bwb horizons. The soil is silty and calcareous (thin carbonate hypocoatings and typic nodules). The microstructure is weak blocky and granular with the silt concentrations on the walls of granule. The Cambisol is overlain by thin tundra gley.

The Bug unit (MIS 2) consists of loess and solifluction beds. The latter is dominated by brown soil material. Soft carbonate nodules and calcified root cells dominate the solifluction bed, whereas disperse powdery lime and pseudomicellia dominate the loess bed.

The Dofinivka unit is represented by a weak calcareous soil with pronounced redoximorphic features in the Bgkb horizon. Moreover, in the Bgkb horizon there are many carbonate rhizoliths and Fe-oxide depletion hypocoatings, whereas Awkb horizon is characterized by weak platy, granular and crumby microstructure. Therefore, soil is classified as Calcaric Gleyic Brunic Regosol.

The Prychornomorya unit is represented by a genuine calcareous loess, where carbonates are represented exclusively by disperse micrite.

The Holocene soil is truncated, including relatively shallow chernic horizon and calcareous Bk horizon that enables to interpret Holocene soil as Calcic Chernozem. Recent soil is characterized by darn brown humus and spongy microstructure with soil fauna excrements.

The grain-size data of the Smykiv section reveals two periods with principally different depositional environment. The first period includes late Dnipro, Kaydaky and Plyluky times showing high sedimentation rates of sands presumably of aeolian origin. In the late Pryluky times ($pl_{3b2}$), drastic changes in depositional environment occurred, and a period of silt sedimentation began, which was probably caused by the rebuilding of the Styr river valley.

Mass specific magnetic susceptibility shows low values in all loess, palaeosol and aeolian sand samples ($7-20 \times 10^{-8}$ $m^3kg^{-1}$), with the exception of the Holocene soil (up to $\times 10^{-8}$ $m^3kg^{-1}$). This suggests very low concentration of ferrimagnets, in particular, lower content of soft magnetic minerals was revealed by magnetic-mineralogical parameters (IRM, S ratio, HIRM). This is typical for other loess-palaeosol sequence of the Volyn-Podillia Upland (Boyanychi, Korshiv, Medzhybizh).

At Smykiv, the Pryluky–Kaydaky palaeosol series demonstrate a higher degree of pedogenesis (indicated by mean $\chi_{fd\%}$ values in the section up to 12–13%) compared to that in the younger interstadial palaeosol units (only 3–3.5%). Relatively high $\chi_{fd\%}$ values (6%) are also observed in the Prychornomorya loess and pseudomorphs (due to reworking by soils).

Rock magnetic data from the Smykiv section supports the hypothesis of the transitional type (between “Chinese” and “Alaskan” types) of palaeoclimate record in north-western Ukraine.

Thus, the high stratigraphic variability of palaeosols at the Smykiv site and nearby sites indicates their high sensitivity to global and regional palaeoenvironmental changes, emphasizing the potential of the sequence for the further interdisciplinary studies.

*The study was partly supported by the National Research Foundation of Ukraine, grant number 2020.02/0406.*

**References**

1. IUSS Working Group WRB, 2022. World Reference Base for Soil Resources. International Soil Classification System for Naming Soils and Creating Legends for Soil Maps.
2. Kachynskyi N.A. Grain-size and microaggregate composition of soil, methods for its study. Moscow: AS USSR, 1958.
3. Stoops G. Guidelines for analysis and description of soil and regolith thin sections. Wisconsin: Soil Science Society of America Medison. 2003.
4. Stoops G., Marcelino V., Mees F. Interpretation of micromorphological features of soils and regoliths (Second Edition). Elsevier, 2018.

DOI: https://doi.org/10.30836/igs.iies.2024.6

**Pyasetska S.I.**

*Borys Sreznevsky Central Geophysical Observatory, Kyiv, Ukraine. E-mail: spyasets@ukr.net*

# SPACE-TIME DISTRIBUTION OF THE GREATEST MASS CASES OF WET SNOW DEPOSITS DURING 1991-2020

Falling of wet snow and its subsequent sticking with the formation of appropriate deposits is a typical phenomenon for the territory of Ukraine. Sleet deposits are one of the types of ice-frost deposits, which are mostly formed from mid-autumn to October, but reach their maximum development in the winter months. They are observed in April, but not every year and only in certain regions. It should be noted that this type of ice-frost deposits is quite dangerous for a number of branches of the economy, and first of all for objects of energy and its transportation, communication, transport and communal sphere. In agricultural production, a layer of wet snow prevents the access of air to winter crops, which leads to the accumulation of carbon dioxide and its evaporation. It should be noted that this type of ice-frost deposits is quite dangerous for a number of branches of the economy, and first of all for objects of energy and its transportation, communication, transport and communal sphere. In agricultural production, a layer of wet snow prevents the access of air to winter crops, which leads to the accumulation of carbon dioxide and its evaporation. Deposits of wet snow that spread over a large area covering several regions are particularly dangerous. It is known that recently, after a certain period of stabilization of the air temperature in the global climate system, its growth has been observed. This is especially noticeable in Europe, which leads to the frequent passage of cyclones with warm fronts and occlusion fronts, which contributes to intensive precipitation of sleet, supercooled precipitation in the form of freezing rain and thaws. All this is the result of climate change due to the increase in air temperature in the global climate system "ocean-atmosphere" and the increase in a number of adverse weather phenomena, which include ice and frost deposits.

Many scientists in the world community are engaged in the study of climate change and adaptation to new realities. The results of research on this issue have been published in IPCC reports [4-6], resolutions of international intergovernmental commissions on climate change, and National Adaptation Programs. In Ukraine, similar studies on climate change and its possible consequences were conducted by V.M. Voloshchuk [1, 2]. His research was based on the semi-empirical model he created for paleo-reconstructions of past climatic eras, which was used to predict the further development of the climate system taking into account its current stat. The obtained results, regarding the increase in the average air temperature and the increase in the number of dangerous weather phenomena, practically coincided with the assessment of international experts. Significant results from the study of climate changes, and as a result, an increase in the frequency of recurrence of certain weather phenomena, are presented in monographs devoted to the climate of Ukraine, published in the early 2000s [3, 8]. The author [7] established a sharp increase in air temperature during 1991-2020 compared to the previous climatological norm of 19961-1990. This indicates the continued probability of the occurrence of favorable conditions for the formation of various types of ice-frost deposits, including wet snow deposits, which are second only to ice deposits in terms of the possibility of their creating a danger for the branches of the economy.

In general, the cases of mass spreading of wet snow deposits on the wires of the ice machine, which would have been observed on 1 date at least in the territory of 2 oblasts, were selected for the study. However, in the presented results, similar cases from 8 regions and more were analyzed for better visualization. In Figure 1, for example, cases of mass deposits of wet snow, which were observed in the territory 10 and more, are presented in the form of maps.

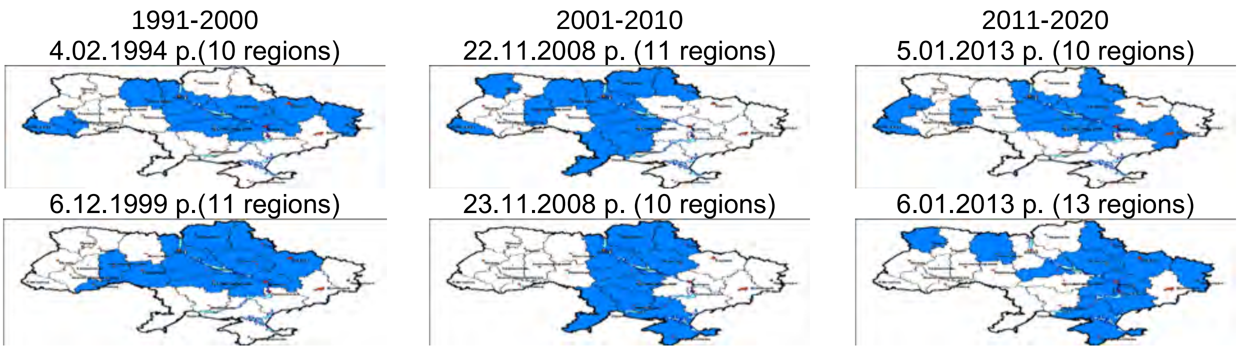


Fig. 1. Cases of the largest mass deposits of wet snow in individual months and years during individual decades of the period 1991-2020

It was established that the largest cases of mass deposits of wet snow in terms of distribution were mainly detected in the second and third decades of the general period 1991-2020. They mostly cover the northern regions from west to east from Zhytomyr Region (sometimes even Volyn) to Chernihiv Region, Sumy Region and Kharkiv Region. and are also combined with separate regions of the central region, mostly Cherkasy, Kirovohrad, Poltava and Dnipropetrovsk regions. Sometimes such a range was expanded at the expense of Vinnytsia and. In some cases, the most large-scale, deposits of wet snow can be observed in 1 date in the territory from the western regions to the northern, northeastern, eastern, central and even some of the southern regions (Odesa). Cases of mass spreading of wet snow deposits in the south mostly cover the Mykolaiv, Kherson, Zaporizhia regions and Crimean Autonomous Republic. In some cases, they can also be observed in Odesa in the west and Donetsk in the east. There have been cases when wet snow deposits with their mass distribution were observed only on the territory of the western regions from Transcarpathia in the west to Volyn, Rivne region and Zhytomyr region in the north and to Khmelnytskyi (sometimes Vinnytsia) in the east. It should be noted separately that on the territory of Ivano-Frankivsk Region, deposits of wet snow in cases of their mass distribution are not often observed compared to other western regions. It should also be said that there are cases of massive distribution of wet snow deposits, the areas of which are located submeridionally from north to south, or sublatitudinally from west to east through the center of the country. The most common cases of wet snow deposits were observed on 16.03.2000, 20.12.2004, 16.01.2009, 28.12.2009, 12.02.2011, 21.01.2012, 06.01.2013, 17.03. 2014, 05.02.2020.

**References**

1. Boychenko. S.G., Voloshchuk V.M., Doroshenko I.A. Global warming and its consequences for the territory of Ukraine. Ukraine geogr. magazine. – 2000. – No. 3. 59-68 p.
2. Voloshchuk V.M. About possible changes in the average annual temperature regime of Ukraine in the first half of the 21st century. Reports of the National Academy of Sciences of Ukraine, 1993. - No. 12, 105-111 p.
3. Climate of Ukraine / Ed. V.M. Lipinsky, V.A. Dyachuka, V.M. Babichenko. K.: Type-vo. Raevsky, 2003. 343 p.
4. Climate Change 2007: Impacts, Adaptation, and Vulnerability (2007). In: Contribution of working Group II to the Forth Assessment Report of the Intergovernmental Panel on Climate Change. M. Parry, O. Canziani, J. Palutkof, et al. (eds.). – New York, Cambridge University Press. P 976.
5. IPCC 2013: Summary for Policymakers. Climate Change 2013: The Physical Science Basis. Contribution of Working Group I to the Fifth Assessment Report of the Intergovernmental Panel on Climate Change. [Stoker T.F., D. Qin. J.K. Plattner, S.M. Tignor, S.K. Allen, J. Boschung, A. Nauels, Y. Xia, W. Bex and P.M. Midgley (eds.) Cambridge University Press, Cambridge, United Kingdom, New York. USA, 1535 p. DOI: https://doi.org/10.1017/CBO978117415324
6. IPCC 2014: Climate Change 2014: Impacts. Adaptation and vulnerability. Part B: Regional aspects. Contribution of Working Group II to the Fifth Assessment Report of the Intergovernmental Panel on Climate Change [Barros V.R., S.B. Field, D.J. Dokken, M.D. Mastrandera, K.L. Mach, T.E. Bilir, M. Charterjee, K.L. Ebi, Y.O. Estrada, R.C. Genova, V. Grima, E.S. Kissel, A.N. Levy, S. MacCracken, P.R. Mastrandrea and L.L. White (eds.)]. Cambridge University Press, Cambridge, United Kingdom, New York. NY, USA 1757-1776 p.
7. Pyasetska S.I., Shcheglov O.A., Grebenyuk N.P. Comparison of fields of average monthly air temperature during the climatic norms of 1991-2020 relative to 1961-1990. Collective monograph. Under the editorship M.S. Painted. – K.: Yaroshenko Ya.V. - 2022. 202-228 p. DOI: https://doi.org/10.51500/7826-23-0.
8. Natural meteorological phenomena on the territory of Ukraine during the last twenty years (1986-2005) / Ed. V.M. Lipinskii, V.I. Osadchyo, V.M. Babichenko. - K.: Nika Center Publishing House, 2006. 311 p.

DOI: https://doi.org/10.30836/igs.iies.2024.5

**Starodubets K., Yaroshovets-Baranova K.**

*Institute of Geological Sciences of the National Academy of Sciences of Ukraine, Kyiv, Ukraine.*
*E-mail: starodubets.kirill@ukr.net, katerina.yaroshovetseo_33@ukr.net*

# LANDFORMS INFLUENCE ON THE TEMPERATURE DISTRIBUTION IN SUBSOIL LAYER

The main aim of this work is to research the distribution of the subsoil layer temperature during the period of stable meteorological conditions in the presence of different landforms.

To achieve the aim, two main tasks were solved.

The first task is to conduct field work, as a result temperature survey of the subsoil layer were performed at 50 research points with step 700 meters on a total area 40 km$^2$ within the limits of the Novomoskovsk district of the Dnipropetrovsk region, Ukraine. At each research point, the following was performed: auger drilling of hole with depth of 1.0 meter, installation of a thermal probe in the hole and recording of temperature value. The equipment and research methodology are patented [1] and described in a number of publications [2-4].

The second task is the processing of the obtained field data and the features research of the area temperature distribution depending on the landform. The influence of meteorological conditions was taken into account.

Survey of the subsoil layer temperature was carried out in the square version for two days, according to the data of the nearest weather station, during fieldwork the weather was cloudless, there was no precipitation, the average value of the temperature showed a slight increase.

The results of the temperature survey are presented in a graph (Figure 1) obtained during August 25 and 26, 2018.

On the first day of fieldwork, measurements were taken on a plain, which is represented by agricultural lands, with absolute heights 120-130 meters. The last research point was carried out on the slope to lowland number 1.

On the second day of fieldwork, measurements were continued in lowland number 1, the width of lowland varies from 50 to 100 meters, the absolute heights are 100-110 meters, the vegetation is represented by shrubs and single trees, the soil is moistened, movement of the temperature survey took place along the lowland number 1. The following 7 points of survey were carried out on the upland plateau, the width of plateau varies from 500 to 600 meters with absolute heights 130-140 meters, the vegetation is represented by wild grasses and shrubs, movement of the temperature survey took place along the upland plateau, the corresponding changes in the measured temperature are recorded on the graph. Further observation points were made in lowland number 2 and on slopes to it, the width of the lowland number 2 varies from 100 to 200 meters, the absolute heights 100-110 meters, the vegetation is represented by shrubs and single trees, the soil is wet in places, movement of the temperature survey took place along the lowland.

Given the absence of a significant difference in meteorological conditions for the two days of fieldwork, no correction was made for the difference in temperature when graph constructing.

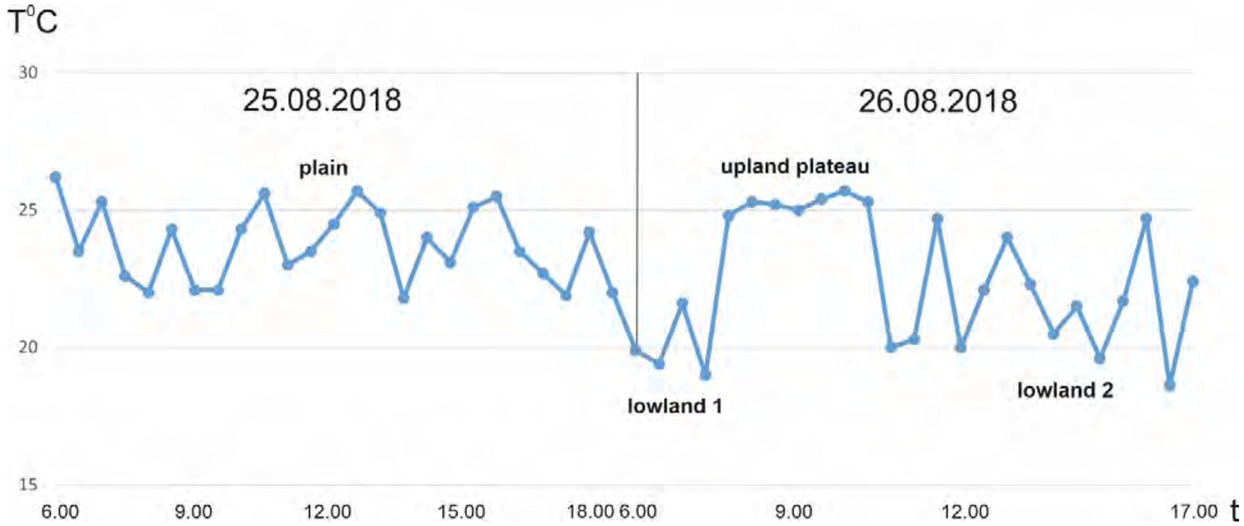


Fig. 1. Temperature distribution graph of the subsoil layer at depth 1 meter on the research area, August 25-26, 2018

According to the results of the conducted survey, data on the temperature distribution at a depth of 1 meter were obtained and analyzed.

As a conclusion, in the summer period of high air temperatures, in the absence of other significant factors of influence, such as urbanized areas, water objects, uneven distribution of green spaces and forests, precipitation, – the distribution of the subsoil temperature at depth of 1 meter actually reflected the relief of the research area. When evaluating average values: the maximum value is typical for local highlands, an intermediate value for plains, and a minimum value for local lowlands.

**References**

1. Bagrii I.D., Gozhik P.F. Complex method of structural-thermo-atmogeochemical research (STAGR), author's certificate No. 28176, 31.03.2009, Ukraine.
2. Bagriy I.D. Development of geological-structural-thermo-atmogeochemical technology for forecasting mineral exploration and assessment of the geoecological state of the environment. – Kyiv: Logos, 2013. – 510 p. (In Ukrainian).
3. Bagriy I.D., Gordieieva Yu.K., Glon V.A., Kulish A.P., Starodubets K.M. Structural geothermal atmo-hydrological-geochemical studies of the territory of the Bobrikivska depression. Geoinformatika, 2017. Volume 62, № 2. P. 5-13. (In Ukrainian).
4. Starodubets K.M. Interpretation of results of structural-thermal-atmogeochemical research on the Voskresenivska area. Geological Journal, 2018. Volume 362, № 1. P. 89-94. DOI: https://doi.org/10.30836/igs.1025-6814.2018.1.126573 (In Ukrainian).

DOI: https://doi.org/10.30836/igs.iies.2024.47

**Bondarenko L., Halchenko Z., Kirichenko V., Kryuchkova S., Ostapenko N.**

*Institute of Geotechnical Mechanics named after M.S. Polyakov National Academy of Sciences of Ukraine, Dnipro, Ukraine. E-mail: larisabondarenko102@gmail.com, zorichka85@gmail.com, vakirichenko62@ukr.net, svetlanakriuchkova69@gmail.com, ianatali1978@gmail.com*

# ON THE QUESTION OF THE PROBLEM OF DISTURBED LANDS UNDER THE CONDITIONS OF THE STATE OF WAR AND THEIR RESTORATION

The main component of the natural environment and the biosphere in general is soil - a limited, irreplaceable and difficult-to-renew natural resource that performs important functions: productive (biomass production, nutrition), ecological (biogeochemical, geohydrological, bioenergetical, biological), social, informational, and others. "Land is the main national wealth under the special protection of the state" - the Article 14 of the Constitution of Ukraine was established.

Due to the full-scale Russian invasion of Ukraine about a third of all chernozems of the European continent and 9% of the world's chernozems significantly disturbed by military action. More than 20% of all Ukrainian lands and protected areas of Ukraine occupied, and about 1 million hectares a total area damaged. Shell craters, steel parts from air bombs, artillery shelling and drone attacks, explosions, oil leaks and pollution from burnt military equipment, compaction and burning of fertile soil and vegetation lead to complex land damage (mechanical, physical, chemical and biological). Restoration of lands can take a long time. According to the Operational Headquarters at the State Environmental Inspectorate of Ukraine, the total environmental (land, water, landscape, nature reserve) damages as a result of the armed aggression of the Russian Federation amount to about 2 trillion UAH., and the estimated area of disturbed soil reaches about 900,000 hectares.

The total amount of damage caused to the soils of Ukraine (taking into account the costs of reclamation, restoration of reclamation systems, cleaning of contaminated soils and littered land plots, direct and indirect losses) amounts to almost 1.2 trillion UAH, or 34 billion dollars USA [1].

One of the most acute problems of the Ukraine is the mine contamination of the territories, the area of which, according to the State Emergency Service, is about 170,000 km$^2$ (almost two Moldova or two Austria). According to the UN Office for the Coordination of Humanitarian Affairs, since 2014, almost 2 million residents of Ukraine have already lived surrounded by landmines. During this period, hundreds of civilian casualties recorded due to incidents involving explosive ordnance. At the same time, the demining of territories will remain a priority in the work of the State Service of Ukraine for Emergency Situations for a long period. The post-war experience of the Balkan countries shows that it can last more than 20 years, and the estimated cost of complete demining of Ukrainian lands can reach 50 billion US dollars.

The special danger of environmental terrorism today is the use of large dangerous objects (atomic, electronic, chemical and environmental), such as: the targeted destruction by the RF military of the Kakhovska HPP and the Kakhovka reservoir, the real threat of damage to Zaporizhska NPP and the use of nuclear weapons.

Modern military aggressions are environmental terrorism, that is, a manifestation of serious crime that can affect not only public safety and public order, but also the peace and security of humanity on a global scale. Today, a number of methods of active influence on the environment for military purposes already been created. For example, the artificial destruction of the ozone layer, the scattering and formation of clouds and fog, the initiation of earthquakes, the creation of tsunami-type tidal waves, the influence of tropical cyclones, the use of atmospheric currents for the transfer of radioactive and other substances, the creation of disturbance zones in the ionosphere. Each method poses a danger both to the participants in the armed conflict and to other states. According to the IAEA, more than 10 million sources of ionizing radiation used in the world today. Now, the nuclear confrontation of the parties may be replaced by a less visible, but no less dangerous ecological confrontation with the use of the following types of environmental weapons (according to the structure of natural spheres): meteorological, hydrobiospheric, lithospheric, climatic [2].

Industrially developed regions with a high population density are the most vulnerable to the impact of damaging factors of a military nature and environmental/technological terrorism. Technological terrorism can defined as a set of innovative ways of carrying out military/terrorist actions (which today also include aerospace and information terrorism).

The danger increases as the ability of military aggressors/terrorists to use industrial toxic substances increases. Ukraine has already accumulated a huge amount of radioactive waste. The total volume of radioactive waste is about 3,300-4,600 thousand m$^3$, and 13 thousand m$^3$ of liquid radioactive waste and 28 thousand m$^3$ of solid radioactive waste generated annually at the nuclear power plant alone. The current state of affairs in the field of radioactive waste management does not provide the necessary level of protection, which increases the likelihood of military attacks and terrorist acts.

All the considered processes, which are further intensified and complicated by military actions on the territory of Ukraine, are to one degree or another related to physical and geographical conditions.

Based on the analysis of hydrophysical and biotic disturbances during land use, the features of their parameterization are determined as the basis of innovative technologies in land restoration (Table 1).

Table 1. The list of land disturbances due to the influence of the main hydrophysical, biotic phenomena and hostilities and the features of their parameterization in land use

| *Land use* | |
|---|---|
| *Disturbances of lands* | *Restoration of lands* |
| *Influence of the main hydrophysical phenomena and military operations and the features of their parameterization* | |
| Rehabilitation of technogenically disturbed lands | Formation of a secondary surface to prevent gravity, surface runoff, wind erosion, solar radiation |
| Disturbances of landscapes | Partly – the reproduction of landscapes, partly – a change in the type of land use |
| Land erosion | Changes in the morphological structure of the surface, distribution of precipitation flows, aggregation of granulometric particles |
| Physical degradation, decrease in water permeability | Soil compaction |
| Presence of mines and contamination from weapons | Demining territories and mechanical land clearing |
| *Influence of the main biotic phenomena and features of their parameterization* | |
| Destruction of forests and natural reserve lands | Restoration of forests and lands of the nature reserve fund |
| Depletion of soils | Application of biotic technologies for restoration of soil fertility |
| Soil fertility decline | Introduction of innovative technologies in selection work |
| Wind erosion | Applying plants for strengthening the soil |
| Rehabilitation of technogenically disturbed lands | Returning natural soil fertility through artificial plantings and changing the type of agricultural use |

Technogenic losses of land include: extraction of mineral raw materials, oil, gas, amber; cutting down forest belts in the south of Ukraine (will lead to huge losses of land due to lack of protection against soil erosion); deforestation (especially in mountainous areas), military operations, etc. We observe the emergence of particularly acute contradictions between industrial technologies and the environment in the process of functioning of mining and processing enterprises.

Over many decades of operation of Kryvbas mining and processing enterprises, huge masses of beneficiation waste have accumulated in the tailings, covering an area of about 10,000 hectares and estimated at about 8 billion tons. The total iron content in them is 15-18%, so they can considered as Technogenic deposits [3, 4].

The analysis of parameters of Kryvbas tailings dumps also shows that they have a resource potential of solar generation comparable to their energy consumption (Table 2).

Table 2. Energy consumption and generation potential of solar power plants located on lands disturbed by mining enterprises of Kryvbas

| Mining and processing enterprises | Production volume, million tons | Required power, MW* | Area of disturbed land, ha | Potential power of SPPs, MW |
|---|---|---|---|---|
| Northern mining and processing enterprises | 14,2 | 493 | 2590 | 1290 |
| Central mining and processing enterprises | 8,9 | 309 | 3300 | 1650 |
| Southern mining and processing enterprises | 10,1 | 351 | 1870 | 935 |
| Novokryvorizkyi mining and processing enterprises | 9,6 | 333 | 1760 | 880 |
| Inguletskyi mining and processing enterprises | 14 | 486 | 1530 | 760 |
| TOTAL (all in all): | 56, 8 | 1972 | 11050 | 5515 |

Note.* - The Required power was calculated based on the indicators of the best available mining technologies (The information and technical handbook of the best available technology, 2017).

Rehabilitation of disturbed lands includes the following main directions, as formation of secondary ecosystems; reclamation; melioration. Reclamation, by definition, is a set of works aimed at restoring the productivity of disturbed lands. The technology of activating the formation of secondary soils allows for the disposal of organic waste from municipal, forestry, agriculture and processing industries.

Examples of the use of innovative ecologically oriented strategies in developed economies demonstrate the manifestation of the catalytic effect and the advantages of the effect of dynamic efficiency from their implementation. Taking into account the formation of sustainable development priorities, the green economy can considered the most common strategy.

Innovative green development strategies focus on a combination of important goals such as economic efficiency and appropriate environmental and social standards. It was determined that the use of low-carbon technologies contributes to the reduction of $CO_2$ emissions by 1.5 t/ha [5]. This allows you to avoid additional $CO_2$ emissions during the operation of machines and mechanisms at the mining-technical and biological stages of reclamation.

In general, the methodology for combating environmental risks and environmental terrorism or military threats is a systemic approach. The main measures for environmental restoration include the assessment of damage to the environment caused during military operations, determination of the scope of restoration works, including demining and land reclamation, forest rehabilitation, and landscapes restoration.

According to the estimates of authoritative international experts (for the period until 2030) the implementation of green projects in the world will require attracting additional financing in amount of 90 trillion US dollars, which may make it difficult for Ukraine to obtain similar funds on the period of martial law and restoration [2].

In the coming years, a significant part of the existing fixed assets will replaced due to their obsolescence or due to destruction during military operations or extreme climatic events. In the context of the development of a green economy, this will allow for more intensive implementation of innovative technologies.

Enterprises of the metallurgical complex and mechanical engineering of Ukraine are especially in need of such an update, since the latest technical equipment will be extremely important for the reconstruction of the energy complex, agricultural and chemical industries, logistics networks, as well as for the further strengthening of the defense complex. The state can mainly help in this, using the mechanism of public orders.

The foundation of Ukraine's high competitive status and influence should be a research, educational and law-making strategy, coordinated with the goals of sustainable development, standards of environmental, social and corporate responsibility, recognized and supported at the state level.

**References**

1. Bondar O.I., Mashkov O.A., Zhukauskas S.V., Nigorodova S.A. Methodology for combating environmental threats, risks and environmental terrorism: a systematic approach. Ecological sciences: a scientific and practical journal / Editor-in-Chief O.I. Bondar. Kyiv: DEA. No. 5(24). Vol.1. 2019. 180 p.
2. Roubini N. Project Syndicate. Ours is an era of megathreats.
Mode access: https://www.epravda.com.ua//publications/2023/12/10/707522/.
3. Podrezenko I.M., Ostapenko N.S., Kryuchkova S.V., Kyrychenko V.A., Bondarenko L.V. Peculiarities of ecological assessment of natural and man-made impact on the hydrosphere within urban techno-ecosystems. PDAA Bulletin. No.2. 2019. P. 70-76. DOI: https://doi.org/10.31210/visnyk2019.02.08 PDAA.
4. Semenenko E.V., Medvedeva O.A. Technology of development of man-made deposits of Kryvbass. Mode access: http://www/mining.in.ua.arricles,volume7.3/.
5. Skrypnyk O.O., Ostapenko N.S., Kryuchkova S.V. Reducing greenhouse gas emissions by implementing low-carbon technologies for the use of lands disturbed by mining operations. Agrology, DDAEU. Issue 4(2). 2021. P. 59-64. DOI: https://doi.org/10.32819/021007.

DOI: https://doi.org/10.30836/igs.iies.2024.21

**Kurysh T.**

*Institute of Geography of the National Academy of Sciences of Ukraine, Kyiv, Ukraine.*
*E-mail: kurysh.taras@gmail.com*

# SPATIAL AND FINANCIAL ASPECTS OF LOCAL GOVERNMENT MODERNIZATION: FOREIGN BEST PRACTICES

The modern administrative-territorial system of Ukraine is currently in a transitional stage, undergoing the reform of decentralization of management. This reform opens the way for further progressive transformations of our society. The experience of EU countries shows that the driving force behind their social and economic development is local self-government. In Ukraine, it is the territorial communities whose development prospects are shaped by the needs and positions of their residents. In this process, the state should only perform a protective and regulatory function.

Local self-government, as defined by the European Charter of Local Self-Government approved by the Council of Europe on October 15, 1985. It refers to the right and capacity of local governing bodies to regulate and manage a significant portion of public affairs within the boundaries of the law, in the interests of the local population [2]. Accordingly, capability is a key characteristic of local self-government. Therefore, capable territorial communities are defined as communities of villages (villages, towns) that, through voluntary association, have the ability to independently or through relevant local governing bodies ensure the appropriate level of service provision. This includes areas such as education, culture, healthcare, social protection, and housing and communal services, taking into account human resources, financial support, and infrastructure development within the corresponding administrative-territorial unit [3]. The formation of communities occurred through voluntary association, with consideration given to the opinions of citizens. Additionally, during the planning process for community creation, the potential resource capabilities of the community for economic and social development were determined, and opportunities to provide quality services to citizens were taken into account.

The method of forming capable territorial communities, as defined by the authors of the reform, includes criteria concerning the size, population, accessibility zones of new administrative centers, as well as the presence of social, educational, and household infrastructure. Simultaneously, the financial capacity and infrastructural security of the territorial community depend on various spatial aspects, including socio-geographical factors such as favorable geographical location, effective utilization of the socio-economic and demographic potential of community centers, development of transport links, and availability of natural resources, etc.

During the implementation of the decentralization process of local self-government in Ukraine, the experience of reform processes in European countries was utilized. Specifically, the decentralization of state power in Poland primarily involved the transfer of tasks, competences, powers, financial assets, and funds from the central (higher) level to the territorial (self-government) level. Consequently, communities were granted independent legal status, and property rights were transferred. At the same time, the sources of income for the gminas were identified, ensuring their financial sustainability, and a new differentiated system of subsidies and social protection for the population was established. It's noteworthy that as a result, local government revenues in Poland increased from 150 billion zlotys to 195 billion zlotys between 2011 and 2016, indicating a significant annual growth of local budgets by 5.39% [6]. The positive growth trend in local budgets, particularly in large cities, continues to the present day.

In addition, the Law on Territorial Self-Government was adopted, which defines provincial assemblies representing the communities of residents within those provinces. These assemblies serve three main functions: 1) representing communities in their relations with central state administration bodies; 2) providing platforms for sharing experiences in self-government and, if necessary, serving as mediators between communities and the central government; 3) overseeing and auditing the activities of executive committees, communal enterprises, and organizations. Additionally, in collaboration with these assemblies, communities can form intercommoned associations to address certain tasks delegated to them.

We can agree with A. Chirkin that '... the process of reforming local self-government bodies in Poland is not yet complete. The tendency towards decentralization leads to the fact that the state entrusts gminas with regular tasks, without providing them with budget funds, which significantly complicates the functioning of municipalities. ... Proposals to create another Voivodeship, to unite or even liquidate individual gminas and counties, to change the scope of competence approved for the relevant levels of municipal administration, etc., are being heard more and more often' [6].

Over the past five years, Poland has seen a successful modernization of its local self-government system, evidenced by the strengthening of gminas and counties. This is attributed to numerous state programs aimed at developing small farming, as well as state support of 500 zlotys per month for each child, among others. Furthermore, local self-government bodies, while analyzing the spatial aspects of community development, increasingly seek additional finances for the development of depressed counties and gminas by engaging them in various grant projects or international programs [7]. Concurrently, the financial decentralization of local self-government has contributed to the rapid development of cities in Poland, particularly in cities like Warsaw, Krakow, Wroclaw, Gdansk, Poznan, Katowice, Sopot, Kielce, and others. Clearly, the implementation of the principle of "supporting depressed gminas and not interfering in the development of large cities," given the strengthening trend of uncontrolled urbanization worldwide, now warrants attention in Ukraine as well.

The reform of local self-government bodies is currently one of the most crucial aspects of the transformation period for the Baltic republics. For both Ukraine and the Baltic republics, the main principles of this reform include democratization and decentralization of management, independence of local self-government bodies from the central government, freedom of action within the law, independence of local budgets, and the application of economic management methods rather than command-based approaches. Further implementation of these reforms is necessary to strengthen local communities and provide a wide range of high-quality public services to local residents.

For the Baltic republics, the strategic tasks of reforming local self-government are defined as:

- Introduction of EU and Council of Europe democratic standards in the field of territorial organization of public authorities.
- Liberalization of electoral legislation and widespread implementation of participatory forms of democracy utilizing the potential of "e-democracy."
- Strengthening integration among local communities, considering spatial aspects.
- Development of the local budget system and provision of financial decentralization for local communities.
- Enhancement of the system for equalizing financing for local communities.
- Development of the territorial statistical system.
- Improvement of socio-economic planning methods.
- Implementation of strategic management principles.
- Enhancement of local public services, etc. [4].

Some of the above tasks are being successfully implemented in the Baltic countries already today. In particular, the task of forming powerful territorial communities through their voluntary association and the introduction of financial decentralization. For example, in Estonia, since 2004, the Act "On Support of Voluntary Association" has been in force, and grants for OTG are also provided for. The latter assumes that:

- Each community receives funds in the amount of 50 euros per person.
- The development fund of the newly created OTG ranges from 150,000 to 400,000 euros.
- OTG receives a grant at the end of the year in which the merger was completed.
- Former elected officials of local self-government receive compensation in case of job loss as a result of community unification, etc. [5]."

In most cases, the given stimulating mechanisms catalyzed the unification of territorial communities - cities and volosts. At the same time, the formation of "centers of gravity" is observed - both in Poland and in Estonia, these are large cities.

Ukraine observes the practice of some member states of the Council of Europe regarding a significant share of the population living in the rural areas. Accordingly, when forming rural territorial communities, in order to avoid unwanted mass emigration from these territories, it is necessary to develop effective rural development programs. Their goal should be to diversify the employment structure and create new partnerships between the city and the countryside. Attention should be paid to the development of the agricultural sector, supported by subsidies, and in the private sector it is necessary to develop production and other types of activities that would serve as generators of employment, for example, in the tourism industry. It is important to establish partnership interaction and exchange of experience.

Considering the spatial location of individual territorial communities in mountainous areas of Ukraine, their exceptional potential can be identified as they fulfill ecological, economic, social, cultural, and agricultural functions. Accordingly, the Parliamentary Assembly and the Congress of Local and Regional Authorities of the Council of Europe pay attention to mountain regions in the context of implementing the strategy of social unity. In mountainous regions, many measures of spatial development designed for urban and rural areas can be implemented. At the same time, the comprehensive program for mountain regions should become an independent part of the pan-European program of spatial development, which includes measures of economic and social development, protection and the use of natural resources and takes into account the local traditions and cultural features. The program of spatial development of mountainous regions should also take into account the circumstances that borders separate some regions, so development programs on both sides of the borders should be mutually agreed upon [1].

When creating territorial communities in mountain areas, it is crucial to acknowledge that despite their diversity, which must be preserved and supported, mountain regions face similar economic, social, and environmental challenges due to altitude, topography, and climate. An important aspect to consider is that the natural conditions of mountainous regions not only pose obstacles to their development but also offer opportunities for the local population and the generation of financial resources, ensuring the capacity of the territories. Therefore, achieving a balance between economic and social development and environmental protection is essential in such communities.

The conducted research has identified specific spatial aspects related to the formation of financial resources of territorial communities in Ukraine. Additionally, best practices from European countries have been analyzed to ensure the success of modernizing the system of local self-government and management. These practices serve as examples of the proper implementation of EU values and principles regarding the development of strong local self-government and effective territorial organization of public power through decentralization.

The analysis has revealed that Poland, the Baltic states, and other countries with conditions similar to Ukraine's have achieved significant success in implementing decentralization reforms. These reforms have led to the creation of strong regions with considerable autonomy and adequate financial resources. As Ukraine pursues candidacy for EU membership, there is an urgent need to effectively utilize the experience of aligning the administrative-territorial system with European standards.

**References**


1. Kuybida V.S., Negoda V.A., Tolkovanov V.V. (2009). Regional development and spatial territory planning: experience of Ukraine and other Council of Europe states: a collection of regulations and scientific and analytical materials on regional development and spatial planning. Kyiv: Publishing Kramar. 2009, 170 p.
2. European Charter of Local Self-Government [Electronic resource]. – Mode access: https://zakon.rada.gov.ua/laws/show/994_036#Text.
3. Kozina V. "Formation of favorable territorial communities", Derzhsluzhbovets, May, 2015/No. 5. [Electronic resource]. - Mode access: https://i.factor.ua/ukr/journals/ds/2015/may/issue-5/article-7879.html.
4. Local self-government in Ukraine and foreign countries: comparative legal aspects: monograph / edited by O. V. Batanov, O. V. Marcelyak, A. Berlinguer. Kyiv: OSNOVA Publishing House, 2020. – 672 p.
5. Tkachuk A.F. Estonia: local self-government. Working notes. Kyiv: ICC "Legal Status", 2014 - P. 12-13.
6. Chirkin A.S. Constitutional and legal regulation of local self-government in Poland, Hungary, the Czech Republic: monograph. Kharkiv: Yurayt, 2019. – P. 116-117.
7. Zaucha J., Brodzicki T., Ciołek D., Komornicki T., Mogyła Z., Szlachta J., Zaleski J. Territorial dimension of growth and development. – Correct citation: Warsaw: Difin, 2015, 457 p.

DOI: https://doi.org/10.30836/igs.iies.2024.24

**Kushnir A., Marushchynets A., Leiberiuk O., Shvaiko V., Molodyka V.**

*Institute of Geography of the National Academy of Sciences of Ukraine, Kyiv, Ukraine.*
*E-mail: kushnir.paleogeo@gmail.com*

# PECULIARITIES OF THE RESILIENCE RESEARCH OF THE AGRARIAN SPHERE OF THE KYIV PRYDNIPROVIA REGION, AFFECTED BY RUSSIAN AGGRESSION

Russia's invasion has caused enormous damage to Ukraine's agricultural sector, with reduced crop areas, lower production volumes, damaged production facilities, shortages of labour, equipment and fuel, disruption of logistics routes, etc. The World Bank estimates that in the first year of the war, Ukraine's agricultural sector suffered losses of USD 8.72 billion, with total economic losses amounting to USD 31.5 billion. The territory of Kyivske Prydniprovia (Kyiv, Zhytomyr, Chernihiv, Cherkasy regions) was negatively affected from the first days of the full-scale invasion. Some of the territorial communities were occupied or active hostilities were taking place within their borders.

We consider the agricultural sector an independent formation that includes interrelated components: agriculture, the territory with its natural conditions and resources, as well as the population living on these territories and engaged in agricultural activities. The agricultural sector is not only a production entity, but also a place of human activity. Accordingly, this understanding of the agricultural sector is closely correlated with the concept of sustainable development, which is based on the close interconnection of environmental, economic and social problems of human development and the understanding that their solution is possible only on a comprehensive basis, taking into account the balance of interests of nature and society. Achieving this development involves harmonious growth in three main aspects - economic, social and environmental.

In this context, our scientific task is to assess resilience as the ability to change, adapt and recover from crises and destruction in the territories directly affected by russian aggression.

The issue of resilience in the agricultural sector is quite diverse and has its own research experience. A summarizing publication on indicators for assessing the resilience of the agricultural sector is written by Joshua F. Cabell and Myles Oelofse [1]. Based on a review of the literature on the resilience of socio-ecological systems, the authors identified 13 indicators for the agricultural sector. When they are identified in a functioning agricultural sector, we can talk about the degree of its resilience. These are the following indicators: socially self-organized; ecologically self-regulated; appropriately connected; functional and response diversity; spatial and temporal heterogeneity; exposed to disturbance; coupled with local natural capital; reflective and shared learning; globally autonomous and locally interdependent; honors legacy; builds human capital; reasonably profitable. Each individual indicator has its own definition, features and a brief description of what to look for in order to identify the indicator.

Joel Tallaksen [2], substantiating the theoretical provisions of agricultural resilience, concludes that there are three groups of factors that determine it: economic, environmental and social. He also notes that if all three of them do not work together, the system is out of balance and eventually fails. By understanding the problems in each of these three groups, it is possible to better determine how to improve the resilience of the agricultural sector. He points to three factors that need to be considered to make the system more resilient: persistence, adaptability and transformation. Persistence is the ability to cope with short-term challenges, which does not necessarily mean significant changes in operations. Adaptability is the ability to make drastic changes to the way the business operates in order to maintain profitability in the long term. Transformation - the ability to rebuild the farm to complement or replace the existing system.

A group of European researchers [3], studying the basis for assessing agricultural resilience, also notes the above challenges and complements them to some extent. They consider economic (falling commodity prices, new competitors, internationalization, etc.), environmental (extreme weather events, heavy metal pollution, etc.), social (available labour force, access to social services for workers, etc.) and institutional (sanctions, changes in environmental regulations, war, etc.) issues that affect the resilience of the agricultural sector. In each of these aspects, they distinguish between temporary shocks (extreme weather events, falling commodity prices, etc.) and long-term stresses (climate change, war, etc.). They propose to define three resilience capacities: robustness, adaptability and transformability. Robustness is the ability of an agricultural system to withstand stresses and (un)expected shocks. Adaptability is the ability to change the composition of inputs, production, marketing and management in response to shocks and stresses, but without changing structures and mechanisms. Transformability is the ability to significantly change the internal structure and mechanisms of the farming system in response to major shocks or prolonged stress.

The practice of assessing the resilience of the agricultural sector of individual countries, territories, and farms is based on the above theoretical provisions and has a number of specific features in each case. For example, to analyses the resilience of the agricultural sector when comparing two peasant communities in Latin America (Brazil and Colombia), a conceptual and methodological framework was proposed in which such aspects as the agricultural structure and activities of the peasant communities are included as determining factors [4]. The authors believe that resilience is the result of complex interactions between ecological, economic, social and cultural systems and cannot be analyses by looking at each component in isolation. The proposed methodology for measuring the resilience of rural communities is based on the quantification and weighting of 17 variables, each with its own percentage weight. All variables are related to a specific criterion (there are 8 of them), and the criteria in turn correspond to one of 4 factors. This methodology for determining resilience is clear in terms of the weight assigned to each variable (indicator/criterion). At the same time, these variables are subjective, as the vast majority of them relate to a given oblast and given communities.

As a result of the introduction of the EU's Common Agricultural Policy, Lithuania also assessed the resilience of the agricultural sector. It was based on the analysis of purely economic indicators of this sector [5] and had a multifactorial approach [6]. The study used data from the Lithuanian Statistical Service and the Farm Accounting Data Network (FADN) for the period 2010-2019. This approach is certainly one of the most extensive in terms of the level (national) and volume of statistical information used. The main functions analysed were: production of food at affordable prices, guarantee of farm viability, and provision of employment opportunities with decent income for agricultural workers. All indicators of the functions were presented in monetary terms (million euros) and calculated using the formula.

Ukrainian research practice in the field of agricultural resilience is rather limited. It is located at the intersection of assessments of the overall impact of military operations on the agricultural sector of Ukraine [7, 8] and theoretical aspects of studying the resilience of various sectors of the economy [9, 10]. One of the most comprehensive works on the resilience of the agricultural sector of Ukraine is the material of the State Institution «Institute for Economics and Forecasting of the National Academy of Sciences of Ukraine», presented at the end of 2023 [11]. These research findings are complemented by interviews with civil society representatives, politicians, and agribusiness representatives conducted in 2022-2023. This work was supported by the Transnational Institute (TNI) and the Swedish Research Council for Sustainable Development FORMAS, and is presented in the form of a report in Ukrainian and English.

The above theoretical provisions and practices of assessing the resilience of the agrarian sphere in the world have become the basis for outlining the main aspects of such work within the scope of territorial communities of the Kyivske Prydniprovia affected by Russian aggression. In our opinion, such an assessment should include interrelated components: 1) changes in the structure of agriculture as a basic system-forming economic activity; 2) natural conditions, resources and the impact of military operations on them; 3) the population living on these territories and changes in their social conditions. This work is planned to include a comparison of the relevant indicators before the large-scale invasion and after the de-occupation. The approach is based on the use of analytical data with a geographical aspect. This analysis will be based on field research (selection of soil samples, interviews, etc.), software that allows to trace the change in the use of agricultural areas and create mapping schemes for processing spatial data, including primarily the use of GIS tools. In particular, satellite imagery from Planet Labs with medium spatial resolution (3 m per pixel) will be used.

This topic is the subject of the research project «Resilience and potential for restoring the agrarian sphere of territorial communities of Kyivskoho Prydniprovia affected by Russian aggression» in accordance with the order of the Presidium of the National Academy of Sciences of Ukraine of 19.02.2024 No. 101 «On the Results of the 2023 Competition for NAS Grants by Research Laboratories/Groups of Young Scientists of the National Academy of Sciences of Ukraine for Research in Priority Areas of Science and Technology Development in 2024-2025».

**References**

1. Joshua F. Cabell, Myles Oelofse. An indicator framework for assessing agroecosystem resilience. Ecology and Society. Vol.17 (1), 2012. http://dx.doi.org/10.5751/ES-04666-170118.
2. Tallaksen J. What is Agricultural Resilience? [Electronic resource]. – Mode access: https://wcroc.cfans.umn.edu/about-us/wcroc-news/ag-resilience.
3. Miranda P.M. Meuwissen, Peter H. et al. A framework to assess the resilience of farming systems. Agricultural Systems. Agricultural Systems. Vol. 176. 2019. https://doi.org/10.1016/j.agsy.2019.102656.
4. Córdoba C., Triviño C., Calderón J.T. Agroecosystem resilience. A conceptual and methodological framework for evaluation. PLOS ONE 15(4): 2020. https://doi.org/10.1371/journal.pone.0220349.
5. Morkūnas M., Volkov A., Pazienza P. How Resistant is the Agricultural Sector? Economic Resilience Exploited. Vol. 11 (3), 2018, 321-332. https://doi.org/10.14254/2071-789X.2018/11-3/19.

6. Volkov, A.; Žičkienė, A.; Morkunas, M.; Baležentis, T.; Ribašauskienė, E.; Streimikiene, D. A Multi-Criteria Approach for Assessing the Economic Resilience of Agriculture: The Case of Lithuania. Sustainability 2021. https://doi.org/10.3390/su13042370.
7. Nehrey M., Trofimtseva O. Analysis of the agriculture sector of Ukraine during the war. Bulletin of V. N. Karazin Kharkiv National University Economic Series, 2022, (102). P. 49-56. https://doi.org/10.26565/2311-2379-2022-102-06.
8. A year of war in numbers for the agricultural sector [Electronic resource]. – Mode access: https://www.ucab.ua/ua/pres_sluzhba/novosti/rik_viyni_v_tsifrakh_dlya_agrosektoru.
9. Pyrozhkov C.I., Bozhok E.B., & Khamitov H.B. National resilience of the country: strategy and tactics of anticipation of hybrid threats. Visn. Nac. Akad. Nauk Ukr., 2021, (8). P. 74–82. https://doi.org/10.15407/visn2021.08.074.
10. Khaustova V.Ye., Reshetnyak O.I. Resilience of Economy: Its Essence and Challenges for Ukraine. Business Inform, 2023, 7. P. 30-41. https://doi.org/10.32983/2222-4459-2023-7-30-41.
11. Mamonova N., Borodina O., Kuns B. Ukrainian agriculture in wartime. Resilience, reforms, and markets [Electronic resource]. - Mode access: https://www.tni.org/en/article/ukrainian-agriculture-in-wartime.

*DOI: https://doi.org/10.30836/igs.iies.2024.26*

**Varukha A.**

*Chornobyl Radiation and Ecological Biosphere Reserve, Kyiv, Ukraine.*
*Institute of Geography of the National Academy of Sciences of Ukraine, Kyiv, Ukraine.*
*E-mail: avarukha@gmail.com*

# DEVISING A MODEL PROTECTED AREA MANAGEMENT EFFECTIVENESS EVALUATION METHOD FOR THE CHORNOBYL RADIATION AND ECOLOGICAL BIOSPHERE RESERVE USING THE THEORY OF CHANGE APPROACH TO ENSURE RESERVE'S SUSTAINABLE DEVELOPMENT

The effectiveness of protected area management is essential for their success in safeguarding bio- and landscape diversity as well as ensuring sustainable development [1]. Protected areas (PAs) without effective management won't provide other benefits either. It is important to evaluate the management effectiveness of PAs to keep track of the progress toward the commitments of the strategy and make any necessary adjustments. Effectiveness assessments are crucial to understanding whether and why PAs are working or not, and how to improve PAs' quality [2].

Aiming to evaluate the protected area management effectiveness (PAME) the International Union for Conservation of Nature World Commission for Protected Areas (IUCN-WCPA) developed a special framework [3]. It became the basis of many PAME assessment methods in the world. Including one of the most used ones - Management Effectiveness Tracking Toll (METT) [4]. It has been used occasionally by some EU Member States to assess the management effectiveness of their Natura 2000 sites or their protected areas. Some countries adapted the method accordingly with their PAs peculiarities creating national METT-based PAME-evaluation methods.

Currently, there is no approved method for assessing the effectiveness of protected area management in Ukraine on the national level. However, there was a pilot project on assessing the PAME in national parks in the Carpathian region which showed an average of 53% in management effectiveness [5]. Low efficiency of protected areas in Ukraine, including not only national parks but biosphere reserves, is the existing problem that continues to emerge. War-induced challenges protected areas face only highlight the urgent need for improvement of PAs management in Ukraine and therefore the need to evaluate their effectiveness.

For now, the situation is: there is no PAME evaluation conducted in the PAs regularly as there are no obligations (from the Ministry of Environment and Natural Resources of Ukraine) on PAs, including the Reserve, to use some PAME method(s) (as we know it) and to conduct evaluations - so, PAs does not conduct it. The Ministry has micro-capacity in the management of the PA system (less than 20 people work in the relevant PA departments). PAs as institutions sometimes are very weak, as well as PA staff, who are underpaid, underskilled, and unmotivated to revise their management using some foreign method(s).

National Parks and Biosphere Reserves have a 10-year management plan and have had to review it at the end of the 10 years while creating a new management plan. But often organizations that create new management plans do it poorly, there are no criteria or Ministry's recommendations on how to do it properly - how to review the efficiency of the PA and no guidelines for providing recommendations for its improvement.

Chornobyl Radiation and Ecological Biosphere Reserve (ChREBR or Reserve), which was founded in 2016 and began to operate in 2017, has special functioning conditions as it is located within the Chornobyl Exclusion Zone (CEZ), occupying 87% of CEZ territory. The ChREBR was established to preserve the biodiversity that has recovered after the accident.

Protected area (PA) management of the ChREBR must be assessed to identify the current level of it's effectiveness and possible ways of improvement.

METT could be a basis for devising the model PAME evaluation method for the ChREBR. The standard METT questionnaire cannot reflect all the intricacies of managing such a specific PA as the Chornobyl Reserve (limitations in types of natural resources use due to radiation contamination (including forestry, recreation, etc), management measures. Radiation security is number one priority of the management). Therefore, our goal is to increase the management effectiveness of the Reserve by developing and establishing a Model Monitoring Method for PAME in the Chornobyl Radiation and Ecological Biosphere Reserve.

We choose to use the Theory of change (result chain) method used in conservation project management to reach our goal – devise an appropriate model PAME evaluation method for ChREBR. Theory of change is an approach that describes how with conservation interventions we can achieve desired outcomes.

Applying the theory of change approach and using Miradi software (a digital tool for conservation project management) we developed a specific result chain for our task (Fig. 1).

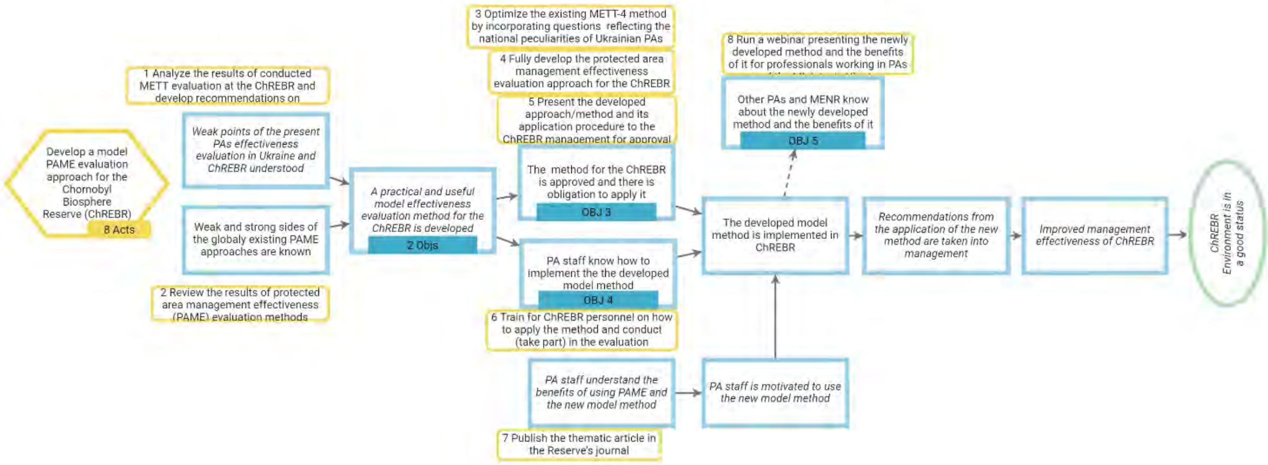


Fig. 1. Theory of change (Result chain) for devising the model protected area management effectiveness evaluation method for the Chornobyl Radiation and Ecological Biosphere Reserve developed using Miradi software

By devising a model PAME evaluation method for the Chornobyl Radiation and Ecological Biosphere Reserve, the Reserve's management effectiveness will be improved and create a positive example for the country. The Reserve can become a pioneer among PA in Ukraine in establishing a specific PAME Monitoring Plan. This Plan will ensure the sound PAME of the Reserve as well as will ensure its sustainable development.

*We are grateful to the Klaus Toepfer Fellowship Programme and Volodymyr Milushev for providing the theory of change perspective on the issue discussed in the paper.*

**References**


1. Geldmann, J., Manica, A., Burgess, N.D., Coa, L. & Balmford, A. (2019). A global-level assessment of the effectiveness of protected areas at resisting anthropogenic pressures. Proceedings of the National Academy of Sciences of the United States of America, 116 (46), 23209-23215.
2. Chen H., Zhang T., Costanza R., Kubiszewski I. (2023). Review of the approaches for assessing protected areas' effectiveness. Environmental Impact Assessment Review, Volume 98, 106929.
3. Protected Planet. (2023). Management Effectiveness (PAME). [Electronic resource]. - Mode access: https://www.protectedplanet.net/en/thematic-areas/protected-areas-management-effectiveness-pame?tab=Methodologies.
4. IUCN. (2021). Management Effectiveness Tracking Tool (METT): New edition of the METT Handbook launched. [Electronic resource]. - Mode access: https://www.iucn.org/news/protected-areas/202112/management-effectiveness-tracking-tool-mett-new-edition-mett-handbook-launched.
5. Support to Nature Protected Areas of Ukraine. (2020) A national version of the methodology for assessing the management effectiveness of Ukrainian protected areas was formed within the SNPA project. [Electronic resource]. - Mode access: http://snpa.in.ua/en/v-ramkah-proektu-sformuvaly-natsionalnu-versiyu-metodyky-dlya-otsinyuvannya-efektyvnosti-upravlinnya-pryrodno-zapovidnymy-terytoriyamy-v-ukrayini/.

*DOI: https://doi.org/10.30836/igs.iies.2024.48*

**Halchenko Z., Ostapenko N., Kryuchkova S., Kirichenko V., Bondarenko L.**

*Institute of Geotechnical Mechanics named after M.S. Polyakov National Academy of Sciences of Ukraine, Dnipro, Ukraine. E-mail: zorichka85@gmail.com, ianatali1978@gmail.com, svetlanakriuchkova69@gmail.com, vakirichenko62@ukr.net, larisabondarenko102@gmail.com*

# ON THE QUESTION OF METHODOLOGICAL FEATURES OF ENVIRONMENTAL FORECASTING UNDER THE CONDITIONS OF THE STATE OF WAR

In the conditions of martial law, risk assessment of the implementation of geological and mining projects and the environmental justification of the innovative possibilities of acceptable technological solutions, acquires particular importance. Defining risk responses is currently the weakest point in the risk management process.

To build a universal methodology for the complex analysis of dangerous man-made risks, the problem of the "critical limit" is sometimes singled out, that is, a set of critical limitations, and the basic principle of risk assessment is called the "critical limit principle". Thus, it is possible to estimate the value of risk as the ratio of expected values to the critical value (for all components of the environment, both at the global and regional levels).

The risk of the impact of man-made activity on the environment is the probability of the occurrence of an event that has adverse consequences for the environment and is caused by the negative impact of economic or other activities, emergency situations species of man-made [1]. Such a negative feature as the absence of certain conditions and technologies for the use of material resources in a closed cycle determines the modern "Production-Consumption" system, which leads to the formation of a huge amount of industrial and household waste. At the same time, as a rule, their processing is either technically impossible, or economically impractical, or both. As a result, irreversible losses of renewable and non-renewable natural resources and dangerous pollution of the environment are have observed, that are repeatedly intensified by military actions.

The technologies for extraction and processing of mineral raw materials cause especially unjustified consumption of natural resources and the accumulation of large volumes of waste. The actual solution to these problems is determination the risks of the operation of mining enterprises and hydro-technical structures, including. In the conditions of martial law, the definition and assessment of environmental risks creates the necessary basis for the application of legal norms of the European direction and state mechanisms of administrative and economic influence in order to achieve an acceptable level of risk and safe landmarks.

At the ecosystem level, the indicators of zones of ecological losses determined by spatial characteristics (by indicators of relative and absolute area and ratios of their areas). Under conditions of the same stage of disruption of geoecosystems, a higher level of danger have will be observed where there is an increase in the relative disturbed area. As a result, the spatial criterion of zones of geoecological losses is the heterogeneity of destabilizations, for example, the relative area of the land (in %) removed from the land use: under normal conditions − less than five, in the ecological risk zones − 5-20, of crisis − 20-50, of disaster − more 50.

For an objective assessment, criteria for identifying environmental damage based on the rate of increase in adverse changes in the environment are required. The probability of realization of forecasts of natural and man-made hazards is determined by the area affected or the recurrence of the event.

Material damage $D_m(H)$, presented in the form of area affected by a single manifestation of danger *H*, can defined as:

$$D_m(H) = V_m(H) \cdot S_0 = S_H \cdot S_0 \cdot S_t^{-1} \,, \qquad (1)$$

Where $V_m$ *(H)* – the degree of damage to the territory under the impact of a certain danger,

$S_H$ – the area affected by a single manifestation of danger *H*,

$S_0$ – the area of the hazard object of the developed part of the territory,

$S_t$ – the total area of the territory.

From this, the risk of damage (destruction) of a unit of area within the developed part of the territory $S_0$ in time and space by danger *H* and the full integral risk of losses in this event are calculate, according to the formulas:

$$R_{sm}(H) = P^*(H) \cdot V_m(H) \ , \tag{2}$$

$$R_m(H) = P^*(H) \cdot D_m(H) = R_{sm}(H) \cdot S_0 \ , \tag{3}$$

Where $P^*(H)$ – the recurrence of the danger ($H$), which is numerically equal to its statistical probability.

Formula (2) characterizes the material risk of specific losses from a unit area of both the object and the entire assessed territory per unit of time, which can be expressed through the dimension ha/ha/year; $km^2/km^2$/year. This risk is usually called the "specific risk of damage to the territory", specifying in each case the specific nature of the consequences of the damage. The material risk of damage to the territory is the basis for determining other types of risks and losses from extraordinary and catastrophic events, in particular, the risk of land destruction because of hostilities.

Specific damage risk can have used for mapping and comparative assessment of the risk of dangerous phenomena, especially in the absence of reliable information about the location and cost of individual objects, as well as for determining indicators of the stability of territories in conditions of military operations. The full value of the damage risk obtained by formula (3) determines the conditional rate of land loss within the developed part of the territory. Values of the damage and risk for the entire territory (if it is accepted as an object of danger) can have obtained by formulas (1, 2), considering the $S_0 = S_t$.

Since tailings dumps are an integral part of the process of the beneficiation of poor iron ores, practically all the mining and processing enterprises are carry out monitoring the state of tailings dumps and auxiliary structures, develop projects to increase the capacity of their existing tailings dumps. Today about 2 billion $m^3$ of beneficiation waste accumulated in Kryvbas, and up to 10,000 hectares of agricultural land occupied by the tailings dumps [2]. During the period from 1961 to the present day, the five active mining and processing enterprises of Kryvbas was stored iron quartzite beneficiation waste in six tailings dumps. The waste from the mining and processing enterprises of Kryvbas contains up to 25% of total iron and about 12-13% of magnetic iron. The reserves of iron ore tailings in these storages are estimated at more than 8 billion tons, the content of magnetic iron in which varies from 3,0% to 7,17%, and of total iron − from 15,7% to 18,6% [3, 4]. Tailings dumps of beneficiation waste of the mining and processing enterprises of Kryvbas are of interest, both promising man-made deposits and sources of ecological danger.

The construction of a predictive assessment for any natural and man-made negative phenomenon should begin with the definition of such categories as “Essence / State / Relationship / Predictive assessment” according to a simplified scheme. These categories should be determined for all indicators that are have represented the characteristics of ecological, social and economic consequences in a certain sequence of four stages, the content of which proposed in the Table 1.

Table 1. Structured form of four consecutive stages of predictive assessment of dangerous natural and man-made phenomena considering the risks

| *Sequence of categories* | *Four stages and essence of assessment* | | | |
|---|---|---|---|---|
| | I | II | III | IV |
| *Logical sequence* | The essence of a negative phenomenon | State of danger | Relationships (interactions and connections) | Development of forecast assessment |
| *Process sequence* | Process analysis of activation mechanisms | System analysis of geotechnical system monitoring data | Correlation analysis of basic factors | Determination of negative consequences |
| *The resulting sequence* | Construction of the system of direct and indirect factors of negative impact | Justification of the system of basic factors | Determination of indicators for the geotechnical system | Assessment of risks of various degrees of danger (including military actions) |

Innovative solutions for the introduction of unmanned aerial vehicles as a component of aerospace systems are needed in the management of monitoring the quality of the environment and the operational determination of the risks of man-made impact. At the same time, the degree of operational awareness of relevant state and municipal institutions and relevant specialized emergency and rescue formations, which allows online monitoring of the situation [5], increases. Today in Ukraine, the problem of the effectiveness of management of environmental monitoring for the operative identification of risks of man-made impact is relevant. In countries such as the United States of America, Canada, Germany, France, and Great Britain, this problem are successfully solving with the help of technologies of geo-intelligent decision-making systems, the core of which is satellite systems of remote sensing of the Earth [6].

Risk assessment of the operation of existing storage facilities and mineral processing products at mining enterprises caused by man-made and environmental factors is an important step in ensuring safety and optimizing production. This process should be include the following steps:

1 – Risk identification: assessment of potential hazards associated with the processes of raw material storage and processing. These can be landslides, soil and water pollution, man-made accidents and others.

2 – Analysis of compliance with safety standards: assessment of the extent to which storage facilities and processing processes comply with international and national safety standards.

3 - Classification of storages and processing products: distribution of storages and products by risk level, for example, high risk, medium risk and low risk, which helps to prioritize the implementation of measures.

4 – Development of risk minimization strategies: development and implementation of risk reduction plans in storages and processing processes, and improvements technologies, implementation of monitoring systems and other measures on security issues.

5 – Security audit: regular analysis of the security of the processes of storage and processing to identify new risks and tracking the effectiveness of implemented risks minimization measures.

6 – Documentation and reporting: maintaining relevant documentation on risk assessment, and measures taken and reporting support to relevant regulators.

7 – Implementation of the innovative available technologies to minimize or eliminate risks.

The classification of risks and safety in the mining industry is a complex and multifaceted process that requires the integration of specialized expertise in geology, engineering, ecology, mining technologies and industrial production safety.

For the increase the level of man-made and ecological safety of potentially dangerous productions and reduce the level of risk of emergency and catastrophic situations, it is necessary to create a complete interdepartmental system of integral monitoring and forecasting of emergency situations.

In the future, it is necessary to study the dynamics of deflation and migration processes, which are associated with functioning tailings dumps and lead to changes in the components of the environment - soils, surface and underground waters, bottom sediments, and landscapes and local geoecosystems.

The main direction of further research is the determination of environmental risks of the operation of tailings dumpi of mining enterprises and innovative possibilities of eliminating the shortcomings of existing technologies of iron ore extraction and beneficiation. For to determining potential risks, and to reveal the potential of an accessible comprehensive assessment (with comparing the expected risks/losses) of mining and processing enterprises, innovative support of environmental monitoring is needed.

**References**

1. Lysychenko G.V., Zabulonov Yu.L., Khmil G.A. Natural, man-made and environmental risks: analysis, assessment, management. Kyiv: Naukova dumka. 2008. 542 p.

2. Gubina V.G. Iron-containing waste from enterprises of the mining and metallurgical complex of Ukraine. Geological and mineralogical bulletin. No. 1-2 (23-24). 2010. P. 97-100.

3. Kopach P.Y., Yakubenko L.V., Romanenko V.N. [et al.] Prospects for involvement in the operation of man-made deposits (for example, Ukraine and Georgia). Ecology and nature management. Issue 16. 2013. P. 210-217.

4. Medvedeva O.A. Kryvbass tailings ponds, problems and features of their operation. Geotechnical mechanics. Issue 103. 2012. Dnipropetrovsk. P. 279-285.

5. Klymenko M.O. Environmental monitoring. Kyiv. 2006. 360 p.

6. Lyalko V.I., Fedorovskyi O.D., Kostyuchenko Yu.V. Multispectral methods of remote sensing of the Earth in nature management tasks. Kyiv. 2006. 357 p.

DOI: https://doi.org/10.30836/igs.iies.2024.9

**Koptieva T.**

*H.S. Skovoroda Kharkiv National Pedagogical University, Kharkiv, Ukraine.*
*E-mail: koptevatania36@hnpu.edu.ua*

# THE SINKHOLES OF THE SURFACE TIER OF MINING LANDSCAPES IN THE KRYVYI RIH LANDSCAPE-TECHNICAL SYSTEM

The Kryvyi Rih landscape-technical system (the KLTS) is a system that was formed 150 years ago and has completely transformed natural landscapes into anthropogenic ones in such a short period of time. Mining landscapes are of particular importance in the KLTS, which are complex dynamic systems that determine the emergence of derivative processes and phenomena [4]. They are the leading factors in the formation of the surface tier of mining landscapes and cause natural and technological emergencies. The surface tier of the KLTS mining landscapes is represented by surface facilities and structures: quarries, dumps, sludge dumps, mining and processing plants, etc [3]. During active mining of iron ore in the KLTS, derivative processes and phenomena appear on the surface layer, which lead to the emergence of technogenic hazards, especially in the KLTS landslide zones.

Earth surface displacement zones usually arise as a result of underground mining, and this, in turn, forms a dip and subsidence relief on the surface layer.

The dip relief is actively developing in the northern and central part of the KLTS. The sinkhole relief is the end result of the process of rock displacement, which is activated by the use of a subsurface rock collapse system during mining operations [2]. The essence of such system is that the roof of underground cavities of significant total volumes, which are formed after mines have mined the upper horizons of ore-bearing layers (up to 300 m in depth), is artificially collapsed, thus filling the space. According to G.I. Chernoho research, surface displacement begins approximately one to two months after the deposit has been mined over a significant length or after most of the target areas have been excavated at a certain horizon [5]. The collapse can also occur uncontrollably due to the Earth's gravity, as well as due to drilling and blasting operations in the mining allotment.

On the territory of the KLTS, the largest shifts are observed on the territories of Sukha Balka OJSC, Rosa Luxemburg Ore Mining Department, Ordzhonikidze Saksahan Mine, and Kirov Ore Mining Department. According to Palienko research, the area of landslides and sinkholes in the KLTS is estimated at more than 3.3 thousand hectares [1].

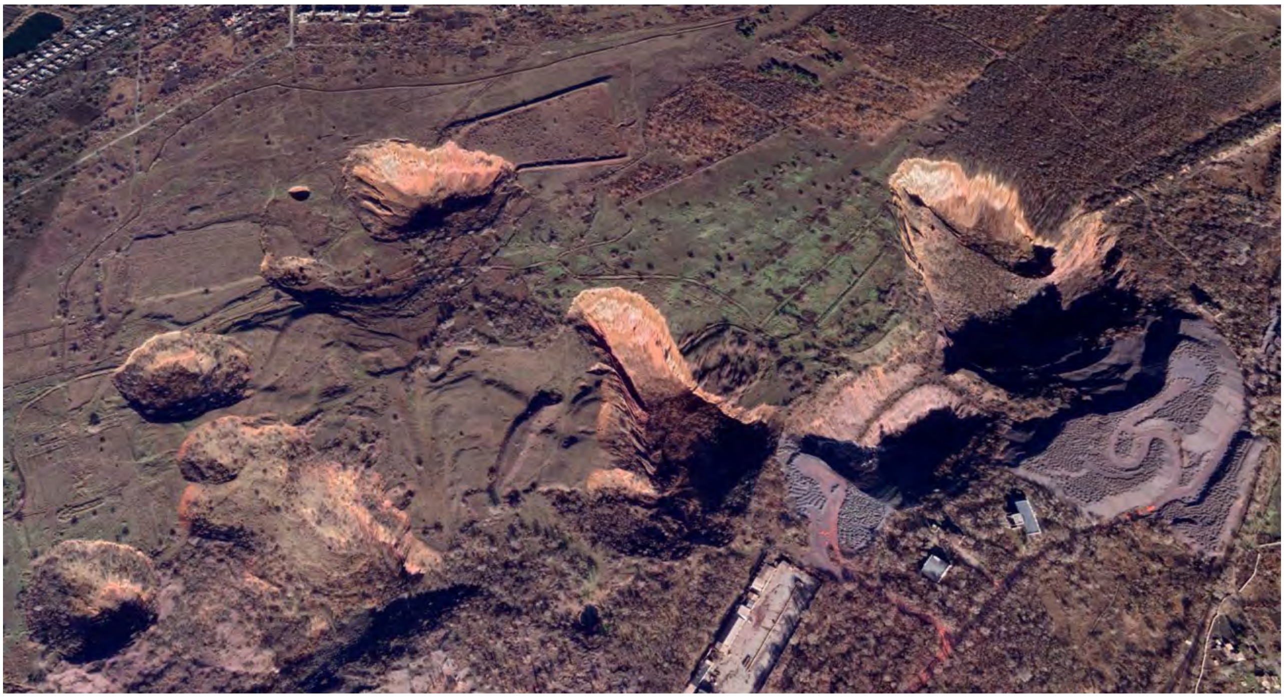

Fig. 1. Sinkholes formed on the territory of the Ordzhonikidze Mine Administration

Sinkholes are meso-relief forms in size; the size of modern sinkholes reaches 100-150 m in depth, and their diameter ranges from several tens of meters to 200-500 m. Each sinkhole has a number of morphological elements, such as a rim, slopes, and a cone-shaped bottom [1].

The first forms of sinkhole relief were recorded in the 1930s and continue to form in the twenty-first century. On June 13, 2010, as a result of the collapse of the ceiling of the working chambers of the -477 m horizon of the Ternivska mine, a sinkhole was formed in an area of 16 hectares, with a depth of 80-82 m in the lying block and 5-20 m in the hanging block, which is called the "Dragon's Nest" of the KLTS industrial mountaineering and tourism, and several profile sinkholes were recorded in this area (Fig. 1).

The formation of the next sinkhole was recorded on August 17, 2010 at a depth of 20 m in the central City District, according to Zadorozhnia G.M., the occurrence of this sinkhole is associated with the self-collapse of rocks in the worked-out pre-revolutionary mine horizons.

Also, as a result of the earthquake that occurred on January 14, 2011 with a magnitude of 3.9, a sinkhole was formed in the territory of the Kirov Mining District sinkhole zone. The sinkhole is located within the supposititous landslide zone, which is formed as a result of mining operations at a depth of -1045 m.

Recently, on March 29, 2024, a large-scale sinkhole was formed on the territory of the Kirov Mining Administration, near the Halkovskyi Kut, with a width of about -100 meters and a depth of 200 meters. This sinkhole is still expanding in morphometric characteristics (Fig. 2).

Fig. 2. A sinkhole on the territory of the Halkovskyi Kut the KLTS

In general, sinkhole processes lead to the formation of fundamentally new landscape complexes at the level of terrain types, the further development of which is determined by landscape formation processes.

Thus, sinkholes are a phenomenon that is formed on the surface tier of the KLTS mining landscapes and passes into the underground tier; a considerable number of sinkholes have been recorded on the KLTS territory, so optimization measures to prevent technogenic hazards should be introduced in this system now [2]. A large percentage of the KLTS territory requires mining and technical reclamation of the failed relief, primarily backfilling and leveling, but recently, sinkholes have been occurring that are large-scale and dangerous. It is also necessary to investigate the entire KLTS territory and draw up detailed maps of the sinkhole terrain and potential areas where sinkholes may form in order to stop mining and reduce and prevent the construction of the KLTS settlement landscape.

Sinkhole zones are complex paradynamic systems, in which the leading role is played by mineral migration (development of landslides, landslides, and landslides on the slopes of sinkholes), water migration (outflow of deep groundwater and formation of reservoirs at the bottom of sinkholes). The migration of biogenic matter (formation of vegetation cover, animal colonization) is somewhat slowed down due to unfavorable environmental conditions that form in sinkholes.

**References**

1. Denysyk H.I., Zadorozhnia H.M. Derived processes and phenomena in the landscapes of technogenesis zones: monograph. Vinnytsia: Vinnytsia regional publishing house, 2013. 220 p. (In Ukrainian).
2. Koptieva T.S. The development of gravity relief and its consequences on the territory of the Kryvyi Rih landscape-technical system. Environmental safety – modern directions and prospects of higher education:

coll. theses add. II International internet conf., Kharkiv, 2th5 of February 2022. Kharkiv, 2022. P. 59–61. (In Ukrainian).
3. Koptieva T.S. Altitudinal differentiation and diversity of mining landscapes of Kryvorizhzhia: monograph: TVORY. 2023, 138 p.: ill. - ("Modern Nature and Landscapes of Ukraine") (In English).
4. Koptieva T.S. Mining landscapes of Kryvyi Rih landscape technical system. Man and the environment. Problems of neoecology. Issue 35. 2021, P.18-26. DOI: 10.26565/1992-4224-2021-35-02 (In English).
5. Chernyyi H.I. Displacement of rocks on the lying side in the Kryvyi Rih Basin, Kyiv.: Publishing house of the Academy of Sciences of the Ukrainian SSR, Institute of Mining, 1959. 67 p. (In Ukrainian).

DOI: https://doi.org/10.30836/igs.iies.2024.19

**Medvedieva O., Halchenko Z.**

*M.S. Poliakov Institute of Geotechnical Mechanics of the National Academy of Scienses of Ukraine, Dnipro, Ukraine. E-mail: medvedevaolga1702@gmail.com, zhalchenko85@gmail.com*

# ASSESSMENT OF THE NATURAL RESOURCE POTENTIAL OF ROCK DUMPS IN MINING REGIONS

An important condition for the smooth functioning of all sectors of the economy is to ensure sustainable energy supply. Today, the threat of depletion of mineral resources is the most acute, so it is important to find and use alternative energy sources to meet energy needs. It is important to take into account their environmental friendliness and renewability.

Ukraine is an energy-dependent country, with imports amounting to about 72%. Therefore, taking into account the negative impact on the environment, the development and use of renewable energy sources (RES) is a priority to ensure the energy independence of our country.

The ability of the natural complex or its individual components to satisfy society's needs for energy, raw materials, and the implementation of various types of economic activity constitute its natural resource potential.

The degree of transformation of the natural resource potential of territories disturbed by mining operations determines the possibility of reclamation or use of these territories for the needs of society.

The most interesting thing today is the attraction of land unsuitable for agricultural needs for renewable energy sources - solar panels, wind turbines, or the creation of forest park recreation areas.

The prospects for the use of renewable energy sources on technologically altered lands in mining regions are very high. There is no doubt that the level of specific energy consumption in Ukraine is higher than it could or should be, especially in comparison with neighboring EU countries. The main obstacles to the development of renewable energy sources and improvement of energy efficiency in Ukraine include the following: insufficient popularization and awareness of renewable energy and energy efficiency measures and their application; insufficient technical development; and excessive market regulation. It should also be noted that there is a significant shortage of land plots for renewable energy facilities, which is not available in mining regions.

The most promising direction of renewable energy is the use of wind turbines. The objects of the technogenic landscape of mining areas are characterized by a significant height in relation to the daytime surface level. This value reaches 100-120 m and can increase with time. Taking into account that wind speed increases with height, the energy potential of the territory where such objects are located also increases [1].

Wind energy has long been viewed as a clean, inexhaustible source of energy. The shortage of non-renewable energy sources and growing dependence on imported fuels have led to a revival of research aimed at expanding the ability to convert wind energy into a usable form of energy.

Advantages of wind energy [2]:

– low cost of production;

– wind power can compete with nuclear, coal and gas power;

– zero cost of the fuel component, the energy source is inexhaustible and available in unlimited quantities;

– environmentally acceptable energy;

– energy production is not accompanied by carbon dioxide emissions;

– wind energy does not have risks associated with the volatility of fossil fuel prices;

– wind power allows us to avoid dependence on energy imports;

– modular design, quick installation;

– electricity supply is comparable in volume to traditional generation methods;

– dispersion over the territory;

– wind power does not interfere with agriculture and industrial activities near wind farms;

– the possibility of using technologically disturbed lands in mining regions.

In modern conditions, man-made mining landscapes are not only widespread, but also quite diverse.

In Ukraine, the most perspective resource waste should include [3]:

1) tailings of ferrous and non-ferrous metal ore enrichment, the total reserves of which (Kremenchutsk-Kryvorizkyi Iron Ore Basin) already reach 2.5 billion tons with a total iron content of 14-20%, and in the Nikopol-manganese ore district - 240 million tons, the content manganese in which is 10-15%. Utilization of sludge from the Mykolaiv alumina plant will allow obtaining gold-rutile-zirconium (gold – 36-42%, zircon – 40-60%, rutile – 14-20%) concentrates;

2) lost mineral raw materials of previously developed deposits, the volume of which reaches 30-40% of outlined reserves, the content of total iron in which is 45-67%;

3) lost mineral raw materials of previously developed deposits, the volume of which reaches 30-40% of outlined reserves, the content of total iron in which is 45-67%;

4) stocks of poor and oxidized ores, which are stored in dumps.

The use of these resources will allow obtaining additional volumes of iron ore concentrate and materials for the construction industry.

The second effective way of using the natural potential of man-made landscape objects is wind energy. Let's consider the wind energy potential of external dumps. In a wind flow, the wind speed increases with increasing height above the Earth's surface. Objects of man-made landscape of mining areas (dumps) are characterized by a significant height in relation to the day surface mark. This value reaches 100-120 m and may grow over time.

Electricity generation in the conditions of Kryvbas dumps by vertical and horizontal wind turbines with a capacity of 100 kW is presented in Table 1 [3].

Table 1. Electricity generation in the conditions of Kryvbas dumps by vertical and horizontal wind turbines with a capacity of 100 kW

| Wind speed, m/s | Number of days with wind, per year, days | Capacity of a vertical wind turbine, %. | Electricity generated, kW-days | Capacity of a horizontal wind turbine, %. | Electricity generated, kW-days |
|---|---|---|---|---|---|
| 1.8 | - | - | - | - | - |
| 2 | 9 | 1 % | 9 | | |
| 2.5 | 12 | 2 % | 24 | | |
| 3 | 67 | 6 % | 402 | | |
| 4 | 76 | 13 % | 988 | | |
| 5 | 79 | 22 % | 1738 | 1 % | 79 |
| 6 | 54 | 34 %; | 1836 | 3 % | 162 |
| 7 | 36 | 46 % | 1656 | 7 % | 252 |
| 8 | 18 | 57 % | 1026 | 12 % | 216 |
| 9 | 6 | 70 % | 420 | 22 % | 132 |
| 10 | 4 | 84 % | 336 | 38 % | 152 |
| 11 | 2 | 100 % | 200 | 48 % | 96 |
| 12 | 1 | 100 % | 108 | 59 % | 59 |
| 13 | 1 | 100 % | 108 | 80 % | 80 |
| 14 | - | 100 % | - | 100 % | - |
| Total | 365 | - | 8849 | - | 1228 |

Based on the results of Table 1, in Kryvyi Rih, vertical wind turbines can produce electricity more than 7 times more than traditional (horizontal) wind turbines.

The objects of the technogenic landscape of mining areas, for example, Kryvbas, where average annual wind speeds rarely exceed 3.5-4.5 m/s and are characterized by a significant height of 100-120 m in relation to the day surface level and variability, therefore, in the conditions of mining regions, it is effective to use wind turbines with a vertical axis of rotation of the turbine with a magnetic levitating bearing.

Based on the above, it follows that wind turbines will not pollute air, water, soil, or generate hazardous waste when generating electricity, as is the case with mining and transportation of minerals in mining regions. They do not deplete natural resources such as coal, oil and gas and do not cause environmental pollution. Clean wind energy can reduce the environmental damage caused by fuel-based energy in Ukraine. In addition, the possibility of involving technologically disturbed lands in mining regions (including through the placement of wind turbines) in the economic activities of individual regions and the country as a whole is particularly promising.

**References**

1. Medvedieva O.O., Halchenko Z.S., Shustov O.O., Akhmetkanov D.K. Prospects for the use of technologically disturbed lands in mining regions for the location of renewable energy sources facilities. Geo-Technical mechanics Interdepartmental collection of scientific works Issue 165, 2023. pp. 17-27.

2. Pivniak H., Shkrabets F., Neuberg N., Tsyplenkov, D. *Osnovy vitroenerhetyky: pidruchnyk* [Basics of wind energy: a textbook], Dnipropetrovsk, Ukraine, 2015. 335 p.

3. Kopach P.I., Yakubenko L.V., Mormul T.M., Danko T.T., Gorobets N.V., Halchenko Z.S. Assessment of natural resource potential of territories disturbed by mining works in the context of effective use of post-technogenic landscape, Geo-Technical mechanics Interdepartmental collection of scientific works, Issue 162, 2022. pp. 38-47.

## NATIONAL ACADEMY OF SCIENCES OF UKRAINE
## DEPARTMENT OF GEOSCIENCES

**INSTITUTE OF GEOLOGICAL SCIENCES NAS OF UKRAINE**
**M.P. SEMENENKO INSTITUTE OF GEOCHEMISTRY, MINERALOGY AND ORE FORMATION NAS OF UKRAINE**
**SUBBOTIN INSTITUTE OF GEOPHYSICS NAS OF UKRAINE**
**INSTITUTE OF GEOGRAPHY NAS OF UKRAINE**
**STATE INSTITUTION SCIENTIFIC CENTER FOR AEROSPACE RESEARCH OF THE EARTH OF THE INSTITUTE OF GEOLOGICAL SCIENCES NAS OF UKRAINE**
**UKRAINIAN MINERALOGICAL SOCIETY**
**INTERNATIONAL ASSOCIATION OF SEDIMENTOLOGISTS**
**INTERNATIONAL ASSOCIATION ON THE GENESIS OF ORE DEPOSITS**

# IDEAS AND INNOVATIONS IN EARTH SCIENCES

## PROCEEDINGS OF THE 10TH INTERNATIONAL GEOSCIENCES CONFERENCE OF YOUNG RESEARCHERS
## Kyiv, 23-24 May, 2024

Compiler: Starodubets Kyrylo

Development of the original layout and typesetting: Starodubets Kyrylo

Cover design: Halyna Kuzmanenko, Starodubets Kyrylo

Information about the publisher

Printing LLC "GNOSIS". Kyiv, Mezhihirska 82-a.
Certificate of registration of the subject of the publishing business in the State Register of Publishers, Manufacturers and Distributors of Publishing Products,series DK No. 2328 dated 10/26/2005
Signed for printing on 05/08/2024. Format 60x90/8. Mind. printing. sheet 16,5. Edition 8 approx.
Deputy No. 5865.